

Inaugural dissertation  
for  
obtaining the doctoral degree  
of the  
Combined Faculty of Mathematics, Engineering and Natural Sciences  
of the  
Ruprecht - Karls - University  
Heidelberg

Presented by

M.Sc., Pharm. Cong Si Tran

Born in Dong Thap, Vietnam

Oral examination: 06.09.2022

**Functional importance of the lipid kinase  
phosphatidylinositol 4-kinase III alpha on  
cytoskeletal organization and its impact on  
hepatitis C virus-induced liver pathogenesis**

**Referees: Prof. Dr. Volker Lohmann  
Prof. Dr. Ralf Bartenschlager**

## **Declaration**

The applicant, Cong Si Tran, declares that he is the sole author of the submitted dissertation and no other sources for help apart from those specifically referred to have been used. Additionally, the applicant declares that he has not applied for permission to enter examination procedure at another institution and that this dissertation has not been presented to other faculties and has not been used in its current or in any other form in another examination.

---

Date

---

Signature

## TABLE OF CONTENTS

---

# TABLE OF CONTENTS

TABLE OF CONTENTS .....	I
ACKNOWLEDGEMENTS.....	V
LIST OF ABBREVIATIONS .....	VI
ZUSAMMENFASSUNG.....	VII
SUMMARY .....	IX
1. Introduction .....	1
1.1. PI4KA/ PI4P and other phospholipid kinases/ phosphoinositides .....	1
1.1.1. General aspects.....	1
1.1.2. PI4P and PI4Ks family .....	3
1.1.3. PI4KA structure, localization and function .....	5
1.2. Cytoskeleton, focal adhesion in relationship with cell shape, cell motility and cancer progression.....	6
1.2.1. Cytoskeleton network.....	6
1.2.2. Cell migration and invasion in connection with cytoskeleton.....	7
1.2.3. Cell shape and cytoskeleton.....	9
1.2.4. Cell shape and cancer .....	10
1.2.5. Focal adhesion.....	11
1.2.6. The liver and hepatocellular carcinoma (HCC) .....	12
1.3. HCV .....	14
1.3.1. General aspects.....	14
1.3.2. HCV genome, proteins and its life cycle .....	15
1.3.3. Cell culture and animal models for studying HCV .....	18
1.3.4. HCV and PI4KA .....	20
1.3.5. HCV and cytoskeleton .....	21
1.4. Objectives of this study .....	22
2. Materials and methods .....	24
2.1. Materials .....	24
2.1.1. For cell culture work .....	24
2.1.2. Antibodies and molecular probes for Western blot, Immunofluorescence and Immunohistochemistry .....	25
2.1.3. Chemicals, reagents used in Western blot, immunofluorescence microscopy.....	26
2.1.4. Buffers and Solutions used in this study .....	27
2.1.5. Inhibitors and activators.....	28
2.1.6. Chemicals, enzymes, kits and miscellaneous materials .....	28
2.1.7. Bacteria .....	29

## TABLE OF CONTENTS

---

2.1.8. Mammalian cells .....	29
2.1.9. Oligonucleotides .....	31
2.1.10. Plasmids .....	31
2.2. Methods .....	31
2.2.1. Preparation of plasmid constructs.....	31
2.2.2. Cell culture.....	34
2.2.3. Preparation of HCV RNAs by <i>in vitro</i> transcription.....	35
2.2.4. HCV RNA electroporation for virus production and replication assay.....	35
2.2.5. HCV infection .....	36
2.2.6. HCV RNA replication assay .....	36
2.2.7. Production of lentiviruses, adenoviruses and transduction on target cells.....	37
2.2.8. RNA extraction, cDNA synthesis and qRT-PCR.....	37
2.2.9. Western blot .....	38
2.2.10. Coimmunoprecipitation assay .....	39
2.2.11. Microscopy: bright field (cell morphology) and confocal (immunofluorescence) .	39
2.2.12. Biochemical determination of cellular PI(3,4)P2 levels using PI(3,4)P2 ELISA Mass Kit.....	40
2.2.13. Human phosphor kinase array and Cytoskeleton array .....	40
2.2.14. Cell proliferation, migration and invasion assay .....	42
2.2.15. Mice experiments .....	43
2.2.16. Statistical analysis and softwares .....	44
3. Results .....	45
3.1. Screening for factors contributing to PI4KA's signaling-induced liver pathogenesis ...	45
3.2. PI4KA is important for cellular morphogenesis.....	48
3.2.1. Silencing of PI4KA induces morphological changes.....	48
3.2.2. Inhibition of PI4KA leads to the same changes in cell morphology and the effect is dose-dependent.....	52
3.2.3. Expression of enzymatically active PI4KA reshapes cell morphology back to untreated condition.....	54
3.3. PI4KA is a driver for cell invasion and migration.....	55
3.4. PI4KA upregulates phosphorylation of Paxillin and Cofilin .....	59
3.4.1. Immunofluorescence combined with live -cell imaging reveals dynamic changes in cell cytoskeleton in PI4KA knockdown cells.....	59
3.4.2. Suppression PI4KA activity and/or expression reduces levels of p-Paxillin and p- Cofilin.....	64
3.4.3. Both PI4KA abundance and activity are important for the phosphorylation of paxillin and cofilin.....	65

## TABLE OF CONTENTS

---

3.4.4. Constitutive active p-Paxillin reverts morphological changes and regains motility loss induced by silencing of PI4KA.....	66
3.4.5. FA numbers are linked to PI4KA expression and activity .....	68
3.5. PI4KA activation by HCV enhances paxillin and cofilin phosphorylation.....	70
3.6. PI(3,4)P2 is a downstream effector of the pathways regulated by PI4KA .....	73
3.6.1. Screening for downstream effector phosphoinositide kinases .....	73
3.6.2. Knockdown PIK3C2G phenocopies effects on cell morphology and phosphorylation levels of Paxillin and Cofilin observed with silencing of PI4KA .....	76
3.6.3. Viral RNA replication is not dependent on expression of any phospholipid kinase other than PI4KA.....	78
3.6.4. PIK3C2G regulates FA and cell invasion similarly as PI4KA.....	81
3.7. PI(3,4)P2 pools at cell plasma membrane are dependent on PI4KA expression and activity.....	83
3.8. AKT2 is the mediator linking signaling from PI4KA, PIK3C2G to PXN and further downstream.....	89
3.8.1. Silencing PI4KA or PIK3C2G reduces phosphorylation of AKT2.....	89
3.8.2. HCV activates AKT2 at S474 and this correlates with PI4KA activity .....	92
3.8.3. AKT2 is enriched in PI(3,4)P2-containing structures at cell plasma membrane....	93
3.8.4. AKT2 interacts with paxillin .....	93
3.8.5. A pan-AKT activator SC79 reverts the effects on cell morphology and on p-PXN and p-CFL1 levels mediated by PI4KA inhibition in cancer cells .....	94
3.8.6. Constitutive active AKT2 reverts morphological changes induced by silencing of PI4KA.....	96
3.9. Validation of key phenotypes in mice .....	96
3.9.1. Hydrodynamic injection of plasmids expressing PI4KA or HCV nonstructural proteins.....	97
3.9.2. Injection of human liver cancer cells with modulated PI4KA expression into SCID mice .....	99
3.9.3. Autologous transfer of murine HCC derived cells with modulated PI4KA expression.....	101
3.9.4. HCV infection of human-liver chimeric mice.....	101
4. Discussion.....	103
4.1. Important roles of PI4KA on cell morphology revealed by loss-of-function experiments .....	104
4.2. Role of PI4KA on cell migration and invasion.....	105
4.3. Role of PI4KA on cytoskeleton and FA .....	105
4.4. Identification of p-paxillin and p-cofilin as cytoskeletal proteins regulated by PI4KA.	106
4.5. Discovering PIK3C2G as a downstream kinase of the pathway .....	107
4.6. Detection of PI(3,4)P2.....	109
4.7. AKT2 as the downstream kinase.....	110

## TABLE OF CONTENTS

---

4.8. Roles of HCV .....	111
4.9. Efforts to validate key phenotypes in more physiological models .....	113
4.10. Implications of PI4KA, PIK3C2G and AKT2 in cancer progression and as cancer therapeutic targets .....	114
4.11. Outlook .....	116
5. References.....	118
Publications and presentations.....	134
Publications .....	134
Presentations.....	134
Appendix .....	136

# ACKNOWLEDGEMENTS

First of all, I would like to deeply thank Prof. Dr. Volker Lohmann for offering me an opportunity to perform my PhD thesis under his supervision. This allowed me to make one of my big dreams since my childhood come true: studying in and discovering about Europe which before I thought it could hardly ever happen. I also feel really thankful to many open and friendly discussions about the projects with Volker and his kind supports for many other aspects. Furthermore I really appreciate the trust and freedom which he has offered me to work on the projects and to improve myself.

I am very thankful to Prof. Dr. Ralf Bartenschlager, Prof. Dr. Friedrich Frischknecht and Dr. Viet Loan Dao Thi for their willingness to be the members of my PhD defense board. My thanks to Ralf as well for the nice discussions everytime I presented my project in our department seminars and retreats.

I would also like to thank the members in my last four TAC meetings: Kai Breuhahn, Darjus Tschaharganeh and Marco Binder for their valuable time and inputs which they have contributed into shaping this PhD thesis in a nice story. I would also like to send big thanks to all the collaborator partners and people who have contributed to this project: AG. Darjus Tschaharganeh (Marco Breinig, Kai Volz), AG. Kai Breuhahn (Jennifer Schmitt), AG. Tanja Poth, AG. Matti Sällberg (Jingyi Yan, Lars Frelin, Gustaf Ahlen), AG. Heikenwälder (Suzanne Faure-Dupuy, Tobias Riedl), AG. Vibor Laketa, AG. Florian Kühnel (Bettina Mundt, Malin Peter).

My big thanks will also be sent to our lab and department members who have not only helped me specifically in the project but also offered a nice environment for me to work and develop myself and to have a comfortable life in a completely different culture. My special thanks I would like to send to Ombretta Colasanti, my dear friend who has been with me from the first date of my PhD thesis and new life in Heidelberg city, helping me in many things both in and outside the workplace. I would also like to send my big thanks to Rahel Klein who has also shared a lot of experiences with me and given a lot of supports to me. I am highly thankful to Pilar who has been very friendly and supportive whenever I need her helps or instructions. I would also like to thank Uli, Sabine, Alessia, Fredy, Franzi, Sandra, Marie and many other people in the department with whom I have always had friendly conversations and a lot of supports. Thank Sungmin, Tengfeng, Philipp S., Dominik, Santa, Noemi and other lab members who have been with me not only in the lab but also sharing experiences in several nice activities outside the workplace. I also would like to thank my two students, Julia and Stefan who have contributed their time and efforts to the project and shared with me also a lot of nice moments, especially Julia who was with me for almost a year for her lab rotation and master thesis later. I consider many of you as not just colleagues but friends.

Con cảm ơn Mẹ! Vì có Mẹ mà con được trưởng thành như ngày hôm nay. Dù Mẹ không còn hiện diện trên cõi đời này, con biết Mẹ vẫn dõi theo hành trình của con và ủng hộ con. Cảm ơn gia đình, đặc biệt em Thu đã chăm sóc Ba để anh có thể yên tâm ở nơi xa. Thương cả nhà! Cảm ơn chị Hằng, bạn Thu đã rất nhiệt tình giúp đỡ mình trong suốt thời gian qua. Cảm ơn thật nhiều những người bạn và thầy, cô ở Việt Nam, Hàn Quốc và nhiều nơi khác vẫn thỉnh thoảng nhắn tin trò chuyện, động viên trong những lúc mình khó khăn nhất. Cảm ơn các bạn Việt Nam ở Heidelberg đã chia sẻ nhiều khoảnh khắc đẹp trong suốt thời gian mình ở đây. Vielen Dank an meine Mitschüler Mitschülerinnen und Lehrerin Katia aus den Deutschkursen, die viele schöne Erfahrungen mit mir in Heidelberg geteilt haben.



## LIST OF ABBREVIATIONS

---

### LIST OF ABBREVIATIONS

aa	amino acid	HCV	hepatitis C virus
ATP	adenosine-5'-triphosphate	HCC	hepatocellular carcinoma
AU	arbitrary unit	Jc1	Japanese chimera 1
BSA	bovine serum albumin	JFH-1	HCV isolate (= Japanese with fulminant hepatitis)
cc	cell culture	mut	mutation
CFL1	cofilin	MW	membranous web
CIP	calf intestinal alkaline phosphatase	NS	non-structural
DAPI	4',6-diamidino-2-phenylindole dihydrochloride	NT	non-targeting
DMEM	Dulbecco's modified eagle medium	PI	phosphatidylinositol
DMSO	dimethyl sulfoxide	PI4K	phosphatidylinositol 4-kinase
DNA	deoxyribonucleic acid	PI4KA	phosphatidylinositol 4-kinase type III alpha
DTT	dithiothreitol	PI4P	phosphatidylinositol 4-phosphate
E. coli	Escherichia coli	PI(3,4)P2	phosphatidylinositol 3,4-bisphosphate
ECM	extracellular matrix	PVDF	polyvinylidene fluoride
EDTA	ethylene diamine tetraacetic acid	RNA	ribonucleic acid
EGTA	ethylene glycol tetraacetic acid	rpm	revolution per minute
EMT	Epithelial-mesenchymal transition	RT	room temperature (20 - 25°C)
ER	endoplasmic reticulum	SDS	sodium dodecyl sulfate
FA	Focal adhesion	sh	short hairpin
FCS	fetal calf serum	TGN	trans-Golgi network
gt	genotype	wt	wild type
h	hour		

# ZUSAMMENFASSUNG

Die Dynamik von Phosphoinositiden spielt eine entscheidende Rolle bei einer Vielzahl von Zellfunktionen und bei der Entstehung von Krankheiten. Es gibt immer mehr Hinweise darauf, dass Phosphatidylinositol (PI) 4-Phosphat (PI4P) in zahlreichen wichtigen Signalwegen eine signifikante wichtige Rolle spielt. Für die Umwandlung von PI in PI4P sind Enzyme der Phosphatidylinositol-4-Kinase (PI4K)-Familie erforderlich, zu der die Phosphatidylinositol-4-Kinase III alpha (PI4KA) als wichtiges Mitglied gehört. Eine neuere Studie hat einen Zusammenhang zwischen einer hohen Expression von PI4KA und einem undifferenzierten Status sowie einer schlechten Prognose des hepatozellulären Karzinoms (HCC) nahegelegt, obwohl der Mechanismus noch nicht entdeckt wurde. Das Hepatitis-C-Virus (HCV) ist einer der wichtigsten ätiologischen Faktoren im Zusammenhang mit HCC. Darüber hinaus aktiviert HCV PI4KA über Wechselwirkungen mit den nichtstrukturellen (NS) Proteinen NS3-NS5B, um ausreichend PI4P für eine effiziente Genomreplikation bereitzustellen. Ziel dieser Arbeit war es daher, die Auswirkungen der PI4KA-Signalwege auf die Leberpathogenese und die möglichen Beiträge von HCV in diesem Prozess mechanistisch zu verstehen.

In dieser Studie habe ich mit Hilfe von shRNA-vermitteltem Gen-Silencing und einem spezifischen Inhibitor herausgefunden, dass PI4KA über sein Produkt PI4P die Phosphorylierung von Paxillin (PXN) und Cofilin (CFL1), in HCC-Zelllinien mit hoher Expression der Phospholipidkinase positiv reguliert. PXN und CFL1 sind zwei wichtigen Zytoskelettproteinen, welche die Aktindynamik regulieren/steuern, nämlich Paxillin (PXN) und Cofilin (CFL1), in HCC-Zelllinien mit hoher Expression der Phospholipidkinase positiv reguliert. Eine erhöhte PXN- und CFL1-Phosphorylierung wurde mit morphologischen Unterschieden in Verbindung gebracht/assoziiert, darunter die Ausbreitung von Zellen, eine erhöhte Anzahl von fokalen Adhäsionen und eine höhere Zellmotilität im Vergleich zu Zellen mit geringerer Expression und/oder Aktivität von PI4KA. In Übereinstimmung mit diesen Ergebnissen führte die Aktivierung von PI4KA bei HCV-Infektion oder Expression von NS3-5B zu einem weiteren Anstieg von p-PXN und p-CFL1, zu einer erhöhten Anzahl von fokalen Adhäsionen und einer verstärkten Invasivität der Zellen, was auf die PI4P-Konzentration als treibende Kraft schließen lässt. Diese Phänotypen sind Kennzeichen des epithelial-mesenchymalen Übergangs, was auf eine wichtige Rolle von PI4KA bei der Krebsentstehung hindeutet.

Um den Mechanismus zu verstehen, wie PI4KA die Dynamik des Zytoskeletts reguliert, untersuchte ich die PIP-Synthesewege, indem ich auf die Expression verschiedener Phospholipidkinasen abzielte, die mit PI4P verbunden sind/als Substrat verwenden. Dieser Ansatz zeigte, dass nur das Ausschalten der Phosphatidylinositol 3-kinase C2 domain-containing subunit gamma/Phosphatidylinositol-3-Kinase C2-Domäne-enthaltenden Untereinheit gamma (PIK3C2G), einer Lipidkinase, die für die Herstellung von Phosphatidylinositol(3,4)-Bisphosphat [PI(3,4)P<sub>2</sub>] aus PI4P verantwortlich ist, führte zu ähnlichen Phänotypen, die auch bei in zellulären Zytoskelett-assoziierten Signalwegen in PI4KA-Knockdown-Zellen beobachtet wurden, insbesondere in PI4KA-Knockdown-Zellen auf zellulären Wegen, die mit dem Zytoskelett zusammenhängen, beobachtet wurden, und führte zueinandergehend mit zu einer geringeren Ausbreitungsmorphologie, einer Herabregulierung von p-PXN/p-CFL1 und einer Dämpfung der verminderten Invasivität der Zellen. Darüber hinaus verringerte die Ausschaltung von PI4KA oder PIK3C2G die Häufigkeit von spezialisierten PI(3,4)P<sub>2</sub>-Strukturen an der Plasmamembran der Zellen. Diese PI(3,4)P<sub>2</sub>-enthaltenden Strukturen wurden mit sind wahrscheinlich Invadopodien in Verbindung gebracht, die von Krebszellen für ihre Invasivität genutzt werden, was auf einen engen Zusammenhang zwischen den beiden Lipidkinasen und der Zellinvasion hindeutet. Um die Proteinkinase zu identifizieren, die erhöhte PI(3,4)P<sub>2</sub>-Konzentrationen mit Zytoskelettveränderungen verbindet, habe ich einen menschlichen humanen Kinase-Array in Kombination mit einer Western-Blot-Analyse eingesetzt. Dabei zu diesem Zweck wurde festgestellt, dass korrelierte die p-AKT2-Konzentrationen mit den PI4KA- und PIK3C2G-Konzentrationen korrelierend sind. Außerdem war AKT2 innerhalb an den invadopodienähnlichen Strukturen angereichert. Die AKT2-Aktivität korrelierte mit der Phosphorylierung von PXN und CFL1, sowie mit Veränderungen der Zellmorphologie. Eine HCV-Infektion oder -Expression hingegen stimulierte die AKT2-Phosphorylierung und erhöhte den PI(3,4)P<sub>2</sub>-Spiegel an der Zellplasmamembran. Diese Daten legen nahe, dass AKT2 die vorherrschende Proteinkinase ist, die PI4KA/PIK3C2G mit den nachgeschalteten Zielen Substraten PXN und CFL1 verbindet.

## ZUSAMMENFASSUNG

---

Um die in HCC-Zelllinien beobachteten Schlüsselphänotypen zu verifizieren, wandte ich physiologischere Modelle an, einschließlich der Expression von HCV-Proteinen in primären menschlichen Hepatozyten und mehreren Mausmodellen. Diese Ansätze unterstützten das Konzept der PI4KA-Häufigkeit Abundanz und -Aktivität als Schlüsselregulatoren der Zellmorphologie und -motilität über die Stimulierung der Phosphorylierung der Zytoskelettproteine PXN und CFL1.

Zusammenfassend zeigen meine Daten, dass PI4KA über das Signalmolekül PI(3,4)P2 und seinen nachgeschalteten Mediator AKT2 auf zelluläre Wege Signaltransduktionspfade aktiviert einwirkt, die die Zellmorphologie und die Dynamik des Aktinzytoskeletts steuern und damit das Fortschreiten von Krebs begünstigen. HCV trägt also über die Aktivierung von PI4KA zur Pathogenese der Leber bei und vermittelt ähnliche Phänotypen wie die erhöhte PI4KA-Expression, die in von HCC abgeleiteten Zellen beobachtet wurde.

# SUMMARY

Phosphoinositide dynamics play a crucial role in a diverse range of cellular functions and in the development of diseases. Among them, accumulating evidence suggests significant contributions of phosphatidylinositol (PI) 4-phosphate (PI4P) in numerous important signaling pathways. The conversion to PI4P from PI requires enzymes of the phosphatidylinositol 4-kinase (PI4K) family in which phosphatidylinositol 4-kinase III alpha (PI4KA) is an important member. A recent study has suggested a connection between high expression of PI4KA and undifferentiated status and poor prognosis of hepatocellular carcinoma (HCC), although the mechanism has yet to be discovered. Hepatitis C virus (HCV) is one of the main etiological factors associated with HCC. In addition, HCV activates PI4KA via interactions with nonstructural (NS) proteins NS3-NS5B to provide sufficient PI4P for efficient genome replication. The aim of this work was therefore to mechanistically understand the impact of PI4KA signaling pathways on liver pathogenesis and the potential contributions of HCV in this process.

In this study, by using shRNA mediated gene silencing and a specific inhibitor, I found that PI4KA via its product PI4P positively regulated levels of phosphorylation of two important cytoskeletal proteins regulating actin dynamics, paxillin (PXN) and cofilin (CFL1), in HCC derived cell lines with high expression of the phospholipid kinase. Increased PXN and CFL1 phosphorylation was associated with morphological differences including cell spreading, increased numbers of focal adhesions (FAs) and higher cell motility as compared to cells with lower expression and/or activity of PI4KA. In agreement with these results, the activation of PI4KA upon HCV infection or expression of NS3-5B further increased p-PXN and p-CFL1, resulted in elevated numbers of FAs and enhanced cell invasiveness, suggesting PI4P concentration as the driving force. These phenotypes are hallmarks of epithelial–mesenchymal transition, implying important roles of PI4KA in cancer progression.

To understand the mechanism how PI4KA regulated cytoskeletal dynamics, I evaluated PIP synthesis pathways by targeting different phospholipid kinases which are connected to PI4P. This approach revealed that silencing of Phosphatidylinositol 3-kinase C2 domain-containing subunit gamma (PIK3C2G), a lipid kinase responsible for producing phosphatidylinositol (3,4)-bisphosphate [PI(3,4)P<sub>2</sub>] from PI4P, led to similar phenotypes observed in PI4KA-knockdown cells on cytoskeleton-related cellular pathways, leading to less spreading morphology, downregulation of p-PXN/p-CFL1 and dampening of cell invasiveness. Furthermore, knockdown of PI4KA or PIK3C2G reduced the abundance of PI(3,4)P<sub>2</sub> specialized-enriched structures at the cell plasma membrane. These PI(3,4)P<sub>2</sub> containing structures had been linked to invadopodia which are utilized by cancer cells for their invasiveness, suggesting a strong connection of the two lipid kinases with cell invasion. To identify the protein kinase connecting increased PI(3,4)P<sub>2</sub> levels with cytoskeletal changes, I applied a human kinase array in combination with western blot analysis. To this end, p-AKT2 levels were found to be correlated with PI4KA and PIK3C2G abundances. Furthermore, AKT2 was enriched at the invadopodia-like structures. AKT2 activity was correlated with the phosphorylation of PXN and CFL1 and changes in cell morphology. HCV infection or expression in contrast stimulated AKT2 phosphorylation and enhanced PI(3,4)P<sub>2</sub> at the cell plasma membrane. These data suggested AKT2 as the predominant protein kinase linking PI4KA/PIK3C2G with the downstream targets PXN and CFL1.

To verify the key phenotypes observed in HCC-derived cell lines, I applied more physiological relevant models, including expression of HCV proteins in primary human hepatocytes and several mouse models. These approaches supported the concept of PI4KA abundance and activity as key regulators of cell morphology and motility via stimulating phosphorylation of the cytoskeletal proteins PXN and CFL1.

In conclusion, my data demonstrate that PI4KA functions on cellular pathways governing cell morphology and actin cytoskeleton dynamics favorable for cancer progression via the signaling molecule PI(3,4)P<sub>2</sub> and its downstream mediator AKT2. HCV, therefore, contributes to liver pathogenesis via activating PI4KA, mediating similar phenotypes as increased PI4KA expression observed in HCC derived cells.

# INTRODUCTION

# 1. INTRODUCTION

## 1.1. PI4KA/ PI4P and other phospholipid kinases/ phosphoinositides

### 1.1.1. General aspects

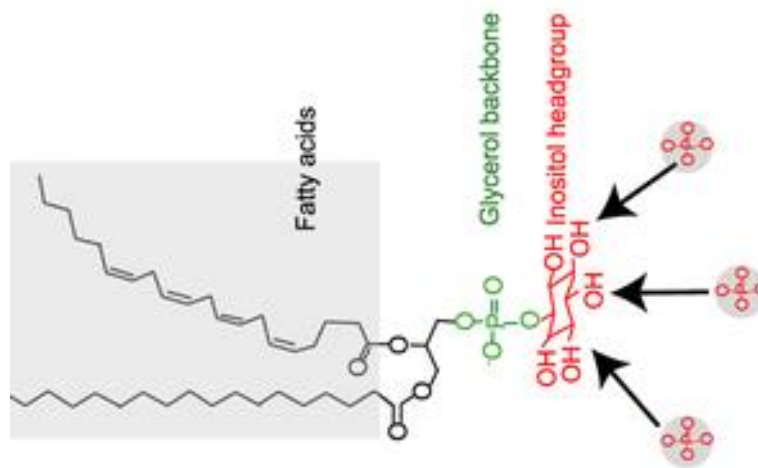
Life requires a delicate coordination of various cellular events including cell growth, cell cycle progression, cell adhesion, cell motility and apoptosis which are tightly regulated by a plethora of signaling pathways in a spatial and temporal manner (1). Signal transductions modulated by phosphoinositides have been proven to play central roles in a wide range of cellular activities (1,2). These signal molecules have become more attractive as a research topic in recent years. Dysregulation of these pathways is now considered one of the leading causes of many diseases, including cancer (1).

Phosphoinositides (PIs) are low-abundant phospholipid residents of the cytoplasmic leaflet of cellular membranes (3,4). These molecules are amphiphilic with a polar inositol head group facing towards cytoplasm or inside intracellular organelles and hydrophobic fatty acid tails embedded in the lipid bilayer (4) (**Figure 1A**). The key feature of the phosphoinositide signaling system is the interconversion among the seven phosphoinositides and phosphatidylinositol, performed by different phosphoinositide kinases, phosphatases and other phosphoinositide-modifying enzymes (5). In human there are 19 genes encoding for the catalytic subunits of the different phosphoinositide kinases. They are divided into different groups according to the corresponding hydroxyl groups of the inositol ring which they are responsible for phosphorylation: PI3Ks (class I, II and III), PI4Ks (type II and III) and PIP5Ks (type I, II and III) (6). Phosphorylation of the hydroxyl-groups on the inositol ring gives rise to a total of seven different PI species, including 3 phosphatidylinositol mono-phosphates (PI3P, PI4P and PI5P), 3 phosphatidylinositol bi-phosphates (PI(3,4)P<sub>2</sub>, PI(4,5)P<sub>2</sub> and PI(3,5)P<sub>2</sub>) and one phosphatidylinositol tri-phosphate (PI(3,4,5)P<sub>3</sub>) and rendering these phospholipid molecules negatively charged (4,7) (**Figure 1A** and **Figure 2A**). These phosphoinositides are located in various cell compartments at different densities which regulate a variety of signaling pathways in cells (6, **Figure 2A**).

Phosphoinositides take part in key biological processes via recruitment and allosteric activation of signaling proteins to specific intracellular locations. In addition, these small molecules also regulate the function of integral membrane proteins by changing their allosteric conformation or modulating their coupling to protein binding partners (**Figure 1B**). Their coordination with lipid kinases, phosphatases and lipid transport proteins can further mediate lipid transport processes and generate concentration gradients (7). Dysfunction of these enzymes has been found to exert critical impacts on progression of many diseases, including cancer, immune disorders, developmental disorders and inflammatory diseases (7).

# INTRODUCTION

A



B

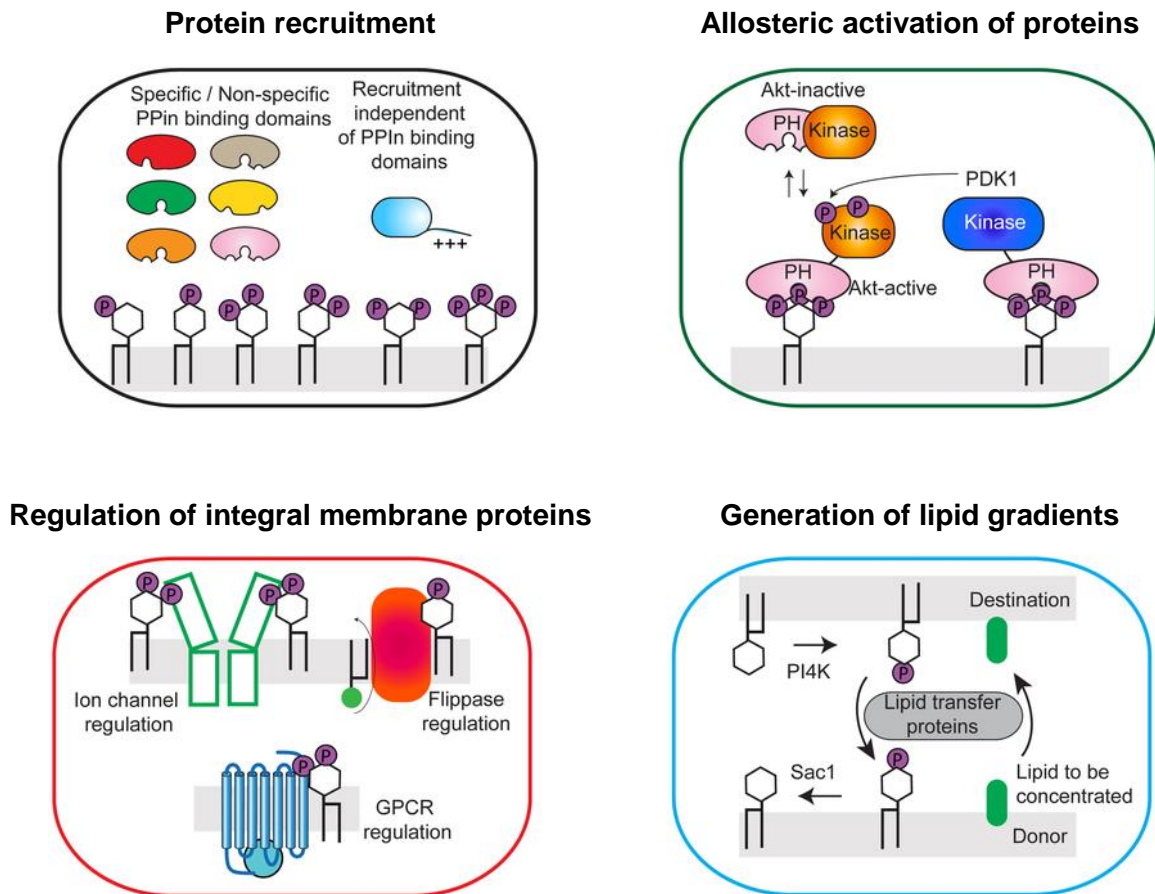


**Figure 1. Schematic illustration of phosphatidylinositol, its PI derivatives and their mechanistic function in cell biology.** A. Chemical structure of phosphatidylinositol and its possible phosphorylated positions (indicated by arrows) for the PIs synthesis. Figure was adapted from (4). B. Contributions of PIs in key cellular signaling events. Figure was adapted from (7).

### 1.1.2. PI4P and PI4Ks family

Phosphatidylinositol 4-phosphate (PI4P) is the most abundant monophosphorylated derivative of phosphatidylinositol (PtdIns) in cells (9). Synthesis of PI4P is carried out by phosphatidylinositol 4-kinases (PI4Ks) which catalyze D-4 phosphorylation of the inositol ring of PIs (9). In cooperation with PI4Ks, PI4P phosphatases and kinases that further phosphorylate PI4P work together to maintain PI4P steady-state levels (10). Phosphorylation at the D3 or D5 position on the inositol ring of PI4P by the class II PI3Ks (PIK3C2A, PIK3C2B and PIK3C2G) or type I PIP5Ks (PIP5K1A, PIP5K1B, PIP5K1C), respectively leads to production of the two important messenger molecules PI(3,4)P<sub>2</sub> and PI(4,5)P<sub>2</sub>. The last phosphoreceptive site on PI(4,5)P<sub>2</sub> is a substrate of class I PI3Ks (PIK3CA, PIK3CB, PIK3CD and PIK3CG) (6, **Figure 2B**). Several pools of PI4P are present in cells as a result of different localization and non-overlapping contributions of 4 human PI4Ks. They are found however most abundantly at the Golgi, plasma membrane and secretory vesicles which attribute to functions of PI4III $\beta$ , PI4KIII $\alpha$  and the type II PI4K, respectively (11,12). PI4P synthesized by PI4Ks have been long considered as an intermediate product for PI(4,5)P<sub>2</sub> at the plasma membrane but recent studies have shown its important functions uncoupled from PI(4,5)P<sub>2</sub> in many aspects of cell biology (9).



# INTRODUCTION

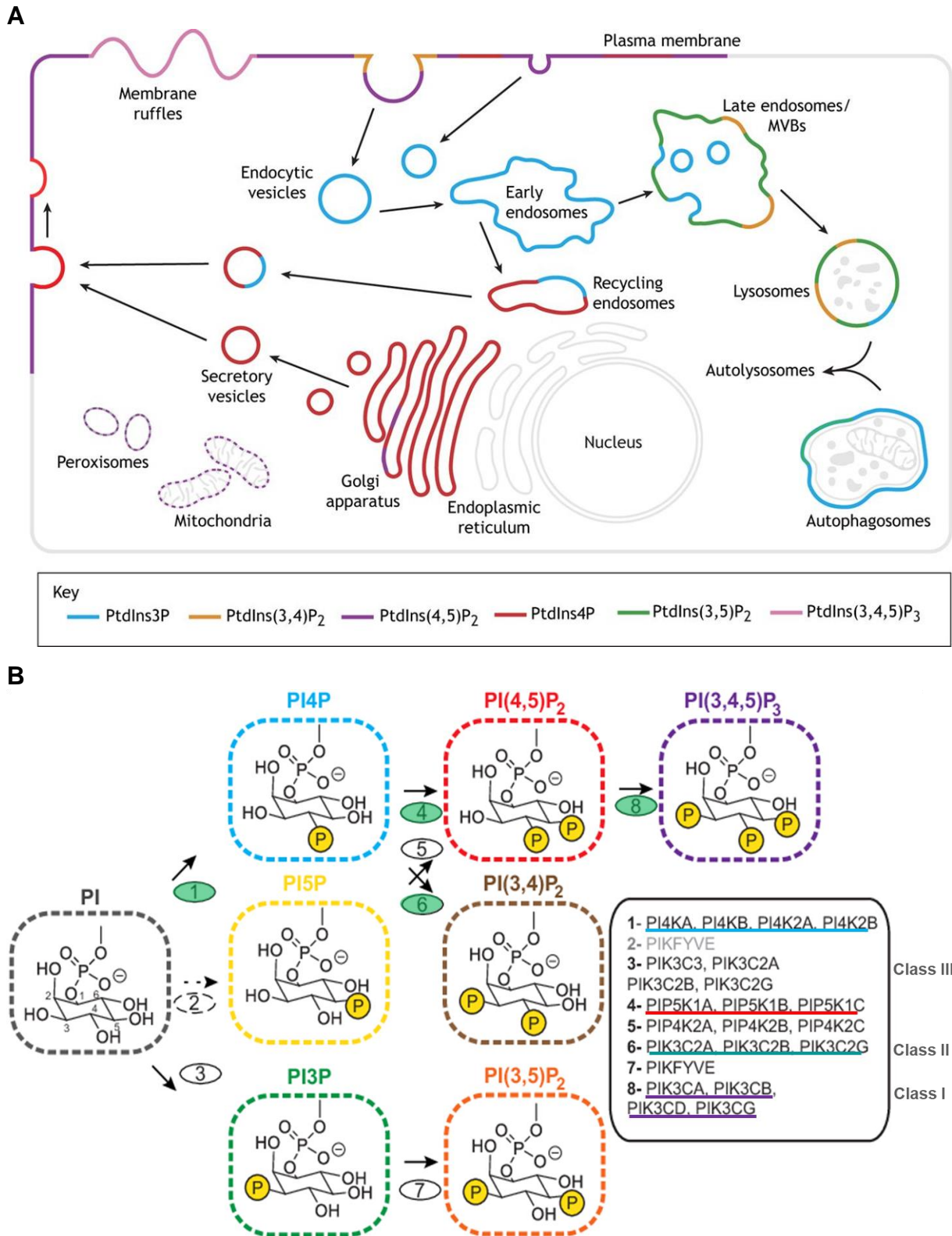


**Figure 2. Distribution and interconversion of human phosphoinositides.** **A.** Schematic illustration of PIs distribution in cells. Figure was adapted from (1). **B.** Phosphorylation at the D3, D4, D5 on the inositol ring of phosphatidylinositol by several classes of phospho lipid kinases leads to production of 7 phosphoinositides. Figure was adapted from (6).

Classification of PI4Ks are based on their sensitivity to specific chemical compounds: type II PI4Ks are adenosine-sensitive while type III PI4Ks are wortmannin-sensitive (11,12). The former are much smaller (**Figure 3**), act primarily as monomers and due to the intrinsic

## INTRODUCTION

presence of lipidation sites they are always associated at membranes (6). The initially described type I PI4Ks were later classified as PI3Ks, leaving no genuine type I PI4Ks nowadays (13). The type III PI4Ks consists of the two proteins PI4KIII $\alpha$  and PI4KIII $\beta$ , which are encoded by PI4KA and PI4KB genes, respectively, (**Figure 3**) and are regulated in the forms of heteromeric protein complexes (6). Both proteins of the type III PI4Ks are conserved in yeast and are known to be hijacked by numerous positive strand RNA viruses, including Hepatitis C virus (HCV), Polioviruses, Enteroviruses, Cardioviruses, and Coxsackieviruses (14,15,16,17,18). These viruses activate either proteins to generate membranes enriched in PI4P which are crucial for viral replication by promoting the exchange and enrichment of specific lipids at these replication sites (6).

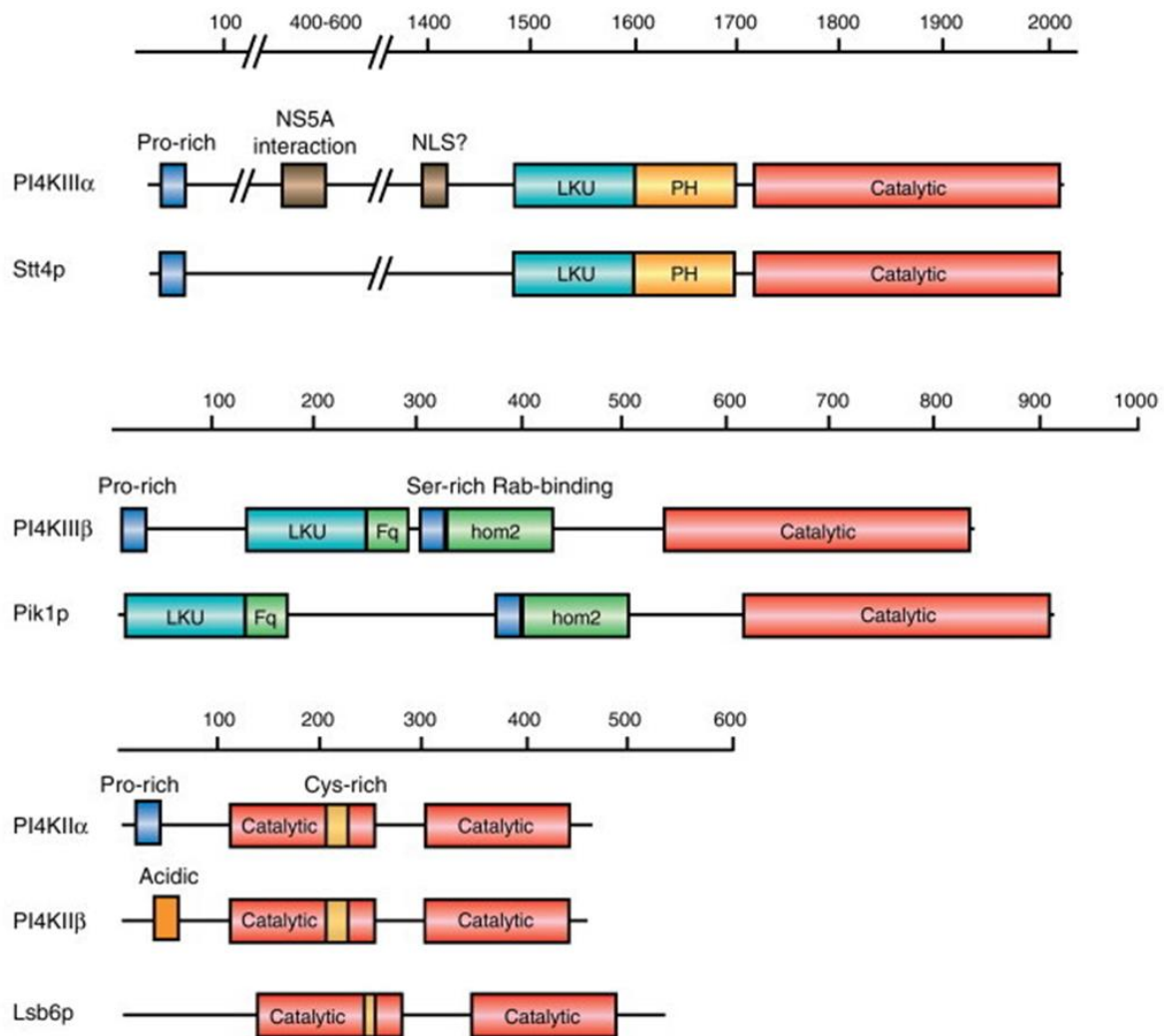


**Figure 3. Schematic illustration of domain organization of the PI4K proteins and their yeast homologs.** Figure was adapted from (19). Note that the NS5A interaction region has not been confirmed in a more recent study (20).

### 1.1.3. PI4KA structure, localization and function

In term of size, PI4KA is the largest member in the PI4Ks family (**Figure 3**). The mRNA is 6309 nt long and encodes a 240 kDa protein with 2012 amino acid. The catalytic module is located at the very C terminus (aa residues 1597–2085) and represents only a small portion of the entire molecule (21) (**Figure 3**). PI4KA mutant variants K1792L, D1899A and D1957A

## INTRODUCTION

---

with mutations located in the catalytic domain have been shown to be catalytically inactive (22). The N-terminal portion has no homology to other known proteins but plays important role in the shuttling of PI4KA to the plasma membrane (23). Proline rich regions reside at the very N terminus, followed by a nuclear localization signal (NLS), lipid kinase unique domain (LKU) and pleckstrin-homology domain (PH) (24,25) (**Figure 3**).

In terms of organ distribution, high expression of PI4KA was found in heart, brain, placenta, skeletal muscle, kidney, spleen, thymus, prostate, ovaries, small intestine and colon. Only little amount was detected in lung, liver, pancreas, testis, and leukocytes (21).

While its yeast ortholog Stt4 resides mainly at the cell plasma membrane where it exerts an important role in maintaining cell wall integrity and in proper organization of the actin cytoskeleton, PI4KA was firstly suggested as an ER resident protein in mammalian cells (11). However, this lipid kinase was also detected in different organelles, such as in the Golgi apparatus membranes (12) or in the nuclei of neuronal cells, COS-7 or B50 cells, or in the nucleoli in rat brain cells (26,27). More importantly, ample evidence have suggested PI4KA as the only kinase responsible for PI4P pools at the cell plasma membrane (11,23,28).

PI4KA, however, does not permanently reside at the plasma membrane but is recruited in a complex with at least two accessory proteins EFR3A/B (Efr3 in yeast) and TTC7A/B (Ypp1 in yeast). In addition, FAM126 helps in recruiting PI4KA to PM by forming a tight heterodimer with and stabilize TTC7 (29). Cryo-EM reveals that PI4KA forms a dimer of heterotrimers with TTC7 and FAM126 which is essential for a stable assembly and activity of PI4KA. In these protein complexes FAM126 acts as a central scaffold which is enwrapped by TTC7. TTC7 interacts directly with PI4KA and mediates the activation of this kinase via interaction with the plasma membrane resident EFR3 (29).

### **1.2. Cytoskeleton, focal adhesion in relationship with cell shape, cell motility and cancer progression**

Phosphoinositides are known to be involved in many important cell functions, not solely acting in classical signal transduction at the cell surface, but also via regulation of membrane traffic and the cytoskeleton. Having served as platforms for protein recruitment as well as direct regulators of cytoskeletal proteins, these small molecules contribute to the organization and dynamics of the cytoskeleton network (30,31).

#### **1.2.1. Cytoskeleton network**

The cytoskeleton meshwork is made of three main cytoskeletal filaments: the microfilaments (actin), intermediate filaments and microtubules. It is highly structured, adaptive and dynamic to provide quick reorganization in response to external and internal stimuli (32 and **Figure 4**). The involvement of numerous cytoskeletal proteins and signal molecules make this network one of the most complex and functionally diverse structures in cells (32). The differences in mechanical stiffness, polarity, assembly and disassembly dynamics and associated molecular motors distinguish the cytoskeletal polymers (33).

## INTRODUCTION

Spatial organization of the cell contents, providing physical and biochemical connections with extracellular environment, and generation of coordinated forces for cell movement and cell shape alteration are the three broad functions which have been attributed to the cytoskeleton (33). Several classes of regulatory protein complexes contribute to forming the architecture of the cytoskeleton network, starting from initiation of filament formation by nucleation-promoting factors, trigger and sustain filament growth by groups of polymerases, termination of filament growth by capping proteins, organization of higher-order network structures by cross-linkers and stabilizing proteins, and disassembly of filaments by depolymerizing and severing factors (33).

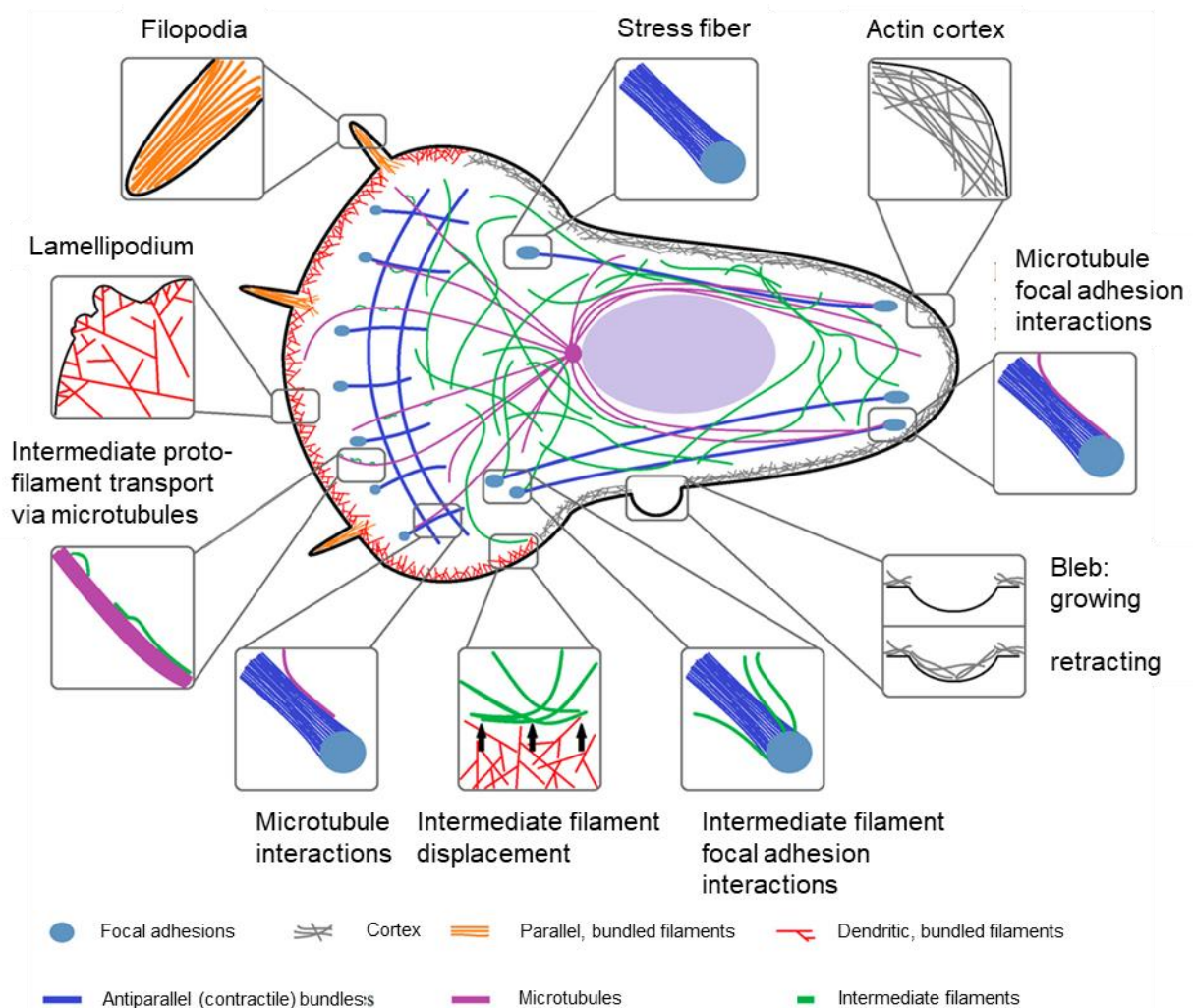


**Figure 4. Organization and interactions of the key components of cytoskeleton network.** (adapted from 32)

### 1.2.2. Cell migration and invasion in connection with cytoskeleton

Most of cancer deaths link to metastasis. In this highly selective process, cancer cells move from a primary site to a distant site or organ. A metastatic cascade comprises of multiple steps: detachment from the primary site, migration and invasion, intravasation and extravasation (cells transport through blood vessels and evade anoikis), and establishment of a secondary tumor. In this process a substantially temporal and spatial reorganization of the cell cytoskeleton is required for cell movement and alterations in cell shape (34).

## INTRODUCTION

---

In order to initiate and maintain cell motility, modification of cell shape and stiffness is necessary to facilitate the interaction with the surrounding tissue. In this process formation of cell protrusions or cell extensions occurs to support cell migration (**Figure 5**). These special structures all contain filamentous actin and trigger extracellular matrix (ECM) recognition and binding. Based on morphology and dynamics, they are classified as lamellipodia, filopodia (or podosome for early filopodia), pseudopodia (or ruffles for early pseudopodia), and invadopodia (35, **Figure 4** and **Figure 5**).

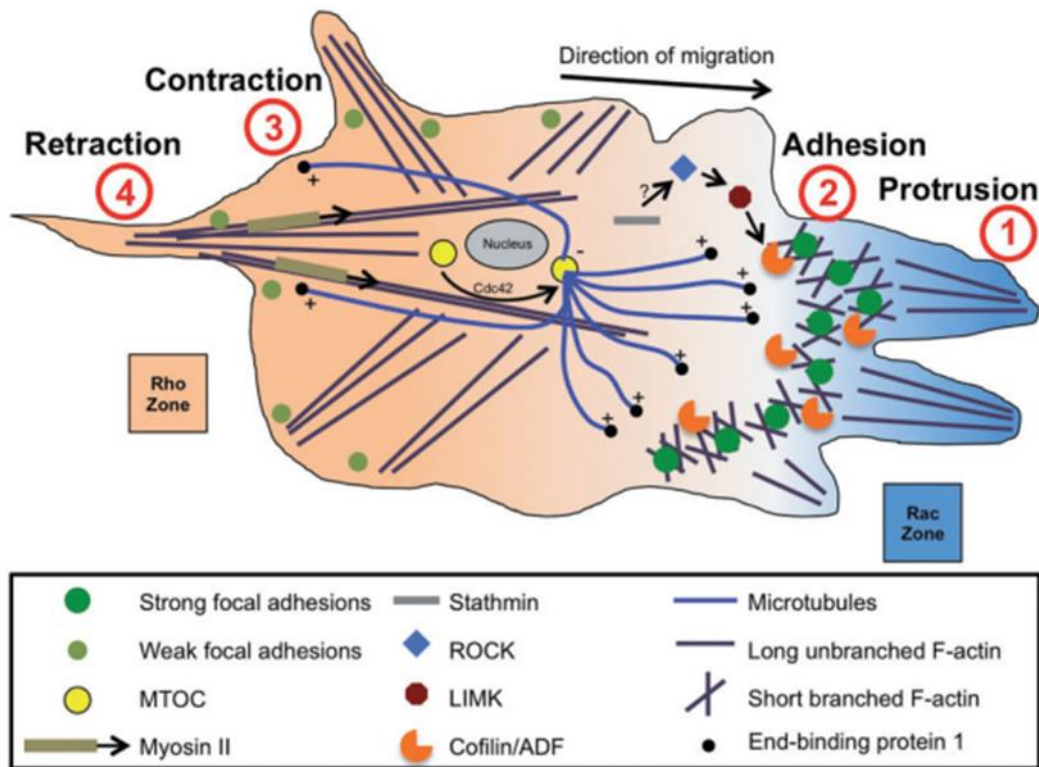
Focalized adhesion dynamics and actomyosin polymerization and contraction are the key for cellular migration. Growth of cell protrusions is the first step which initiates binding to the adjacent ECM via adhesion molecules. Small focal complexes are then formed via coupling of integrins to actin cytoskeleton. These focal complexes can grow further and stabilize to become focal adhesions (FAs). In the meantime, elongation and assembly of actin filaments occur with the aids of cross-linking proteins. It is then the turn of actomyosin contraction to shorten the cell's length axis while generating inward tension towards FAs. Interactions of cell-ECM in the back are resolved and FAs are disassembled, allowing the cell to slowly glide forward (35).

Cell invasion is defined as the penetration of tissue barriers and requires the cooperation of cell migration, proteolysis to degrade ECM and cell adhesion. Several proteases are recruited towards attachment sites to degrade ECM components, most notably the family of metalloproteinases (35).

Cell migration and invasion are not only utilized by cancer cells but also play pivotal roles in many other biological processes, including embryonic morphogenesis, immune surveillance, and tissue repair and regeneration (36).

# INTRODUCTION

A



B

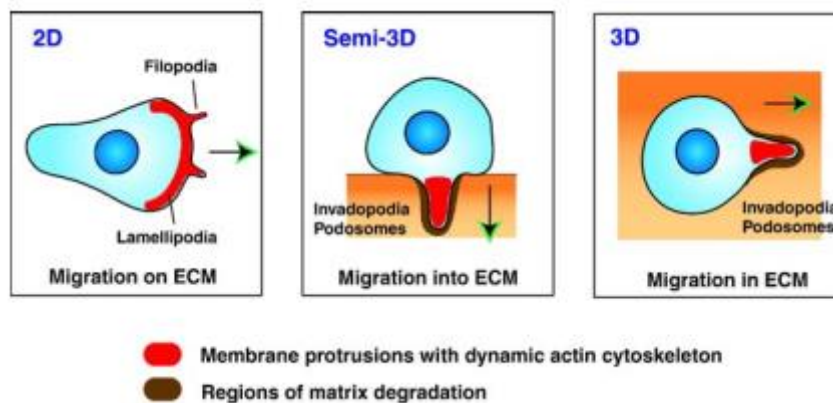


**Figure 5. Cell migration and different membrane protrusions/extensions are required in different environment. A.** Cell migration requires coordination of several steps (adapted from (34)), starting from cell protrusion and adhesion (which require the activity of Rac (Rac zone)), to cell contraction and in the end cell retraction (with the involvement of Rho (Rho zone)). Short, branched F-actin filaments are localized at the leading edge whereas long, unbranched F-actin stress fibers are mostly found at the rear. Microtubules with one ends initiating from the microtubule-organizing centre (MTOC) near the nucleus. LIMK, Myosin II, Cofilin/ADF, ROCK, Stathmin are shown as cytoskeletal regulatory and associated proteins. **B.** Different actin structures are required for cell migration, depending on ECM (adapted from (36)). Filopodia and lamellipodia are cell protrusions formed when cells migrating on 2D substrates whereas invadopodia and podosomes are needed for cell migration into ECM in 3D.

## 1.2.3. Cell shape and cytoskeleton

Cell shape is connected with many important cell functions such as apoptosis and proliferative capacity. There are many factors which contribute to shaping morphology of cells but the most important determinant is a complex and dynamic interaction among its

## INTRODUCTION

---

cytoskeleton, the plasma membrane, and the ECM. In different species and organs, the factors can include the protrusive force of actin polymerization and tension in the plasma membrane, lipid constituents of the plasma membrane, membrane-binding proteins that induce curvature, the presence and strength of adhesive structures at the cell periphery (37).

Cell shape is determined by a balance of internal and external forces as well as the mechanical characteristics of the cell. The force generation is provided by the cytoskeleton and therefore it is the key determinant of cell morphology. Changes in cell morphology occur permanently throughout cell development until their final differentiated state is reached and therefore, cell shape has a strong connection with cell fate. The activation of signaling pathways that govern relevant cytoskeleton dynamics is usually a result of cell fate decision (namely proliferation, apoptosis or differentiation) and thus, cell fate determinants are often found upstream of the cell morphology apparatus. Cell shape, however, in many cases can affect the intrinsic state of the cell and therefore, also exert influence on how cells react to external signals to make a cell fate decision (38).

In motile cells, actin polymerization occurs proximal to the plasma membrane and thus is the key to shape it. Actin filaments are polar structures with two distinct ends, differentiated by their shapes when decorated with myosin heads, a barbed end and a pointed end. Addition of actin monomers occurs mainly at the barbed ends whereas pointed ends are where actin disassembly taking place. Many regulatory factors of the actin polymerization machinery are either membrane-anchored small G proteins of the Rho family or phospholipids and help orientate newly polymerized actin to the direction of cell migration with their barbed ends directed towards the plasma membrane (39).

### **1.2.4. Cell shape and cancer**

In response to different stimuli, cells can change their shape. Cell shape has been considered as one of the most important determinant of cell function, including metabolism, differentiation, cell growth and apoptosis (40). Cell shape transition has proven to exert significant impact on both gene expression and enzymatic reactions (41). Assessment of cellular morphology from tumor tissue samples is, therefore, one of the important criteria in tumor grading which helps to predict the clinical outcome of cancer (42).

Changes in cell morphology are often the result of alterations in cytoskeletal properties and expression of adhesion proteins. Analysis of morphometric characteristics can detect changes in expressional pattern of genes with cytoskeletal functions which drive morphological alterations and predict metastatic capacity (42). On the other hand, detectable shape changes can result from acquisition of invasive properties due to genomic changes and therefore, provides information about the cell state (42).

In addition, induction of epithelial-mesenchymal transition (EMT) by matrix metalloproteinases in epithelial cells also requires changes in cell shape. EMT is a reversible cellular process in which epithelial cells lose their cell-cell adhesion and cell polarity, acquiring mesenchymal phenotypes and behaviours which then become more motile and

## INTRODUCTION

---

migratory. In this context, spread morphology could imply the occurrence of EMT in epithelial cells. (40).

### 1.2.5. Focal adhesion

Focal Adhesions are macromolecular multiprotein assemblies which connect actin stress fibers to the ECM and thus translate the force on stress fibers into cell movement. The ATP-driven movement of the myosin filaments along the polarized actin filaments produces force which then leads to stress fiber contraction and a pulling force on the FA complex. The stress fibers associated with FAs are classified into 3 types: Ventral stress fibers transverse through the whole cell and are connected with FAs at either end; dorsal stress fibers stretch upwards to the nucleus and the dorsal cell surface and are associated with FAs on one end near the cell front; recently discovered cortical stress fibers are linked to FAs at both end but are thinner and less contractile than ventral stress fibers (43 and **Figure 6A**).

The combination of myosin-II contractility and the stiffness of the ECM determine the force experienced by FAs. In response to the level of force, FAs change in number, size and composition. They are flat and elongated structures and typically range from 1–5  $\mu\text{m}$  in length, 300–500 nm in width and, have an average diameter of 50 nm (43).

The formation of new FA complexes starts with the binding of integrin transmembrane receptors to the ECM which then leads to clustering and subsequent activation of the integrins inducing conformational changes. This step is followed by a recruitment of more than 30 adaptor proteins which in turn acts as a feedback loop to promote further integrin activation and clustering of more integrins as well as provides a platform for the engagement of the hundreds of other FA proteins. This eventually leads to the recruitment of an actin stress fiber (43). FA complexes are highly dynamic with continuous events of assembly and disassembly. The lifetime of FA depends on several factors and lasts on average an hour (43).

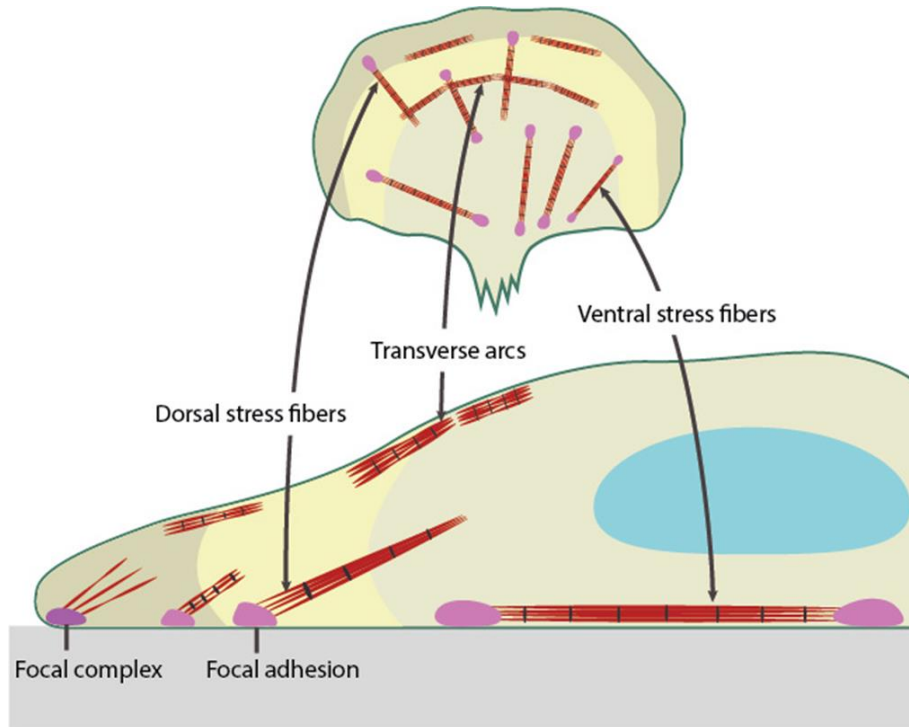
FA complexes are built in a layered manner with dozens to hundreds of proteins present in each layer (**Figure 6B**). This starts with the bottom layer where paxillin is of central importance for FA formation, continues with middle layer where talin is one of the very first proteins to bind to clustering integrins and vinculin forms a bridge between the layers, adds to the top with the actin-interacting proteins such as zyxin and VASP (43). Due to its particularly large number of potential binding partners, paxillin has been considered to be the main adaptor protein connecting all functional modules of FAs (43).

There is a strong correlation between size and shape of FA. Using a wide range of substrate stiffness, it was revealed that large FAs had a tendency of elongation while rounded shapes were associated with small FAs. There were moderate correlations between cell speed and FA size. In fast moving cells, FAs were larger and more elongated (44).

Due to their importance in cell adhesion and force transmission, FAs play key role in cell migration and thus of focus in cancer research. In aggressive forms of cancer, integrins and other FA components are often upregulated and are actively involved in EMT (43).



A



B

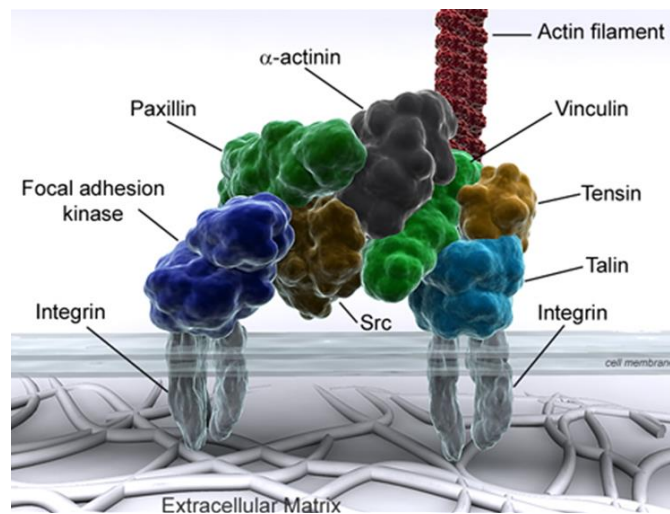


**Figure 6. View on FA architecture and components.** A. FA distribution in connection with stress fibers. Figure was adapted from (45). B. A layer view of main constituents of FA. Figure was adapted from (46).

### 1.2.6. The liver and hepatocellular carcinoma (HCC)

The liver is a central hub for many important physiological processes, including macronutrient metabolism, regulation of blood volume, immune system support, endocrine control of growth signaling pathways, homeostasis of lipid and cholesterol, and the breakdown of xenobiotic compounds (47).

There are more than 20 cell types residing in the liver and spatiotemporally cooperating to shape and maintain hepatic function at multiple levels. The majority of the liver volume is made of hepatocytes which account for many functions of the liver. This is followed by cholangiocytes lining the lumen of the bile ducts. Stellate cells in their quiescent state store

## INTRODUCTION

vitamin A in the lipid droplets, however when activated upon liver damage they proliferate and progressively lose vitamin A stores. They are responsible for deposition and organization of collagen in the injured liver, contributing to scarring of the liver – an important step leading to liver cirrhosis and end stage liver disease. Other important liver residents are Kuffer cells which function as macrophage to recognize pathogenic stimuli introduced through the portal circulation. Liver sinusoidal endothelial cells form fenestrated sieve plates at the sinusoidal lumen which is critical for exchange of proteins and particles between plasma and the cell types of the liver, while maintaining certain barrier functions (47 and **Figure 7**).

The lobule is the functional structural unit of the liver. Around the central vein, hepatocytes are organized in a typically hexagonal shape. A partitioning of functions based on localization divides the lobule into three distinct ‘zones’ in which hepatocytes differ in metabolic gene expression and functionality. This leads to the difference in characteristics of the blood composition entering and exiting the lobule. Hepatic artery, portal vein, and bile ducts form the portal triads residing at the vertices of the lobule (47 and **Figure 7**).

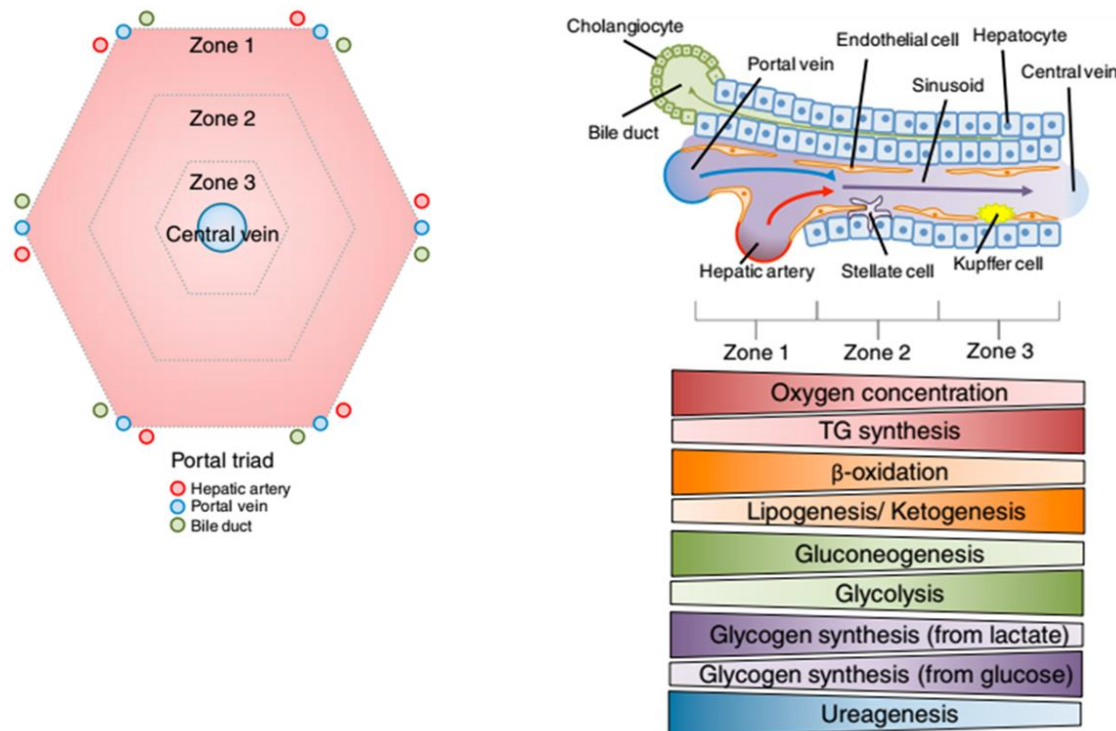


**Figure 7. Organization of the liver. Adapted from (47)**

Being the sixth most common cancer and the fourth leading cause of cancer-related death worldwide, liver cancer still pose an extreme risk to global health (48). HCC is the most prevalent malignancy of the liver, accounts for approximately 90% of the cases and is the third most leading cause of cancer death worldwide. Hepatitis B (HBV) and Hepatitis C viruses are the major etiologies for HCC development of which HBV accounts for 50-80% of the virus-associated HCC cases. With the advancement of high efficacy direct-acting-antivirals the risk attributed to HCV infection has substantially reduced but is still the predominant causative factor in Western Europe, North America and Japan. Even after HCV clearance patients who already developed cirrhosis are still at high risk for HCC. While alcohol intake is still the main etiological factor in Central and Eastern Europe, non-alcoholic

## INTRODUCTION

---

steatohepatitis (NASH) is growing rapidly and is expected to become the main cause for HCC in the future, especially in high-income countries (49).

The treatment for HCC is assigned according to tumor stages classified by the Barcelona Clinic Liver Cancer staging system. Resection, transplantation and local ablation are methods of choice for early-stage patients, whereas transarterial chemoembolization (TACE) is preferably applied for patients at intermediate stages. Systemic therapies are the first choice for those with advanced disease. Six drugs have been approved for systemic therapies in HCC, including atezolizumab plus bevacizumab, sorafenib, lenvatinib, regorafenib, cabozantinib and ramucirumab (49).

### 1.3. HCV

#### 1.3.1. General aspects

Hepatitis C was firstly described in 1975 as non-A, non-B hepatitis (50,51). Initially perceived as a minor disease because of the lack of significant morbidity during the acute phase of infection, it gradually became apparent that this form of hepatitis frequently persisted as a chronic condition that could slowly lead to chronic hepatitis and liver cirrhosis, which in turn potentially progresses to end-stage liver disease and HCC (52). In 1989, a single cDNA clone derived from the hepatitis-associated virus was successfully identified, which paved the way for further development on diagnostic tests (51,53). This discovery together with further success in achieving cell culture, replicon, infectious virus models and the advancement in modern technologies have shaped much better understanding on virology as well as led to the development of several classes of antiviral drugs with excellent efficacies.

According to estimates from 2017, 71 million people are chronically infected with HCV worldwide (54). However, despite the availability of efficient therapies, HCV-infected patients who already developed cirrhosis or chronic liver damage with bridging fibrosis are still at high risk of developing HCC even after successful cure from the virus infection (48).

Approximately 80% HCV-infected individuals become chronic carriers which are at risk of developing severe liver diseases. It is estimated that liver cirrhosis occurs in 10-20% of the patients and 1-5% eventually develop HCC within 20-30 years (55). It is believed that signaling and metabolic pathways modulated by HCV as well as chronic inflammation induced by host antiviral immune responses account for liver fibrogenesis in HCV-infected patients (55).

HCV isolates are classified into 8 genotypes based on the phylogenetic and sequence analyses of viral genomes and further dissected into 67 subtypes (56). This extraordinary variability is likely due to high error rates of RNA polymerases and a massive number of infectious particles (approximately  $10^{12}$ ) produced per day in an infected patient. This diversity of HCV genomes is also associated with clinical outcome and poses a challenge for development of antiviral therapies covering all isolates.

### 1.3.2. HCV genome, proteins and its life cycle

HCV is an enveloped virus, containing a positive sense, single stranded RNA genome. The virus belongs to the Hepacivirus genus of the Flaviviridae family. The approximately 9.6 kb HCV genome contains a single open reading frame encoding a polyprotein which is processed into 10 mature proteins by cellular and viral proteases: structural proteins core, E1, E2 and nonstructural proteins p7, NS2, NS3, NS4A, NS4B, NS5A and NS5B (57 and **Figure 8A**).

HCV particles contain the single stranded RNA genome, core protein and the two envelope proteins E1 and E2 (**Figure 8B**). They are 50-80 nm in size and strongly associated with cellular lipoproteins. Core protein is one of the major components of HCV particle and interacts with genomic RNA to build the viral nucleocapsid. Interaction of core with lipid droplets is required for the recruitment of other viral components participating in the process of viral assembly. The envelope glycoprotein complex made of non-covalent heterodimers of E1 and E2 is another important component of the viral particle. They are the major determinants of the viral entry, being involved in receptor binding and fusion process with host endosomal membrane and also play important role in viral particle formation (reviewed in 57).

The small hydrophobic viroporin p7 with cation ion channel activity and NS2 with cysteine protease activity are not parts of the viral particle but coordinate in regulation of core trafficking and E1-E2 migration to the virion assembly site. p7 is furthermore important for capsid assembly and development as well as for the egress of HCV particles by helping in neutralizing acidic compartments within the secretory pathways. The NS2-3 protease activity cleaves the polyprotein at the NS2/3 junction (reviewed in 57).

HCV significantly rearranges intracellular membranes to create so-called “membranous webs” (MWs) which are the sites for viral RNA replication. In this regard, the non-structural proteins NS3/4A, NS4B, NS5A and NS5B (NS3-5B) together induce these membrane alterations and form the replication machinery to synthesize positive sense RNA genomes through a negative strand intermediate. NS3 itself has protease and helicase activity. During the processing of the HCV polyprotein, NS3 firstly cleaves NS4A from itself and NS4B and subsequently associates with NS4A as a complex to further perform the cleavages at the NS4B/5A and NS5A/5B junctions (57). NS4B is an integral membrane protein and plays a major role in the rearrangement of host cell membranes for replication complex formation (57,58). NS5A is a multifunctional phosphoprotein which contributes significantly to the formation of replication organelles and the recruitment of the replicase around LDs which facilitates viral assembly (59). NS5B is an RNA-dependent RNA polymerase and is the key enzyme of RNA synthesis.

HCV particles circulate as a complex of virion and lipoproteins, called lipoviroparticle (**Figure 8B**). The HCV life cycle is divided into several steps (**Figure 8B**), beginning with the binding of envelope proteins E1 and E2 to glycosaminoglycans or LDL receptors on cell surface. Several other cellular entry factors are further involved in the process of viral entry, including scavenger receptor SRB1, tetraspanin CD81 and tight-junction proteins CLDN1 and OCLN.

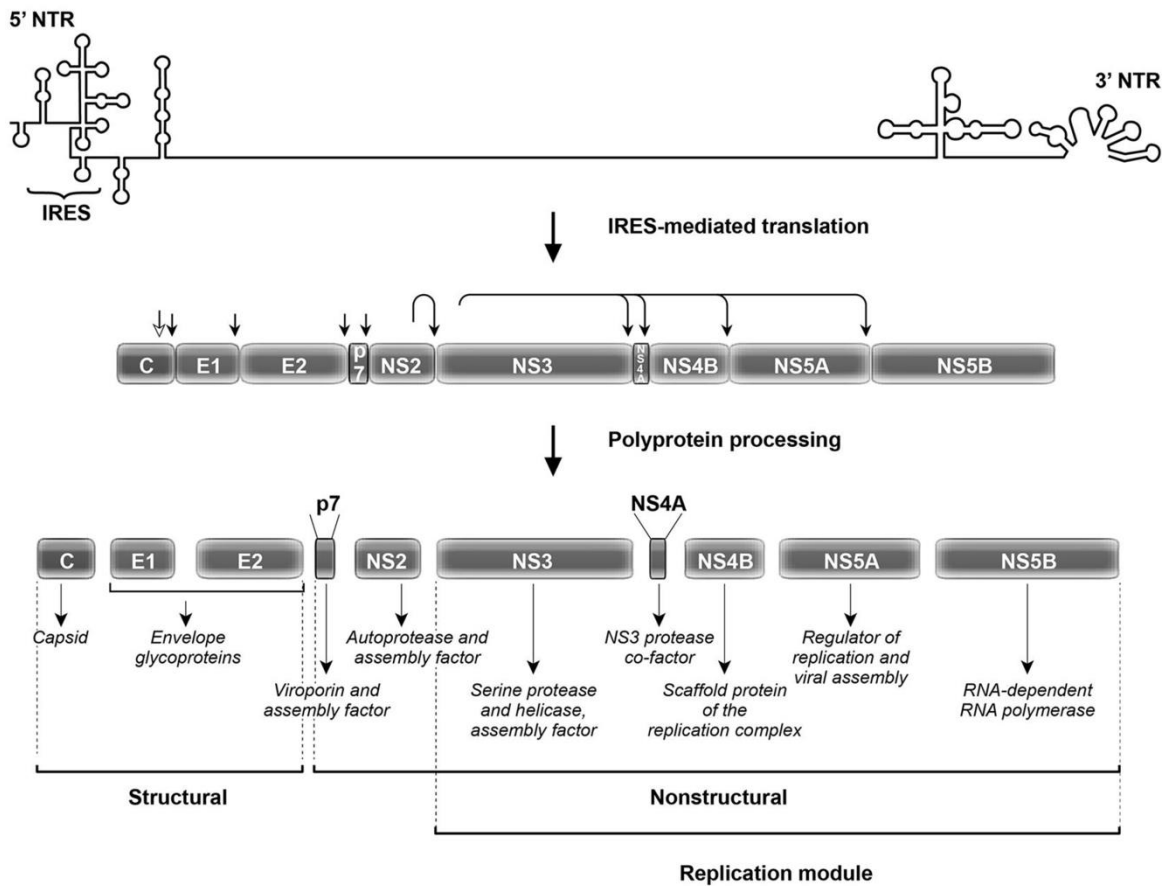
## INTRODUCTION

---

Internalization of HCV particles via clathrin-mediated endocytosis is followed by membrane fusion which takes place in endosomes, allowing the viral genome to be released in the cytoplasm. Translation is mediated by the HCV internal ribosome entry site (IRES), resulting in translation of the polyprotein. The viral polyprotein is then co- and post-translationally processed by host and viral proteases into the mature proteins. Non-structural proteins NS3 to NS5B then induce massive rearrangement of cellular membrane to generate the MW, consisting of heterogeneous double membrane vesicles and multi-membrane vesicles and serving as a platform for viral replication. Synthesis of a negative-strand RNA occurs and provides a template for generation of positive-strand RNA genomes which is subsequently used for polyprotein translation or packaging into new virions. Viral particle assembly is thought to take place on lipid droplets in close proximity to the MW. Several viral proteins have been suggested to be involved in the transfer of core, E1-E2 and RNA genome to the assembly site. New virions are then released via the exocytic pathway in cooperation with the ESCRT-machinery or spread via cell-to-cell contact (57,58,59).

# INTRODUCTION

**A**



**B**

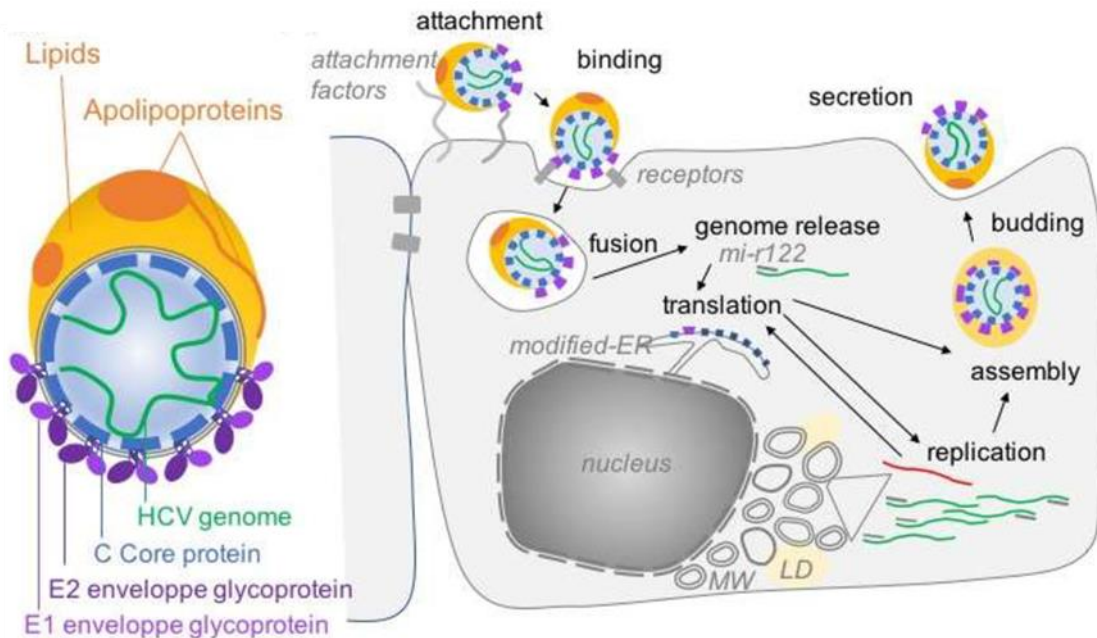


**Figure 8. HCV proteins and its life cycle. A.** Translation and processing of HCV polyprotein. **B.** HCV lipoviral particle (left) and its life cycle. Figures were adapted from (57)

### 1.3.3. Cell culture and animal models for studying HCV

Since the discovery of HCV, developing a cell culture system for HCV replication was a central focus of many research groups. However, it took 24 years from the first description of nonAnonB hepatitis and 10 years from the discovery of HCV as the etiological agent until the first subgenomic replicon became available in 1999 (60,61,62 and **Figure 9A**). This important hallmark of HCV research has facilitated better understanding on HCV RNA replication step and provided an important tool for studying antiviral drugs. This was followed by the establishment of retrovirus-based pseudoparticle systems a few years later, allowing scientists to study HCV entry (62, **Figure 9A**). In 2005, a fully permissive cell culture model of HCV was established, paving the road for further research studies on all steps of the virus life cycle as well towards a better understanding of virus-host interactions and viral pathogenesis (62, **Figure 9A**). The first system was based on a single genotype (gt) 2a isolate originated from a Japanese patient with fulminant hepatitis (JFH1). This virus isolate replicates in cell culture efficiently without the need for adaptive mutations and is able to release viral particles in supernatant, so-called infectious cell-culture HCV (HCVcc) (62). Since then, other full-length cell culture infectious virus constructs and chimeric genomes of other genotypes based on the gt 2a replication machinery were developed (63,64,65,66,67,68,69,70). A gt 2a/2a chimera with J6CF and JFH1 derived sequences fused via a site located right after the first transmembrane domain of NS2 is the most efficient construct with 100-1000 fold higher infectious titer (63). This chimera, designated as Jc1, is the most widely used virus strain for studying HCV infection in cell culture. Other HCV genotype recombinants were developed based on JFH1 with the structural genes (Core, E1, E2), p7, and NS2 derived from gt 1a (H77S, TN), 3a (S52, DBN3a), 4a (ED43), 5a (SA13, ), 6a (HK6a), etc. allowing virus production and facilitating genotype-specific studies of HCV *in vitro* (64,65,66,67,68,69,70). The discovery of Huh7-derived hepatoma cell lines which highly support HCV replication was also a major landmark in HCV research. Huh7.5 and Huh7-Lunet are still the central models for HCV research. These human hepatoma cell lines are also models for studying HCC. Hep3B, PLC/PRF/5 and HepG2-CD81 (HepG2 exogenously expressing HCV entry receptor CD81) allows HCV entry (and RNA replication) to some extent. However HCV particle production was completely abrogated in these cells, limiting their use in studying HCV infection (71). PH5CH (generated by immortalizing primary hepatocytes with the T antigen of simian virus 40) supported HCV replication at low level but virus production was also restricted (review in 72,73). Due to the lack of many features of hepatocytes in Huh7-derived cells, especially the impaired innate immunity response, other cell including Hep3B, HepG2, HepaRG (a naturally immortalized hepatic cell line, retaining many characteristics of primary human hepatocytes), PH5CH, HHT4 (a telomerase-immortalized human hepatocyte-derived cell line) and especially primary human hepatocytes have been used for validation (57). It is noteworthy that PI4KA expression was found higher in Huh7-derived cell lines (Huh7-Lunet, Huh7.5, etc.) than in HepaRG and PHH (or normal liver tissue), respectively (74,75). Expression of PI4KA was correlated with undifferentiation status and proliferative rate of the liver cell lines as well as of HCC (74).

## INTRODUCTION

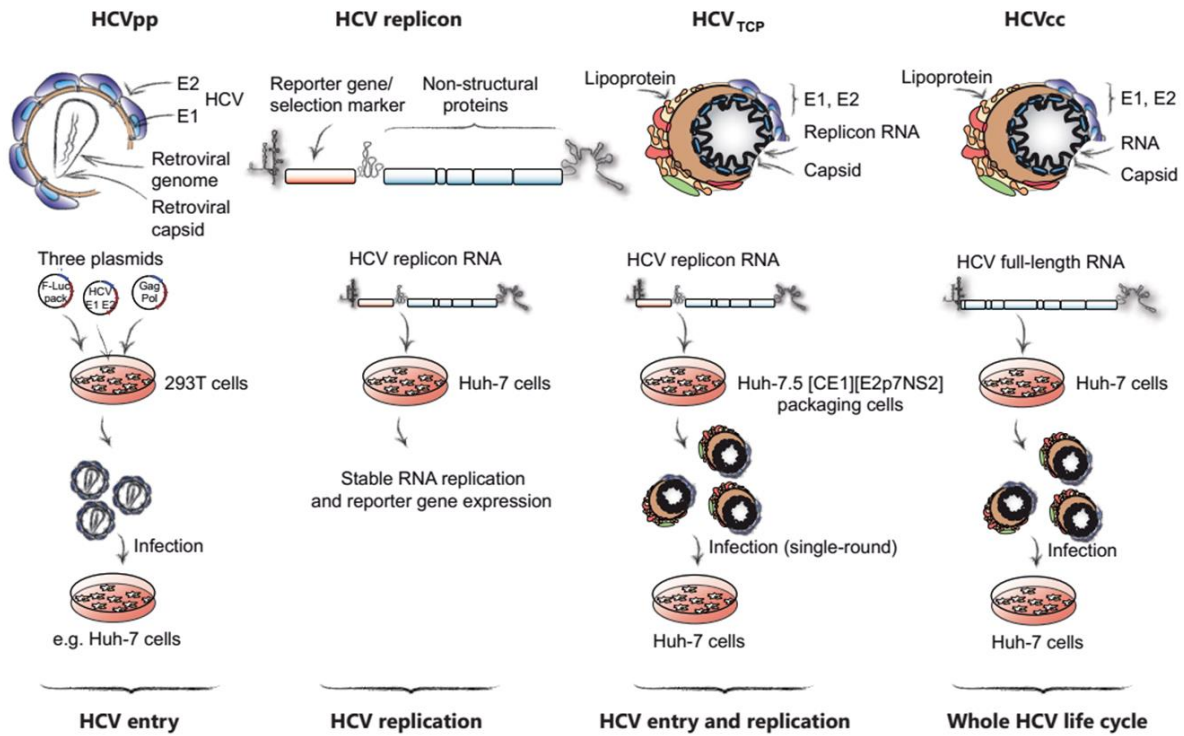
---

For *in vivo* studies, the chimpanzee was the only animal susceptible to HCV infection besides humans. The use of chimpanzees in HCV research had significantly contributed to the discovery of this virus as well as to the uncovering of host–virus interactions, particularly in the aspects of cellular immunity and preclinical analysis of antiviral strategies. However due to ethical constraints, limited availability and the high costs associated with this model, there has been a special need for alternative animal models, ideally and especially supporting a persistent infection in order to study pathological aspect of this virus such as steatosis, fibrosis, cirrhosis and HCC. The development of such animal models has been challenging due to the narrow host range of HCV (76). Four approaches however have been proposed and proven to be helpful to some extent (**Figure 9B**). First, HCV homolog GBV-B and a number of recently identified HCV-related hepaciviruses and pegiviruses could be used as HCV surrogate model to infect other animal species. Second, taking advantage of error-prone replication of HCV, several attempts have been made in adapting the virus to mice by cultivation of HCV in mouse cells or cells expressing murine entry proteins. Third, by supplementing mice with human proviral factors or depleting murine interference factors, HCV infection in transgenic mice even with intact innate immune system was possible to some extent. Last but not least, immunodeficient chimeric mice having liver xenografted with human hepatocytes is an advanced model which supports robust and reproducible infection of both natural virus isolates and cell-culture produced HCV (reviewed in 76).



# INTRODUCTION

**A**



**B**

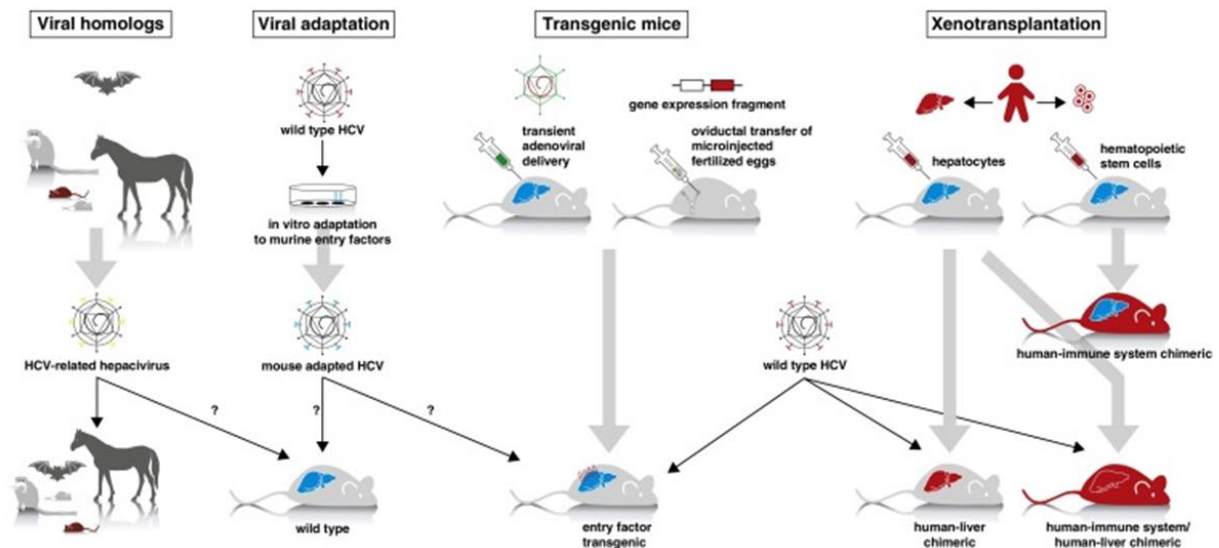


**Figure 9. Important cell culture systems and animal models for HCV research.** **A.** Different cell culture systems for studying key steps in HCV life cycles, including HCV pseudo particles (HCVpp) to study HCV entry step, HCV replicon for studying viral RNA replication, HCV transcomplemented particles (HCV<sub>TCP</sub>) cover entry and replication steps, Cell culture-derived HCV for studying the whole viral life cycle (adapted from (62)). **B.** Four approaches for studying HCV *in vivo*, including the usage of HCV homologs, adaptation of virus or host for permissive infection, or xenotransplantation. Figure was adapted from (76).

## 1.3.4. HCV and PI4KA

PI4KA is an essential host factor for HCV replication. Several research groups independently had published its important functions in relationship with the virus at approximately the same time via different screening techniques for viral host factors (77,78,79,80,81,82,84,85). Yet it

## INTRODUCTION

---

is highly agreed that this lipid kinase is foremost important for the replication step of viral RNAs. Silencing of PI4KA reduced substantially viral replication in both HCV replicon (subgenomic and full-length) and infection models (77,78,79,80,81,82,84,85). This effect seemed to be independent of cell line (81) and viral genotypes (79,81). Furthermore, upon the PI4KA depletion, the MW was strongly disturbed with abolished formation of multi membrane vesicles and reduced size of double membrane vesicles but very homogenous and aggregated into huge clusters (78,81,85). The association of PI4KA with the viral replication complex was further revealed by its colocalization with HCV replicase components NS5A and dsRNA (78,82). Importantly, PI4KA activity was enhanced via its interaction with viral protein NS5A, subsequently led to induced production and intracellular accumulation of PI4P (81,84).

HCV NS5A is made of 3 domains, separated by 2 low-complexity sequences (86). Domain 1 of NS5A is responsible for the binding with PI4KA and activation of this kinase (81). Further examination revealed that a highly conserved sequence at the C-terminus of D1, designated as PI4KA functional interaction site (PFIS) is critical for interaction with PI4KA. Mutations at this region (including the mutant PPH) interrupt the interaction with PI4KA, abrogating HCV replication, PI4KA activation and PI4P induction (87). Furthermore, a mutation at the position S2208 in the HCV gt2a isolate JFH1 (S2204 in the gt1b Con1) also impaired PI4KA activation and HCV replication (75,87). In addition to NS5A, NS5B was also found to interact with PI4KA (81). Expression of NS3-5B either via polyprotein overexpression or HCV subgenomic replicon is sufficient to activate PI4KA and to induce formation of MW which is important for HCV replication (81). Since any HCV mutations disrupting interactions with PI4KA also impairs HCV replication (75,87), overexpression of HCV NS3-5B is the model of choice in place of HCV replicon or infectious model when comparing effects of different mutants on PI4KA activity.

Although interactions between HCV and the phospholipid kinase PI4KA have been intensively studied and so much has been discovered about their roles in HCV replication, the effects of these interactions in HCV-induced liver pathogenesis remains to be elucidated. Recently, an elevated expression of PI4KA (2.1 times higher) was found in a subset of HCC tissue samples in comparison with normal reference samples (74). There was however no significant difference in mRNA expression of PI4KA in HCC patients with and without HCV. Furthermore *in vitro* and *in vivo* studies suggested that this increased expression of PI4KA was associated with hepatic dedifferentiation and active proliferation in both liver cancer cell lines and HCC tumors. More importantly, patients with PI4KA upregulation had shorter disease-specific survival as well as higher risk of tumor recurrence (74). PI4KA could therefore be a potential link between HCV and HCC.

### 1.3.5. HCV and cytoskeleton

It has been shown that many viruses manipulate the cytoskeleton network during their infection, including HCV. In this regards microtubule and actin filaments, which often have parallel or cooperative functions in orchestrating membrane trafficking, contributed significantly to the process of viral RNA replication (88,89). In both HCV-infected cells and

## INTRODUCTION

---

replicon cells, HCV replication complexes were aligned along microtubules and actin filaments tracks which likely served as a platform for the movement of HCV replication complexes to access other areas in the cell (89). Inhibition of microtubules and actin polymerization by several inhibitors such as vinblastine sulfate, colchicine, cytochalasin B and D reduced viral RNA replication or disrupted the movement of replication complexes (88,89). Furthermore, microtubule aggregates and microtubule paracrystals were observed in HCV-infected hepatocytes and in cells transfected with HCV replicon, respectively (88).

Besides the functional importance in the replication of HCV RNAs mediated via its interactions with viral proteins NS3 and NS5A (89), microtubules also play significant roles in the entry, postfusion, assembly and egress of HCV via HCV core and NS5A (91,190). Interaction of core with  $\alpha$ - and  $\beta$ -tubulin enhances tubulin polymerization (90). Furthermore transport of core-NS5A complexes (or the assembled virions) from ER to lipid droplets and from early-to-late endosomes to the plasma membrane for viral assembly and release requires microtubules (190).

### 1.4. Objectives of this study

Recent studies indicated possible contributions of PI4KA/PI4P to liver pathogenesis. On the one hand increased expression of the enzyme was correlated with the poor prognosis of liver cancer patients, implying the important contribution of this kinase to the cancer progression (74). On the other hand, HCV induces PI4KA activity, resulting in strongly elevated intracellular PI4P concentrations. Increased levels of this important lipid were therefore supposed to impact on HCV related liver disease, including increased metastasis rates observed in HCV associated HCC (92,93,94). It was however unclear how PI4KA contributes mechanistically to liver pathogenesis.

The aim of this thesis was to understand mechanisms contributing to the impact of increased PI4KA expression and activity to HCC progression. The association between PI4KA and HCC metastasis, as well as the central role of phosphoinositides in organization of the cytoskeleton suggested a possible impact of PI4KA on cytoskeletal re-arrangements contributing to cancer progression. I therefore aimed to unravel the signaling pathways governed by PI4KA resulting in changes in cytoskeletal organization. Changing abundance and activity of PI4KA in the HCC derived cell line Huh7 cells was chosen as a central model, due to increased PI4KA expression level compared to primary hepatocytes and the susceptibility for HCV infection.

For this purpose, I firstly aimed to evaluate the effects of PI4KA knockdown or inhibition on cell morphology and cell motility via different imaging techniques and assays of cell migration and invasion. Cytoskeleton proteins regulated by PI4KA expression and activity were further identified and evaluated by screening approaches and western blot analysis. In order to understand the mechanism how PI4KA regulated these phenotypes, I aimed to dissect further the pathways by targeting the phospholipid kinases connected to PI4P and evaluated the impacts of PI4KA silencing or inhibition on different PIs abundance. The effects of HCV on these pathways were evaluated using infection and protein expression models, comparing wild type (wt) and mutants incapable of PI4KA activation. Last but not least, I aimed to

## INTRODUCTION

---

validate the key phenotypes using more physiological relevant models. This included the use of primary human hepatocytes expressing different HCV mutants and several mouse models.

# MATERIALS AND METHODS

## 2. MATERIALS AND METHODS

### 2.1. Materials

#### 2.1.1. For cell culture work

**Table 1. Cell culture medium used in this study.**

Chemicals/ Reagents	Manufacturer/ Supplier	Application
DMEM	Life Technologies (41965-039)	Except for PHH and HHT4, all cell lines were cultured in DMEM supplementing with 10% FCS, 1% Pen/Strep and 1% NEAA. Glutamax was supplemented in the culture medium of Hep55.1C
FCS	Capricorn Scientific (FBS-11A)	
Penicillin/Streptomycin	Life Technologies (15140-114)	
Non-essential amino acids (NEAA)	Life Technologies (11140-035)	
Glutamax	Thermo Fisher scientific (35050061)	For Hep55.1C
William's Medium E	Gibco (22551-022)	For PHH
HCM Hepatocyte Culture Medium BulletKit	Lonza (CC-3198)	For HHT4
KnockOut Serumersatz	Lonza (10828010)	
Trypsin	Gibco (35400-027)	0.05 % Trypsin and 0.02 % in PBS 1X
EDTA	Merck (6361-92-6)	

**Table 2. Selection antibiotics used in this study for cell culture work.**

Chemicals/ Reagents	Manufacturer/ Supplier	Application
Blasticidin	Life Technologies (R21001)	50 µg/ml
Geneticin G418	Santa Cruz (sc-29065B)	500 µg/ml
Puromycin	Clontech (8052-1)	10 µg/ml
Zeocin	Invitrogen (R250-05)	5 µg/ml

**Table 3. Reagents used for cell electroporation**

Chemicals/ Reagents	Manufacturer/ Supplier	Application
Glutathione	Sigma Aldrich (G6013)	Cell electroporation
Hepes Buffer 1M	Life Technologies (15630056)	Cell electroporation

**Table 4. Reagenst used for cell transfection**

Chemicals/ Reagents	Manufacturer/ Supplier	Application
OptiMEM	Life Technologies (31985047)	Transfection
Polyethylenimine (PEI)	Polysciences (23966)	Transfection HEK293T
TransIT-LT1	Mirus (MIR 2304)	Transfection Huh7-Lunet

## MATERIALS AND METHODS

### 2.1.2. Antibodies and molecular probes for Western blot, Immunofluorescence and Immunohistochemistry

**Table 5. List of primary antibodies used in this study**

Antibody	Specificity	Supplier	Dilution
α-PI4KA	Rabbit IgG pAb	Cell Signaling (4902S)	WB 1:1000
α-GAPDH	Mouse IgG1 mAb	Santa Cruz (sc-47724)	WB 1:1000
α-mCherry	Rabbit IgG mAb	Cell Signaling (43590S)	WB 1:1000 IP 1:100
α-PXN	Mouse IgG1 mAb	Sigma-Aldrich (05-417)	WB 1:1000 IP 1:100
α-p-PXN Y31	Rabbit IgG pAb	Invitrogen (44-720G)	WB 1:1000 IF 1:100
α-CFL1	Rabbit IgG mAb	Cell Signaling (5175S)	WB 1:1000
α-p-CFL1 S3	Rabbit IgG mAb	Cell Signaling (3313S)	WB 1:1000
α-AKT2	Rabbit IgG mAb	Cell Signaling (3063S)	WB 1:1000 IF 1:100
α-p-AKT2 S474	Rabbit IgG mAb	Cell Signaling (8599S)	WB 1:1000
α-AKT1	Rabbit IgG mAb	Cell Signaling (2938T)	WB 1:1000
α-p-AKT1 S473	Rabbit IgG mAb	Cell Signaling (4060S)	WB 1:1000
α-E-cadherin	Rabbit IgG mAb	Cell Signaling (3195S)	WB 1:1000
α-Tubulin	Mouse IgG2β,κ mAb	GenScript (A01410)	WB 1:5000
α-NS5A	Mouse IgG2α mAb	9E10, gift from C.M. Rice, Rockefeller University, N.Y	WB 1:10000 IF 1:500
α-PI4P	Mouse IgM mAb	Echelon (Z-P004)	IF 1:100
α-PI(3,4)P2	Mouse IgG mAb	Echelon (Z-P034)	IF 1:100
α-PI(4,5)P2	Mouse IgM mAb	Echelon (Z-P045)	IF 1:100
α-PI(3,4,5)P3	Mouse IgM mAb	Echelon (Z-P345)	IF 1:100
α-Src	Rabbit IgG mAb	Cell Signaling (2109T)	WB 1:1000
α-p-Src Y419	Rabbit IgG pAb	R&D systems (AF2685-SP)	WB 1:1000
α-FAK	Rabbit IgG pAb	Cell Signaling (3285T)	WB 1:1000
α-p-FAK	Rabbit IgG pAb	Cell Signaling (3283S)	WB 1:1000
α-HA	Rabbit IgG mAb	Cell Signaling (3724S)	WB 1:1000

**Table 6. List of secondary antibodies used in this study**

Antibody	Type	Specificity	Supplier	Dilution
Mouse HRP	Goat-α-mouse	Mouse polyclonal	Sigma-Aldrich (A4416)	WB 1:5000
Rabbit HRP	Goat-α-rabbit	Rabbit polyclonal	Sigma-Aldrich (A6154)	WB 1:5000
Alexa Fluor 488	Goat-α-mouse	Mouse IgM	Invitrogen (A21042)	IF 1:500
Alexa Fluor 488	Donkey-α-mouse	Mouse IgG	Invitrogen (A21202)	IF 1:500
Alexa Fluor 488	Goat-α-rabbit	Rabbit IgG	Invitrogen (A-11008)	IF 1:500
Alexa Fluor 568	Goat α-mouse	Mouse IgG2α	Invitrogen (A-21134)	IF 1:500

## MATERIALS AND METHODS

**Table 7. List of molecular probes used in this study**

Molecular probes	Specificity	Source	Application
DAPI ((4',6-diamidino-2-Phenylindole dihydrochloride))	DNA	Invitrogen (D21490)	1:4000, 1 min, post 2 <sup>nd</sup> antibodies incubation
Rhodamine Phalloidin	F-Actin	Invitrogen (R415)	1:1000 (Stock 200 U/ml), 45 min with 2 <sup>nd</sup> antibodies
SiR-Actin	Actin	Spirochrome	25 nM in both labeling (6h) and imaging medium in combination with verapamil 10 $\mu$ M in imaging medium
SiR-Tubulin	Tubulin	Spirochrome	500 nM in labeling medium for 6h, followed by 100 nM in imaging medium. Verapamil 100 $\mu$ M in both labeling and imaging medium

### 2.1.3. Chemicals, reagents used in Western blot, immunofluorescence microscopy

**Table 8. Chemicals and reagents for Western blot and immunofluorescence microscopy**

Chemicals/ Reagents	Supplier	Application
$\beta$ -Mercaptoethanol	Aldrich	Western blot
Acrylamide/Bis Solution (29:1)	Carl ROTH	Western blot
Complete Protease Inhibitor Cocktail	Roche	Western blot
ECL Plus Western Blot Detection System	Amersham/Perkin-Elmer	Western blot
Prestained protein marker	New England Biolabs	Western blot
PVDF Western blot membrane	Merck Milipore	Western blot
TEMED	AppliChem	Western blot
Tween20	Thermo Scientific	Western blot
Bovine Serum Albumin (BSA)	Sigma (A3294-50G)	IF, Western blot
Paraformaldehyde	Electron Microscopy Sciences	IF: fixation
Paraformaldehyde		IF: fixation
Glutaraldehyde	Merck (1042390250)	IF: fixation
Saponin	Sigma (S7900)	IF: permeablization
Digitonin	Sigma	IF: permeablization
Triton X-100	Merck	IF: permeablization
Fluoromount G	SouthernBiotech	IF: mounting



## MATERIALS AND METHODS

### 2.1.4. Buffers and Solutions used in this study

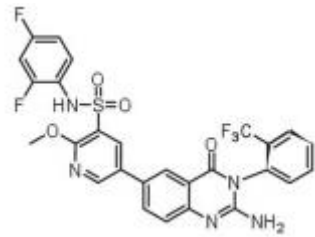
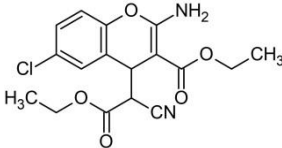
**Table 9. Buffers and solutions used in this study**

Buffers/ Solutions	Components	Application	
PBS 1X	140 mM NaCl, 8 mM Na <sub>2</sub> HPO <sub>4</sub> ·2H <sub>2</sub> O, 2 mM NaH <sub>2</sub> PO <sub>4</sub> ·2H <sub>2</sub> O	Cell culture	
Cytomix	120 mM KCl, 0.15 mM CaCl <sub>2</sub> , 10 mM potassium phosphate buffer (pH 7.6), 25 mM Hepes, 2 mM EGTA, 5 mM MgCl <sub>2</sub> , pH 7.6. 2 mM ATP and 5 mM glutathione freshly added before use	Cell electroporation	
Luciferase lysis buffer	1 % Triton X-100, 25 mM glycyl glycine, 15 mM MgSO <sub>4</sub> , 4 mM EGTA, 10% Glycerol, storage at 4 °C. 1 mM DTT freshly added before use	Luciferase assay	
Luciferase assay buffer	25 mM glycyl glycine, 15 mM K <sub>3</sub> PO <sub>4</sub> (pH 7.8), 15 mM MgSO <sub>4</sub> , 4 mM EGTA. 1 mM DTT and 2mM ATP freshly added before use		
Luciferase (Firefly) substrate solution	0.1 mM luciferin in 25 mM glycyl glycine solution		
RIPA buffer (1X in PBS)	50 mM Tris-HCl (pH 7.4), 1% NP-40, 0.25% sodium deoxycholate, 150 mM NaCl, , 1 mM EDTA. 1 Complete Protease Inhibitor Cocktail tablet per 50 ml	Western blot	
Laemmli buffer 6X	375 mM Tris HCl (pH 6.8), 9% SDS, 50% glycerol, 0.03 % bromophenol blue, 9% β-mercaptoethanol		
SDS-PAGE resolving gel buffer	1.5 M Tris-HCl pH 8.8, 0.4 % (w/v) SDS		
SDS-PAGE stacking gel buffer	1 M Tris-HCl pH 6.8, 0.8 % (w/v) SDS		
TGS 10X buffer	250 mM Tris, 1.92 M glycine, 1 % (w/v) SDS		
Western blot wet transfer buffer (10X)	25 mM Tris Base, 150 mM Glycine pH 8.3. Add 20 % (v/v) methanol to 1X solution before use.		
TBS 10X buffer	0.2 M Tris base, 1.5 M NaCl		
Western blot washing buffer 1X TBS Tween	1X TBS, 0.25 % Tween 20		
Western blot blocking buffer	1X TBS Tween, 5 % milk powder or 5% BSA		
Ponceau S solution	1.3 mM Ponceau S, 0.874 M acetic acid (glacial)		
TAE (50x)	242 g Tris, 100 ml 0.5 M Na <sub>2</sub> EDTA (pH 8.0) and 57.1 ml glacial acetic acid, adjusted to 1 l with H <sub>2</sub> O		Gel electroporesis
Transcription buffer RRL (5x):	400 mM Hepes (pH 7.5), 60 mM MgCl <sub>2</sub> , 10 mM spermidine, 200 mM DTT		<i>In vitro</i> transcription
Paraformaldehyde (4%)	40 g paraformaldehyde dissolved stirring at 60 °C in 1 l PBS, adjust to pH 9 with NaOH		IF

## MATERIALS AND METHODS

### 2.1.5. Inhibitors and activators

**Table 10. Inhibitors and activators used in this study**

Reagents	Formulation	Sources	Application
PI4KA Inhibitor F1		gift from J. Botyanszki (Preparation of quinazolinone derivatives as antiviral agents. PCT International Patent Application WO 201287938 A1,..)	Inhibit PI4KA activity
AKT Activator SC79		Abcam (ab146428)	binds to the pleckstrin homology domain of Akt, Enhances Akt phosphorylation by upstream protein kinases

### 2.1.6. Chemicals, enzymes, kits and miscellaneous materials

**Table 11. List of chemicals, reagents and miscellaneous materials used in this study**

Chemicals/ Reagents	Supplier	Application
Agarose	VWR	Nucleic acids
DNA marker	Thermo Scientific	Nucleic acids
NucleoSpin® Gel and PCR Clean-up	Macherey-Nagel (MN) (740609.250)	Nucleic acids
NucleoSpin® Plasmid	Macherey-Nagel (MN) (740588.250)	Nucleic acids
NucleoSpin® RNA II Kit	NucleoBond® AX 500	Nucleic acids
Phusion Flash Master Mix	Thermo Scientific (F-548)	Nucleic acids
T4 DNA Ligase	Thermo Scientific (EL0016)	Nucleic acids
NEBuilder® HiFi Assembly Master Mix/	NEB	Nucleic acids
NEBuilder® HiFi Assembly Cloning Kit	NEB	Nucleic acids
NucleoBond Xtra Midi EF	Macherey-Nagel (740420.10)	Midi kit for endotoxin-free plasmid DNA
Ampicillin	VWR	Bacteria culture, cloning
Kanamycin	Applichem	Bacteria culture, cloning
D-Luciferin	PJK GmbH	Luciferase assay
Glycylglycine	Sigma Aldrich	Luciferase assay
DMSO	Sigma	Inhibitor experiments
Hydrogene peroxide (H <sub>2</sub> O <sub>2</sub> ), 30 %	Merck	HCV titrating

## MATERIALS AND METHODS

---

### 2.1.7. Bacteria

**For usual DNA cloning**, the E. coli strain DH5 $\alpha$  was used (F<sup>-</sup>, 80dlacZ $\Delta$ M15,  $\Delta$ (lacZYA-argF)U169, deoR, recA1, endA1, hsdR17 (r-K<sup>-</sup>, m<sup>+</sup>K), phoA, supE44, -), thi-1, gyrA96, relA1) (95).

**For cloning pAd vector for adenovirus-mediated gene expression**, Adtrack competent bacteria (Adeasy) were used: BJ5183: endA1 sbcBC recBC galK met thi-1 bioT hsdR (Strr) (96)

**For retransformation of pWPI vector**, HB101 strain was used: F<sup>-</sup> mcrB mrr hsdS20(rB-mB-) recA13 leuB6 ara-14 proA2 lacY1 galK2 xyl-5 mtl-1

rpsL20(SmR) glnV44  $\lambda$ - (97)

### 2.1.8. Mammalian cells

All eukaryotic cells were cultured in Dulbecco's modified Eagle's medium (DMEM; Gibco) containing 10% FCS (Seromed), 1% penicillin/streptomycin (Gibco), 2 mM L-glutamine (Gibco) and 1% non-essential amino acids (Gibco) at 37 °C in a constant humid atmosphere containing 5% CO<sub>2</sub>. Mycoplasma contamination was regularly tested using a commercially available system (MycoAlert Mycoplasma Detection kit; Lonza).

**Table 12. List of cell lines used in this study**

Cell line	Description
Huh7	Human liver carcinoma cell line which was originally taken from a liver tumor in a 57-year-old Japanese male in 1982
Huh7 shNT	Huh7 cells stably expressing non-targeting shRNA sequence under selection of Puromycin
Huh7 shPI4KA	Huh7 cells stably expressing shPI4KA under selection of 10 $\mu$ g/ml Puromycin
Huh7-Lunet	Subclone of Huh7 cells. Generation by curing a persistent replicon cell line, supports high level RNA replication
Huh7-Lunet shNT	Huh7-Lunet cells stably expressing non-targeting shRNA sequence under selection of Puromycin
Huh7-Lunet shPI4KA	Huh7-Lunet cells stably expressing shPI4KA under selection of Puromycin
Huh7-Lunet shPI4KA + vector	Huh7-Lunet cells stably expressing shPI4KA and either vector, HA-PI4KA wt or HA-PI4KA D1957A, respectively under selection of Puromycin and Blasticidin
Huh7-Lunet shPI4KA + HA-PI4KA wt	
Huh7-Lunet shPI4KA + HA-PI4KA D1957A	
Huh7-Lunet shPI4KB	Huh7-Lunet cells stably expressing shRNA against the respective gene under selection of Puromycin
Huh7-Lunet shPI4K2A	
Huh7-Lunet shPI4K2B	
Huh7-Lunet shPIP5K1A	

## MATERIALS AND METHODS

Huh7-Lunet shPIP5K1B	Huh7-Lunet cells stably expressing shRNA against the respective gene under selection of Puromycin
Huh7-Lunet shPIP5K1C	
Huh7-Lunet shPIK3CA	
Huh7-Lunet shPIK3CB	
Huh7-Lunet shPIK3CD	
Huh7-Lunet shPIK3C2A	
Huh7-Lunet shPIK3C2B	
Huh7-Lunet shPIK3C2G	
Huh7.5	Curing Huh7 HCV replicon cells with alpha interferon, highly permissive for HCV infection, high CD81
Huh7.5 shNT	Huh7.5 cells stably expressing shNT under selection of Puromycin
Huh7.5 shPI4KA	Huh7.5 cells stably expressing shPI4KA under selection of Puromycin
Hep3B	Hepatoma cell line taken from liver tissue of an 8-year-old, Black youth with liver cancer
Hep3B-shNT	Hep3B cells stably expressing shNT under selection of Puromycin
Hep3B-shPI4KA	Hep3B cells stably expressing shPI4KA under selection of Puromycin
HepG2	Human cell line isolated from a HCC of a 15-year-old, white, male youth
HHT4	hTERT-immortalized human liver epithelial cells, derived from human hepatocytes which were infected with a replication defective retrovirus encoding hTERT, gift from K. Breuhahn
Hep55.1C	Mouse hepatoma cells, established from the primary HCC of C57BL/6J mice, gift from F. Kühnel
HEK 293T MCB	The GMP-compliant generation of a Master Cell Bank of HEK 293T cells which is a derivative of human embryonic kidney 293 cells and contains the SV-40 antigen (98). They are highly transfectable and have been widely used for retroviral and lentiviral production and gene expression as well as protein production. This is a gift from Birke Bartosch.
PHH	Primary human hepatocytes were prepared in house at Heidelberg University Hospital. The human liver tissue used to extract PHHs were obtained from a patient undergoing liver cirrhosis which was approved by the French National Ethics Committee and legal instances.

## MATERIALS AND METHODS

---

### 2.1.9. Oligonucleotides

All primers used for qRT-PCR are listed in **Appendix 3**. Primers used for cloning shRNAs are listed in **Appendix 4**. All oligonucleotides were obtained from Sigma Aldrich and resuspended in water at the concentration 100  $\mu$ M and stored at -20°C.

### 2.1.10. Plasmids

All plasmids used in this study are listed in **Appendix 6**.

## 2.2. Methods

### 2.2.1. Preparation of plasmid constructs

#### 2.2.1.1. Cloning

#### Constructions of PWPI based vectors and other expression plasmids

For cloning of usual expression plasmids, primers were designed to amplify the DNA of interest, resulted in PCR products with restriction sites at both ends to facilitate ligation into a target vector. 2X PhusionFlash High-Fidelity Mastermix (Thermo Scientific) were used for PCR reaction according to the manufacturer's instructions with few modifications. The PCR program was in brief described below.

**Table 13. PCR program for cloning**

Step	Temperature	Duration	
1	98 °C	30 s	
2	98 °C	10 s	Repeat 25x step 2-4
3	55-65 °C	20 s	
4	72 °C	30 s per kb	
5	72 °C	5 min	

Construction of pWPI-BLR-PI4KA wt and pWPI-BLR-PI4KA D1957A with silent shRNA escape mutations were described elsewhere (87). PIK3C2G, PXN and CFL1 genes were amplified and introduced into AsiSI and Ascl sites of the pWPI vector using the primers listed in the **Appendix 5**. Constitutive active mutants Y31D of PXN and S3A of CFL1 were cloned by introducing the following nucleotide exchanges T91G, T7G, respectively. All the mutations were introduced by overlap extension PCR.

#### Cloning shRNA constructs

For constructions of shRNAs, Katahdin algorithms (<http://katahdin.cshl.org/siRNA/RNAi.cgi?type=shRNA>, maintained by Sachidanandam Lab) was used to design a 97-mer oligonucleotide containing microRNA-based shRNA targeting sequence (**Appendix 4**) was designed against each corresponding gene. In order to clone into pAPM vector, XhoI and EcoRI sites were introduced to the 5'-end of sense and antisense sequence, respectively as followed: for sense primers, the sequence tcgagaaggatat was added in 5' of the 97-mer oligonucleotides and the last A was deleted; while anti-sense primers was designed by reversing the sequence of the oligonucleotide and

## MATERIALS AND METHODS

---

adding aat in 5' and atataccttc in 3'. Each pair of sense and antisense primers was annealed by boiling at 95°C for 5 min, followed by 30 min incubation at room temperature and 5' phosphorylated using T4 PNK (New England Biolabs) to produce respective DNA insert suitable for cloning into pAPM vector. Non targeting shRNA and shPI4KA were described previously (81) with the targeting sequences provided below.

### **Cloning pAd constructs for adenovirus-mediated gene expression**

HCV NS3-5B expressions were achieved via adenovirus transduction which is generated according to the protocol published by Agilent Technologies (99) with some modifications. In brief, HCV NS3-5B wt and mutants (S232A and PPH) were cloned into pShuttle-CMV vector. The plasmids were then linearized with PmeI and then 1 µg of the purified DNA was electroporated into 50 µL BJ5183 electroporation competent cells bearing pAdEasy-1 supercoiled vector to allow recombination occurs.

#### **2.2.1.2. Restriction enzyme digestion**

All restriction endonucleases, buffers and reagents were obtained from New England Biolabs and handled according to the manufacturer's instructions. The amount of plasmids, purified PCR DNA fragments, enzymes and reaction volume was adjusted in each reaction in respect to the purpose, the size and the number of restriction sites present in each plasmid/DNA. If necessary (but not always), 10 U/µl calf intestinal alkaline phosphatase (CIP) were added for dephosphorylation to avoid religation. Depending on the size of residual fragments and the complexity of samples DNA fragments were either directly purified by NucleoSpin Extract® II Kit (Macherey & Nagel) or a step of agarose gel electrophoresis was added beforehand.

#### **2.2.1.3. Ligation**

Typically 50 ng of vector backbone was used for ligation. A vector: insert molar ratio of 1:5 – 1:9 was used to calculate the amount of required insert. Ligation was prepared in 20 µl volume containing 1 µl T4 DNA ligase and carried out at RT for 1-2 hours or at 16°C overnight. The ligation mix was directly transformed into competent bacteria.

#### **2.2.1.4. Transformation (heat shock and electroporation)**

Homemade CaCl<sub>2</sub>-competent E.coli DH5α or commercial competent HB-101 were thawed and incubated with 0.5 µl of established plasmid or 20 µl ligation product on ice for 15 min. This was followed by a heat shock at 42°C for 1 min and then an incubation on ice for 5 min. 900 µl of LB medium were added and bacteria were incubated at 37°C for 30 min up to 6 h with agitation on a heat-block at 800 rpm. Either 50-100 µl of cell suspension for re-transformation or all the cell suspension in the case of ligation (after a centrifugation at 500 rpm for 3 min, 900 µl supernatant was removed) were plated on agar plates containing appropriate antibiotic selection. Colonies were grown overnight in an incubator at 37°C.

Electroporation of DNA into bacteria was performed according to an instruction manual provided by Agilent Technologies (99) with some modifications. In brief electroporation cuvettes (0.2 cm gap) were pre-chilled on ice. Electroporation competent cells harboring

## MATERIALS AND METHODS

---

pAdEasy-1 supercoiled vector were thawed and mixed with 1  $\mu$ g of linearized, dephosphorylated shuttle vector and keep on ice for 10 min. This bacteria-DNA mix were then subsequently transferred into a pre-chilled cuvette and electroporation was performed with an electroporator with the following settings: 200  $\Omega$ , 2.5 kV, 25  $\mu$ F. 1 ml of sterile LB broth was immediately added and the cell suspension was transferred into a new eppi and incubated at 37°C for 1 h with agitation on a heatblock at 800 rpm. 100  $\mu$ l of cell suspension was plated on agar plates containing Kanamycin and incubated overnight at 37°C.

### **2.2.1.5. Agarose gel electrophoresis**

In order to evaluate cloning success, RNA quality, identify DNA from PCRs or restriction digestion or to isolate DNA fragments of specific length for further downstream applications, agarose gel electrophoresis was performed to separate nucleic acid molecules by their size in an electrical field. 0.8-1% (w/v) agarose gels were prepared by dissolving agarose in 1x TAE buffer with boiling, followed by staining with DNA stain. The solidified agarose gels were run horizontally in 1x TAE buffer at 100-120 V for 15-30 min and the DNA was visualized by UV light and documented with an electronic gel imaging system. In the case of preparative gels, the band of interest was quickly cut out using a sharp scalpel and purification of DNA was done using the NucleoSpin Extract® II Kit according to the manufacturer's protocol.

### **2.2.1.6. Measurement of nucleic acids concentration**

Nucleic acids have absorbance maxima at 260 nm and the "A260 unit" is used as a quantity measure for nucleic acids. In addition, the ratio of the absorbance at 260 and 280 nm (A260/280) is used to assess the purity of nucleic acids. Concentration and purity of nucleic acid solutions was determined by a spectrophotometric analysis using a NanoDrop Spectrophotometer (Thermo Scientific,). A 260/280 ratio of ~1.8 is generally accepted as "pure" for DNA; aratio of ~2.0 is generally accepted as "pure" for RNA.

### **2.2.1.7. Plasmids extraction**

#### **Mini prep**

A single colony of bacteria harboring plasmid of interest was inoculated in 5 ml LB overnight at 37°C, 180 rpm shaking in the presence of a selection antibiotic (Ampicillin or Kanamycin). The bacteria pellet was collected by centrifugation at 600xg, 10 min and plasmid DNA was isolated and purified using the NucleoSpin® Plasmid kit (Macherey & Nagel) according to the manufacturer's protocol. 50  $\mu$ l of distilled water was used to elute bound plasmid DNA from purification column and sequencing was performed by Eurofins Genomics.

#### **Maxi prep**

Plasmids from mini prep with correct sequencing were used for retransformation. A single colony of bacteria harboring plasmid of interest was inoculated in 50 ml – 400 ml LB (whether it is high or low copy plasmid) overnight at 37°C, 180 rpm shaking in the presence of a respective selection antibiotic (Ampicillin or Kanamycin). The bacteria pellet was collected by centrifugation at 600xg, 10 min and plasmid DNA was isolated and purified using the using the NucleoSpin® Plasmid kit (Macherey & Nagel) according to the manufacturer's protocol.

## MATERIALS AND METHODS

---

200 - 1000  $\mu$ l of distilled water was used to elute bound plasmid DNA from purification column. Sequencing was performed to ensure that correct constructs were used for experiments.

### **Endotoxin-free plasmids extraction**

The envelope of gram-negative bacteria, including the E. coli DH5 $\alpha$  used for plasmid extraction, is made of two lipid membranes. Lipopolysaccharides (LPS), also known as endotoxins, are a central component of the outer membrane of these bacteria. These LPS trigger inflammatory responses of the mammalian immune system and therefore should be removed from plasmid preparations for animal experiments. The plasmid preparation is in general similar to other plasmid preparation but NucleoBon Xtra EF (Macherey-Nagel) helps to reduce the endotoxin level to <0.05 EU/ $\mu$ g plasmid DNA.

### **2.2.2. Cell culture**

#### ***Culturing and passaging***

All cell monolayers were grown in 100 or 150 mm dishes (Corning, BD Falcon or Greiner bio-one) with DMEM complete in the presence of antibiotic selection if necessary or HCM Hepatocyte Culture Medium BulletKit (for HHT4) or William's Medium E medium (for PHH). Except for PHH all cells were routinely split twice a week at a split ratio of 1:5 to 1:10 depending on their current growth rate and their confluency. For this purpose cultured medium was aspirated, cells were washed once or twice with PBS and were detached using 1-2 ml of trypsin/EDTA with 3-5 min incubation at 37°C. Cells were then resuspended in appropriate culture medium before redistribution to a new cell culture dish.

#### ***Determining cell numbers***

To acquire a proper number of cells for experimental seeding, cells were trypsinized and then passed through a 1 ml pipette tip several times to singularize cells. 10  $\mu$ l of the cell solution were either transferred to a counting slide for automatic counting using TC20 automated cell counter (Biorad) or to a haemocytometer (Neubauer cell counting chamber) for manual counting. In the later case haemocytometer and the cover slip were always cleaned with 70 % (v/v) ethanol prior to use. The number of cells within 4 large quadrants was counted with the aid of an inverted light microscope and an average number was taken. The cell number per ml is calculated by multiplying the amount of cells in one quadrant by 10,000.

#### ***Storage and thawing cells***

To produce cell stocks for long-term storage, confluent cell monolayers were trypsinized and cell pellets were collected by centrifugation at 700 rpm for 5 min. Cells were then resuspended in FCS containing 10% (v/v) DMSO and 1.8 ml of the cell solution were distributed in each cryo tubes. Cells were then transferred to -80C for several days before storing long-term in liquid nitrogen.



## MATERIALS AND METHODS

---

To obtain a fresh cell culture batch, cells were thawed from a frozen cell stock by incubating quickly in a water bath at 37°C and transferring into 10 ml of warm culture medium in a 50 ml conical tube. Medium containing DMSO was then removed by a centrifugation at 700 rpm for 5 min and cell pellets were resuspended in fresh culture medium before plating in a proper cell culture vessel. Cell condition was monitored a day post seeding and antibiotic selection was added in the case of stable cell lines.

### ***Cell culture and experimental setup with stable cell lines***

To eliminate false interpretation which might be caused due to different cell batches, all the stable cell lines from an experiment were always prepared from the same parental cell line at the same starting point and were kept passaging at the same time. The cell origins, passage numbers, culture medium, etc. were therefore identical among the stable cell lines in the same experiment. The lentiviruses used to express the genes of interest (shRNAs, exogenous expression) in an experiment were also prepared at the same time side by side. Possible false-positive observation coming from antibiotic selection was also eliminated by including always appropriate control (pAPM-shNT in the case of knockdown, PWPI-empty vector in the case of overexpression).

### **2.2.3. Preparation of HCV RNAs by *in vitro* transcription**

In order to ensure transcripts with defined 5'-ends, plasmids were linearized using an appropriate restriction enzyme, or a construct was used that encoded for the genomic ribozyme of hepatitis  $\delta$  ( $\delta$ g) downstream of the 5'-end of the RNA. DNA was extracted using a NucleoSpin® Gel and PCR Clean-up kit and resuspended in RNase-free H<sub>2</sub>O. 5  $\mu$ g DNA were mixed with 80 mM HEPES, pH 7.5, 12 mM MgCl<sub>2</sub>, 2 mM spermidine, 40 mM DTT, 3.125 mM of each nucleoside triphosphate, 1 U/ $\mu$ l RNasin (Promega) and 0.8 U/ $\mu$ l T7 RNA polymerase (Promega). The reaction was incubated at 37 °C and after 2 h additional 0.4 U/ $\mu$ l T7 RNA polymerase was added for another 2 h. Finally, 1 U/ $\mu$ g DNA RNase-free DNase (Promega) were added. RNA was extracted by adding 60  $\mu$ l 2 M sodium acetate (pH 4.5), 440  $\mu$ l H<sub>2</sub>O and 400  $\mu$ l water-saturated phenol. The sample was mixed, incubated on ice for 10 min and centrifuged at 14,000 rpm and 4 °C for 10 min. Supernatant was transferred to a new tube and mixed with an equal volume of chloroform. The sample was mixed again and centrifuged for 3 min at 14,000 rpm and RT. To precipitate the RNA, 0.7 volumes of isopropanol were added to the supernatant. After 15 min spin at 14,000 rpm, RT, the pellet was washed once with 70% ethanol and then resuspended in RNase-free H<sub>2</sub>O. Concentration was determined using a Nanodrop Lite (Thermo Scientific) and RNA integrity was checked by agarose gel electrophoresis.

### **2.2.4. HCV RNA electroporation for virus production and replication assay**

HCVcc was produced according to the protocol published previously (100) with some modifications. In brief,  $6 \times 10^6$  Huh7.5 cells was resuspended in 400  $\mu$ l of Cytomix buffer supplemented with 2 mM ATP and 5 mM glutathione and mixed with 10  $\mu$ g of invitro-transcribed RNAs from full-length pFK-JFH1-J6-dg or the respective pFK full-length viral vectors and transferred into a 4 mm cuvette. Electroporation of RNA was set at 975  $\mu$ F and

## MATERIALS AND METHODS

---

270 V. 2-3 electroporations were combined, resuspended in 20 mL DMEM and cells were seeded in a 20 cm dish. The cells were cultured for 4 days and the supernatant were collected and filtered via a 0.45 µm filter. Virus titer was determined and virus stock was stored at -80°C. Virus titer was determined using method described by Lindenbach (101) which based on NS5A expression via immunohistochemistry.

For HCV RNA replication assay, instead Huh7-Lunet and RNA transcribed from replicon construct pFK-i389 Luc NS3-3' JFH wt were used. For RNA electroporation, single cells were washed with PBS and resuspended in Cytomix to  $1 \times 10^7$  cells/ml for Huh7-Lunet. In a cuvette 200 µl of cells were mixed with 2.5 µg of HCV RNAs and electroporation was performed at 975 µF and 166V. Cells were then resuspended in 6 mL complete DMEM and were seeded in 6 well-plates as follows: 2 mL each for sets of 4 h and 24 h time point, 1 mL each for sets of 48 h and 72 h time point.

### 2.2.5. HCV infection

One day prior to infection Huh7.5 cells were seeded in 6-well plates or 10 cm dishes. Cells were inoculated with HCVcc at MOI 0.5 for 6 h. Cells were then washed twice with PBS and then DMEM complete was replaced.

### 2.2.6. HCV RNA replication assay

Transient HCV replication was carried out as previously described (102) with minor modifications. In brief, replicon encoding plasmid DNA pFK-I341PI-Luc/NS3-3'/JFH1 with all HCV parts derived from HCV isolate JFH1 (gt 2a) (in which its replication amplifies to high levels without the need for cell culture adaptation but is highly dependent on PI4KA expression) and harboring hepatitis delta virus ribozymes was used for invitro transcription. 2.5 µg of purified RNA was electroporated into  $2 \times 10^6$  Huh7-Lunet cells. Cells were then resuspended in 6 ml DMEM complete supplemented with 10 mM HEPES. 2 mL aliquots were seeded into each well of a 6-well plate for 4 h and 24 h time points, and 1 mL for 48 h and 72 h time points. Replication was determined by measuring firefly luciferase activity at the indicated time points post-electroporation and was normalized for transfection efficiency to the value obtained at 4 h time point.

To quantify luciferase reporter assay, cells were lysed in 350 µL Fluc lysis buffer (1% Triton X-100, 25 mM Glycine-Glycine (pH 7.8), 15 mM MgSO<sub>4</sub>, 4 mM EGTA (pH 7.8), 10% glycerol and 1 mM DTT). 100 µL of cell lysate was then mixed with 360 µL Fluc assay buffer (15 mM K<sub>3</sub>PO<sub>4</sub> (pH 7.8), 25 mM Glycine-Glycine (pH 7.8), 15 mM MgSO<sub>4</sub>, 4 mM EGTA (pH 7.8), 1 mM DTT and 2 mM ATP). 200 µL luciferin (200 nM in 25 mM Glycine-Glycine) was then injected and measured for 20 sec in a tube luminometer (Lumat LB 9507; Berthold Technologies, Freiburg, Germany).

## MATERIALS AND METHODS

---

### **2.2.7. Production of lentiviruses, adenoviruses and transduction on target cells**

#### **2.2.7.1. Lentivirus production and transduction**

One day prior to transfection,  $6 \times 10^6$  293T cells were seeded per 10 cm-diameter dish in DMEM complete. 30 min before transfection, medium was replaced by serum-free DMEM. For transfection, 5.15  $\mu\text{g}$  packaging plasmid (pCMV-Gag-Pol), 1.72  $\mu\text{g}$  of the VSV envelope glycoprotein expression vector (pMD2-VSVG) and 5.15  $\mu\text{g}$  of transfer vector encoding either the respective shRNAmir and puromycin resistance (pAPM) or the respective shRNAmir-escape variants and blasticidine resistance (pWPI) were mixed in 360  $\mu\text{L}$  Opti-MEM (mixture A). In a separate tube 36  $\mu\text{L}$  polyethylenimine (PEI) was mixed with 360  $\mu\text{L}$  Opti-MEM (Mixture B). Mixture B was then added dropwise to Mixture A, followed by a vortex for 10 seconds and 20 min incubation at room temperature. The transfection mixture was then added dropwise to different area of the dishes and was distributed evenly by gently rocking the culture vessel back-and-forth and from side-to-side. 6 h post-transfection medium was replaced with DMEM complete, followed by 3 days incubation. Lentivirus-containing-supernatant was harvested and filtered through a 0.45  $\mu\text{m}$  filter and was used to transduce target cells. Cells were then subjected to selection with medium containing appropriate antibiotics (2.5  $\mu\text{g}/\text{mL}$  puromycin and/or 10  $\mu\text{g}/\text{mL}$  blasticidin) after one day of transduction.

#### **2.2.7.2. Adenovirus production and transduction**

Expected p-Ad vectors bearing HCV NS3-5B were then linearized with PacI. 5 $\mu\text{g}$  of the corresponding linearized plasmid was transfected into  $7 \times 10^5$  293T cells per 60-mm dish and incubated for 8 days. Cells were collected and resuspended in serum-free DMEM. Cell suspension was then subjected to four rounds of freeze/thaw by alternating the tubes between the  $-80^\circ\text{C}$  freezer and the  $37^\circ\text{C}$  water bath with vortexing briefly after each thaw. Supernatant collected after centrifugation at 12000 xg for 10 min was used as primary viral stock and used to amplified virus titer by infection fresh HEK293T cells, followed by similar procedures for collecting virus. Virus titer was determined by plaque assay as described in the protocol. Target cells were transduced with virus stock and media was replaced after one day, followed by another 2 days of incubation.

### **2.2.8. RNA extraction, cDNA synthesis and qRT-PCR**

#### **2.2.8.1. RNA extraction**

To verify knockdown efficiency via quantification of mRNA level of the gene of interest and to determine HCV intracellular RNA levels, cellular and viral RNAs were extracted using NucleoSpin RNAII kit (Macherey-Nagel) according to the manufacturer's instruction and 60  $\mu\text{L}$  of RNA-free water was used for elution.

#### **2.2.8.2. cDNA synthesis**

Complementary DNA (cDNA) was synthesized using a High Capacity cDNA Reverse Transcription kit (Applied Biosystems) and was diluted 1:10 with water before subjecting to qRT-PCR. The master mix and PCR program for cDNA synthesis were as follows:

## MATERIALS AND METHODS

**Table 14. Master mix for cDNA synthesis**

Reagent	Volume
10x RT buffer	1 $\mu$ l
25x dNTP Mix (100 mM)	0,4 $\mu$ l
10x RT Random Primers	1 $\mu$ l
RNase inhibitor	0,5 $\mu$ l
Enzyme (MultiScribe 50 U/ $\mu$ l)	0,5 $\mu$ l
Water	1,6 $\mu$ l

**Table 15. PCR program for cDNA synthesis**

Step	Temperature	Time
1	25°C	10 min
2	37°C	120 min
3	85°C	5 min

### 2.2.8.3. qRT-PCR

qRT-PCRs were performed in triplicate using an iTaq Universal SYBR Green kit (Bio-Rad) with a Bio-Rad CFX96 Touch Real-Time PCR system, and data were analysed using the corresponding software. The tables below show components of master mix and PCR program.

**Table 16. Master mix for qRT-PCR**

Reagent	Volume
2x iTaq Universal Bio-Rad	7,5 $\mu$ l
Primer sense (5 $\mu$ M)	1,5 $\mu$ l
Primer antisense (5 $\mu$ M)	1,5 $\mu$ l
H <sub>2</sub> O	1,5 $\mu$ l
cDNA	3 $\mu$ l

**Table 17. PCR program for qRT-PCR**

Step	Temperature	Time	
1	95°C	3 min	
2	95°C	10 sec	44 times
3	60°C	30 sec	

### 2.2.9. Western blot

Cells seeded in 6-well plates were washed twice with PBS, harvested by lysis with 90  $\mu$ l per well of lysis buffer containing 20 mM Tris HCl (pH 7.2), 150 mM NaCl, 10% glycerol, 1% NP-40, 10 mM NaF, 30 mM sodium pyrophosphate, 1 mM EDTA, 1 mM Na<sub>3</sub>VO<sub>4</sub>, 1 mM phenylmethylsulfonyl fluoride (PMSF), and a protease inhibitor cocktail) and incubated on ice for 20 min. Supernatant collected after centrifugation at 13500 rpm at 4°C was mixed with Laemmli 6X buffer (375 mM Tris.HCl, 9% SDS, 50% glycerol, 0.03% bromophenol blue and 9%  $\beta$ -mercaptoethanol) and was heated 5 min at 95°C and loaded onto polyacrylamide-SDS gel. After electrophoresis proteins were transferred to a PVDF membrane and was blocked in 5% milk (in PBS supplemented with 0.25% Tween (PBS-T)) for 1 h. After over-night incubation of the membrane at 4°C with primary antibodies diluted in PBS-T supplemented with 1% BSA, the membrane was washed 3 times for 15 min with PBS-T and incubated with secondary antibodies conjugated to horseradish peroxidase diluted in PBS-T supplemented with 1% milk for 1 h at RT. After extensive washing bound antibodies were detected with the ECL Plus Western Blotting Detection System (GE Healthcare Europe, Freiburg, Germany). The antibodies and corresponding dilutions were listed in **Table 5** and **Table 6**.

## MATERIALS AND METHODS

---

### 2.2.10. Coimmunoprecipitation assay

### 2.2.11. Microscopy: bright field (cell morphology) and confocal (immunofluorescence)

#### ***Bright field microscopy***

To obtain bright field microscopic images, cells were seeded in 6-well plate and cell morphology was monitored over time. Images were usually acquired 2-3 days post seeding when cells reach 50-75% confluence using an inverted phase contrast microscope (Nikon) with 20x objective lens. Images were then processed using Fiji, scale bars was added, brightness and contrast was adjusted with the same parameters among the images in the same set to provide a clear observation.

#### ***Immunofluorescence***

Cells were firstly subjected to either intracellular or plasma membrane staining protocol.

#### ***Intracellular staining***

Intracellular PIs (PI4P, PI(3,4)P2, PI(4,5)P2 and PI(3,4,5)P3) and HCV NS5A were stained as described elsewhere (20). In brief, cells seeded on coverslips were washed twiced with PBS before fixation in 4% paraformaldehyde (PFA) for 15 min. Cells were then permeabilized with 50  $\mu$ g/ml digitonin for 10 min and blocked in 3% bovine serum albumin (BSA) for 30 min. Cells were incubated with primary antibodies diluted in 3% BSA either at room temperature (RT) for 2 h or at 4°C overnight. Cells were further incubated with Alexa 488- or 561-conjugated secondary antibodies (Invitrogen, Molecular Probes) in 3% BSA for 45 min at RT with a dilution of 1:500. Nuclei were stained using 4',6-diamidino-2-phenylindole (DAPI) for 1 min at a dilution of 1:4000. Cells were mounted with Fluoromount G (Southern Biotechnology Associates, Birmingham, AL, USA).

#### ***Plasma membrane staining***

**Table 18. Buffers used for plasma membrane staining**

Buffer A	4% FA and 0.2% GA in PBS
Buffer B	PBS containing 50 mM NH <sub>4</sub> Cl
Buffer C	5% (v/v) NGS, 0.5% saponin in buffer B
Buffer D	in 5% NGS (v/v) and 0.1% saponin in buffer B
Buffer E	2% FA in PBS

Plasma membrane PIs (PI4P, PI(3,4)P2, PI(4,5)P2 and PI(3,4,5)P3) were stained as previous study (103). In brief, after aspirating media, buffer A was added directly to allow fixation at room temperature for 15 min. After 3 times rinsing with buffer B, slides were place on ice and cells were blocked for 45 min with buffer C, followed by primary antibodies in buffer D for 2 h. After 3 washes with buffer B, secondary antibodies prepared in buffer D were added and incubated for 45 min. Nuclei was stained with DAPI for 1 min, followed by 4 times rinsing with buffer C. Cells were then post-fixed with buffer E on ice for 10 min and at

## MATERIALS AND METHODS

---

room temperature for 10 min. After 2 times rinsing with buffer B and one time with distilled water, cells were mounted with Fluoromount G.

Whole-cell z-stacks for PIs analysis were acquired with a Leica SP8 confocal laser scanning microscope. Quantification of intracellular and plasma membrane PIs signals was described before (81). The following primary antibodies and corresponding dilutions were used: m $\alpha$ PI4P (Echelon Biosciences Inc., cat. no. Z-P004; 1:100), m $\alpha$ PI(3,4)P2 (IgM) (Echelon Biosciences Inc., cat. no. Z-P034; 1:100), m $\alpha$ PI(4,5)P2 (IgM) (Echelon Biosciences Inc., cat. no. Z-P045; 1:100), m $\alpha$ PI(3,4,5)P3 (IgM) (Echelon Biosciences Inc., cat. no. Z-P345; 1:100), m $\alpha$ NS5A (IgG2 $\alpha$ ) (9E10, a generous gift from C.M. Rice, The Rockefeller University, New York; 1:500).

### **2.2.12. Biochemical determination of cellular PI(3,4)P2 levels using PI(3,4)P2 ELISA Mass Kit**

Total cellular PI(3,4)P2 were extracted using a protocol for phospholipids extraction of Echelon (104). In brief,  $5 \times 10^6$  cells were harvested in 5 mL ice cold 0.5M Trichloroacetic Acid (TCA) and incubated on ice for 5 min. After centrifugation at 1500 rpm for 5 min, the pellet was washed with 3 mL 5% TCA supplemented with 1 mM EDTA, followed by another centrifugation at 1500 rpm for 5 min. Neutral lipids were removed by adding into the pellet 3 ml of MeOH: CHCl<sub>3</sub> (3:1), vortexing 3 times over 10 min at room temperature and centrifuging at 1500 rpm for 5 min. Acidic lipids including phospholipids was extracted using 2.25 ml of MeOH: CHCl<sub>3</sub> : 12 M HCl (80:40:1), followed by vortexing 4 times over 15 min at room temperature and centrifuging at 1500 rpm for 5 min. The supernatant was then transferred into new 15 mL centrifuge tube, followed by adding 0.75 mL of CHCl<sub>3</sub> and 1.35 mL of 0.1 M HCl, vortexing and centrifuging at 1500 rpm for 5 min. Organic (lower) phase containing phospholipids was collected into clean 2ml vial and dried under hood. Dried phospholipids were stored at -20C. Relative amount of PI(3,4)P2 was determined by PI(3,4)P2 Mass ELISA kit (Echelon) according to manufacturer's instructions. In principle, samples containing PI(3,4)P2 were incubated with PI(3,4)P2 detector protein and then added to the PI(3,4)P2-coated plate for competitive binding. Amount of PI(3,4)P2 detector protein bound to the plate was detected using a peroxidase-linked secondary detection reagent and colorimetric substrate which yielded signal at absorbance 450 nm. This is inversely proportional to the samples' amount of PI(3,4)P2.

### **2.2.13. Human phosphor kinase array and Cytoskeleton array**

#### **2.2.13.1. Human phospho-kinase array**

Sample preparation and assay were carried out according to the manufacturer's instruction (Proteome Profiler, R&D systems, #ARY003B) with few modifications. In brief, Huh7-Lunet cells stably expressing shNT, shPI4KA or shPIK3C2G were cultured in 15cm dishes and cell lysates were collected in 500  $\mu$ l lysis buffer 6 (with scraper, rock on ice for 30 min, centrifuge for 5 min at 14000xg). The supernatant were collected and protein concentration was determined by Bradford assay. 600  $\mu$ g of total protein diluted in Array Buffer 1 from each sample were divided evenly into two parts and each was incubated overnight at 4°C with

## MATERIALS AND METHODS

---

either membrane A or B (already blocked with Array Buffer 1) separately. The membranes were washed three times with 1x Wash buffer before an incubation with the respective Detection Antibody Cocktail A or B for 2 hours at RT. This was followed by another incubation with diluted Streptavidin-HRP (in 1X Array Buffer 2/3) and prepared Chemi Reagent Mix with three washes in between. The membranes were then treated with an ECL detection kit (PerkinElmer) and chemiluminescence was recorded using ECL imaging system (Intas).

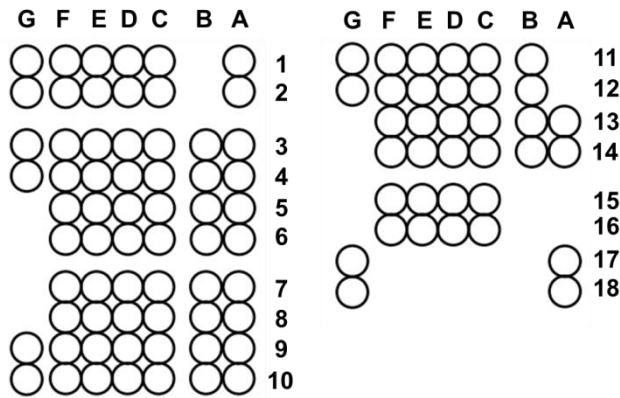


**Figure 10. Human phospho-kinase array coordinates**

## MATERIALS AND METHODS

**Table 19. Human phospho-kinase array coordinates**

Membrane/Coordinate	Target/Control	Phosphorylation Site	Membrane/Coordinate	Target/Control	Phosphorylation Site
A-A1, A2	Reference Spot	—	A-F3, F4	Chk-2	T68
A-A3, A4	p38 $\alpha$	T180/Y182	A-F5, F6	FAK	Y397
A-A5, A6	ERK1/2	T202/Y204, T185/Y187	A-F7, F8	PDGF R $\beta$	Y751
A-A7, A8	JNK 1/2/3	T183/Y185, T221/Y223	A-F9, F10	STAT5a/b	Y694/Y699
A-A9, A10	GSK-3 $\alpha/\beta$	S21/S9	A-G1, G2	Reference Spot	—
A-B3, B4	EGF R	Y1086	A-G3, G4	PRAS40	T246
A-B5, B6	MSK1/2	S376/S360	A-G9, G10	PBS (Negative Control)	—
A-B7, B8	AMPK $\alpha$ 1	T183	B-A13, A14	p53	S392
A-B9, B10	Akt 1/2/3	S473	B-A17, A18	Reference Spot	—
A-C1, C2	TOR	S2448	B-B11, B12	Akt 1/2/3	T308
A-C3, C4	CREB	S133	B-B13, B14	p53	S46
A-C5, C6	HSP27	S78/S82	B-C11, C12	p70 S6 Kinase	T389
A-C7, C8	AMPK $\alpha$ 2	T172	B-C13, C14	p53	S15
A-C9, C10	$\beta$ -Catenin	—	B-C15, C16	c-Jun	S63
A-D1, D2	Src	Y419	B-D11, D12	p70 S6 Kinase	T421/S424
A-D3, D4	Lyn	Y397	B-D13, D14	RSK1/2/3	S380/S386/S377
A-D5, D6	Lck	Y394	B-D15, D16	eNOS	S1177
A-D7, D8	STAT2	Y689	B-E11, E12	STAT3	Y705
A-D9, D10	STAT5a	Y694	B-E13, E14	p27	T198
A-E1, E2	Fyn	Y420	B-E15, E16	PLC- $\gamma$ 1	Y783
A-E3, E4	Yes	Y426	B-F11, F12	STAT3	S727
A-E5, E6	Fgr	Y412	B-F13, F14	WNK1	T60
A-E7, E8	STAT6	Y641	B-F15, F16	PYK2	Y402
A-E9, E10	STAT5b	Y699	B-G11, G12	HSP60	—
A-F1, F2	Hck	Y411	B-G17, G18	PBS (Negative Control)	—

### 2.2.13.2. Cytoskeleton antibody array

Huh7-Lunet cells were treated with 0.05  $\mu$ M PI4KA-F1 or DMSO for 3 days. Cells were then washed 5 times with cold PBS and cell pellets were collected by a centrifugation at 700 rpm, 5 min. Cell pellets were then transferred to Fullmoon for further assay. In brief, protein was extracted using non-denaturing lysis buffer and protein concentration was measured. Protein samples were then biotinylated. These labeled samples were then incubated with antibody array and detection was facilitated by dye conjugated streptavidin.

### 2.2.14. Cell proliferation, migration and invasion assay

#### Cell proliferation

Cell proliferation was assessed by CellTiter 96® Aqueous One Solution Cell Proliferation Assay Kit (Promega) according to the manufacturer's instruction. Tetrazolium compound [3-(4,5-dimethylthiazol-2-yl)-5-(3-carboxymethoxyphenyl)-2-(4-sulfophenyl)-2H-tetrazolium,



## MATERIALS AND METHODS

---

inner salt (MTS) is bio-reduced by NADPH or NADH in metabolically active cells into a colored formazan product. Assay was carried out at 4, 24, 48 and 72 h.

### ***Wound healing and cell migration***

Cell migration was evaluated using wound healing assay in which the gap is created by using the ibidi Culture-Insert 2 Well to obtain a high reproducibility due to the defined size of the cell-free gap. While trypsinization of cells occurred, the inserts were plated into a 24-well plate. Cells were seeded at the density of to have a 100% cell confluency to minimize the effect of cell proliferation on the assay. To assure cell attachment pictures were taken at 4h post seeding and served as control starting point of the assay using phase contrast microscopy. Cells were further monitored and images were then taken at 24 and 48h post seeding. Images of each gap created by the insert were taken at the two ends and the exact same gap position was monitored during the entire experiment.

### ***Cell invasion***

Cell invasion assay was carried out using BioCoat Matrigel Invasion Chamber (Corning) according to manufacturer's instructions. In brief, prior to cell seeding Matrigel inserts in 24-well plate were rehydrated with serum-free DMEM for 2 h in humidified tissue culture incubator (37°C, 5% CO<sub>2</sub>). Media was removed carefully to avoid disturbing the layer on the membrane. Cells were seeded at the density of  $1.25 \times 10^4$  per well (0.5 mL) onto upper layer of the insert in serum-free DMEM. 0.75 mL complete DMEM was placed in each well under the insert to serve as the chemoattractant. Cells were incubated for 20 h in humidified tissue culture incubator. Invading cells were stained by 0.5% Crystal violet and counted with the aid of an inverted microscope.

## **2.2.15. Mice experiments**

### ***Hydrodynamic injection of plasmids expressing PI4KA or HCV nonstructural proteins***

Endotoxin-free plasmids for expressing HCV or PI4KA were prepared and handed over to Marco Breinig and Kai Volz (AG. Tschaharganeh, DKFZ) for the work in mice. The mice used in these experiments were C57Bl6/N SOPF, female and 8 weeks old. For each mice 20 µg of respective plasmids together with 4 µg of SB plasmid were prepared in 2 mL of 0.9% NaCl. Hydrodynamic tail vein injection was performed in 5-7 seconds with pre heat up of animals (with 15 min red light). BD 3 mL syringes (REF309658) and BD Microlance needles (REF303800) were used. The mice were sacrificed 4 weeks after the injection and their livers were collected. These livers were divided into two parts: one was fixed overnight in PFA 4% in cold room with rotation and the others were snap-frozen at -80°C. The fixed samples were delivered to Center for Model System and Comparative Pathology (CMCP) – Heidelberg University Hospital for immunohistochemistry staining and images were scanned in the NCT-Gewebebank. Pathological status of the samples was further evaluated using HSE staining by Dr. Tanja Poth. For each frozen liver, several small pieces were taken and pooled together for a representative sample. Protein lysates were extracted using 200 µL lysis buffer with the aid of Dounce tissue grinder (Sigma Aldrich, D8938). Expression of p-paxillin, p-cofilin, total paxillin, total cofilin and Gapdh was assessed by western blot.

## MATERIALS AND METHODS

---

### ***Injection of human liver cancer cells with modulated PI4KA expression into SCID mice***

Huh7-Lunet cells were firstly transduced with adenoviruses expressing a firefly luciferase to favor *in vivo* monitoring of the injected cells and tumor formation. These cells were then either stably knocked down of PI4KA or control silenced using lentiviral-mediated gene transduction. Morphology of these cells as well as expression levels of PI4KA was assessed to ensure an efficient silencing. Cells were then delivered to AG. Sällberg (Karolinska Institute) for *in vivo* experiment. 200  $\mu$ l cell suspension of either 1 or  $5 \times 10^6$  cells were subcutaneously injected into nude mice and IVIS Spectrum *in vivo* imaging was performed at day 0, 3, 5, 10, 14, 18 and 21. At day 21 the mice were sacrificed and organs were collected including livers, lungs, spleen and tumors.

### ***Autologous transfer of murine HCC derived cells with modulated PI4KA expression***

Mouse hepatoma cells Hep 55.1C (gift from Prof. Florian Kühnel – Hannover University) were transduced with adenoviral expressing shNT or shPI4KA and stable cell lines were selected with puromycin. Cell invasion was assessed to confirm the phenotype caused by silencing of PI4KA. The works with mice were kindly performed by the research group of AG. Kühnel. In brief, the cells were intravenously infiltrated into immuno-competent mice C57BL/6. As a surrogate to characterize cell invasiveness *in vivo*, growth of lung colonies was monitored. Lung tumor burden was examined at the day 26<sup>th</sup> post injection.

### ***HCV infection of human-liver chimeric mice***

The work with chimeric mice was performed by the research group of Prof. Philip Meuleman at Ghent University. Homozygous uPA+/+-SCID mice were transplanted with primary human hepatocytes and then infected with viral inoculum from the serum obtained from a patient after liver transplantation, containing a novel gt1b isolate (GLT1) via intrasplenic injection. The mice were sacrificed at 8 weeks post infection. Expressions of human albumin, HCV NS5A and p-paxillin in mice livers were assessed by immunohistochemistry on consecutive slices which was performed by the research group of Prof. Mathias Heikenwälder.

### **2.2.16. Statistical analysis and softwares**

VectorNTI was used to design plasmid maps and analyze DNA sequencing. Sequences of all primers for qRT-PCR were taken from PrimerBank, a public resource for PCR primers (<https://pga.mgh.harvard.edu/primerbank/>). For cloning shRNAs, 97-mer oligonucleotides containing microRNA-based shRNA targeting sequence obtained from Katahdin algorithms were then converted to respective sequences of forward and reverse primers using some self-designed Microsoft excel formulas. Images from western blotting, cell culture microscopy, immunofluorescence microscopy, live cell imaging, and immunohistochemistry were processed and analyzed using Fiji. Microsoft Excel and GraphPad Prism Software were used to perform statistical analyses. Arrangement of figures was carried out using Microsoft Powerpoint and Inkscape. Data are presented as means  $\pm$  standard deviations (SD). The asterisks in the figures indicate significant differences: \*,  $P \leq 0.05$ ; \*\*,  $P \leq 0.01$ ; \*\*\*,  $P \leq 0.001$ ; ns, not significant.

# RESULTS

## 3. RESULTS

### 3.1. Screening for factors contributing to PI4KA's signaling-induced liver pathogenesis

The initial aim of the project was the identification of signaling cascades contributing to pathogenesis mediated by increased levels of PI4P, starting with an unbiased screening approach. The strategy was to use HCV replicon cells or HCV-expressing cells with different capacities of activating the kinase PI4KA and inducing PI4P production and subsequently to identify changes in signaling pathways using a Proteome Profiler Human kinase array in combination with Affymetrix microarray for a transcriptomic profile of these cells. This idea was facilitated by the previous works which had identified some classes of cell culture adapted HCV variants showing different levels of PI4P induction (83 and unpublished data). At first several HCV Con1 (gt 1b) replicon cell lines were established in Huh7-Lunet cells, including two that had mutations in NS4B (V1897L or K1846T), one with a mutation in NS5A (S2204I) and one in NS5B (R2884G). The cell lines were created by electroporation of the respective HCV replicon RNAs and underwent a selection with G418. These HCV variants were classified into two groups with regards to PI4P induction. The mutations on NS5A and NS5B were shown to interrupt the activation of PI4KA whereas the other two mutants could still activate the kinase (unpublished data). It should be mentioned that there was no wt version of this HCV Con1 which could replicate in cell culture. The choice of these HCV variants was also based on previous observation using transient replication assay which showed comparable replication capacities (83) and thus could be a good tool to observe changes regardless of levels of replication. Instead, however, with stable replicons I noticed significantly different replication efficiencies indicated by NS5A expression (**Figure 11A**). The S2204I was the most efficient, followed by the K1846T and R2884G, respectively, and V1897L showed lowest NS5A expression level (**Figure 11A**). In addition, PI4P levels were upregulated in all the HCV stable replicons, with the differences ranging from approximately 4 fold (mutant NS5A and NS5B) to 8 fold (2 mutants NS4B) in comparison with control cells (**Figure 11B**). The differences of PI4P induction between the 2 groups of HCV replicons was only 2 fold (**Figure 11B**) which could make it difficult to expect any significant differences on cell signaling pathways among the groups of HCV replicons. Human phosphokinase array using lysates from these cell lines revealed an upregulation of p-ERK1/2 in all the HCV replicons in which the group of HCV mutants NS4B showed the highest upregulation (6-7 fold), followed by NS5A mutant (5 fold) and NS5B mutant (2.5 fold) (**Figure 11C and D**) which could be validated by Western blotting, even though the magnitude of differences were smaller (**Figure 11E**). There were no further significant changes in other phospho-proteins observed among the replicons which could be shown in the array. These replicons however when passaged over time did not show any noticeable differences in levels of PI4P induction (**Figure 11F**) and the phenotype of p-ERK1/2 was also faded out (**Figure 11G**). This raised concerns on using this model as a solid ground for further investigation as the changes observed among the groups of HCV replicon (with higher and lower PI4P induction) were only marginal and not stable. In parallel, an overexpression system where HCV NS3-5B

## RESULTS

---

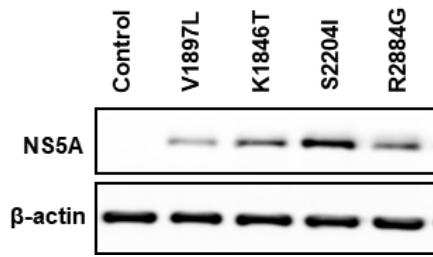
variants with different power of PI4KA activation were expressed in Huh7-Lunet-T7 cells using pTM vector were also tested (**Figure 11H**). Lysates from these cells however did not show any changes in p-ERK1/2 levels in both the array (**Figure 11I**) and western blot analysis (**Figure 11J**).

The failure of all these approaches which aimed to identify signaling molecules regulated by PI4KA using replicon cells and transient overexpression of HCV with different capacities of PI4KA activation lied in many reasons. Firstly, expression of PI4KA is already high in the Huh7-Lunet cells and cell lines which support HCV replication. In order to expect some remarkable changes of the pathways governed by PI4KA, it is necessary to have an extremely high activation or a huge elevation in expression of the kinase. In addition, the levels of PI4P induction between the 2 groups of HCV replicons were not dramatically different. More importantly, signaling pathways regulated by HCV are much more complex than solely an activation of PI4KA, therefore the use of this virus could certainly not reveal a pure picture of the kinase's functions in cells. This should therefore only be used as a supporting tool to study about this kinase as well as to expand our knowledge on the mechanism of the viral pathogenesis.

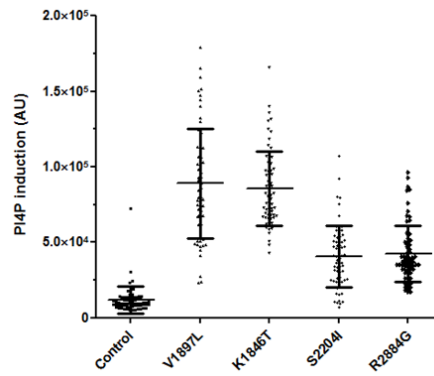
In addition, I also performed comprehensive transcriptomic and phosphoproteomic analysis under conditions of PI4KA knockdown and activation (HCV replicon cells, HCV-infected and uninfected Huh-7.5 cells and Huh-7 cells with specific PI4KA knockdown) to identify changes in intracellular signaling cascades potentially contributing to HCV-induced tumorigenesis mediated by PI4KA. Surprisingly, in the transcriptome there were little differences which could be linked to modulation of PI4P concentrations (data not shown). The phosphoproteomic analysis using Kinexus-Phospho-proteome array KAM-1325, however, revealed significant changes in multiple pathways, many of them linked to cancer development (data not shown). This included among others proteins involved in the Ras/MAPK pathway, cell cycle control, the actin cytoskeleton as well as various receptor and nonreceptor kinases and transcription factors. These findings provided the basis for my further study on signaling pathways regulated by PI4KA/PI4P concentration which potentially contributed to liver pathogenesis.

# RESULTS

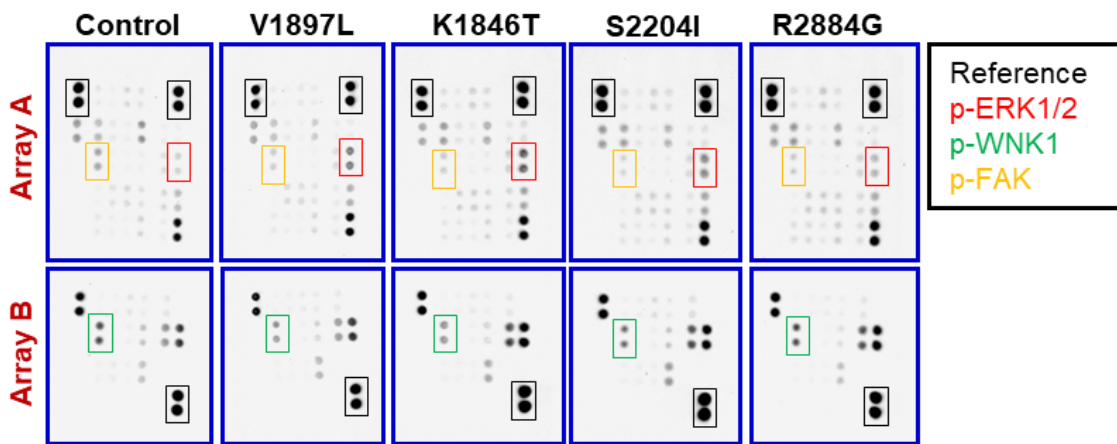
**A**



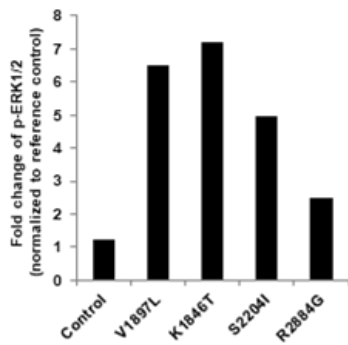
**B**



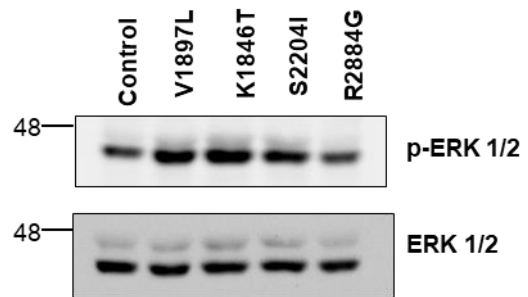
**C**



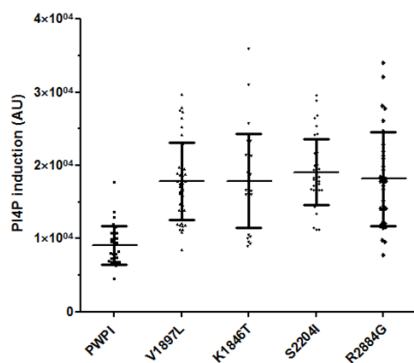
**D**



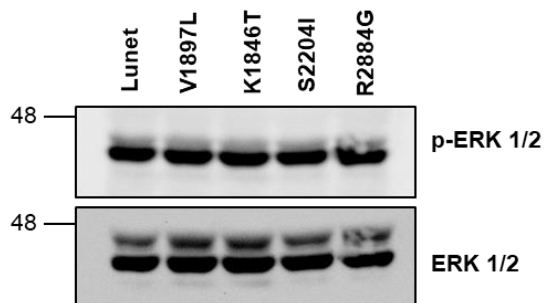
**E**



**F**



**G**



## RESULTS

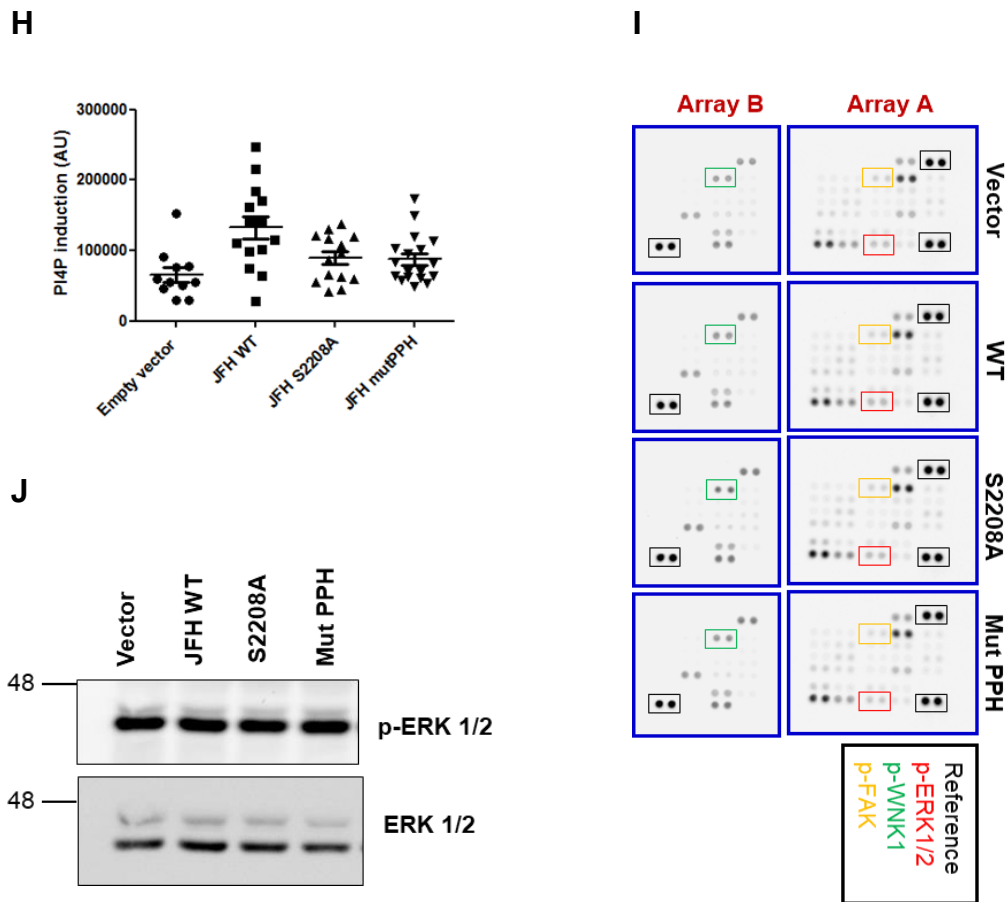


**Figure 11. Initial strategy of using HCV replicons and HCV-expressing cells to identify signaling molecules regulated by PI4KA.** **A.** Huh7-Lunet cells were electroporated with RNAs of HCV subgenomic replicons of isolate Con1 containing mutations in NS4B (V1897L, K1846T), NS5A (S2204I) or NS5B (R2884G). These cells were stably selected by their resistance to G418. Protein lysates were extracted from these cells and Western blot analysis presented expression of NS5A and GAPDH. **B.** Cells were seeded on coverslips and incubated overnight before staining for HCV NS5A (red), PI4P (green) and nucleus (blue) using the respective antibodies and DAPI. Levels of PI4P in these cells were recorded by confocal microscopy and analyzed using Fiji and presented as arbitrary units. **C.** Protein lysates from the cells in **A** were extracted according to the manufacturer's instruction and applied to the human phosphokinase array. **D.** Signal intensities of p-ERK in each condition were quantified using Fiji and relative fold changes in comparison with control cells were presented in Graphpad. **E.** Total lysates were extracted from the cells in **A** and subjected to Western blot for p-ERK detection. **F. and G.** The cells mentioned in **A** after 15 passages were subjected to IF for measurement of PI4P levels and to Western blot for p-ERK analysis, respectively. **H.** Huh7-Lunet cells were transfected with pTM vectors expressing JFH NS3-5B wt or the mutants S2208A, or PPH. PI4P induction in these cells was analyzed as in **B.** **I.** Human phosphokinase arrays were used to analyze cell lysates from **H** as done in **C.** **J.** Protein lysates from **H** was subjected to Western blot for p-ERK analysis.

### 3.2. PI4KA is important for cellular morphogenesis

#### 3.2.1. Silencing of PI4KA induces morphological changes

Given the recently known elevated expression of PI4KA in HCC liver tissue and its association with poor prognosis in liver cancer patients (74) as well as its well-known roles in HCV replication and its activity being upregulated by this virus (77,78,79,80,81,82,84,85), I aimed to decipher the mechanistic link between this lipid kinase and HCC progression as well as a possible manipulation of HCV in this process. Huh7-derived cell lines were central

## RESULTS

---

models in my research due to their support for HCV replication and they were more readily available and easier to handle than primary or primary-like cells. In addition, they showed a clear overexpression of PI4KA compared to primary hepatocytes, in line with their HCC origin (74,75). To investigate the roles of PI4KA and its product PI4P in cell and cancer biology, I firstly employed loss-of-function studies. This approach had benefits over other approaches using overexpression or activation of PI4KA due to intrinsic high expression of PI4KA in the human hepatoma cell lines (74). Reducing expression or activity of PI4KA to more physiological levels found in primary cells would reveal a better picture of possible functions of this kinase, whereas overexpression in cells with close to saturated expression could probably not provoke dramatic changes.

For this purpose, firstly shRNA-mediated gene silencing was introduced into Huh7-Lunet cells by lentiviral transduction. qRT-PCR and Western blot analysis showed 75% and 95% reductions, respectively in mRNA and protein expressions of PI4KA, confirming the successful knockdown of PI4KA (**Figure 12A** and **B**). It was noteworthy that silencing of PI4KA did not affect cell proliferation as shown in **Figure 12C**. Surprisingly, however, striking alterations in cell morphology were observed in PI4KA knockdown cells compared to the control shNT. The first noticeable changes were cell size and shape. In most of the cases control cells were approximately 50  $\mu\text{m}$  in diameter with hexagonal to rounded shape and evenly spread all over the culture matrix. In contrast, PI4KA knockdown cells looked much more compact and smaller in size with diversely irregular shapes. In several cases cells were found elongated, while in other cases cell shrinkage happened in all dimensions. For the most part, shNT-cells were more flattened with rather smooth plasma membranes whereas rough and wrinkly shapes often surrounded by very bright areas were associated with cells expressing shPI4KA (**Figure 12D**). The shrinkage of cell size could also be appreciated by frequent observations of an apparently lower cell density in the case of PI4KA knockdown. Despite this phenotype is often described for cells undergoing apoptosis there was no difference in cell viability (data not shown). Furthermore, cell proliferation (**Figure 12C**) remained at a similar rate as well as nuclear fragmentation was not observed in these cells (**Figure 20**). Furthermore, PI4KA-depleted cells looked much darker with indistinct boundaries between cytoplasm and nucleus which could be due to a condensation of cytosol with its intracellular compartments. Cytoplasms of shNT-cells, on the other hand, were much brighter under light microscope and were visibly distinguished with their nuclear counterparts. Quantification of cells with morphological alterations revealed 71.7% versus 11.1% in Huh7-Lunet expressing shPI4KA and shNT, respectively.

Huh7-Lunet cells were the first choice for my study, since these cells are known to support for HCV RNA replication which was useful for further investigations. In addition, their size, shape and growth behavior were suitable for imaging techniques. To examine if the observed phenotypes of cell morphology were cell lines specific, I in addition implemented Huh7.5 and the parental Huh7. Even though Huh7.5 cells are typically smaller in size, more heterogeneous and often grow in clusters which make them much more challenging for monitoring cell morphology (**Figure 12E**), I however could still record a consistent and significant change in their morphogenesis when PI4KA was depleted. 80.6% of the cell



## RESULTS

---

population showed non-typical cell shape in the shPI4KA expressing cells, whereas in the case of shNT it was 32.7% (**Figure 12E**). Huh7 cells, in general, share similar morphology with the clone Huh7-Lunet and I also recorded 70.8% of PI4KA knockdown cells with morphological changes, whereas it was 19.7% in their counterpart (**Figure 12F**). I also extended my observation to Hep3B cells, a non-Huh7-derived hepatoma cell line. Although it was much more difficult to monitor and record morphology of these cells due to their very light and thin cytoplasm, I noticed that PI4KA depletion caused the above-described alterations in cell morphology with the amounts more than double the case of non-targeting control (55.6% versus 24.5%, respectively) (**Figure 12G**). In conclusion, I observed a very interesting and previously un-described phenotypes caused by PI4KA silencing. The differences in levels of PI4KA expression were strongly associated with a remarkable discrepancy in cell shapes which were recorded across several hepatoma cell lines. Because more expression of PI4KA at mRNA and protein levels were found in HCC samples and the hepatoma cell lines than in normal liver tissues and PHHs (74,75), the differences in morphology between the low and high PI4KA expression groups could reflect the changes in malignancy. These observations provided a firm basis for my further investigations on PI4KA functionalities in cell signalling and its association with liver pathogenesis.

## RESULTS

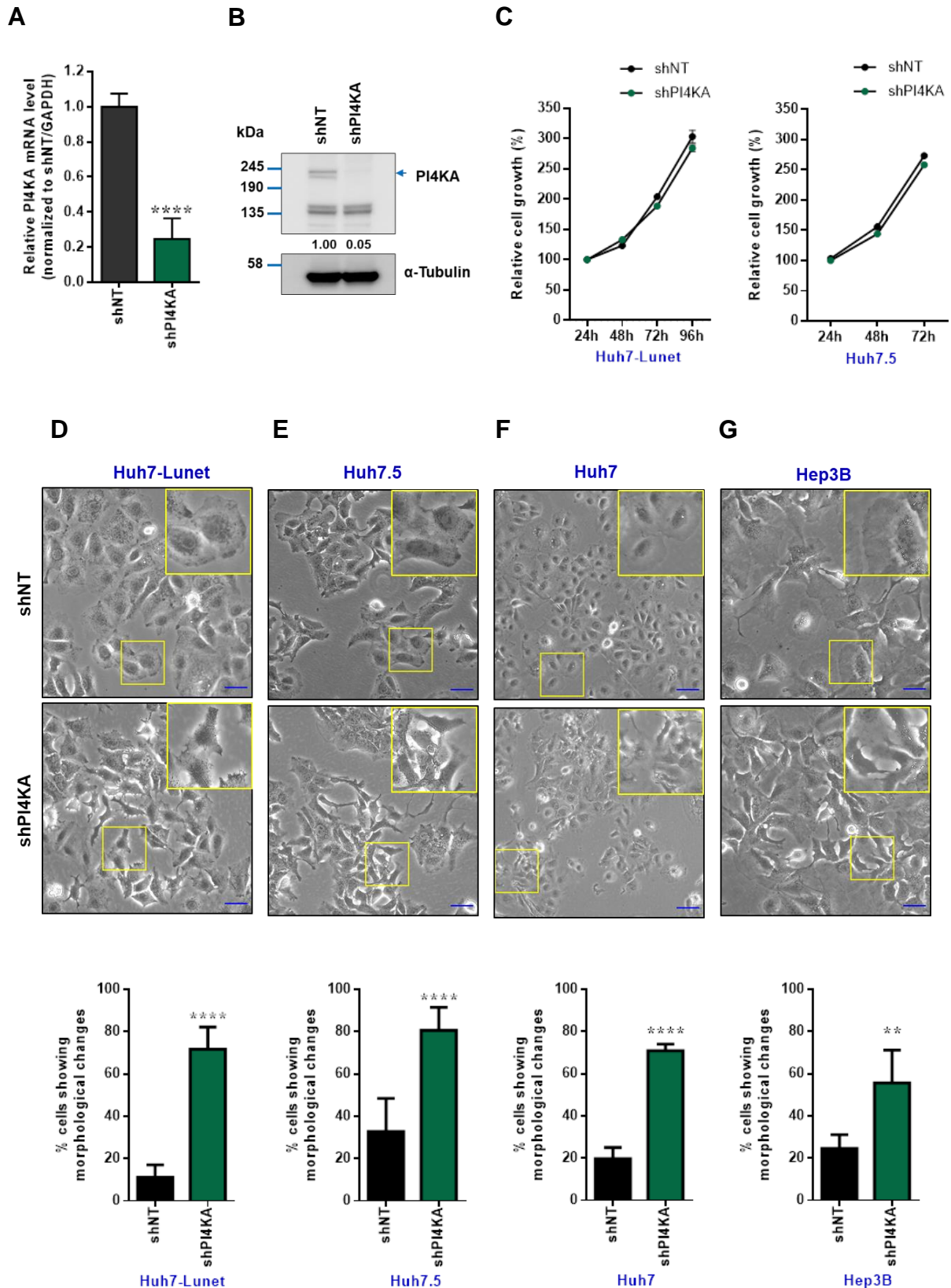


**Figure 12. Knockdown of PI4KA affects cellular morphology but not proliferation.** **A.** Huh7-Lunet cells were transduced with lentiviruses encoding either shNT or shPI4KA and selected with puromycin. The cells were then seeded in a 12-well plate and cultured for 2 days before subjecting to an RNA extraction. qRT-PCR was applied to determine PI4KA expression. Normalization was based on GAPDH expression and relative fold change was expressed as a difference in comparison to the shNT. **B.** The cells from **A** were seeded in a 6-well plate and protein lysates were extracted 2 days

## RESULTS

---

post seeding and immune-blotted using antibodies against PI4KA and  $\alpha$ -tubulin (as a housekeeping protein for normalization). Band intensity was quantified using FIJI and relative fold change of PI4KA expression was presented. **C.** Huh7-Lunet and Huh7.5 expressing shNT or shPI4KA were seeded in a 96-well plate and cell proliferation WST-1 assay was performed at the indicated time point. **D.** Upper panel. Huh7-Lunet-shNT and Huh7-Lunet-shPI4KA were cultured in a 6 well-plate and cell morphology was imaged by bright field microscopy with a 20x objective lens. All images were processed using FIJI and the inserts show magnifications of the boxed areas. Scale bars represent 50  $\mu$ m. Lower panel. Numbers of cells showing morphological changes were counted and percentages of these cells were obtained by dividing to the total number of cells. At least photos of six random areas covering minimum 300 cells in each condition were subjected for quantification. **E., F., G.** were treated as **D** using Huh7.5, Huh7 and Hep3B expressing shNT or shPI4KA, respectively. \*\*\*\* $p < 0.0001$ ; \*\* $p < 0.01$

### 3.2.2. Inhibition of PI4KA leads to the same changes in cell morphology and the effect is dose-dependent

The effects of PI4KA silencing on cell morphology were remarkable. To explore if it was solely a matter of protein expression or enzymatic activity of this protein kinase also played a critical role in shaping cell morphogenesis, a selective inhibitor, namely PI4KA-F1, was applied into the culture medium of Huh7-Lunet and Huh7.5 cells. This drug was shown previously to selectively inhibit PI4KA activity and was also applied to *in vivo* studies due to its better pharmacokinetic properties over other PI4KA inhibitor (105). Indeed, morphological changes with the same features as described by PI4KA silencing were observed consistently in the inhibitor-treated cells (**Figure 13A**). The magnitude of the effects were highly time (data not shown) and dose-dependent (**Figure 13A** and **B**). Cells started to show some alterations in their morphology as soon as an overnight treatment at the highest dose and these differences compared to the control treatment became more and more prominent over time at all the dosages applied (data not shown). These courses of inhibitor treatment also described a clear process of cell shape transformation in response to PI4KA activity. At first some cells showed shrinkage of their cytoplasm which made them look compact and much darker under light microscope. The smooth and round to hexagonal shapes were gradually replaced by rough surfaces with several irregular long extensions likely due to the condensation of cell cytoplasm and the forces created among neighboring cells. At this point the border between cell cytoplasm and nucleus was hardly distinguishable, cells looked much darker and smaller in size and were highlighted by very bright surrounding area. This however did not accompany with their nucleus's size which seemed to be comparable with DMSO-treated control (**Figure 25C**). These changes occurred at several small islands and continuously spread over the whole cell population over time. Although Huh7-Lunet and Huh7.5 differ in their morphology where smaller and more compact shape are with Huh7.5, the transformation in cell shape following the PI4KA inhibitor treatment happened in the same manner with the two cell lines (**Figure 13C** and **D**). The treatment of PI4KA inhibitor F1 at 0.1  $\mu$ M also altered cell morphology of Hep3B as similarly with the other two cell lines (**Figure 13E** and **F**). These data suggested that not only PI4KA expression but more importantly its activity played crucial role in cell shape.

## RESULTS

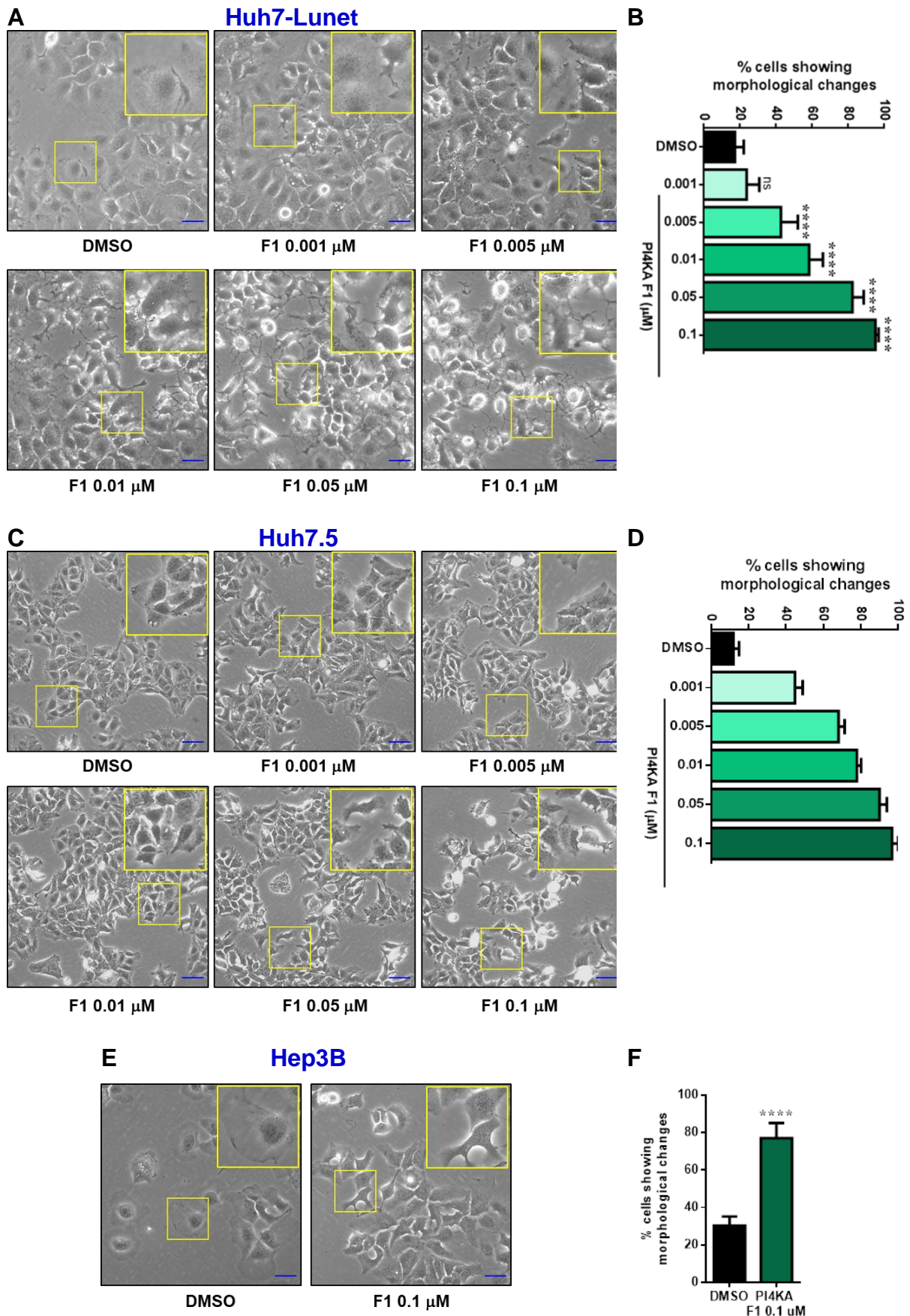


**Figure 13. Inhibition of PI4KA activity alters cell morphology in the same manner as observed with depletion of its expression and the effect is dose-dependent. A.** Huh7-Lunet cells were seeded in a 6 well-plate and incubated overnight. The cells were then treated either with DMSO or the

## RESULTS

---

indicated concentration of PI4KA inhibitor F1. Photos were captured at 48 h post treatment by bright field microscopy with a 20x objective lens. All images were processed using FIJI and the inserts show magnifications of the boxed areas. Scale bars represent 50  $\mu\text{m}$ . **B**. Numbers of cells showing morphological changes were counted and percentages of these cells were obtained by dividing to the total number of cells. At least photos of six random areas covering minimum 300 cells in each condition were subjected for quantification. **C and D** were done as similar as **A** and **B** but with Huh7.5 cells. **E**. Hep3B cells were either treated with PI4KA-F1 inhibitor at 0.1  $\mu\text{M}$  or DMSO-treated for 48 h and cell morphology was imaged by bright field microscopy with a 20x objective lens. **F**. Quantification of cells showing morphological changes were plotted using Graphpad Prism. ns: non-significant; \*\*\*\* $p < 0.0001$ ; \*\* $p < 0.01$ .

### 3.2.3. Expression of enzymatically active PI4KA reshapes cell morphology back to untreated condition

To confirm the importance of PI4KA activity and to verify that the effect of the shPI4KA on cell morphology was specific but not due to an off-target effect, reconstitution of PI4KA expression with or without kinase activity was introduced into the PI4KA knockdown cells via lentiviral-mediated overexpression. To this end, either a full-length PI4KA wt or its mutant version D1957A which has shown to possess no enzymatic activity (22) were used. These genes were expressed using a lentiviral vector expressing a blasticidin resistant protein for stable cell selection. Side by side an empty vector was introduced as a control to eliminate a bias observation which might be caused due to blasticidin used for selection of stable cell lines. Expression of PI4KA was examined and shown in **Figure 18**. Indeed, the described morphological changes due to silencing of PI4KA could only be fully reverted by supplementing PI4KA wt but not by either empty vector or kinase-dead mutant version of the enzyme (**Figure 14A** and **B**). The full reversion of cell shape by PI4KA wt was significant and demonstrated the specificity of this kinase's contribution on cell morphology. Taken together, these data confirmed the specificity of shPI4KA and suggested a strong connection between PI4KA expression and activity and cell morphogenesis.

## RESULTS

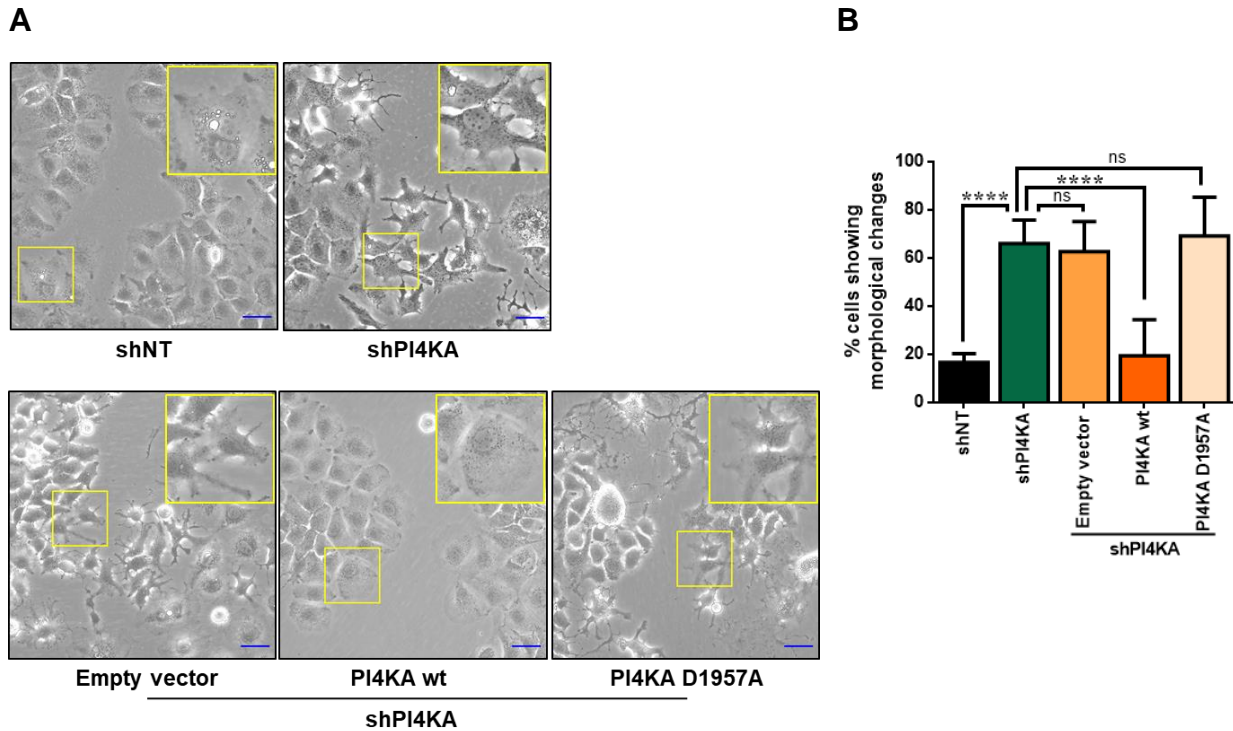


**Figure 14. Reversion of morphological changes due to PI4KA depletion by exogenously expression of wide type PI4KA.** **A.** Huh7-Lunet cells were firstly transduced with lentiviruses expressing shNT or shPI4KA and cultured in the complete medium containing Puromycin. The Huh7-Lunet-shPI4KA cells were then used as parental cells for producing the stable cell lines Huh7-Lunet-shPI4KA + empty vector or + PI4KA wt or + PI4KA D1957A by lentiviral vector-mediated overexpression. These cells were cultured under the selection pressure of blasticidin. The cells were seeded on 6-well plates and the photos of cellular morphology were taken 2 days post seeding when they reached 60-80% confluency using an inverted light microscope with 20x objective lens. The inserts show magnifications of boxed areas. Scale bars represent 50  $\mu$ m. **B.** Numbers of cells showing morphological changes were counted and percentages of these cells were obtained by dividing to the total number of cells. At least photos of six random areas covering minimum 300 cells in each condition were captured. ns: non-significant; \*\*\*\*p<0.0001.

### 3.3. PI4KA is a driver for cell invasion and migration

A previous study showed that PI4KA expression was enhanced in HCC tissues and this higher expression of PI4KA was correlated with poor prognosis of liver cancer patients (74). In this study, I found that PI4KA played important roles in controlling cell shape and manipulations of its expression or activity could drastically alter cell morphology. Transformation from benign to malignant state is often associated with changes in cellular morphology and therefore it was interesting to understand if PI4KA was involved in regulation of cell motility. To explore this possibility both cell migration and cell invasion assays were applied.

In order to obtain reproducibly similar wounding areas, I applied culture-inserts for cell migration assays. These inserts have been used intensively in studying cell migration recently and have advantages over the traditional scratching method since they produce a defined gap size as well as avoid cell and vessel surface damage and gap surface residues due to scratching cells. Using this technique, I firstly examined if silencing of PI4KA had

## RESULTS

---

effects on cell migration. Multiple pilot experiments were performed to obtain an optimal condition for recording cell migration. Antiproliferative drugs or serum-free medium were firstly used for culturing to eliminate the possible interference of cell proliferation, however significant numbers of dead cells were observed and no migration was recorded in all treatment conditions (data not shown). Serum concentration was adjusted to 3% where control cells migrated at an acceptable rate for recording without detectable presence of cell death. Overall, PI4KA-depleted cells migrated at a slower rate than the control cells as shown in **Figure 15A**. At 24h more than 60% of the gap area was covered and the remaining cell-free gap was mostly closed at 48h in Huh7-Lunet-shNT cells. Silencing of PI4KA slowed down the rate of gap closure to about 50% and 80% at 24 and 48h respectively. In support of this observation, inhibitor PI4KA-F1 markedly reduced the ability to close the cell-free gaps compared to the DMSO-treated condition. Here, approximately 50% and 85% of the cell-free gap were covered at 24 and 48 h by the DMSO-treated cells, whereas it reduced to 25% and 40%, respectively, by the inhibition of PI4KA (**Figure 15B**). 1% serum could be used for culturing in absence of cell death and therefore the cells in general migrated as a slower rate and the difference between the treatments was thus more pronounced. The discrepancy in the applied amount of serum in culture could be due to the presence of selection antibiotic in the case of stable knockdown cell lines which could affect cell viability in very low-serum culture medium. These data, however, pointed out to the same direction that both PI4KA expression and activity are important for cell migration.

The involvement of PI4KA in cell motility was further assessed on invasive property using Matrigel Invasion Chambers. In this assay, cells were seeded in the chambers in the presence of lowest possible amount of serum which cells could still tolerate (3% in the case of stable cell lines and 1% in the case of inhibitor treatment). Invasion was triggered by placing 10% complete medium under the chambers. The Matrigel Matrix serves as a reconstituted basement membrane and occludes the pores of the membrane, blocking non-invasive cells from migrating through the membrane. Only invasive cells could degrade this matrix to invade to the bottom part of the chambers. In accordance with cell migration assay, I also observed an approximately 3 times reduction in cell invasion in Huh7-Lunet cells expressing shPI4KA (**Figure 15C**). This observation was further confirmed using mouse hepatoma cells Hep55.1C. These cells in general displayed a better invasive property than Huh7-Lunet, however, silencing of PI4KA also led to a reduction of 60% in their invasiveness (**Figure 15D**). Moreover a similar reduction rate in cell invasion was also observed in cells treated with PI4KA inhibitor F1 in comparison with DMSO treatment (**Figure 15E**). Furthermore, only expression of PI4KA wt but not the mutant version of this kinase could fully restore the invasiveness in shPI4KA cells (**Figure 15F**), confirming that activity of PI4KA was necessary for cell motility including cell invasion and migration. In further experiments, I focused on cell invasion assays as I observed more robust phenotypes and because of its higher relevance for tumor pathogenesis. In order to successfully invade into the surrounding tissue, tumor cells develop several strategies to break down cell-cell contacts and reorganize cell-matrix adhesion sites. Among them, a reversible process known as EMT where non-motile and polarized epithelial cells transform to individually polarized, motile and invasive mesenchymal cells is in many cases utilized by tumor cells for their invasiveness. EMT is

## RESULTS

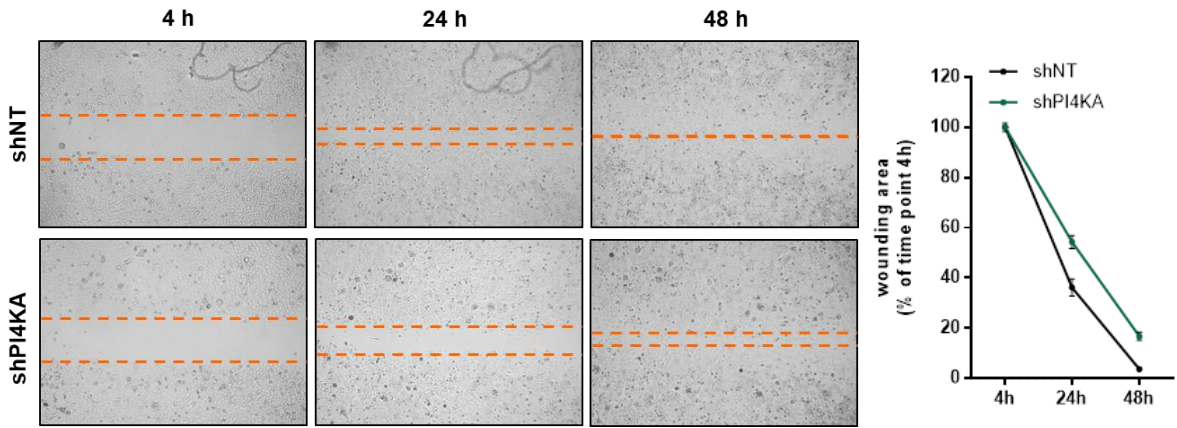
---

recognized by a loss of epithelial cell markers, such as E-cadherin, and an upregulation of mesenchymal markers, such as Vimentin. Immunoblot analysis revealed that E-cadherin expression was consistently higher in PI4KA-silenced cells (**Figure 15G**), indicating a reversion of the EMT process in these cells, accompanying with less invasiveness as shown by the invasion assay. In conclusion these data suggested a significant contribution of the phosphokinase protein PI4KA on cell motility which could favor cancerous progression.

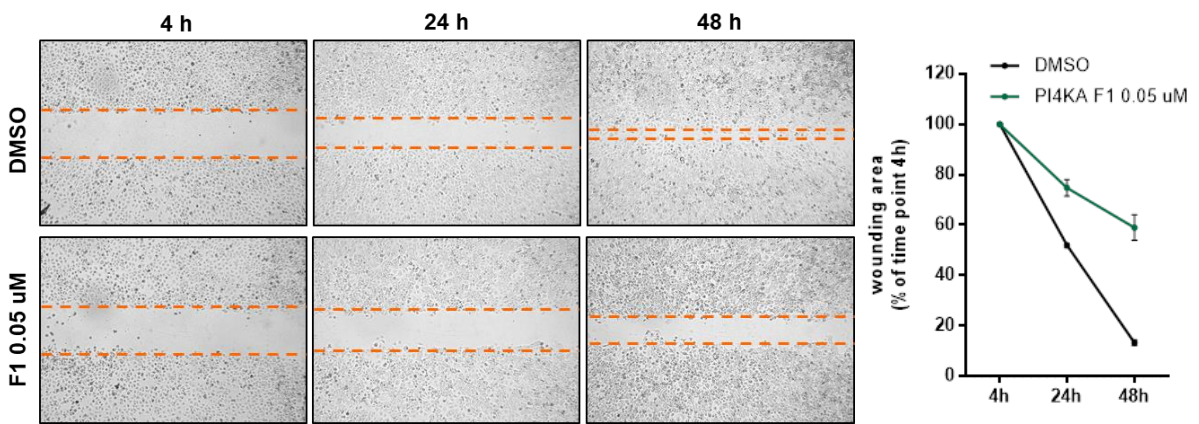


# RESULTS

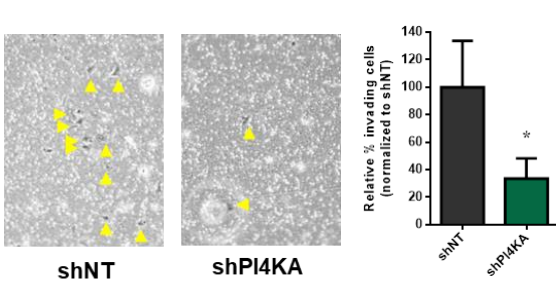
**A**



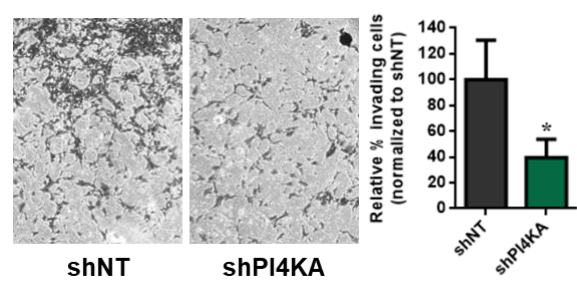
**B**



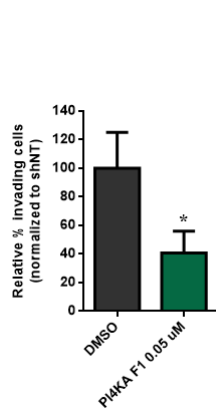
**C**



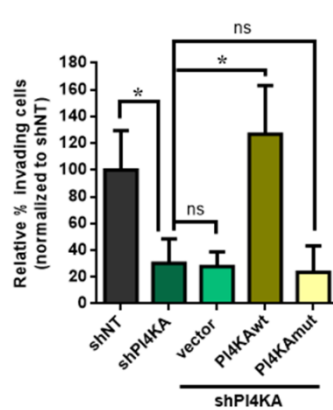
**D**



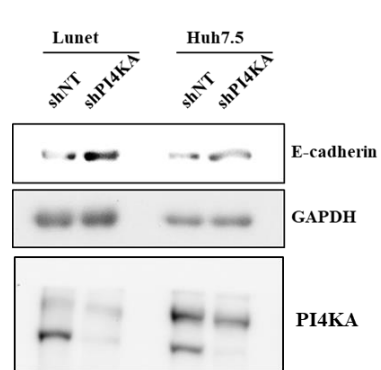
**E**



**F**



**G**



## RESULTS

---

**Figure 15. PI4KA is important for cell migration and invasion.** **A.** Left panel. Huh7-Lunet stably expressing shNT or shPI4KA were seeded in culture-inserts 2 well placed in a 24-well plate. 4 h post seeding the inserts were removed and medium containing 3% FCS was added. Cell-free gaps were imaged using an inverted bright field microscope at the indicated time points. Right panel. Wound closure expressed as the remaining area uncovered by the cells were marked and quantified using FIJI. The scratch area at time point 4 hours was set to 100%. **B.** Left panel. Huh7-Lunet were seeded in culture-inserts 2 well placed in a 24-well plate. 4 h post seeding the inserts were removed and medium containing 1% FCS together with either 0.05% PI4KA-F1 or the same volume of DMSO were added and images were captured at the indicated time points. Right panel. Quantification of wounding area was done as **A.** **C.** Huh7-Lunet stably expressing shNT or shPI4KA were seeded on rehydrated Corning BioCoat Matrigel Invasion Chambers with 8.0  $\mu\text{m}$  PET Membrane in the presence of 3% FCS. These chambers were placed in wells of a 24-well plate containing 10% FCS medium and allowed for a 24 h incubation. Invasive cells attached on the lower surface of the membrane were fixed and stained with crystal violet. Images were recorded using an inverted microscope connected with camera (left panel). Numbers of invasive cells were quantified and relative fold change in the invasiveness were normalized to the Huh7-Lunet-shNT samples. **D.** Experiment was proceeded as **C** using Hep55.1C stably expressing shNT or shPI4KA. **E.** Huh7-Lunet cells were seeded on the Matrigel Invasion Chambers in the presence of 1% FCS and 0.05  $\mu\text{M}$  PI4KA or the same volume of DMSO. Experiment was performed and data were analyzed as **C.** **F.** Invasiveness of Huh7-Lunet expressing shNT or shPI4KA with or without ectopic expression of PI4KA were evaluated as performed in **C.** **G.** Cell lysates from Huh7-Lunet and Huh7.5 expressing shNT or shPI4KA were extracted and Immunoblot analysis was performed to examine protein expression of E-cadherin. ns: non-significant; \* $p < 0.05$ .

### 3.4. PI4KA upregulates phosphorylation of Paxillin and Cofilin

#### 3.4.1. Immunofluorescence combined with live -cell imaging reveals dynamic changes in cell cytoskeleton in PI4KA knockdown cells

Considering the key role of actin cytoskeleton in all morphogenesis processes (106,107) as well as in cell motility (107), I speculated that PI4KA could likely signal reorganization of cytoskeletal structures via a connection with proteins in this network, resulting in the morphological transformation and promotion of cell movement. To test this hypothesis, we examined the three main components of the cytoskeleton network – actin, tubulin and intermediate filaments in shNT and shPI4KA expressing cells using confocal microscopy. We further monitored dynamics of F-actin and tubulin labeled by the fluorophore silicon rhodamine (SiR), a cell permeable and highly specific probe with the help of live cell imaging. This part was mainly performed by Julia Kersten under the supervision and according to experimental design of this PhD candidate. Details of experimental setup, optimization and observation can be found in Julia Kersten's Master thesis (122).

With immunofluorescence, we firstly confirmed my previous observations on morphological changes and further expand our understanding on this dynamic process. The shNT cells were evenly spread with actin fibers, microtubules and intermediate filaments evenly distributed through out the cell body. The actin network was organized in different structures including cell cortex, stress fibres, transverse arcs, lamellipodium and filopodia. In contrast, PI4KA knockdown cells showed actin condensation around the nucleus. Long actin fibres were often missing, leaving these cells with actin network of branched and short filaments, indicating differences in actin polymerization (**Figure 16A**). Live cell imaging in the shNT cells revealed a highly dynamic and constantly rearranging actin network with strongly labeled cell cortex and lamellipodium which are typically involved in cell migration. PI4KA-

## RESULTS

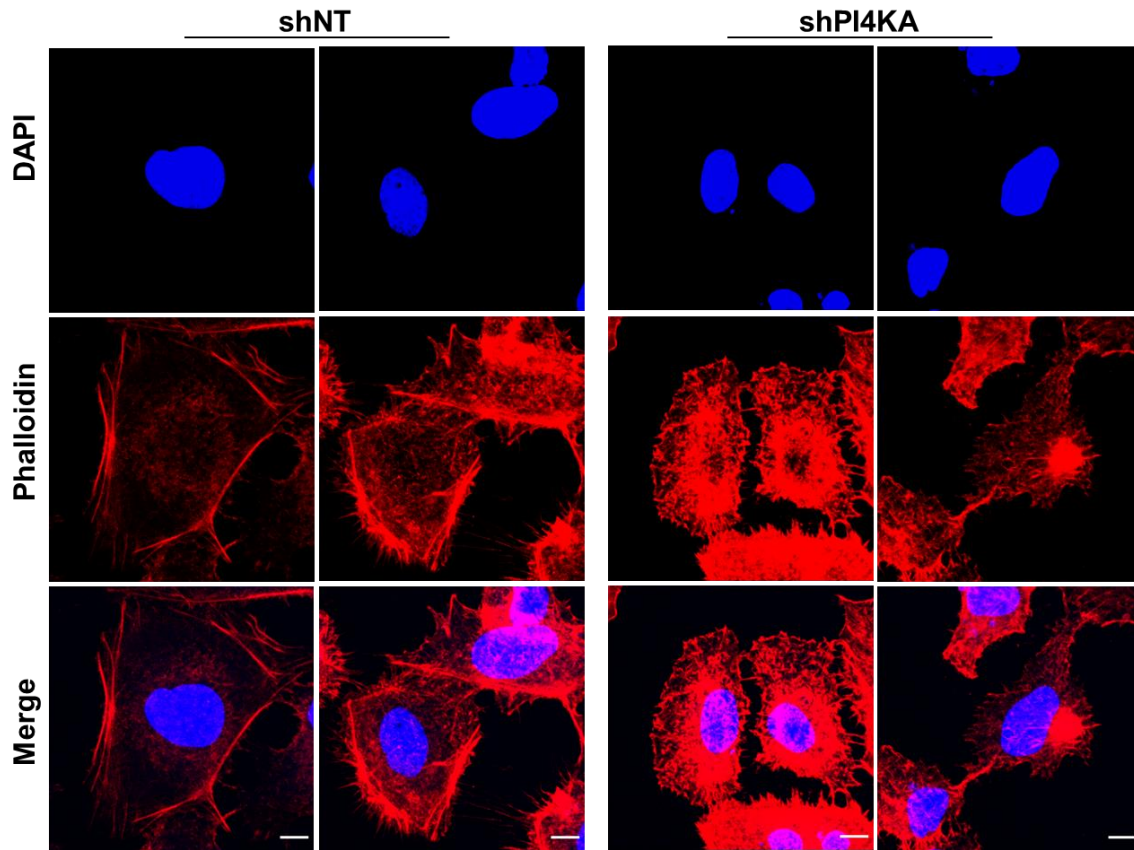
---

depleted cells however were more static with lesser prominent lamellipodia and reduced directional migration (**Figure 16C**), in line with their previously observed reduced motility.

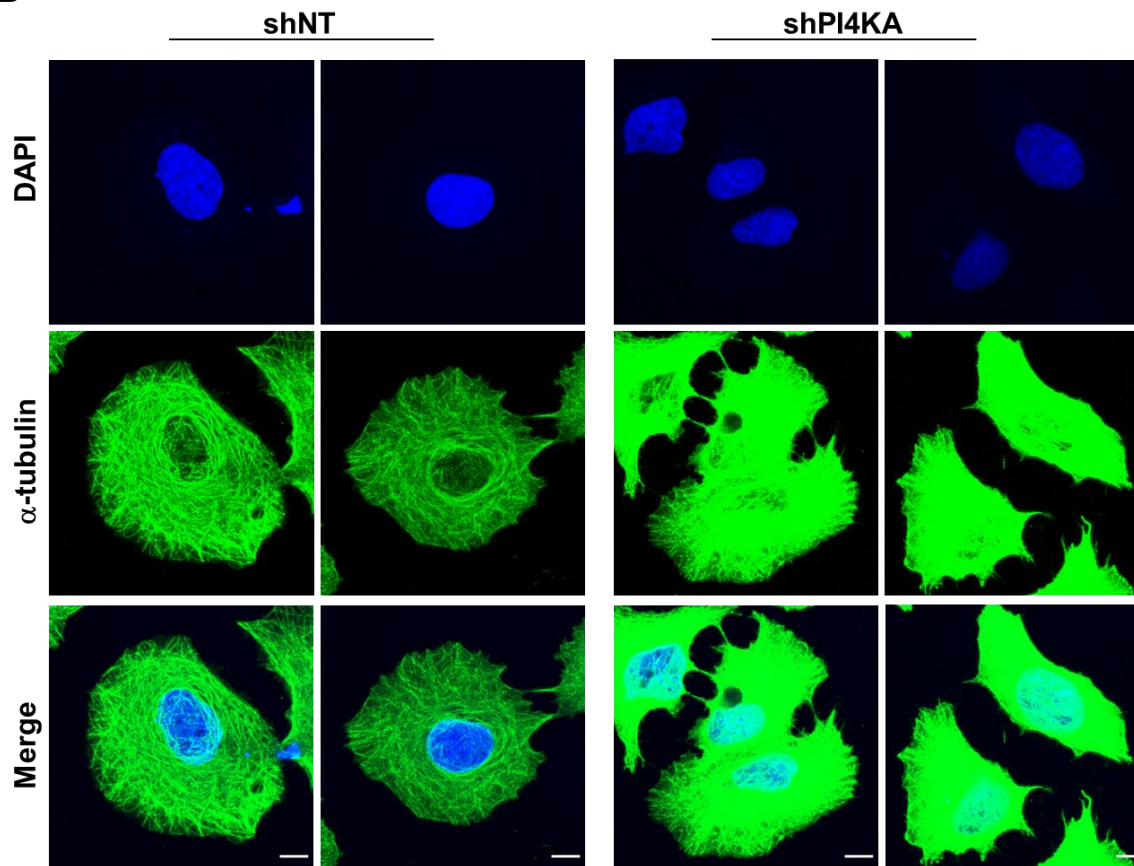
Similarly, microtubules were evenly distributed and organized into a universal fine network in the Huh7-Lunet-shNT cells but PI4KA knockdown also led to highly condensed meshwork of microtubules with many indiscernible fibres (**Figure 16B**). The dynamics and rearrangement of microtubules were also less frequently observed in the cells with lower PI4KA expression (**Figure 16D**). In addition, intermediate filaments revealed by cytokeratin 8 staining also significantly differed between the two cell lines (data not shown). While control cells with high expression of PI4KA showed a widely distribution of fine intermediate fibres, we recorded thicker but shorter patches and filament bundles in cells lacking PI4KA which concentrated densely around the nucleus. Taken together, these data demonstrated that PI4KA depletion overall led to significant alterations in morphology and organization of all the three cytoskeleton components (**Figure 16**).

# RESULTS

**A**

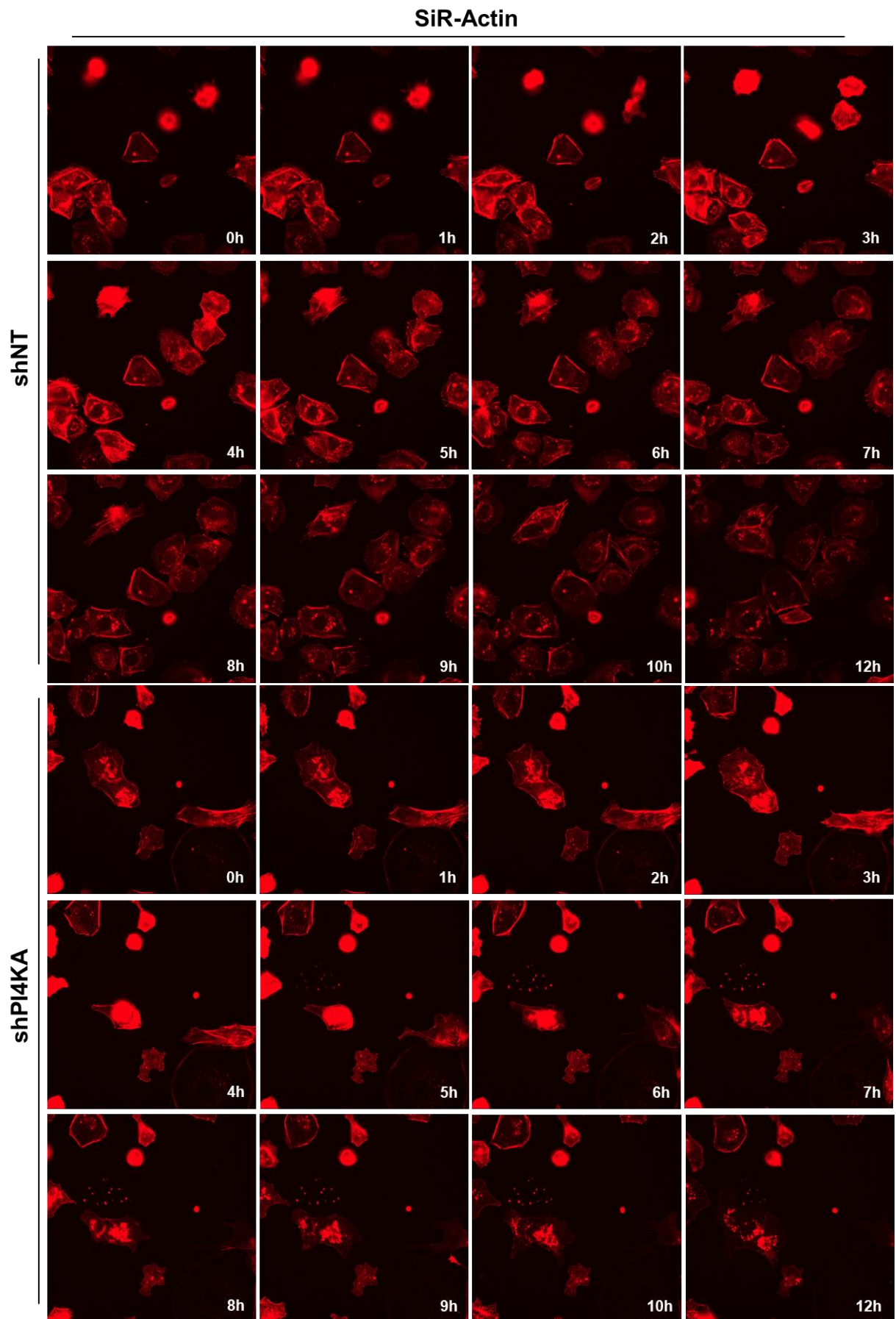


**B**



# RESULTS

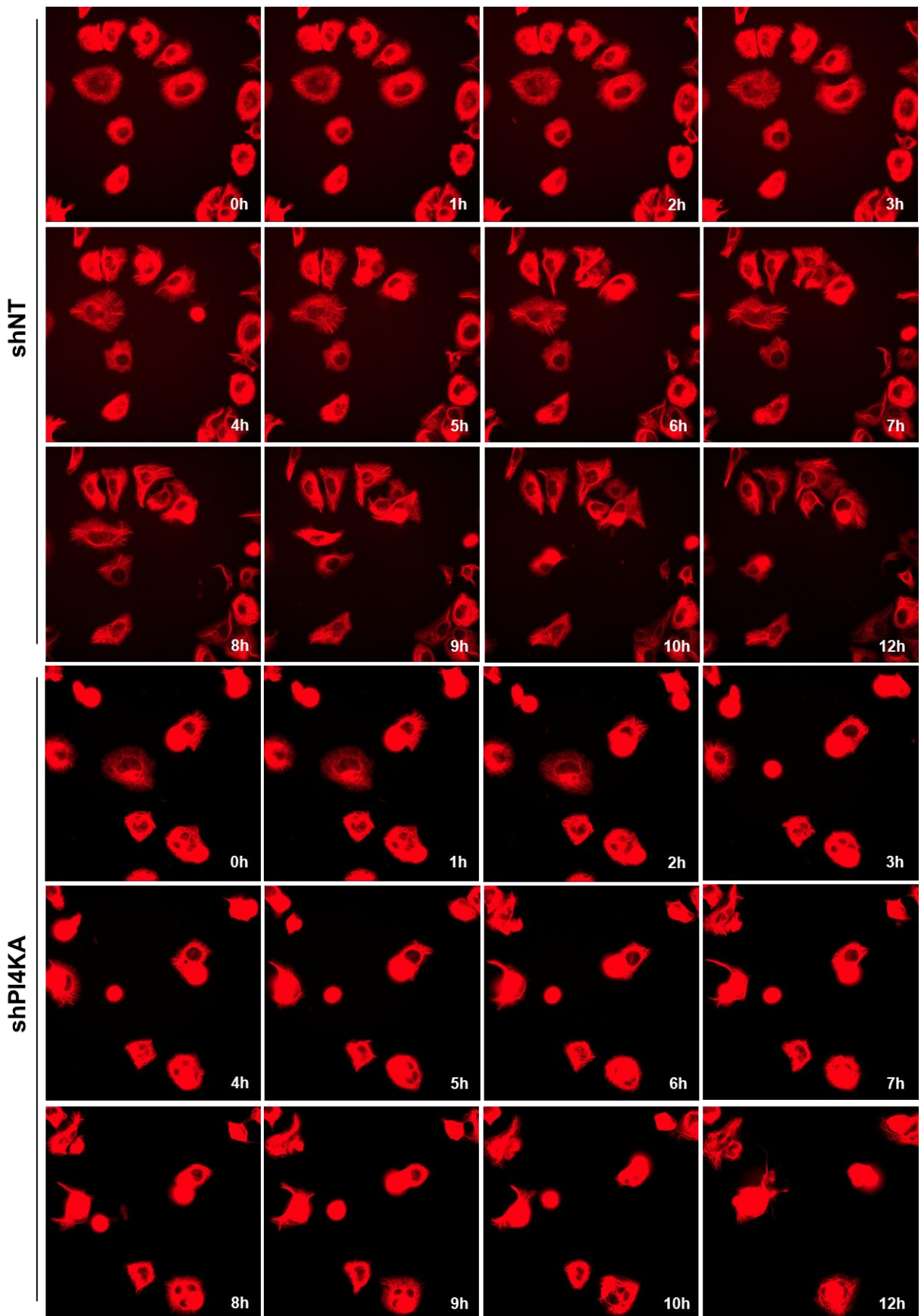
C



# RESULTS

D

SiR-Tubulin



## RESULTS

---

**Figure 16. Silencing of PI4KA leads to dramatic alterations in cytoskeleton network of filaments as revealed by IF and live-cell imaging.** **A.** Huh7-Lunet cells stably expressing shNT or shPI4KA were seeded on coverslips and incubated overnight, followed by a fixation with PFA. F-actin and nuclei were stained with Phalloidin (red) and DAPI (blue), respectively. **B.** Cells were seeded as in **A.** and tubulin and nuclei were stained with an antibody against  $\alpha$ -tubulin (green) and DAPI (red), respectively. Cells were imaged by laser-scanning confocal microscopy. Scale bars represent 10  $\mu$ m. **C.** Huh7-Lunet cells stably expressing shNT or shPI4KA were labelled for 6 h with SiR-actin at 25 nM. Labelling medium was then replaced by non-phenol red imaging medium supplemented with 25 nM SiR-actin and 10  $\mu$ M verapamil. Live-cell imaging was recorded at 30 minutes interval for 12 hours. **D.** Huh7-Lunet cells stably expressing shNT or shPI4KA were labelled for 6 h with SiR-tubulin at 500 nM in the presence of 10  $\mu$ M verapamil. Labelling medium was then replaced by phenol red-free imaging medium supplemented with 100 nM SiR-tubulin and 10  $\mu$ M verapamil. Live-cell imaging was recorded at 30 minutes interval for 12 hours.

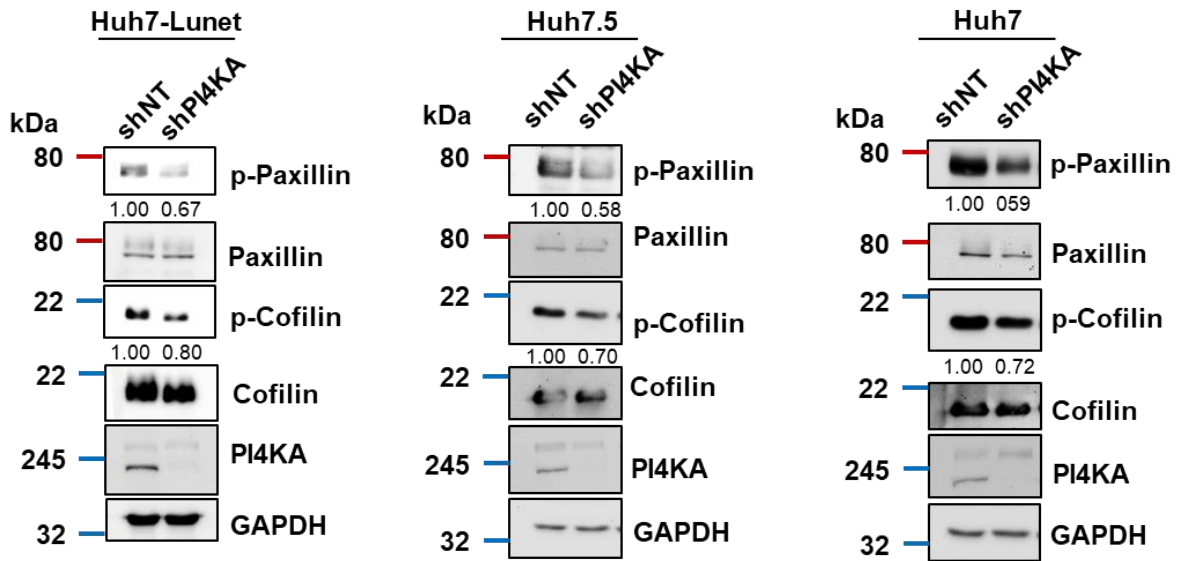
### 3.4.2. Suppression PI4KA activity and/or expression reduces levels of p-Paxillin and p-Cofilin

In search of a possible link between PI4KA and actin cytoskeleton, I came across a recent work of Ziyad and colleagues (108). Applying an antibody array targeting 878 cell signaling proteins using lysates from HEK293 cells transfected with siRNA against PI4KA and control siRNA, the authors identified a variety of dysregulated signaling pathways (108). Interestingly, proteins involved in cytoskeleton regulation were among the most affected in which p-Paxillin (PXN) Y31 and cofilin (CFL1) showed the highest z-scores (108). Applying cytoskeleton phospho antibody array (Full Moon Biosystems), covering 141 highly specific antibodies related to cytoskeleton regulation to Huh7-Lunet treated with PI4KA inhibitor F1, I also identified p-Paxillin Y31 and cofilin, among others, as the proteins with expressions reduced by inhibition of PI4KA activity (**Appendix 2**). Both paxillin and cofilin play key roles in structuring cytoskeletal networks and dysregulation of these two proteins link to many diseases. While the anchorage of the actin cytoskeleton in FA requires proper function of PXN (109), CFL1 enhances actin dynamics by its F-actin-severing and depolymerizing activities (110). They are in addition important in cancer research as their phosphorylation status have been shown to be necessary for cancer cell migration and invasion and involved in chemotherapy resistance (111,112,113,114,115,116).

Based on the screening data from Ziyad S et al. performed in HEK293T cells and my data obtained from the cytoskeleton phospho antibody array, I aimed to know if PI4KA regulated phospho-paxillin (pPXN) and cofilin (CFL1) in human hepatocytes as well, potentially causing the cytoskeletal changes observed in my study. Using shRNA-mediated gene silencing, I indeed observed a significant reduction in the levels of p-paxillin in PI4KA-depleted cells while the total expression of paxillin remained unchanged (**Figure 17A**). Interestingly, even though Ziyad S et al. (108) and my own screening (**Appendix 2**) independently suggested a strong reduction in total expression of cofilin, western blot analysis revealed no major change. However, I instead observed a slight reduction in p-cofilin levels (**Figure 17A**). These phenotypes were consistently revealed in a panel of Huh7-derived cell lines, including Huh7-Lunet, Huh7.5 and Huh7 (**Figure 17A**). The effects of silencing PI4KA on the levels of p-paxillin and p-cofilin was also replicated in Hep3B and HepG2 (**Figure 17B**). These data together indicated that increased expression of PI4KA in liver cancer cells was important for the enhanced phosphorylation of paxillin and cofilin.

## RESULTS

**A**



**B**

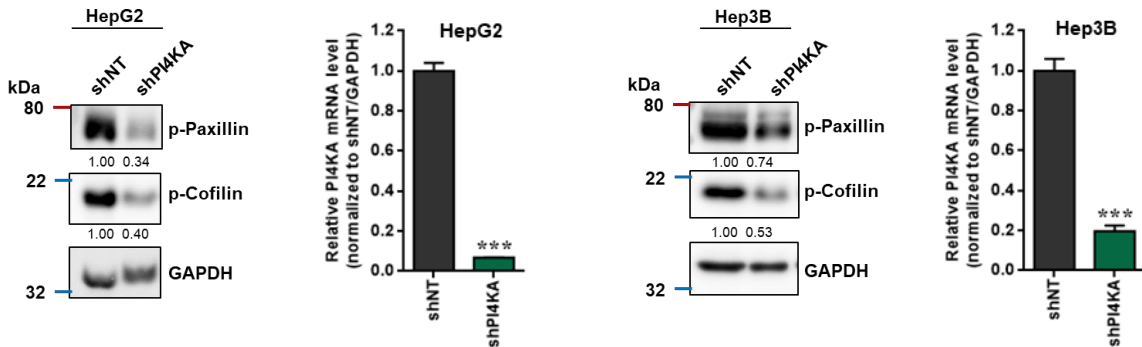


**Figure 17. Silencing of PI4KA reduces phosphorylation levels of phospho paxillin and cofilin.** **A.** Huh7-Lunet, Huh7.5 and Huh7 cells were either stably transduced with lentiviruses expressing shNT or shRNA against PI4KA. Total lysates from these cells were subjected to Western blot for probing phospho and total paxillin and cofilin. Signal intensities of each phospho-protein were quantified using FIJI and normalized to the corresponding total protein. Relative values were then normalized to the corresponding value of the control sample shNT. **B.** Silencing of PI4KA was carried out in HepG2 and Hep3B cells as done in **A.** Signal intensities of p-paxillin and p-cofilin were normalized to GAPDH. Total RNA from these cells were extracted and relative levels of PI4KA were quantified using RT-PCR and plotted on the graphs using Graphpad.

### 3.4.3. Both PI4KA abundance and activity are important for the phosphorylation of paxillin and cofilin

Silencing of PI4KA reduced expression levels of the two phospho proteins, p-paxillin and p-cofilin. To investigate if kinase activity of this enzyme was also associated with phosphorylation of paxillin and cofilin, PI4KA-F1 inhibitor was applied at various doses to Huh7-Lunet. Along with a dose-dependent morphological alteration as mentioned previously, inhibition of the kinase activity also led to a concomitant reduction of p-paxillin and p-cofilin (**Figure 18A**). There was already a drop in phosphorylation of paxillin at the lowest dose of the treatment (by 21% at 0.001  $\mu$ M) and this phosphorylation loss continued down to approximately a half at the two highest doses applied (**Figure 18A**). In contrast, no significant change in the level of p-cofilin was observed at lower doses of the inhibitor and a roughly 20-30% reduction of this phospho protein occurred at 0.05 and 0.1  $\mu$ M treatment of



## RESULTS

the PI4KA inhibitor (**Figure 18A**). This observation was in agreement with the effect of silencing PI4KA on the levels of p-paxillin and p-cofilin (**Figure 17A**), indicating that PI4KA has a stronger influence on phosphorylation of paxillin than that of cofilin. It was also noted that the inhibitor treatment did not affect expression level of PI4KA in cells (data not shown). To further verify the effects of PI4KA depletion as well as activity inhibition on the two phospho proteins, a wt or an inactive mutant of PI4KA was introduced into the PI4KA knockdown cell line. The loss of p-paxillin and p-cofilin caused by silencing of PI4KA could only be reverted by the replenishment of PI4KA wt but not the mutant or vector control (**Figure 18B**), suggesting a tight association of PI4KA abundance and activity with phosphorylation events of the two proteins. Considering these proteins as the key components of cytoskeleton, my data implicated that PI4KA contributed to the cytoskeletal rearrangement transforming cell morphology and favoring cell motility via upregulation of paxillin and cofilin phosphorylation.

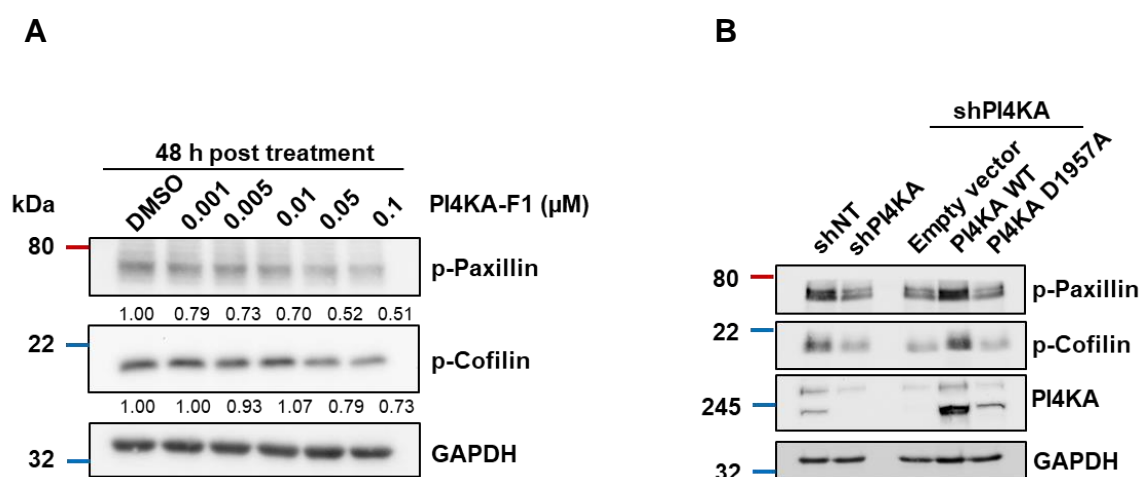


**Figure 18. PI4KA abundance and activity are important for the phosphorylations of paxillin and cofilin.** **A.** Huh7-Lunet cells were treated with DMSO or different doses of PI4KA-F1 and cell lysates were collected at 48 h post treatment and subjected to Western blot analysis for levels of the two phospho proteins paxillin and cofilin. **B.** Huh7-Lunet cells stably expressing shNT or shPI4KA as well as Huh7-Lunet-shPI4KA cells stably expressing PI4KA wt or mutant D1957A or empty vector were seeded on 6-well plates and protein lysates were extracted at 48 h post seeding. Immunoblot analysis was performed to assess the expression of p-paxillin, p-cofilin, PI4KA and GAPDH.

### 3.4.4. Constitutive active p-Paxillin reverts morphological changes and regains motility loss induced by silencing of PI4KA

In this study, I found that lowering PI4KA expression or activity reduced levels of p-paxillin and p-cofilin. Paxillin is a phosphotyrosine-containing protein and is localized to FAs (109). Following integrin-dependent cell adhesion to ECM proteins or stimulation with growth factors, neuropeptides, ligands for G-protein coupled receptors, antigen and physical stress, paxillin is phosphorylated and serves as an adaptor protein to recruit diverse cytoskeleton and signaling proteins for the transmission of downstream signals (109). Paxillin can be phosphorylated at multiple sites, among them tyrosines Y31 (identified in this study) and Y118 are the major phosphorylation sites (109). Cofilin is a small actin-binding protein which regulates spatial and temporal extent of actin filament dynamics. It can be found in multiple cellular compartments (117). Cofilin performs its functions in both initiating asymmetric actin

## RESULTS

polymerization in the first step and recycling actin filaments in later steps (117). The relative balance of actin polymerization and depolymerization controlled by cofilin is determined significantly by the relative concentrations of active cofilin and ATP G-actin. Phosphorylation of cofilin at the Serine S3 disrupts all cofilin–actin interactions (117). Studies have suggested the roles of paxillin and cofilin (un- and phosphorylated forms) in regulation of cancer progression and metastasis but contradictory phenotypes were observed (109,110,111,112,113,114,115,116,117). To clarify if phosphorylation of paxillin and cofilin is important for PI4KA's regulation on cell morphology and cell invasion, I expressed either wt or constitutive active mutant of paxillin and cofilin (PXN Y31D, CFL1 S3A, respectively) in the PI4KA-knockdown cells. As shown in **Figure 19A**, while expression of the constitutive active mutant but not wt of paxillin dramatically reverted the morphological changes observed in PI4KA-knockdown cells, both wt and constitutive active mutant of cofilin showed minor effects. This was in agreement with my previous findings that PI4KA exerted effects on phosphorylation of paxillin in a larger extent than that of cofilin. Moreover, I also found that PXN Y31D could partially restore the invasiveness in shPI4KA cells (**Figure 19B**). These data suggested that paxillin was one of the main downstream signaling molecules of PI4KA in regulation of liver cancer cell morphology and motility.

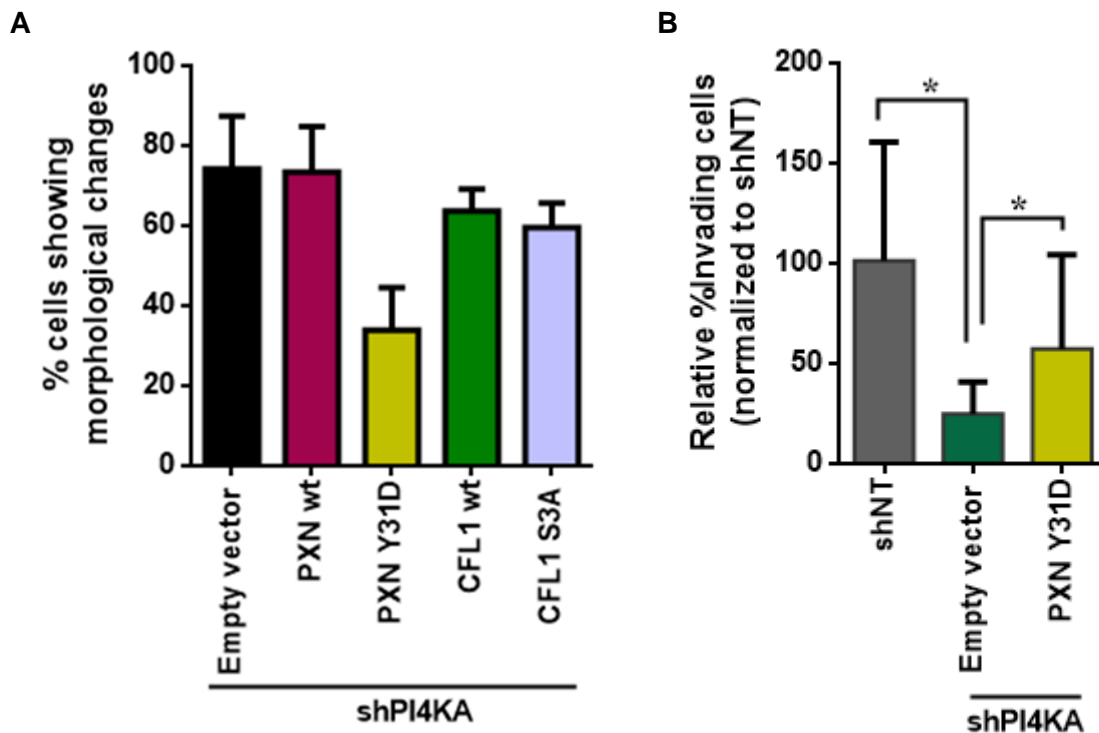


**Figure 19. Reversion of PI4KA silencing effects on cell morphology and cell invasion by constitutive active paxillin.** **A.** Huh7-Lunet-shPI4KA were transduced with lentiviruses encoding either paxillin or cofilin wt or their constitutive active mutants Y31D or S3A, respectively. These cells were seeded in a 6-well plate and morphology of the cells was monitored and recorded using an inverted bright-field microscope. Graph represents percentages of cells showing morphological changes. At least photos of six random areas covering minimum 300 cells in each condition were subjected for quantification. **B.** Huh7-Lunet stably expressing shNT or shPI4KA in the presence of paxillin Y31D or empty vector were seeded on rehydrated Corning BioCoat Matrigel Invasion Chambers with 8.0  $\mu$ m PET Membrane in the presence of 3% FCS. Invasive cells attached on the lower surface of the membrane were fixed and stained with crystal violet. Numbers of invasive cells were quantified and relative fold changes in the invasiveness were normalized to the Huh7-Lunet-shNT samples.

## RESULTS

---

### 3.4.5. FA numbers are linked to PI4KA expression and activity

FAs are large, dynamic multi-protein complexes which contain integrin and provide a link between cytoskeleton and extracellular substrate. As mentioned previously, FAs contribute significantly to regulation of cell shape and cell motility. Since I found that PI4KA expression and activity were important for controlling cell morphology and movement as well as phosphorylation of paxillin, a key component of FAs, I wondered if these special cell structures were regulated by PI4KA as well. To address this question, I stained cells with either paxillin (**Figure 20A**) or p-paxillin (**Figure 20B**) antibody, together with Phalloidin to monitor actin filaments. In both cases I observed a significant reduction in numbers of FAs when cells were PI4KA depleted (**Figure 20A, B and C**). Intensity of p-paxillin stainings was lower in PI4KA-silenced cells while the total paxillin staining was similar between the two samples, further confirmed my previous observation by Western blot (**Figure 17A**). I also noticed that only expression of PI4KA wt but not its enzyme-dead mutant nor empty vector could bring the FA numbers in the PI4KA-silenced cells to the levels in shNT control sample (**Figure 20D**). These data taken together highlighted the importance of PI4KA in regulation of cell adhesion, and thus its potential contribution to cell motility.

## RESULTS

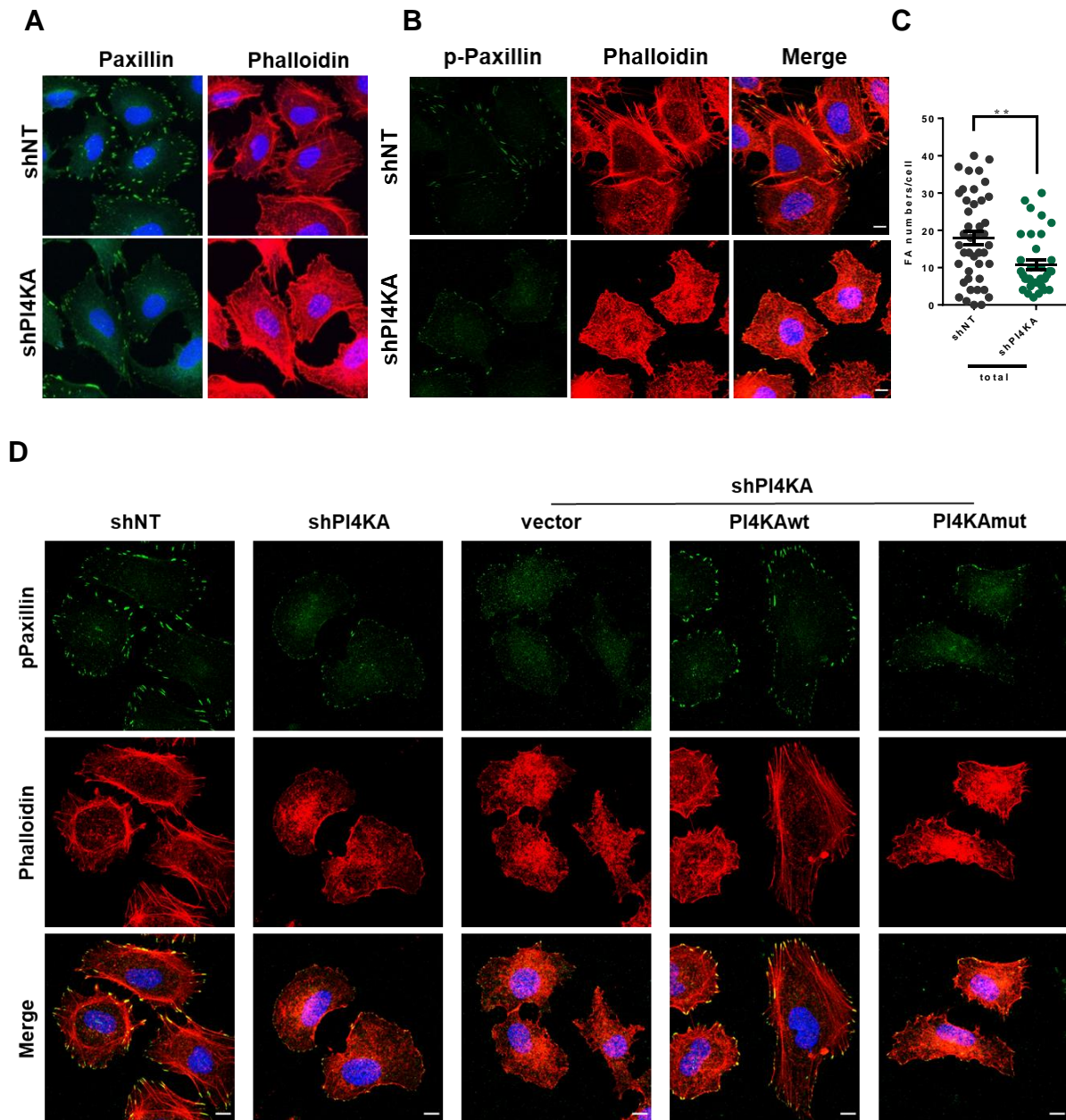


**Figure 20. FA numbers are tightly linked with PI4KA expression and activity.** **A and B.** Huh7-Lunet cells expressing shNT or shPI4KA were seeded on coverslips and incubated overnight. Cells were then stained with either paxillin or p-paxillin antibody. Phalloidin was used to indicate F-actin. Nuclei were stained with DAPI. **C.** Whole-cell Z-stack were recorded to quantify total amounts of FAs using Fiji. At least 30 cells per condition were quantified. **D.** Huh7-Lunet cells stably expressing shNT or shPI4KA as well as Huh7-Lunet-shPI4KA cells stably expressing PI4KA wt or mutant D1957A or empty vector were seeded on coverslips and staining of FA as well as actin filaments were performed as in **B**.

## RESULTS

---

### 3.5. PI4KA activation by HCV enhances paxillin and cofilin phosphorylation

HCV has been shown to activate PI4KA and in turn induce PI4P production at replication site which is important for the integrity of the viral replication complexes (81,84). In this study, I found that expression and activity of PI4KA were required for cell motility via regulation of the cytoskeleton, in particular increased-phosphorylation of paxillin and cofilin. It was, therefore, intriguing to know if the activation of PI4KA by HCV could contribute to the virus-induced liver pathogenesis. To address this question, firstly Huh7.5 cells were either infected with HCV Jc1 virus (gt 2a) or mock infected for 4 days. I confirmed a 2.5 folds induction of PI4P in the infected cells (**Figure 21A**, left panel), indicating an activation of PI4KA. I next sought to determine expression of the two cytoskeletal components paxillin and cofilin. While total levels of paxillin and cofilin remained unchanged, there was a significant up to 3 fold increase in expression of p-paxillin compared to mock-infected cells (**Figure 21A**, right panel). However I only noticed a slight upregulation of p-cofilin in the infected cells in agreement with my previous finding that PI4KA expression and activity positively regulated p-paxillin levels in a stronger manner than p-cofilin. Moreover, using immunofluorescence I also found an approximately 3 fold increase in the number of FAs in the HCV-infected cells, in accordance with previous data showing a positive correlation between PI4KA activity and FA numbers (**Figure 21B**). To corroborate my hypothesis that enhanced phosphorylation of paxillin and cofilin in HCV-infected cells was a result of PI4KA activation, a replication-independent model was utilized where the HCV nonstructural polyprotein NS3-5B (JFH1, gt 2a) was expressed using adenoviral vectors and I firstly applied this to Huh7-Lunet cells. This replication-independent model is known to be sufficient to induce PI4KA activation and allows applying inhibitors and mutants interfering with replication. In this model, HCV NS3-5B wt was shown to induce PI4P about 2 fold whereas 2 variants with mutations in NS5A (namely S2208A and PPH) shown previously to disrupt the interaction with PI4KA (75,87) only slightly increased PI4P levels compared to empty vector (**Figure 21C**, left panel). As shown in the **Figure 21C** (right panel), levels of phospho-paxillin were indeed corresponding to the induction of PI4P in these cells, with 1.84, 1.38 and 1.25-fold upregulation in the HCV NS3-5B wt, mutant S2208A and mutant PPH expressing cells, respectively. I also noticed a minor increase of p-cofilin, in the HCV NS3-5B wt expressing cells but there was not much difference in the magnitude of changes among the HCV variants (**Figure 21C**, right panel). To corroborate my observation in a more physiological model, PHHs were used. However these cells are not permissive for infection as well as difficult to transfect. However, adenoviral transduction was indeed successful in expression of HCV NS3-5B in PHHs (**Figure 21D**). Using this model, I confirmed increased phosphorylation of paxillin and cofilin. I further asked if other HCV genotypes could also upregulate the pathways as observed with the gt 2a Jc1 and JFH1. I therefore transfected full-length RNAs of a panel of cell culture adapted HCV isolates from different genotypes (1a: H77, TN; 3a: DBN3a, S52; 4a: ED43; 5a: 5A13; 6a: HK6a) into Huh7.5 cells via electroporation and examined the levels of PI4P induction in the electroporated cells. I noticed that the levels of PI4P did not necessarily correlate with the expression of HCV NS5A (**Figure 21E**). In case of HK6a, neither NS5A nor

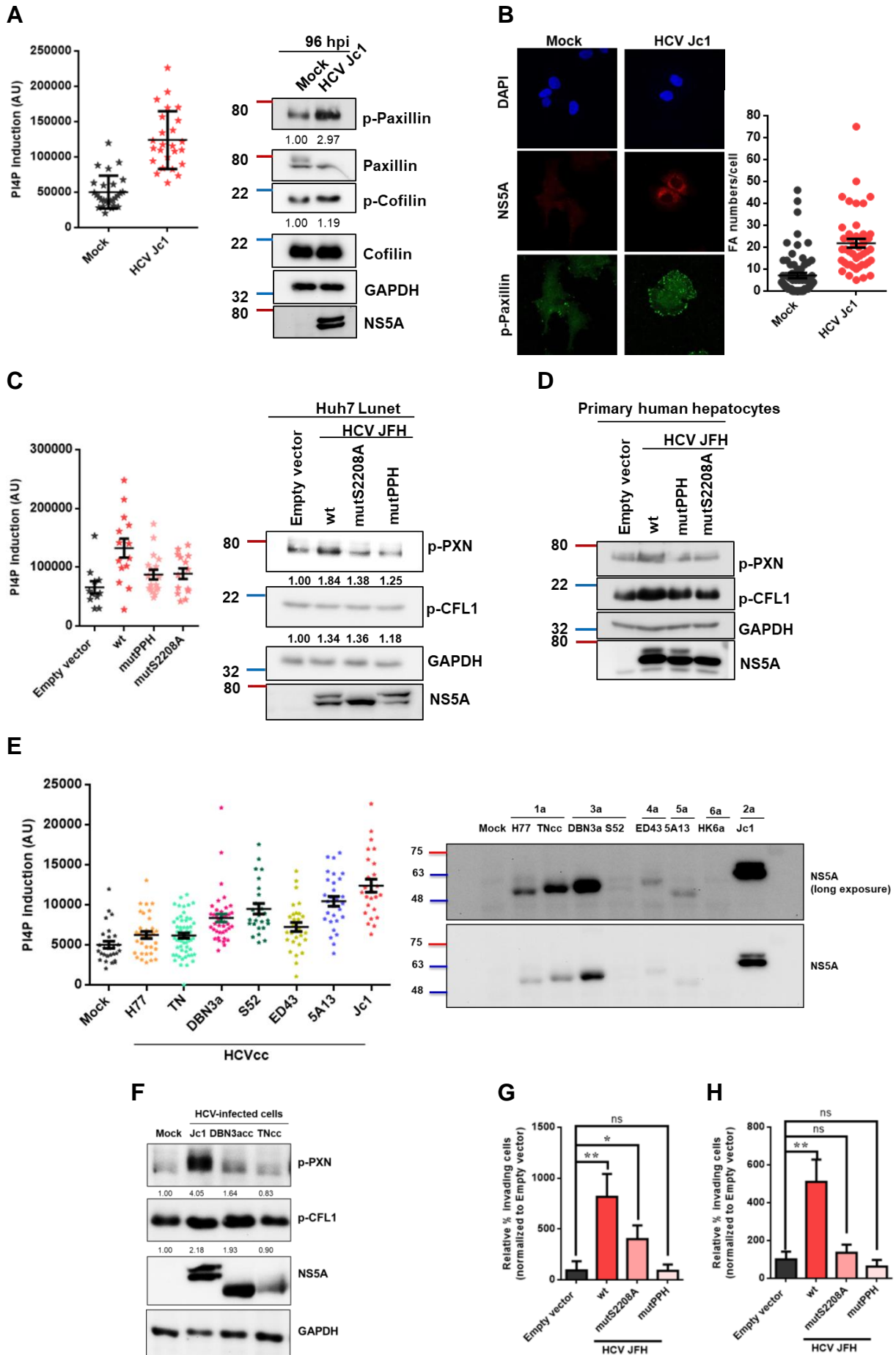
## RESULTS

---

HCV-positive cells (data not shown) were detectable, which might be due to low replication efficiency or lack of reactivity of the antibody. Furthermore, HCV replication and levels of PI4P induction in all the tested samples were not as high as in the case of HCV Jc1 (**Figure 21E**). I selected TNcc and DBN3a for further examination due to their comparable replication efficiency, but lower PI4P induction. I then used cell culture derived viruses of these isolates and infected naïve Huh7.5 cells to investigate the levels of p-paxillin and p-cofilin. There was a strong correlation between levels of PI4P induced and expression of the two phospho proteins. While HCV Jc1 still showed the highest increase, DBN3a could also moderately upregulate the phosphorylation of paxillin and cofilin which correlated with its moderate induction of PI4P (**Figure 21F**). TNcc did not show any significant changes in both phosphorylation of the two proteins and in PI4P levels (**Figure 21F**). Taken together these data indicate that HCV upregulated expression of p-paxillin and to a lesser extent p-cofilin via activation of the lipid kinase PI4KA.

Due to the importance of PI4KA in cell motility, I also examined the invasiveness of HCV-expressing cells. In agreement with my previous findings, cells expressing HCV NS3-5B wt also showed an upregulation of cell invasion to approximately 8 and 5 folds, respectively, in Huh7-Lunet and HHT4. Moderately enhanced cell invasion was still observed in cells expressing the mutant S2208A with 4 and 1.3 folds in Huh7-Lunet and HHT4 cells, respectively, but was completely abrogated in the cells expressing the mutant PPH (**Figure 21G and H**). These data strongly suggested that PI4KA activity linked HCV with upregulated phosphorylation of paxillin and cofilin and with enhanced invasiveness.

# RESULTS



## RESULTS

**Figure 21. HCV-activated PI4KA upregulates p-paxillin and p-cofilin and enhances number of FAs as well as cell invasion.** **A.** Left panel. Huh7.5 cells were either infected with HCVcc Jc1 at MOI=0.5 or mock-infected for 3 days. Cells were then seeded on coverslips, followed by an overnight incubation. Cells were then fixed and PI4P and NS5A (to label infected-cells) were stained using monoclonal antibodies. Nuclei were stained with DAPI. PI4P signals were quantified by recording whole-cell z-stacks and measuring fluorescence intensity using Fiji. At least 30 individual cells were quantified. Right panel. Expression of phosphorylated and total paxillin and cofilin as well as NS5A were assessed by Western Blotting. Band intensities were quantified using Fiji and normalized to relative expression of the respective total proteins. **B.** Infection of Huh7.5 cells with HCVcc Jc1 were done as in **A.** before subjecting to immunofluorescence analysis using antibodies against p-paxillin and NS5A. FA numbers were quantified using Fiji as described above. **C.** Left panel. Huh7-Lunet cells were transduced with adenovirus encoding HCV (JFH1, gt 2a) nonstructural proteins NS3-5B wt or two NS5A mutants (S2208A or PPH) or empty vector for 2 days before seeding on coverslips. Cells were incubated overnight. Staining of PI4P and NS5A as well as quantification of PI4P intensities of the indicated samples were performed as described in **A.** Right panel. Expression of p-paxillin and p-cofilin were assessed by Western blotting and the relative expression of the indicated cells were quantified using Fiji. **D.** PHHs were washed twice with PBS and fresh medium was added. 6 h later, transduction of adenovirus encoding the indicated HCV proteins were performed as in **B.** to verify expression of p-paxillin and p-cofilin in these cells. **E.** Left panel. Huh7.5 were transfected with HCV RNAs from the indicated genotypes using electroporation and levels of PI4P in these cells were quantified using Fiji as described in **A.** Right panel. Expression of NS5A was evaluated by immunoblot analysis. **F.** Huh7.5 cells were infected with HCVcc Jc1, DBN3a or TN for 4 days before subjecting to Western blot analysis using antibodies against p-paxillin, p-cofilin, NS5A and GAPDH. **G.** Huh7-Lunet cells were transduced with adenovirus encoding the indicated proteins for 2 days. Cells were then seeded on rehydrated Corning BioCoat Matrigel Invasion Chambers with 8.0  $\mu\text{m}$  PET Membrane in the presence of 1% FCS. Invaded cells were quantified as described previously. **H.** Quantification of invaded cells was performed in adenovirus transduced-HHT4 cells as in **G.**

### 3.6. PI(3,4)P2 is a downstream effector of the pathways regulated by PI4KA

#### 3.6.1. Screening for downstream effector phosphoinositide kinases

Given the interconversion between the phosphoinositides it was essential to understand whether the cytoskeleton reorganization was modulated directly by PI4P or by an alternative phosphatidylinositol phosphate upon conversion of PI4P. In the latter case, PI(4,5)P2 was the most likely but not sole candidate since the connections between this molecule and FAs formation (118,119) as well as actin polymerization (120) with cell migration and invasion had been evidently proven in numerous studies. In addition, PI(4,5)P2 is the most abundant phosphoinositide and its enrichment in the cytoplasmic leaflet of the plasma membrane accounts for 1–2 mol% of total plasma membrane lipid (121). Synthesis of PI(4,5)P2 from PI4P is catalysed by members of the type I phosphatidylinositol phosphate kinase protein family. This type I PIP5K1s family is composed of the three proteins PIP5K1A, B and C. PI(3,4,5)P3 which is the product of phosphorylated PI(4,5)P2 at position 3 on the inositol ring could possibly be a potential candidate as well since its regulation in cell motility with its strong link to actin reorganization have also been intensively studied (118,120). The conversion of PI(4,5)P2 to PI(3,4,5)P3 is performed by PIK3C1s protein family including PIK3CA, B, D and G. PI(3,4)P2 is synthesized by phosphorylating the PI4P's 3-OH position, which is catalyzed by 3 members of the class II PI3K family, namely PIK3C2A, B and G. However, albeit little information on this molecule was available in literature all the three phosphoinositides were investigated side by side with PI4P to understand the mechanistic



## RESULTS

link of PI4KA with its above mentioned cytoskeletal rearrangement-mediated phenotypes to avoid any bias in my study. Another interesting question was if the phenotypes observed only linked to PI4P produced by PI4KA or could also result from other PI4K family members including PI4KB, PI4K2A and PI4K2B.

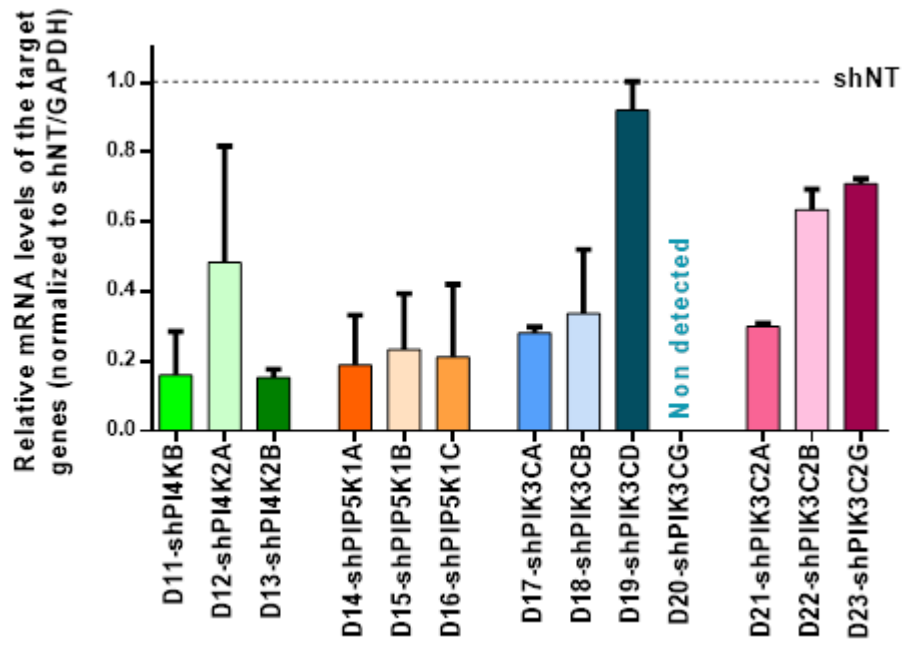
To address my questions, I employed shRNAs targeting all the members of the PIP5K1, PIK3C1, PIK3C2 and PI4K protein families and assessed the changes in cell morphology as well as phosphorylation status of paxillin and cofilin in Huh7-Lunet cells compared to a negative control shNT and a positive control shPI4KA (**Appendix 4**). Knockdown efficiencies of the target genes after transduction with selectable lentiviral vector expressing the respective shRNAs were evaluated using qRT-PCR (primers listed in the **Appendix 3**). All genes showed moderate to high expression in the control shNT cells except for PIK3CG with Ct value of above 39 (**Table 20**), indicating no or extremely low expression of the gene in the Huh7-Lunet cells, which was confirmed by another pair of primers (**Appendix 3**). Regarding the knockdown efficiencies the 7 constructs D11, D13, D14, D15, 16, D17 and D21 targeting PI4KB, PI4K2B, PIP5K1A, PIP5K1B, PIP5K1C, PIK3CA and PIK3C2A, respectively, reduced expression of the corresponding genes by more than 50% (**Figure 22A**) and therefore were used for subsequent experiments. Another round of cloning and testing of shRNAs was carried out to achieve better silencing efficiency for the remained target gene PIK3C2G, which showed only small reduction in the gene expression (**Figure 22B**). In the next attempt for shPIK3C2G all the 3 constructs D31, D32 and D33 showed moderate but acceptable knockdown efficiencies, among them D33 had the strongest effect with 50% reduction in the gene expression and therefore was selected for further analysis (**Figure 22C**), including cell morphology, levels of p-paxillin and p-cofilin and HCV RNA replication. I selected these features for my evaluation over other characteristics (cell migration, invasion or FA numbers) because they were robust enough to implement on my screen with multiple lipid kinases, the availability of materials and time required for the respective assays and their specificities to PI4KA.

**Table 20. Ct values of the phospholipid kinases in Huh7-Lunet shNT-cells**

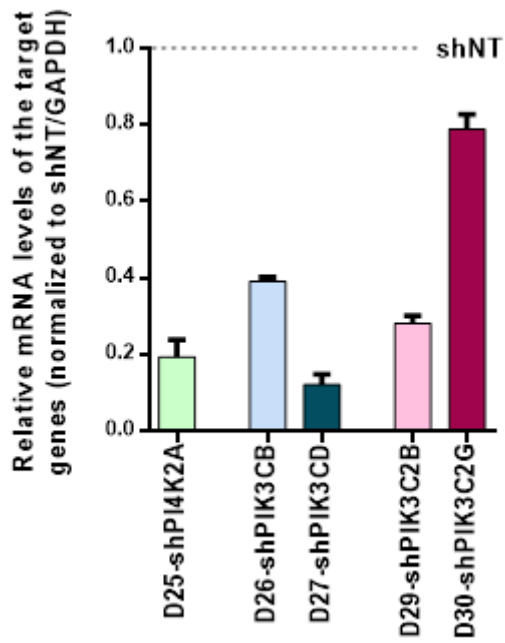
Gene name	Ct value	Gene name	Ct value	Gene name	Ct value
GAPDH	~ 14	PIP5K1A	~ 22	PIK3CD	~ 26
PI4KA	~ 20.5	PIP5K1B	~ 27	PIK3CG	~ 39
PI4KB	~ 21.5	PIP5K1C	~ 22	PIK3C2A	~ 21
PI4K2A	~ 23.5	PIK3CA	~ 24	PIK3C2B	~ 22
PI4K2B	~ 21	PIK3CB	~ 22	PIK3C2G	~ 24

## RESULTS

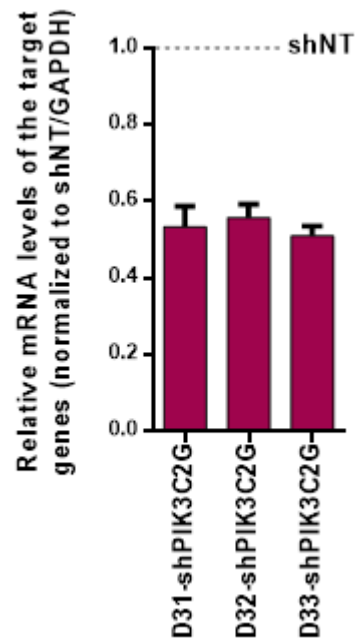
A



B



C



## RESULTS

D

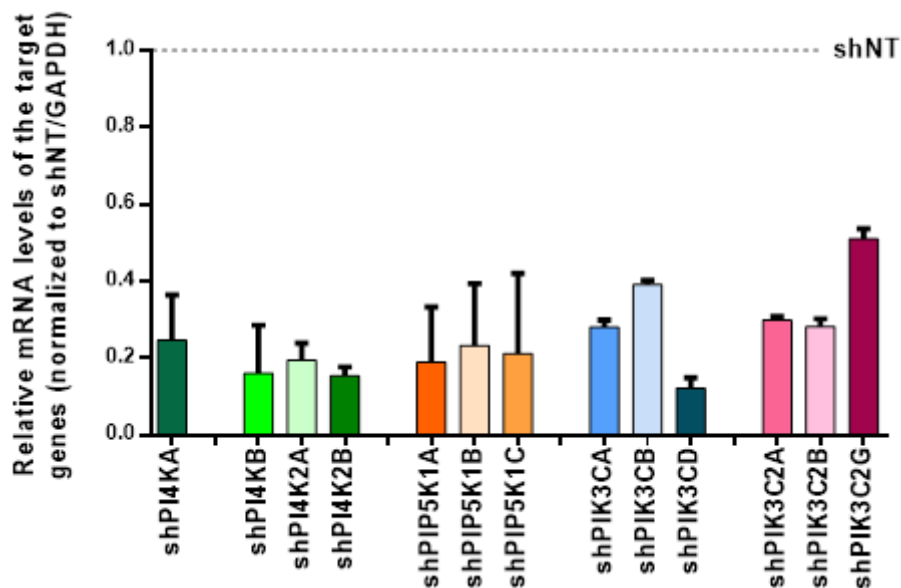


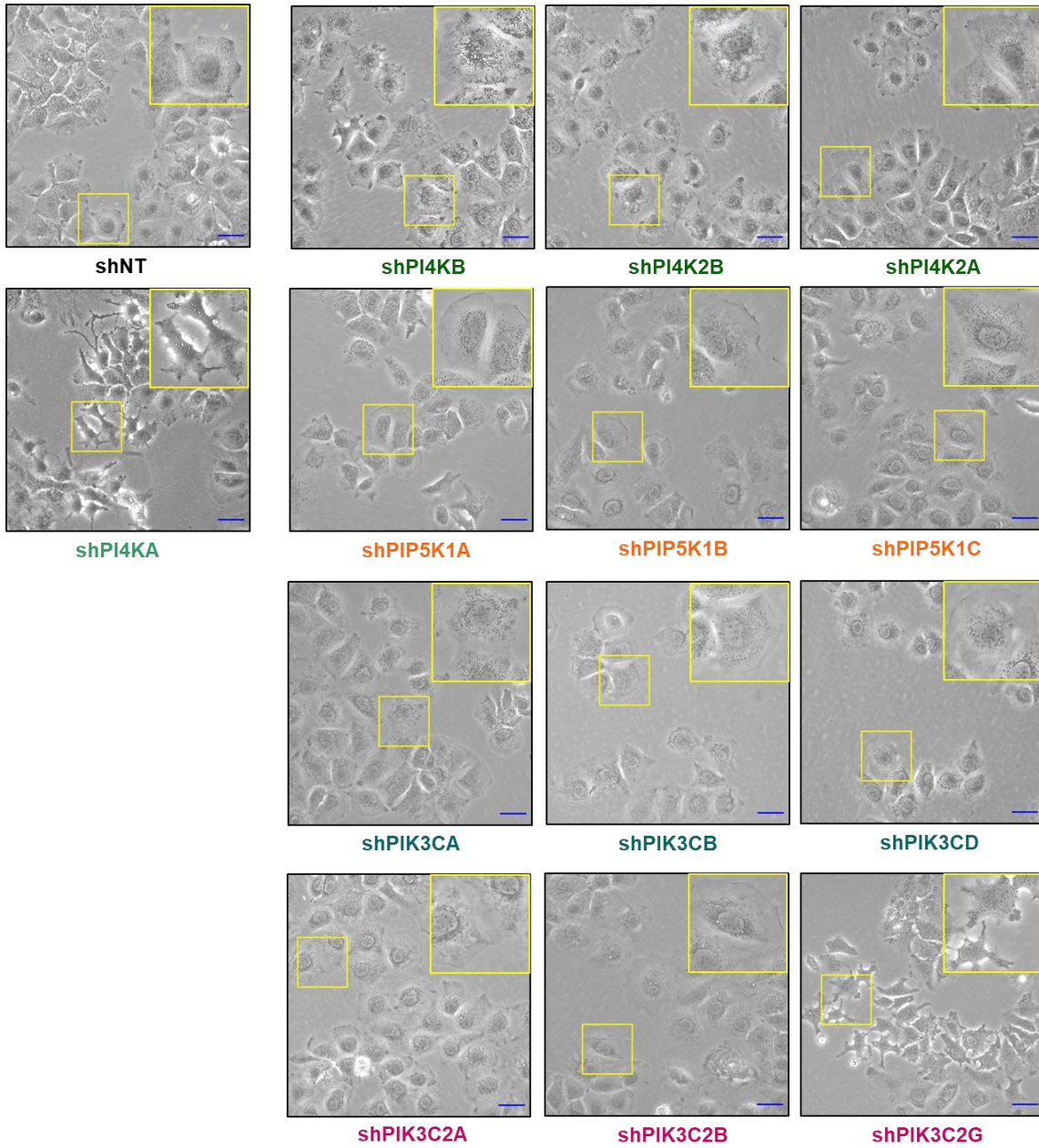
**Figure 22. Constructing shRNAs against PI4Ks, PIP5K1s, PIK3C1s, PIK3C2s proteins.** **A.** Huh7-Lunet cells were transduced with lentiviruses expressing the respective shRNAs. Knockdown efficiencies of the shRNA constructs in the first round tested by qRT-PCR. **B.** Knockdown efficiency of other 5 shRNAs against PI4K2A, PIK3CB, PIK3CD, PIK3C2B and PIK3C2G. **C.** 3 shRNAs against PIK3C2G were further constructed and tested for their silencing efficiencies. **D.** Summary of the shRNA constructs used in the screen and their respective knockdown efficiencies.

### 3.6.2. Knockdown PIK3C2G phenocopies effects on cell morphology and phosphorylation levels of Paxillin and Cofilin observed with silencing of PI4KA

Having established stable cell lines with knockdown efficiencies ranging from 50% (shPIK3C2G) to 88% (shPIK3CD), I firstly assessed cell morphology and phosphorylation levels of paxillin and cofilin. Silencing the other three PI4Ks proteins neither caused any morphological changes nor reduced phosphorylation levels of paxillin and cofilin, indicating that the regulation on this pathway was specific for PI4P originating from PI4KA (**Figure 23A, B and C**). Unexpectedly, however, none of the shPIP5K1s nor the shPIK3C1s cell lines showed morphological changes as observed with PI4KA-silenced cells, suggesting that neither PI(4,5)P<sub>2</sub> nor PI(3,4,5)P<sub>3</sub> were involved in regulation of cell morphogenesis (**Figure 23A and B**). Furthermore only silencing of PIK3CD moderately downregulated expressions of the two investigated phospho-proteins p-paxillin and p-cofilin (35% versus 51% reduction in p-paxillin and 25% versus 49% in p-cofilin in the case of shPIK3CD versus shPI4KA, respectively) but not affected cell morphology (**Figure 23A, B and C**). Surprisingly, only silencing of PIK3C2G showed comparable effects on both cell morphology and expression levels of the two phospho-proteins (**Figure 23A, B and C**), indicating that PI(3,4)P<sub>2</sub> could be involved in the signaling pathway as a downstream effector of PI4P.

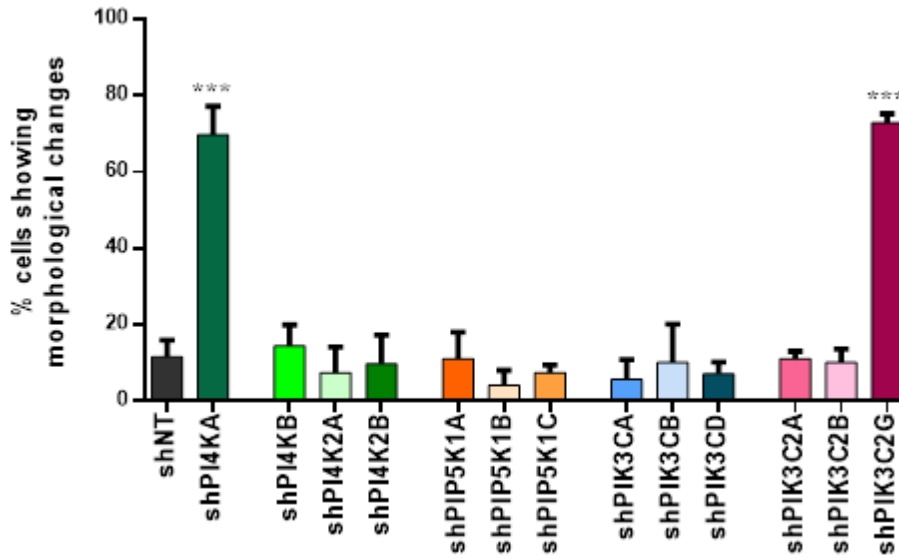
# RESULTS

**A**



## RESULTS

**B**



**C**

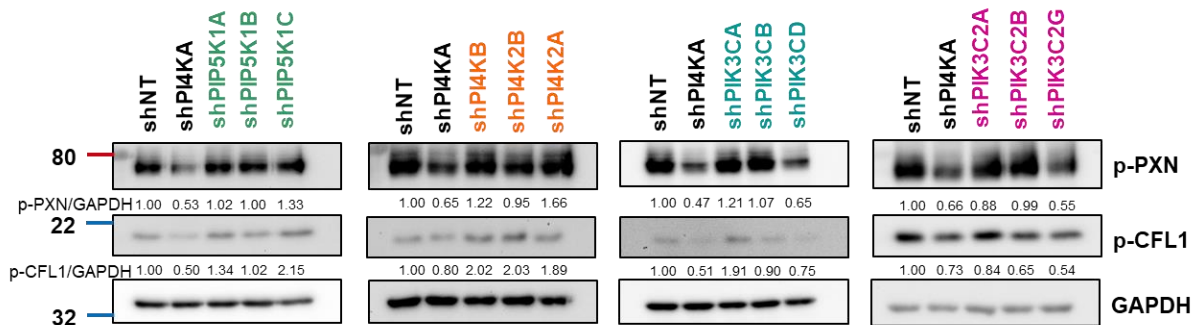


**Figure 23. Identification of PIK3C2G as a downstream kinase of PI4KA in the regulation of cytoskeletal pathways in a PI4P-linked phosphokinases screen.** **A.** Huh7-Lunet cells were transduced with lentiviruses encoding shRNAs against PI4KA, PI4KB, PI4K2A, PI4K2B, PIP5K1A, PIP5K1B, PIP5K1C, PIK3CA, PIK3CB, PIK3CD, PIK3C2A, PIK3C2B, PIK3C2G or non-targeting shRNA for 3 days. Puromycin was applied to select stable cells expressing the corresponding shRNAs. Cells were seeded in 6 well-plates and cell morphology was imaged by bright field microscopy with a 20x objective lens. All images were processed using FIJI and the inserts show magnifications of the boxed areas. Scale bars represent 50  $\mu$ m. **B.** Numbers of cells showing morphological changes were counted and percentages of these cells were obtained by dividing to the total number of cells. At least photos of six random areas covering minimum 300 cells in each condition were subjected for quantification. **C.** Protein lysates from the stable knockdown cell lines were subjected to Western blot analysis for p-paxillin and p-cofilin detection. Band intensity was quantified using FIJI and relative fold changes of p-paxillin and p-cofilin expression were presented.

### 3.6.3. Viral RNA replication is not dependent on expression of any phospholipid kinase other than PI4KA

In this study, I found that PI4KA with its product PI4P increased phosphorylation levels of the two important cytoskeletal modulators paxillin and cofilin, the numbers of FA and cell motility. These phenotypes were characterized as well in the HCV expressing cells and were the results from HCV-activated PI4KA. PI4KA is a critical host factor for HCV replication. The level of PI4P is upregulated in HCV-infected samples and this induction of PI4P was shown to link with the integrity of the viral replication complexes. It was therefore interesting to

## RESULTS

---

investigate if the two roles of PI4KA and its product PI4P in HCV RNA replication and in cytoskeletal regulation were interconnected or independent. One way to address this question could be to employ the stable knockdown cell lines which were created for assessing cell morphology and levels of p-paxillin and p-cofilin as mentioned previously to evaluate the HCV replication kinetics. Since replication of HCV gt 2a JFH-1 is highly dependent on PI4KA expression and activity, I transfected a subgenomic bicistronic luciferase reporter replicon designated i341 PiLuc NS3-3'  $\delta$ g JFH-1 and HCV RNA replication was assessed based on luciferase activity. HCV replication kinetics was monitored over a 72h time course. As previously reported, silencing of PI4KA consistently and profoundly inhibited the viral RNA replication with a 3-4 log reduction compared to the control shNT (**Figure 24A, B, C, D and E**). However, depletion of other phospholipid kinases did not cause any remarkable suppression on HCV RNA replication (**Figure 24A, B, C and D**). Of note, while PIK3C2G shared the similar functionality on cytoskeleton-regulated cell morphology and motility with PI4KA, this kinase seemed not to play critical role on the viral RNA replication (**Figure 24D**). Furthermore silencing of paxillin or cofilin did not lead to suppression of HCV replication either (**Figure 24E and F**). These data highlighted that the regulation of PI4KA on the cytoskeletal axis was likely uncoupled from its role in HCV RNA replication.

## RESULTS

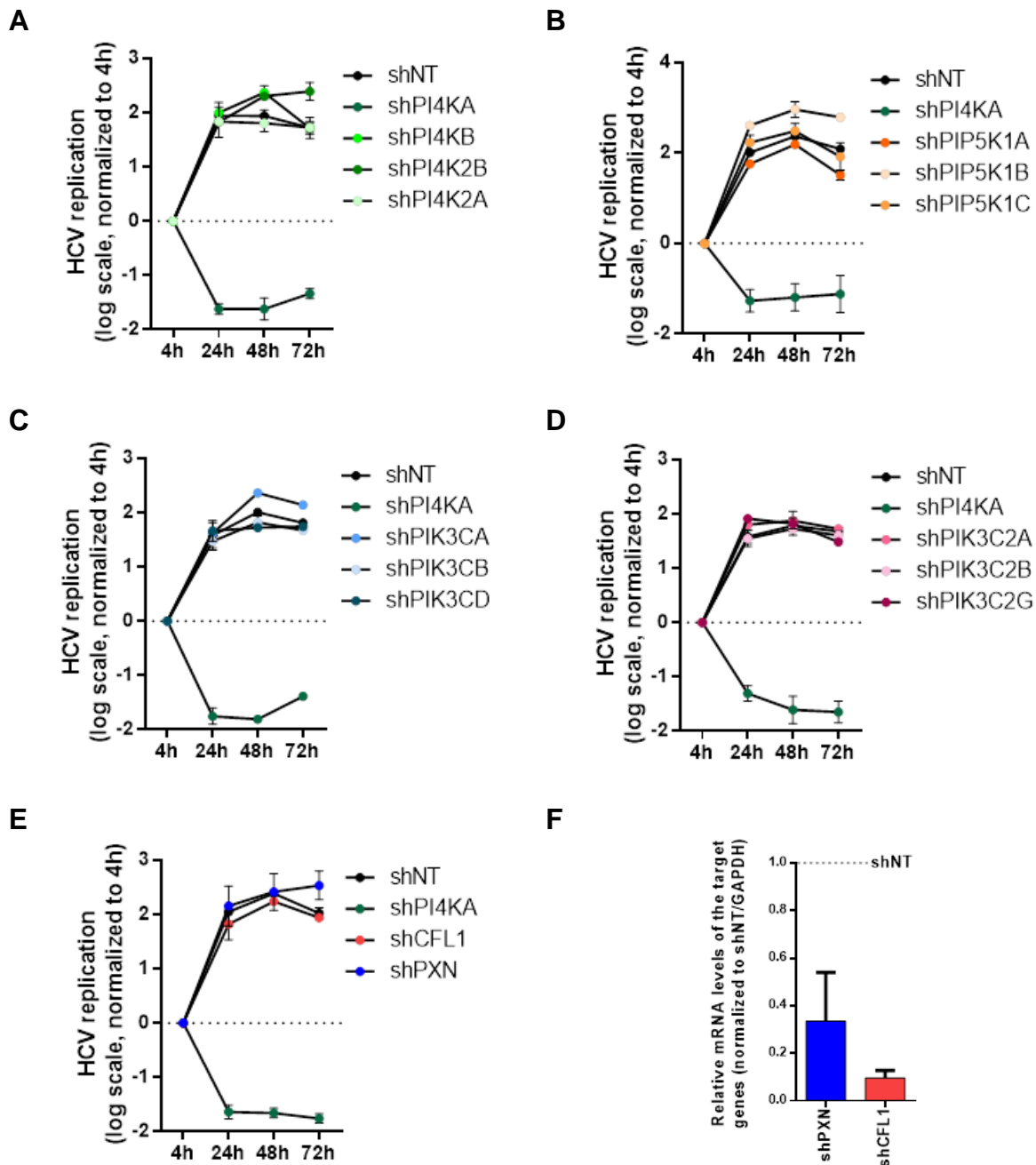


**Figure 24. Only PI4KA but not other PI4P-related kinases or Paxillin or Cofilin is crucial for HCV RNA replication.** **A.** Stable cell lines Huh7-Lunet expressing shNT, shPI4KA or shRNA against other members of the PI4Ks family were generated at the same time by lentiviral transduction. The cells were then electroporated with subgenomic bicistronic luciferase reporter construct pFK i341 PiLuc NS3-3'  $\delta$ g JFH-1. Cells were seeded in 12-well plate and cell lysates were collected at the indicated time points for measuring relative light units (RLU). Values were normalized to 4 h to account for transfection efficiency. **B., C., D.** were performed as **A.** but on PIP5K1s, PIK3C1s and PIK3C2s protein family. **E.** Stable cell lines Huh7-Lunet based expressing shPAXN, shCFL1, shPI4KA or shNT were firstly generated at the same time using lentiviral transduction. HCV RNA replication in these cells were evaluated as done in **A.** **F.** Total RNAs from the Huh7-Lunet-shPAXN, -shCFL1 and shNT were extracted and qRT-PCR was performed to assess knockdown efficiency of the shRNAs.

## RESULTS

---

### 3.6.4. PIK3C2G regulates FA and cell invasion similarly as PI4KA

The screen on cell morphology and levels of the two cytoskeleton phosphoproteins p-paxillin and p-cofilin identified PIK3C2G as a potential kinase working downstream of PI4KA in the pathway. This finding was far from my expectation but it was interesting to investigate further functions of this kinase in regards of the cytoskeleton regulation.

Firstly, specificity of the shPIK3C2G was examined. As shown in **Figure 25A**, ectopic expression of PIK3C2G but not vector could revert the morphological changes caused by silencing of the gene indicating that the effect was specific to this phospholipid kinase.

Furthermore, silencing of PIK3C2G also reduced numbers of FAs and cell invasion by approximately 3 and 2.5 fold, respectively (**Figure 25B** and **C**). PIK3C2G depletion also led to significant changes in cytoskeleton network, especially the effect on actin filaments was as similar as in the case of PI4KA knockdown (122). These data indicated that PIK3C2G shared many similar functions on cytoskeleton-regulated cell morphology and motility with PI4KA and implied that PIK3C2G acted as a downstream kinase in this pathway.



## RESULTS

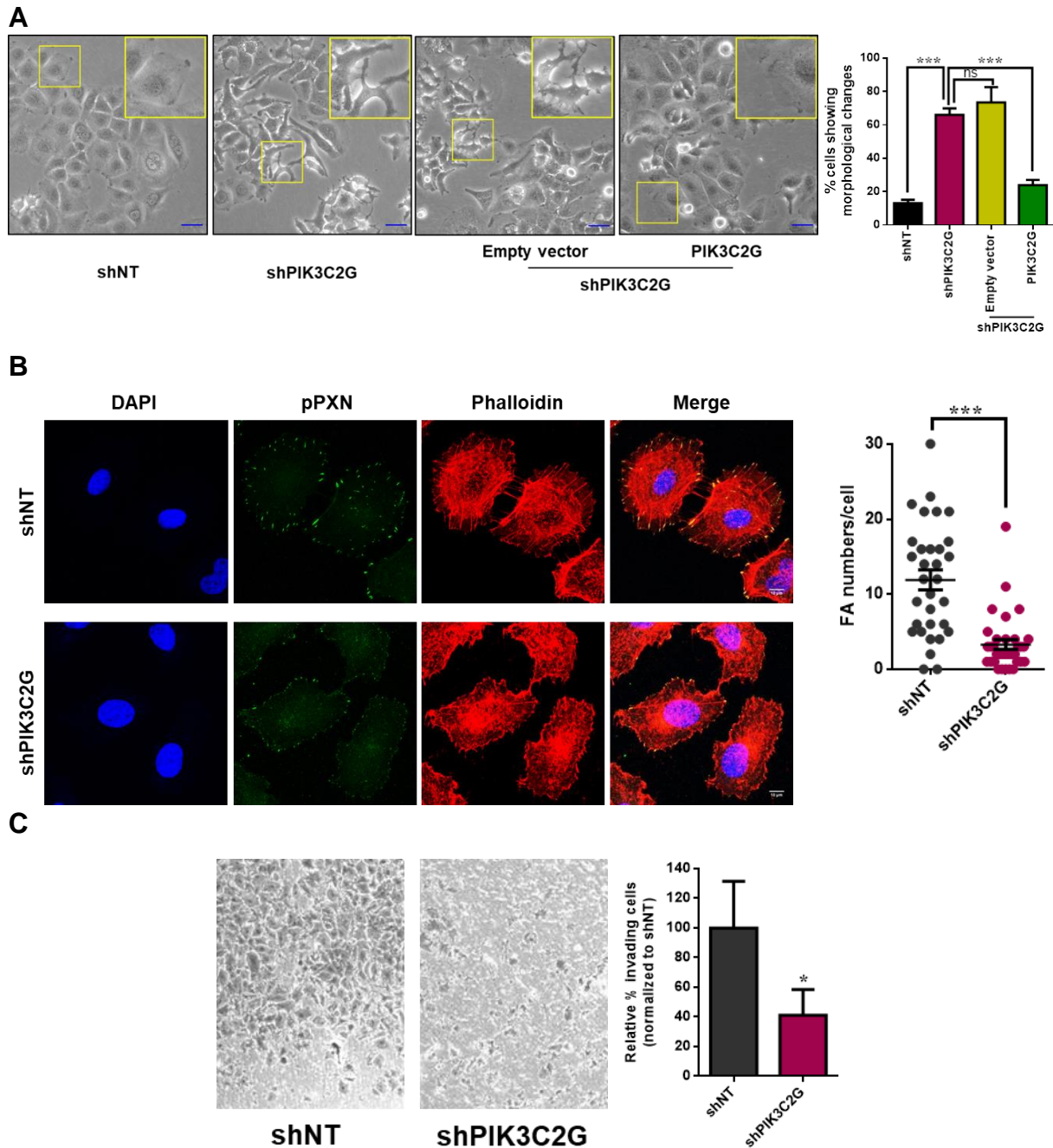


**Figure 25. PIK3C2G regulates cell morphology and enhances FA numbers, cell migration and invasion in the same manner as PI4KA.** **A.** Left panel. Huh7-Lunet cells were firstly transduced with lentiviruses expressing shNT or shPIK3C2G and cultured in complete medium containing Puromycin. The Huh7-Lunet-shPIK3C2G cells were then used as parental cells for producing the stable cell lines Huh7-Lunet-shPIK3C2G + empty vector or + PIK3C2G by lentiviral vector-mediated overexpression. These cells were cultured under the selection pressure of Blasticidin. The cells were seeded on 6-well plates and the photos of cellular morphology were taken 2 days post seeding when they reached 60-80% confluency using an inverted light microscope with 20x objective lens. The inserts show magnifications of boxed areas. Scale bars represent 50  $\mu$ m. Right panel. Numbers of cells showing morphological changes were counted and percentages of these cells were obtained by dividing to the total number of cells. At least photos of six random areas covering minimum 300 cells in each condition were captured. **B.** Left panel. Huh7-Lunet cells expressing shNT or shPIK3C2G were seeded on coverslips and incubated overnight. Cells were then stained with p-paxillin antibody and phalloidin. Nuclei were stained with DAPI. Right panel. Whole-cell Z-stack were recorded to quantify total amounts of FAs using Fiji. At least 30 cells per condition were quantified. **C.** Left panel. Huh7-Lunet stably expressing shNT or shPIK3C2G were seeded on rehydrated Corning BioCoat Matrigel Invasion Chambers with 8.0  $\mu$ m PET Membrane in the presence of 3% FCS. These chambers were placed in wells of a 24-well plate containing 10% FCS medium and allowed for a 24 h incubation.

## RESULTS

---

Invasive cells attached on the lower surface of the membrane were fixed and stained with crystal violet. Images were recorded using an inverted microscope connected with camera. Right panel. Number of invasive cells were quantified and relative fold change in the invasiveness were normalized to the Huh7-Lunet-shNT samples. ns: non-significant; \*:  $p < 0.05$ ; \*\*\*:  $p < 0.001$ .

### 3.7. PI(3,4)P2 pools at cell plasma membrane are dependent on PI4KA expression and activity

PIK3C2G is responsible for converting PI4P to PI(3,4)P2. Since I found that PIK3C2G shared the common pathways with PI4KA, I asked how PI(3,4)P2 was regulated by the two kinases. Two different methods of staining phosphoinositides were applied to differentiate the distribution of PI(3,4)P2 at the plasma membrane versus intracellular compartments (123). The main differences between the two methods are the use of reagents for cell permeabilization and temperature of incubation. While using saponin as a very mild detergent in combination with incubating at 4°C for the whole process of staining allowed me to follow expression of phosphoinositides at or in adjacent to cell plasma membrane. Permeabilization with digitonin and incubation at room temperature could reveal the distribution of these molecules in the intracellular compartments. Applying these approaches in Huh7-Lunet cells showed a wide distribution of PI(3,4)P2 in the whole cell body (**Figure 26A**), in contrast to large clusters underneath the cell plasma membrane at the sites of protrusions (**Figure 26B**). Such PI(3,4)P2-enriched structures had recently been related to invadopodia (124). Invadopodia are specialized cell surface structures which are rich in actin and are utilized by cancer cells to degrade ECM for their invasiveness (124). Interestingly, I found that cells in which PIK3C2G was depleted did not or vaguely showed these PI(3,4)P2 containing structures, and the signals of PI(3,4)P2 were also less intense than those observed in the shNT cells (**Figure 26B**). In contrast I found that PIK3C2G silencing slightly increased the intracellular abundance of PI(3,4)P2 (**Figure 26A**). These data suggested that in our HCC-derived cell culture model, PIK3C2G contributed to the PI(3,4)P2 pools at cell plasma membrane which were linked to invadopodia and cell invasion.

I next sought to determine how PI4KA regulated PI(3,4)P2 distribution in cells using both knockdown and chemical inhibition. In either cases I observed prominent structures enriched in PI(3,4)P2 as described previously in the control cells expressing shNT or treated with DMSO, which were remarkably absent in a large population of PI4KA-silenced cells and PI4KA F1 inhibitor-treated cells (**Figure 26C and D**). This was the same phenotype observed for PIK3C2G knockdown and implied that a fraction of PI4P synthesized by PI4KA was subsequently converted to PI(3,4)P2 at cell plasma membrane by PIK3C2G. It was, however, intriguing that cells lacking PI4KA expression or activity also produced less intracellular PI(3,4)P2 (**Figure 26E**), suggesting that PI4P synthesized by PI4KA via other pathways also contributed to PI(3,4)P2 pools other than the clusters at cell plasma membrane.

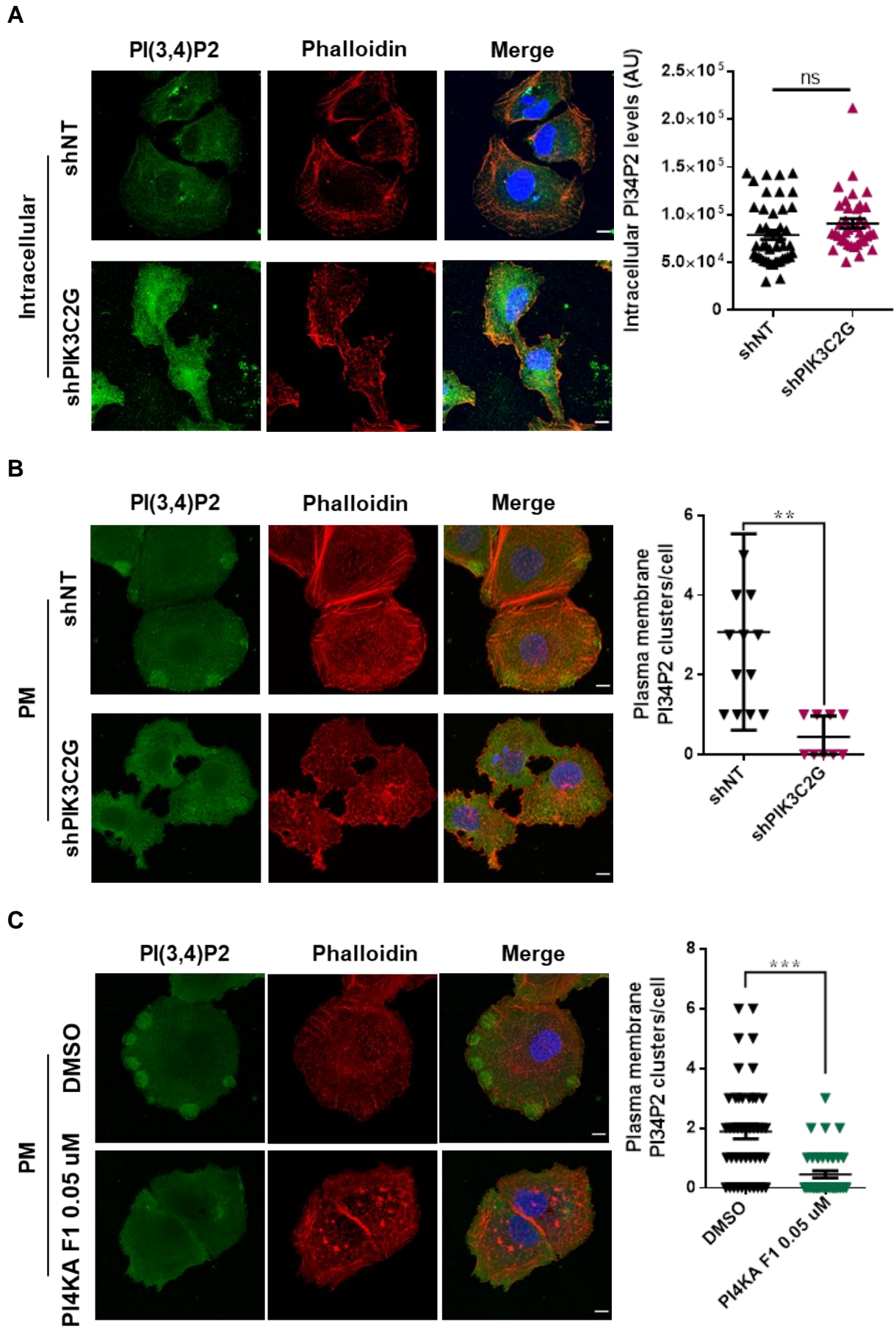
## RESULTS

---

To corroborate my finding of the specific contribution of PI4KA to the special clusters of PI(3,4)P2 at cell plasma membrane, expression of the other two phosphoinositides which are linked to PI4P were also examined. While PI(3,4,5)P3 gathered into some structures reminiscent of the above described PI(3,4)P2-enriched structures, PI(4,5)P2 formed a thick donut-like layer at the plasma membrane (**Figure 26F** and **G**). It was also noteworthy that among the 3 molecules, signal intensities of PI(4,5)P2 were the highest, followed by that of PI(3,4,5)P3 in contrast to low levels of PI(3,4)P2. I did, however, not notice any significant changes in the abundance of the two former molecules in PI4KA knockdown cells (**Figure 26F** and **G**), suggesting that PI4P synthesized by the kinase contributed exclusively to PI(3,4)P2 pools at the cell plasma membrane.

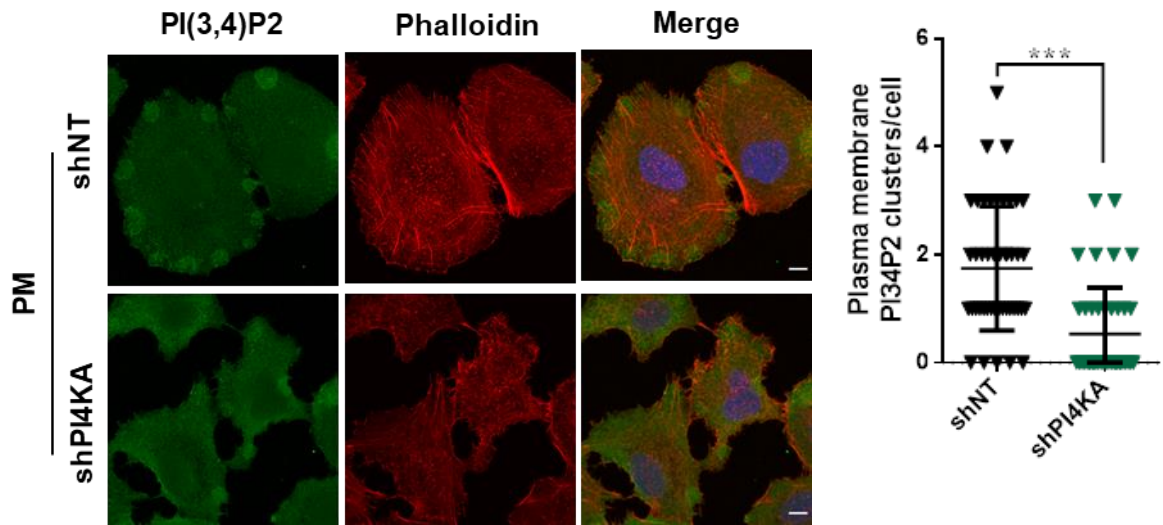
To study the regulation of these phosphoinositides by HCV, I monitored their expression in virus-infected cells compared to mock infection, also using the two different staining methods. It should be however worth to mention that due to the nature of localization, staining HCV proteins did not work with the “plasma membrane” method. Therefore it was impossible to locate HCV-infected cells when I applied this method of immunofluorescence. To overcome this limitation, I aimed to obtain an infection where more than 95% of the cell population was positive with HCV. This was achieved by using Huh7.5 cells inoculated with HCV Jc1cc at MOI = 0.5 and incubated for 6 days (data not shown). At cell plasma membrane I did not observe any changes in the levels of PI(4,5)P2 and PI(3,4,5)P3 (**Figure 26H** and **J**), while HCV infection led to increases in different extent intracellular expression of the two molecules (**Figure 26I** and **K**). In contrast, levels of PI(3,4)P2 in cellular compartments other than plasma membrane were not affected by the viral infection (**Figure 26L**). The presence of these molecules at the cell plasma membrane in Huh7.5 cells were however too low for a proper evaluation (data not shown). I therefore implemented indirect quantification by assessing the total amount of PI(3,4)P2 in these cells using a commercial ELISA (**Figure 26M**). Cells infected with HCV indeed showed higher PI(3,4)P2 levels in total (**Figure 26M**), likely resulting from a surge in the cell plasma membrane pools. These data taken together highlighted the importance of PI4KA and PIK3C2G in regulating plasma membrane PI(3,4)P2 which acted as an important mediator for the observed cytoskeleton rearrangements and cell motility.

## RESULTS

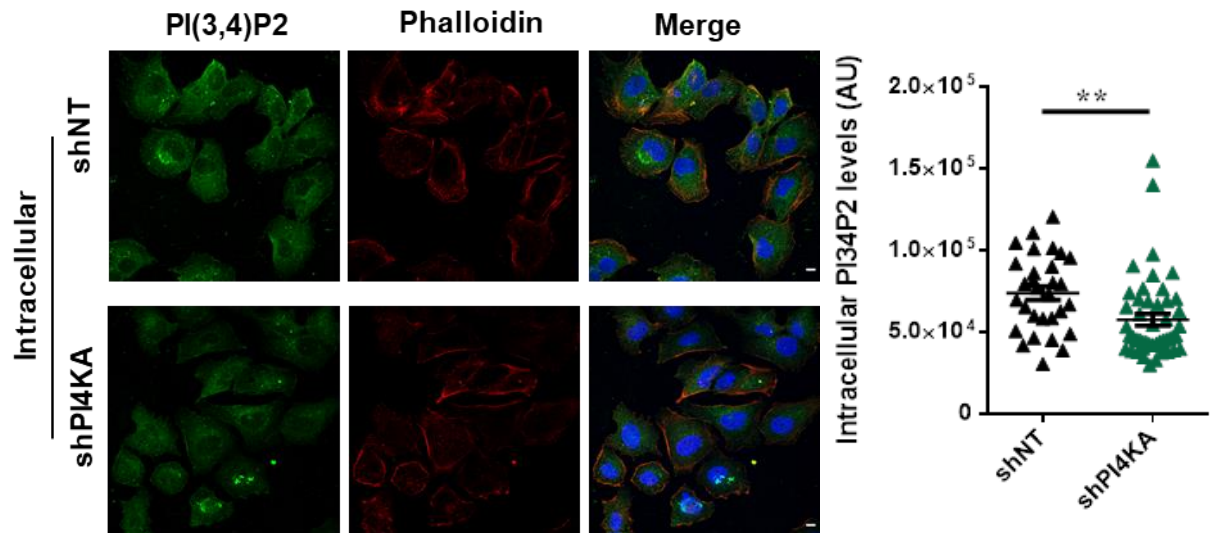


# RESULTS

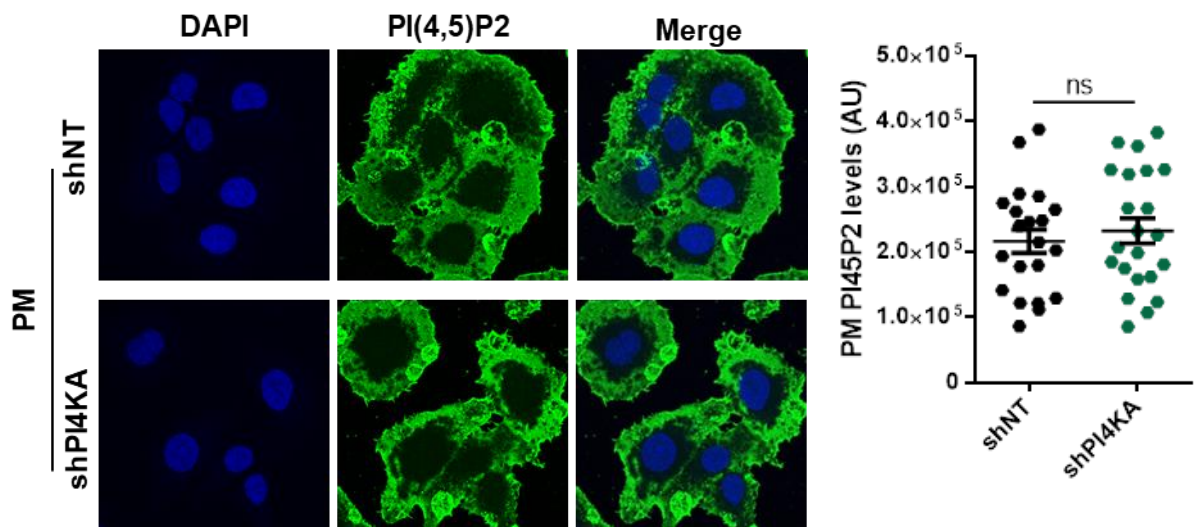
D



E

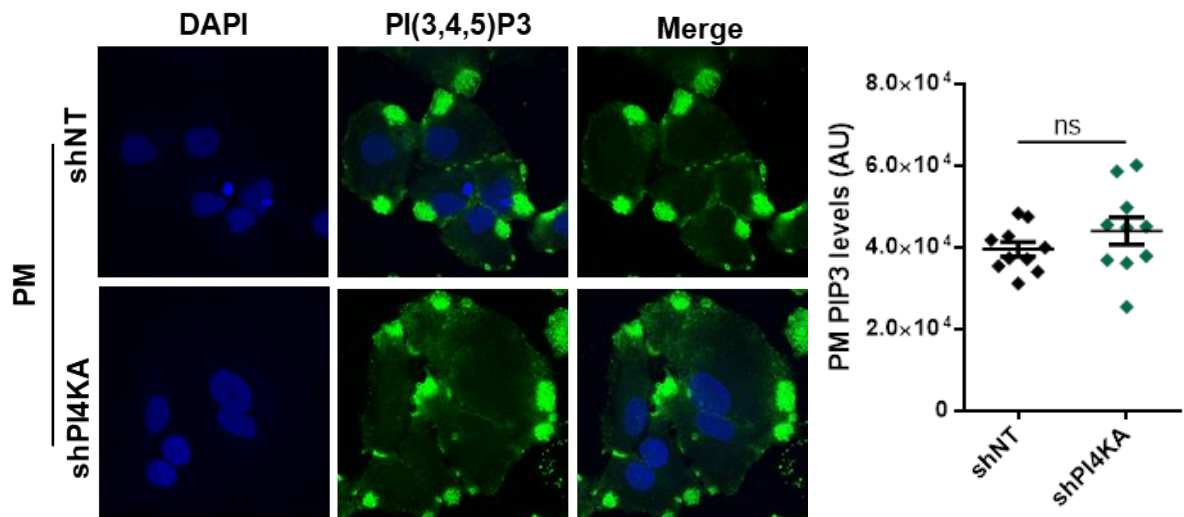


F

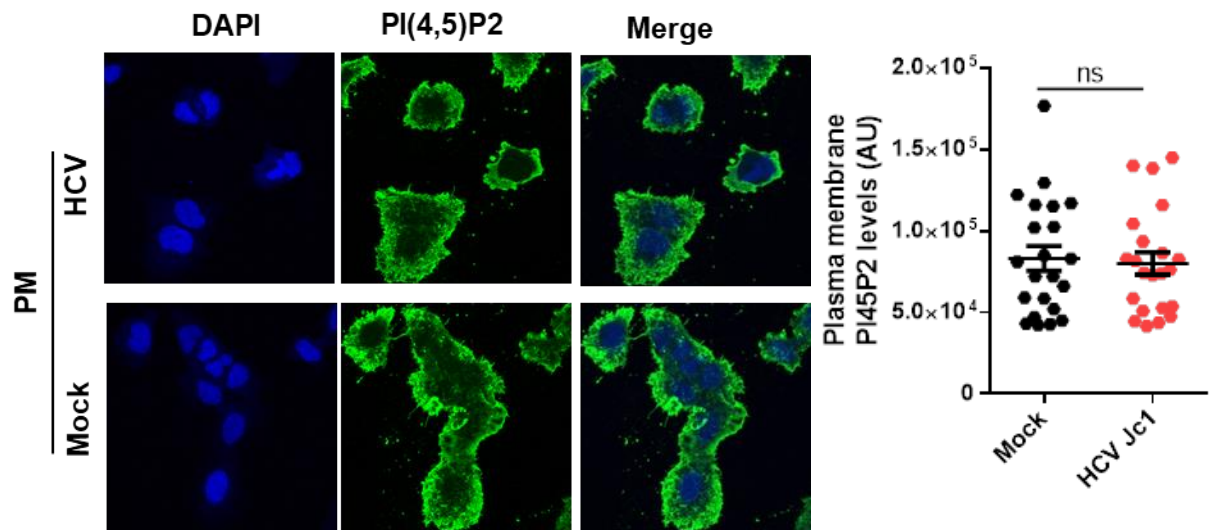


# RESULTS

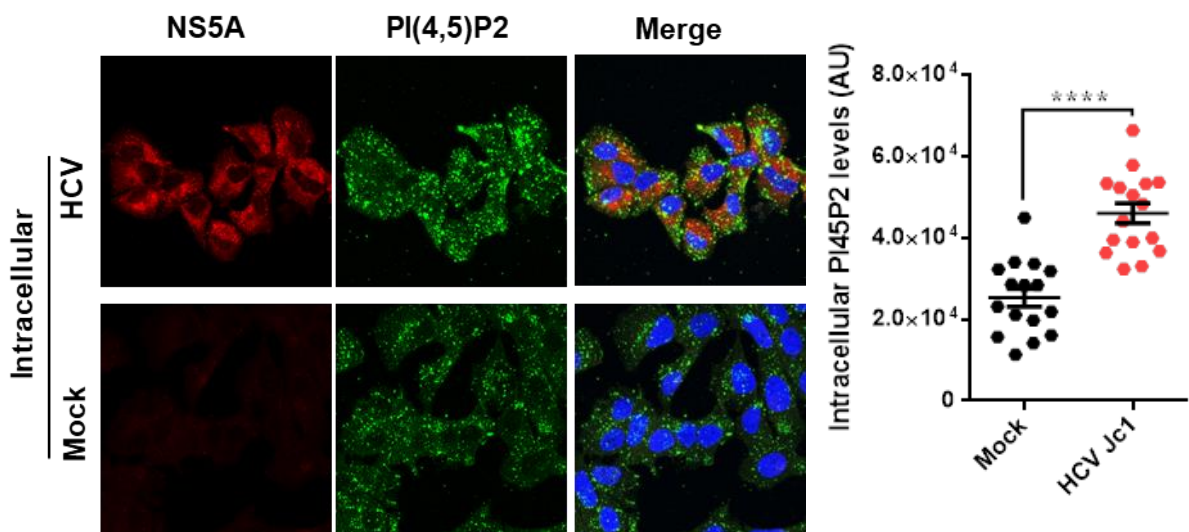
**G**



**H**

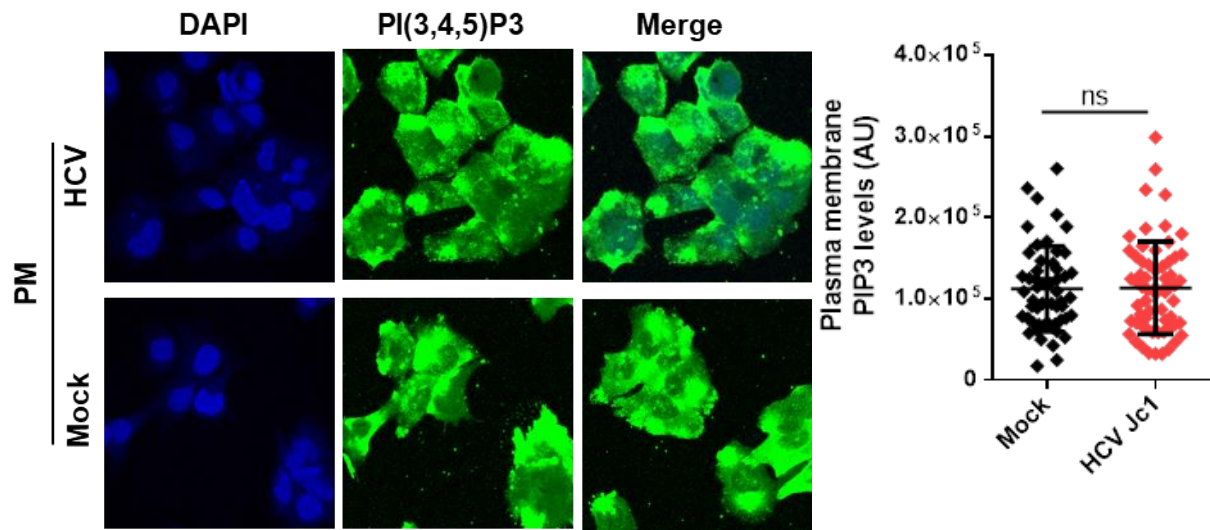


**I**

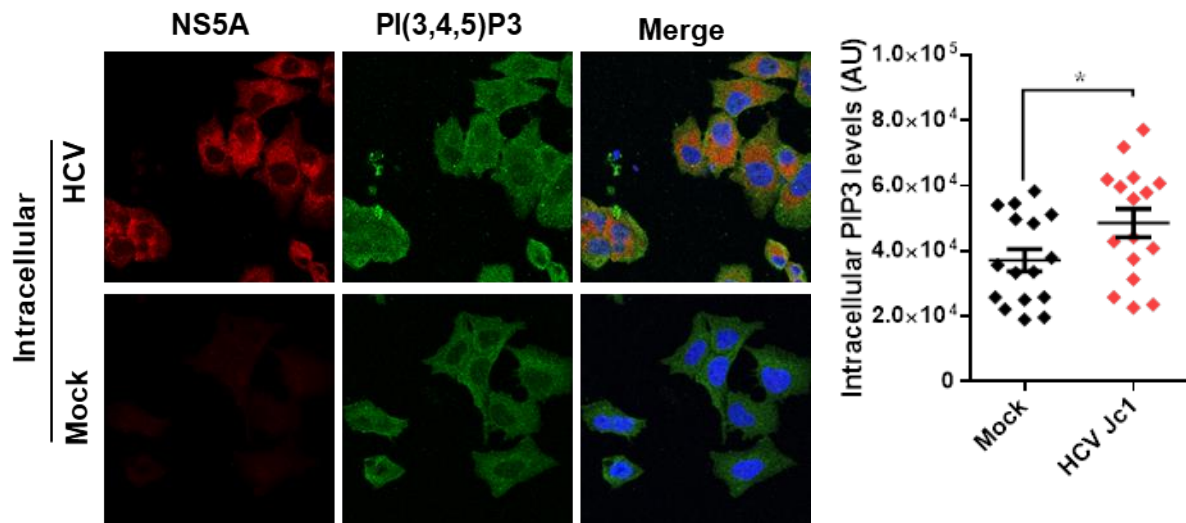


# RESULTS

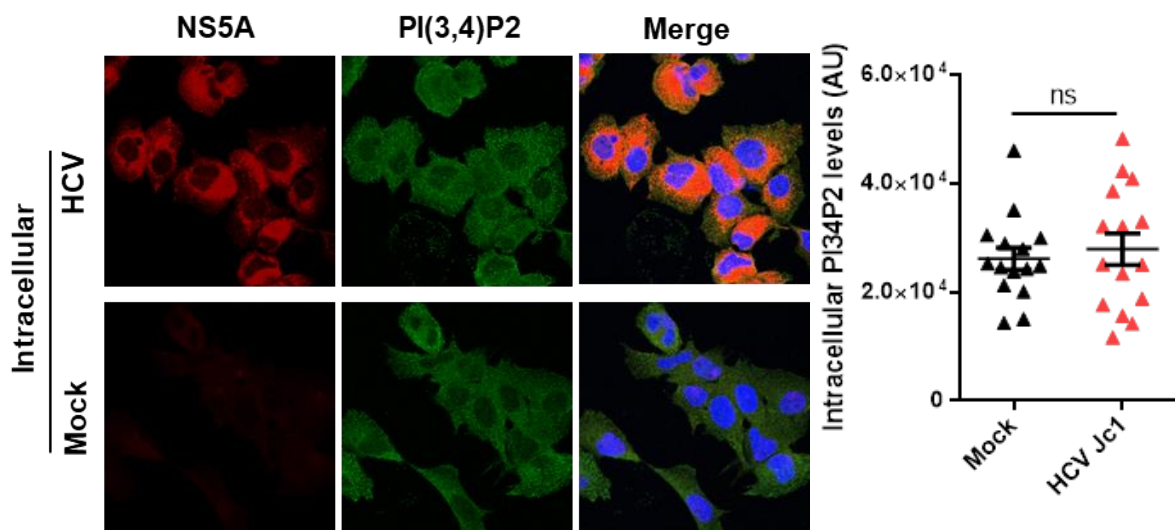
J



K



L



## RESULTS

M

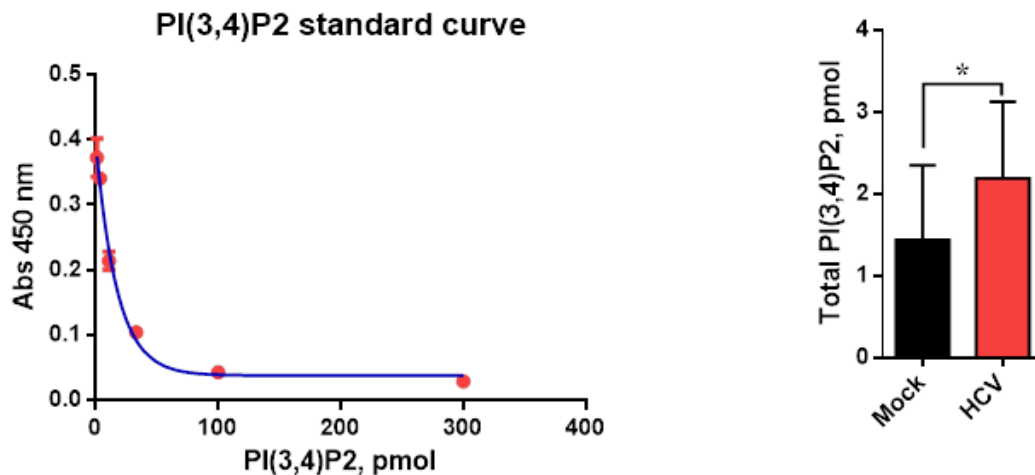


**Figure 26. PI4KA and PIK3C2G are important for plasma membrane pools of PI(3,4)P2.** **A.** Left panel. Huh7-Lunet-shNT and -shPIK3C2G were seeded on coverslips and incubated overnight. Fixation and membrane permeabilization were performed using intracellular staining protocol for phosphoinositides. Cells were then stained with PI(3,4)P2 antibody and phalloidin. Nuclei were stained with DAPI. Right panel. Whole-cell Z-stack were recorded to quantify intracellular amounts of PI(3,4)P2 using Fiji. **B.** Similar to **A** but plasma membrane staining protocol was applied to monitor PI(3,4)P2 at these membranes. Clusters of PI(3,4)P2 were counted per cell and plotted on graph using Graphpad. **C.** Huh7-Lunet were either treated with DMSO or 0.05  $\mu$ M PI4KA F1 for 48 h. Staining, image acquisition, processing and analysis was performed as **B**. **D.** was done as in **B** using Huh7-Lunet expressing shNT or shPI4KA. **E.** was as similar as **A** using Huh7-Lunet-shNT and -shPI4KA. **F.** and **G.** Left panels. Huh7-Lunet-shNT and shPI4KA were seeded on coverslips and incubated overnight, followed by an application for plasma membrane staining of PI(4,5)P2 and PI(3,4,5)P3, respectively. Right panels. Whole-cell Z-stack were recorded to quantify plasma membrane PI(4,5)P2 and PI(3,4,5)P3, respectively using Fiji. **H.** and **I.** Huh7.5 cells were either mock or HCV-infected for 96 h at MOI = 0.5. Either plasma membrane or intracellular staining protocol was applied, respectively to reveal specific pools of PI(4,5)P2 in these cells. Quantification of PI(4,5)P2 were done using Fiji. **J.** and **K.** were done as in **H** and **I**, respectively but PI(3,4,5)P3 antibody was used instead of antibody against PI(4,5)P2. **L.** was done as in **I** using PI(3,4)P2 antibody. **M.** Total cellular PI(3,4)P2 was extracted from mock and HCV-infected Huh7.5 cells using a protocol for phospholipid extraction. Left panel. PI(3,4)P2 standard curve was obtained by plotting the known amount of PI(3,4)P2 against the absorbance at 450 nm corresponding to the amount of PI(3,4)P2 detector protein determined by peroxidase-linked secondary detection reagent and colorimetric substrate. Right panel. Amount of cellular PI(3,4)P2 in Mock and HCV-infected cells were determined using the standard curve.

### 3.8. AKT2 is the mediator linking signaling from PI4KA, PIK3C2G to PXN and further downstream

In the previous chapters, it was shown that PI4KA and the downstream kinase PIK3C2G were important for cell morphology and cell motility via promoting phosphorylation of PXN. In this regards, PI(3,4)P2 - the phosphoinositide product of PIK3C2G kinase - could be the second messenger to convey signals from PI4KA to further downstream. In order to facilitate the phosphorylation of PXN, however, PI(3,4)P2 could not function directly as a kinase but likely played a role in recruiting and activating protein kinases for this purpose.

#### 3.8.1. Silencing PI4KA or PIK3C2G reduces phosphorylation of AKT2

In order to search for a kinase acting downstream of PI4KA and PIK3C2G, I employed a phospho-kinase array. To this end, total protein lysates were extracted from cells expressing



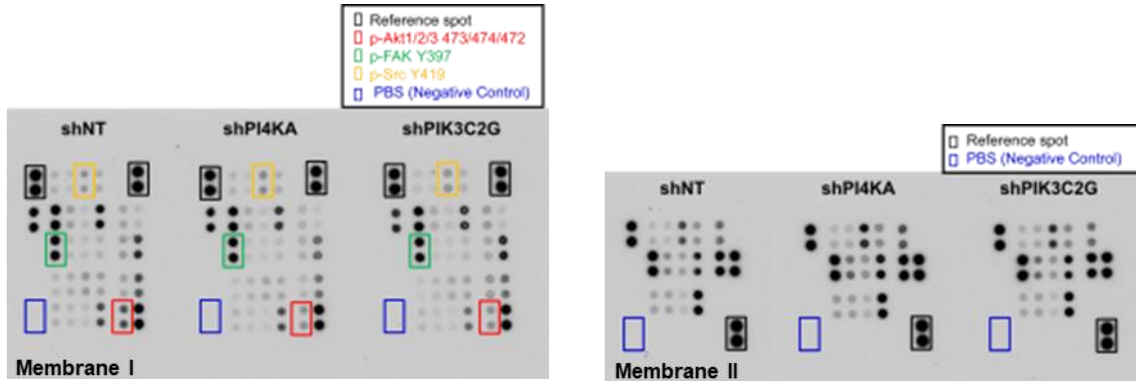
## RESULTS

---

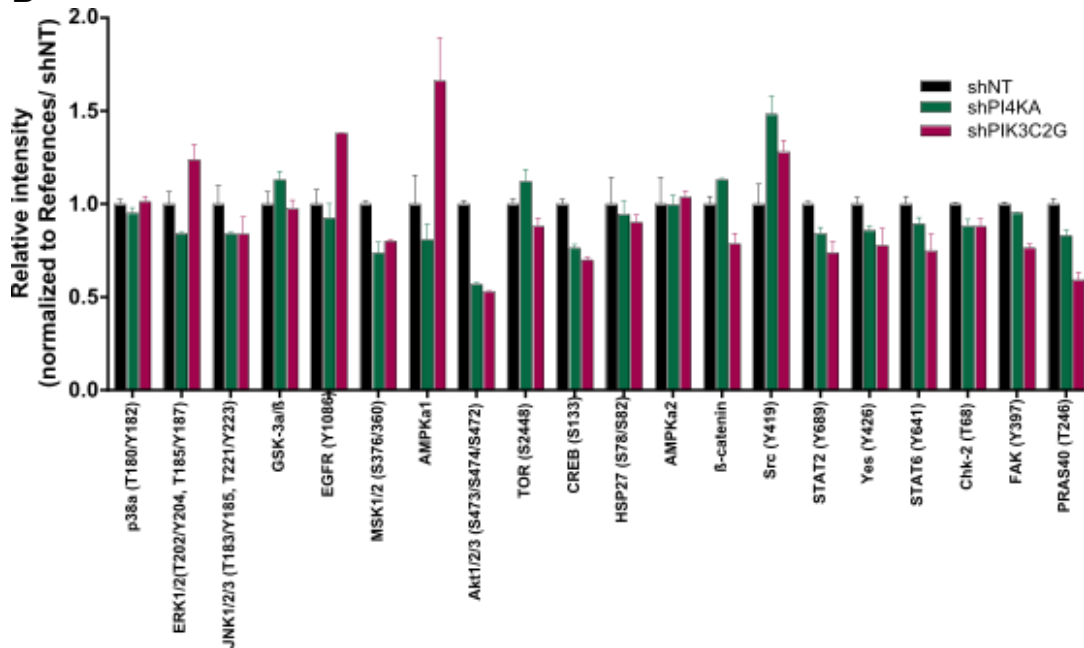
either shNT (control), shPI4KA or shPIK3C2G and incubated with the membrane arrays of spotted antibodies against 37 kinase phosphorylation sites (Material and Method, **Figure 10** and **Table 19**). While signal intensities remained unchanged or slightly altered with other phosphorylation sites, I found concomitantly two times reduction of phosphorylation levels of AKT1/2/3 (Ser 473/474/472) in both PI4KA and PIK3C2G knockdown samples compared to control cell lysate (**Figure 27A** and **B**). Focal adhesion kinase FAK and protein tyrosine kinase Src have frequently been claimed to phosphorylate paxillin (109,125,126). FAK and Src are activated when phosphorylated at tyrosine Y397 and Y419, respectively (127). I did not, however, observe significant impact of silencing PI4KA and PIK3C2G on the levels of these phosphorylation sites (**Figure 27D**). In order to validate the data obtained from the phospho-kinase array, I performed a Western blot using the same lysates. For AKT, I used specific antibodies against phosphorylation sites S473 and S474 of AKT1 and AKT2, respectively. Since AKT3 expression is quite restricted to the brain and a few other organs (128,129), I excluded it from my study. Indeed, I found no quantitative alterations in phosphorylation of both FAK Y397 and Src Y419, whereas phosphorylation levels of AKT1/2 were reduced upon silencing PI4KA (**Figure 27D**). Of note, the AKT2 S474 levels were much more affected than the AKT1 S473 (**Figure 27D**). I also confirmed by Western blot that knockdown of PIK3C2G significantly downregulated the AKT2 S474 level but the effect on AKT1 was only marginal (**Figure 27E**). This was in line with a previous study showing that PIK3C2G selectively activated AKT2 (130). Taken together, these data indicated that AKT2 could work as a mediator to convey signals from PI4KA, PIK3C2G to paxillin and the further downstream pathway. I, nevertheless, could not exclude the possibility that other protein kinases might be involved in this pathway since the human phospho kinase array only covered 37 phosphorylation sites of common kinases and cell transduction signaling pathways are much more complex and often require cooperation of multiple components.

# RESULTS

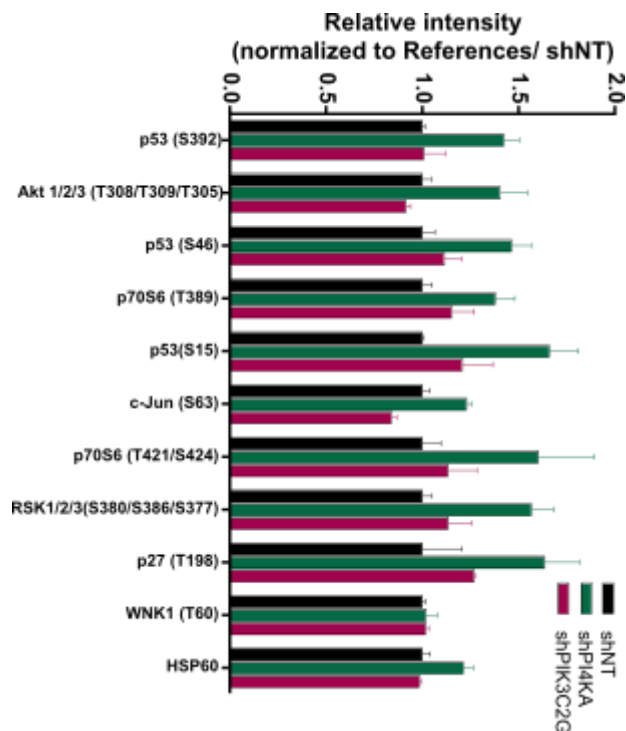
**A**



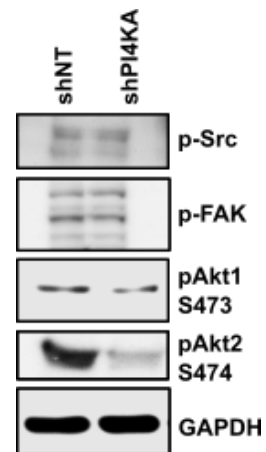
**B**



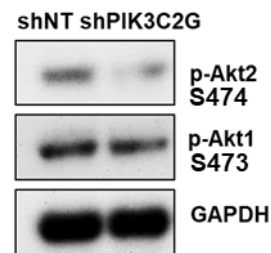
**C**



**D**



**E**



## RESULTS

**Figure 27. Levels of phospho AKT2 S474 is reduced upon silencing PI4KA or PIK3C2G. A.** Huh7-Lunet cells were stably transduced with selectable lentiviral vectors expressing non-targeting shRNA (shNT) or shRNAs targeting endogenous PI4KA (shPI4KA) or PIK3C2G (shPIK3C2G). Protein lysates were extracted and subjected to the Proteome Profile human phospho kinase array kit. Note that the array contains two membranes (I and II). **B.** Protein signal intensities in the membrane I were quantified using Fiji and normalized to the corresponding reference spots of every sample. Relative values were then normalized to the corresponding value of the control sample shNT. Each antibody against the kinase phosphorylation sites were spotted duplicate. Relative signal intensities were plotted on graph using Graphpad. **C.** Was done as in **B** with the membrane II. **D.** Protein lysates were extracted from Huh7-Lunet-shNT and -shPI4KA and levels of p-Src, p-FAK, p-Akt1 S473 and p-Akt2 S474 were determined using Western blot analysis. **E.** Protein levels of p-Akt1 S473 and p-Akt2 S474 were evaluated in Huh7-Lunet expressing shNT or shPIK3C2G.

### 3.8.2. HCV activates AKT2 at S474 and this correlates with PI4KA activity

AKT1 is the most widely studied isoform of AKT. It has been shown previously that HCV activates AKT1 (at both T308 and S473) to promote HCV entry, replication, translation and cell survival (131,132,133). It was, however, unclear whether HCV activates AKT2. Still, this speculation could be true as I demonstrated previously that PI4KA promoted the phosphorylation of this AKT isoform at S474 and HCV is known to activate PI4KA. Indeed, I observed a strong upregulation of p-AKT2 S474 in the HCV Jc1-infected sample compared to the mock infection (**Figure 28A**). This activation of AKT2 by HCV correlated with PI4KA activity (**Figure 28B**), since lower levels of p-AKT2 S474 were observed in cells infected with HCV DBN3acc and HCV TNcc compared to Jc1, corresponding to the PI4P induction levels found for these isolates (**Figure 21E**). The same held true in the HCV expression system using primary human hepatocytes. Only HCV wt but not the two NS5A mutants lacking PI4KA activation could increase the phosphorylation of AKT2 at S474 (**Figure 28C**). My data therefore suggested that HCV activated AKT2 at S474 via promoting PI4KA activity.

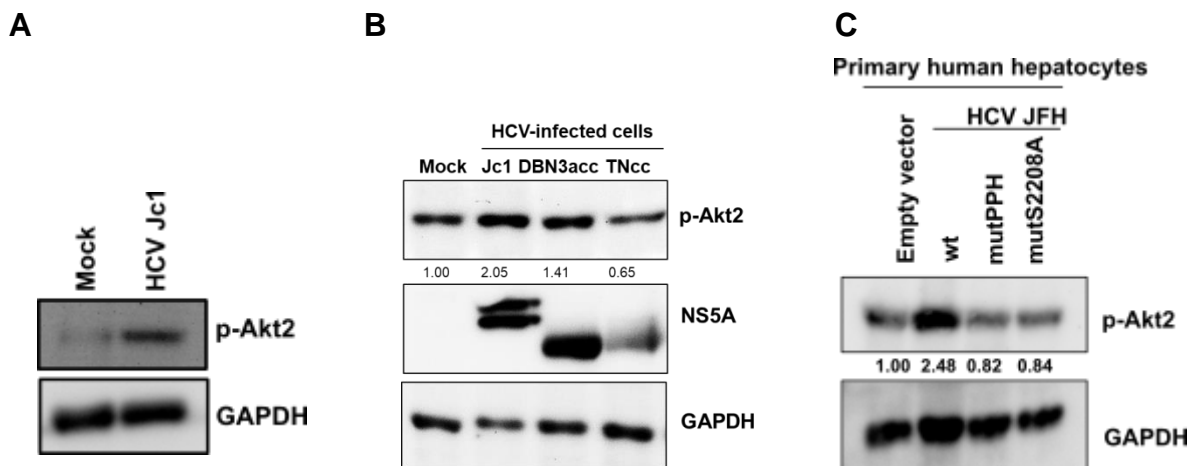


**Figure 28. Levels of phospho AKT2 S474 is increased upon HCV infection or expression. A.** Huh7.5 cells were either infected with HCV Jc1 full-length virus or mock-infected. 6 days post infection cells were harvested and protein lysates were extracted and subjected to Western blot for expression of p-AKT2 S474 and GAPDH. Signal intensities were quantified using FIJI and normalized to GAPDH. **B.** Cell lysates from **F** were used for a detection of p-AKT2. **C.** Primary human hepatocytes were transduced with adenoviruses expressing HCV NS3-5B wt or the indicated mutants. 3 days after transduction cells were harvested and samples were prepared for Western blot as done in **A**.

## RESULTS

### 3.8.3. AKT2 is enriched in PI(3,4)P2-containing structures at cell plasma membrane

Even though it was reported that PI(3,4)P2 activated AKT2 it was not demonstrated how and where these signal molecules interacted (130). Since I suspected that PI(3,4)P2 recruited and activated AKT2 to phosphorylate paxillin and activate further downstream signaling pathways, I firstly sought to clarify where these two molecules localize in cells. To this end plasma membrane staining of PI(3,4)P2 and AKT2 was performed in Huh7-Lunet cells. Immunofluorescence revealed that AKT2 was enriched at the containing PI(3,4)P2 structures supposed to be invasomes (**Figure 29**). This data further favored for my hypothesis that PI(3,4)P2 recruited and activated the kinase AKT2 and consolidated my understanding of the interaction between these two signaling messengers.

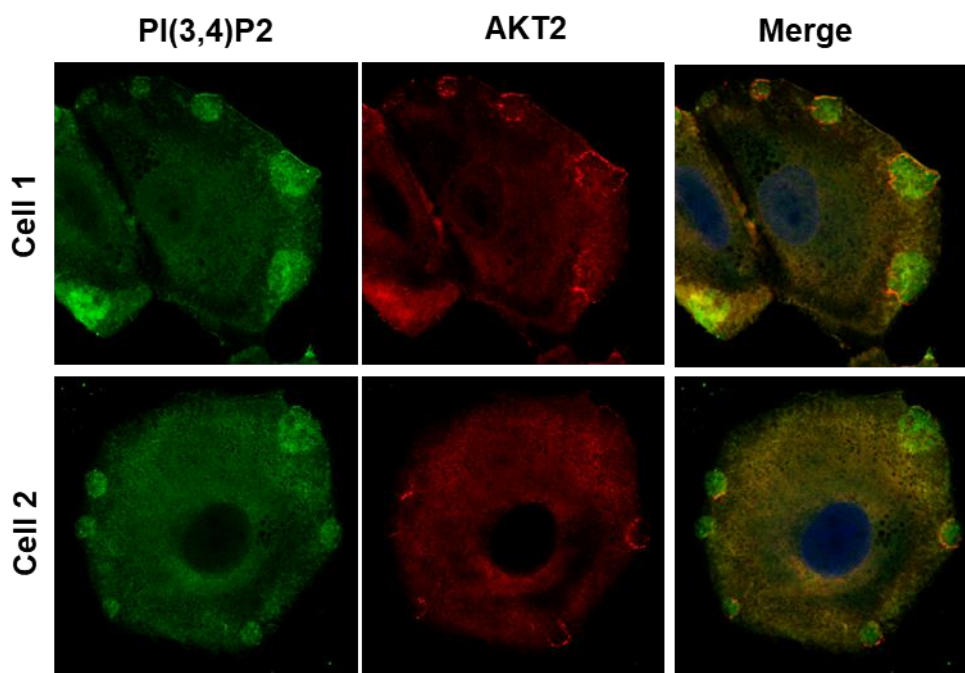


**Figure 29. AKT2 enwrap around special structures containing PI(3,4)P2.** Huh7-Lunet cells were trypsinized and seeded on coverslips. 24 h later the cells were fixed, permeablized and stained for PI(3,4)P2 and AKT2 using the plasma membrane staining protocol (see Material and Methods).

### 3.8.4. AKT2 interacts with paxillin

In my study, AKT2 was identified as a potential kinase to convey signals from PI(3,4)P2 to paxillin. To corroborate my hypothesis, I aimed to examine a possible physical interaction between the two proteins. For this purpose, protein lysates from Huh7-Lunet cells expressing mCherry-AKT2 were either pull-downed with an mCherry antibody or an IgG control. I indeed observed an interaction band of paxillin in the sample immunoprecipitated with mCherry-AKT2 (**Figure 30**), further supporting my hypothesis that AKT2 acted as a mediator kinase to interact with and phosphorylate paxillin.

## RESULTS

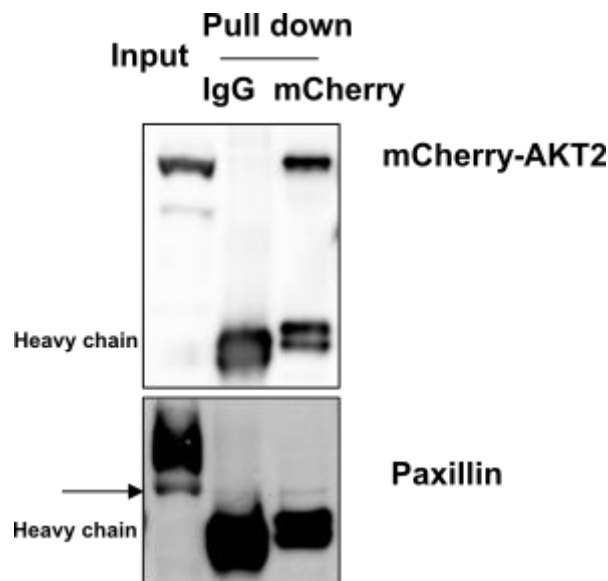


**Figure 30. AKT2 interacts with Paxillin.** Huh7-Lunet cells were transduced with lentiviruses expressing mCherry-AKT2 and selected with Blasticidin. Total cell lysates were immunoprecipitated (Pull down) with either mCherry antibody or IgG control overnight and further with Protein G beads for an hour. Bound proteins were then analyzed by immunoblot (IB) analysis using an anti-Paxillin antibody. The arrowheads denote Paxillin band.

### 3.8.5. A pan-AKT activator SC79 reverts the effects on cell morphology and on p-PXN and p-CFL1 levels mediated by PI4KA inhibition in cancer cells

Since I hypothesized that AKT (specifically AKT2) could act as a mediator kinase which conveyed signals from PI(3,4)P2 to paxillin and further downstream pathways, it was interesting to know if replenishing AKT activity in PI4KA-silenced cells could bring back the phenotypes of non-silenced cells. To this end, Huh7-Lunet cells were treated with PI4KA-inhibitor F1 at 0.05  $\mu$ M for 48 h. Compared to DMSO treatment, these cells showed dramatic morphological changes (second versus first image from the top, **Figure 31A**) as well as a reduction of p-paxillin, p-cofilin and p-AKT2 (lane 2 versus lane 1, **Figure 31C**) as described in detail in the previous sections. These cells were then further treated with SC79, a pan-AKT activator. This AKT activator targets all the three AKT 1/2/3 isoforms and specifically binds to their PHD domains (134). The interaction activates Akt in the cytosol by inducing a conformation change favoring phosphorylation by upstream protein kinases (134). As shown in the **Figure 31C**, treatment with SC79 restored the levels of p-AKT2, indicating a specific effect of this activator. More importantly, this treatment induced changes of cell morphology back to control status (**Figure 31A** and **B**) and reversed the reduction of p-paxillin and p-cofilin in a dose-dependent manner (**Figure 31C**). These data highlighted that AKT (most likely AKT2) activity was important for the PI4KA-regulated cytoskeleton rearrangement.

## RESULTS

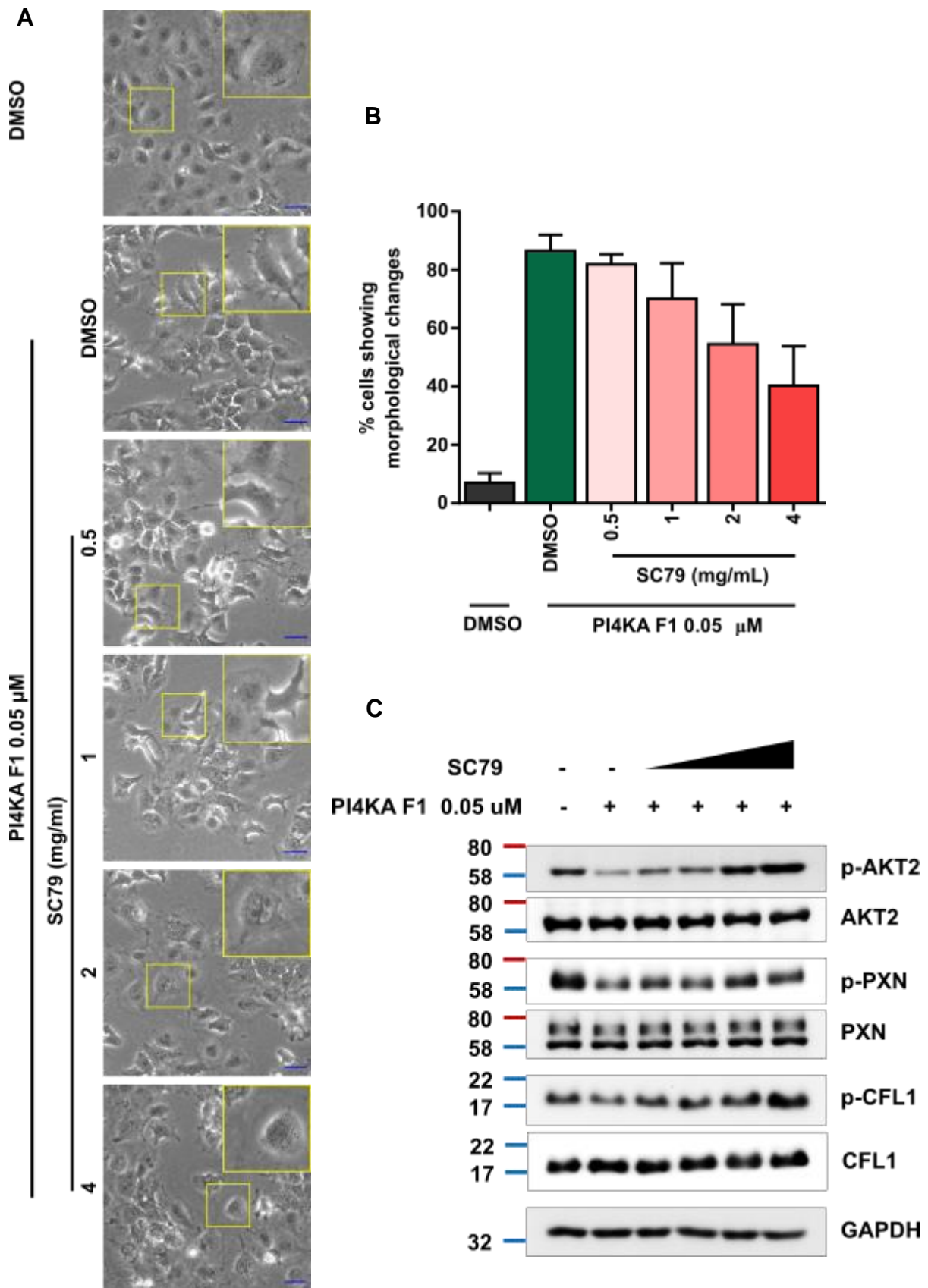


**Figure 31. Reversion of effect of PI4KA inhibition on cell morphology and levels of p-paxillin and p-cofilin by SC79.** **A.** Huh7-Lunet cells were treated with PI4KA inhibitor F1 at 0.05  $\mu$ M for 48 h. SC79 were further added into the culture medium at the indicated concentration for 30 min. Cell morphology was recorded an inverted light microscope with 20x objective lens. **B.** Numbers of cells showing morphological changes were counted and percentages of these cells were obtained by dividing to the total number of cells. At least photos of six random areas covering minimum 300 cells in

## RESULTS

each condition were subjected for quantification. **C.** Protein lysates from the cells in **A** were extracted and subjected to Western blot for further analysis of p-paxillin, p-cofilin, and p-AKT2.

### 3.8.6. Constitutive active AKT2 reverts morphological changes induced by silencing of PI4KA

My previous data showed that silencing of PI4KA reduced AKT2 phosphorylation and I hypothesized that AKT2 bridged PI4KA/PIK3C2G with further downstream cytoskeletal proteins. To further clarify the specificity of AKT2 in the signaling pathways, I constructed plasmids expressing AKT2 wt and constitutive active mutant S474D and introduced to Huh7-Lunet cells expressing shPI4KA via lentiviral transduction. As shown in the **Figure 32**, while AKT2 wt could only to a minor extent reduce the number of cells with morphological changes, its constitutive active mutant significantly reversed the morphological alterations observed in cells with low PI4KA expression. In summary, I found that PI4KA was important for cytoskeleton organization via the pathway PIK3C2G/AKT2 and the two signaling phosphoinositides PI4P and PI(3,4)P2. This pathway in turn positively regulated phosphorylation of paxillin and cofilin, controlling cell morphology and favoring cell motility of liver cancer cells.

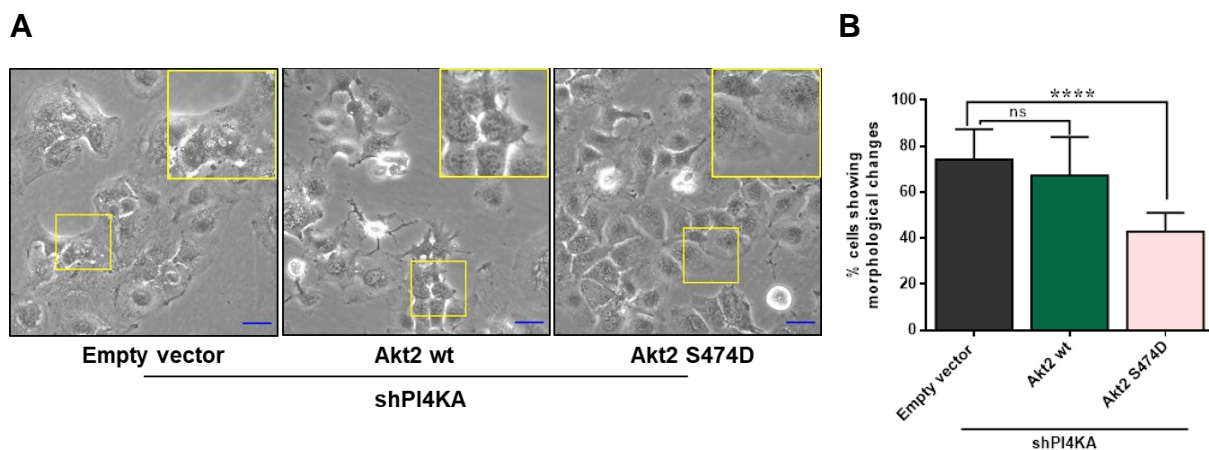


**Figure 32. Reversion of PI4KA silencing effects on cell morphology by constitutive active Akt2.** **A.** Huh7-Lunet-shPI4KA were transduced with lentiviruses encoding either Akt2 wt or constitutive active mutant S474D or empty vector. These cells were seeded in a 6-well plate and morphology of the cells was monitored and recorded using an inverted bright-field microscope. Scale bars represent 50  $\mu$ m. **B.** Graph represents percentages of cells showing morphological changes. At least photos of six random areas covering minimum 300 cells in each condition were subjected for quantification.

### 3.9. Validation of key phenotypes in mice

My data from cell culture highlighted the importance of PI4KA in regulation of cytoskeletal rearrangements which contributed to shaping cellular morphology and favored cell migration and invasion via an elevation of p-paxillin and p-cofilin. Moreover, via activation of PI4KA, HCV up-regulated the transduction pathways. Encouraged by these findings I aimed to validate some key *in vitro* data in mice using different approaches including expression of

## RESULTS

---

PI4KA or HCV via hydrodynamic tail-vein injection, injection of liver cells expressing shNT or shPI4KA and HCV infection in liver-chimeric mice.

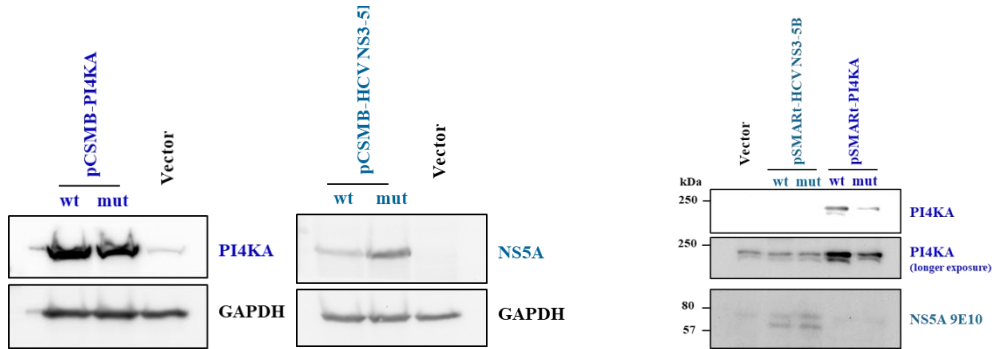
### 3.9.1. Hydrodynamic injection of plasmids expressing PI4KA or HCV nonstructural proteins

To exogenously express PI4KA or HCV NS3-5B in mice, I firstly integrated the genes encoding these proteins into either a Sleeping Beauty (SB) transposon vector or a scaffold/matrix attachment region (pS/MAR) harboring vector with liver-specific promoters (**Figure 33A**). The SB system is well-established in mice, allowing gene delivery specifically into mice hepatocytes (135,136). In this system, hydrodynamic tail vein injection of plasmids harboring a recombinant SB transposon vector and transposase induces selective uptake by hepatocytes. This process of DNA uptake is not well understood but following hydrodynamic injection, the liver is responsible for more than 95% of the expressed transgenic DNA (136). The combination of a nuclear S/MAR element and a human liver-specific promoter  $\alpha$ 1-antitrypsin allows long term expression of a transgene in murine liver after hydrodynamic injection (137,138). The anchorage of episomal vectors to the chromosomal scaffold during mitosis mediated by S/MARs allows persistent gene expression over hundreds of cell divisions. A pair of wt and inactive mutant devoid of PI4KA activity (PI4KAmut) or activation (NS3-5BmutPPH) was included in every setup. Expression of these constructs was firstly tested in Huh7-Lunet cells. As revealed in **Figure 33A**, all the constructs showed detectable expression. These plasmids were then along with Sleeping Beauty transposase or alone (in the case of pSMART) delivered into hepatocytes of mice via hydrodynamic tail-vein injection. 4 weeks post injection the mice were sacrificed and their livers were collected. The organ was divided into two parts with one being snap frozen for immunoblot analysis and the other undergoing a fixation with PFA before subjecting to immunohistochemistry. In order to obtain a representative sample for western blotting, tissues were taken at 3 different positions and pooled together before preparing lysates. Expression of PI4KA wt or HCV NS3-5Bwt in mice led to an overall higher expression of p-paxillin and p-cofilin than in the control samples, while levels of these two phosphoproteins were lower in the case of mice receiving the mutant variants, confirming my previous observation in cell culture that PI4KA and HCV-activated PI4KA positively regulated p-paxillin and p-cofilin (**Figure 33B, C and D**). Furthermore, livers of mice expressing PI4KA wt or HCV wt also had higher scores of steatosis and hepatocellular hypertrophy, as evaluated by Dr. Tanja Poth (**Appendix 1**). These data taken together further supported my hypothesis that PI4KA contributed to the liver pathogenesis via regulation of cytoskeletal pathways also *in vivo*.

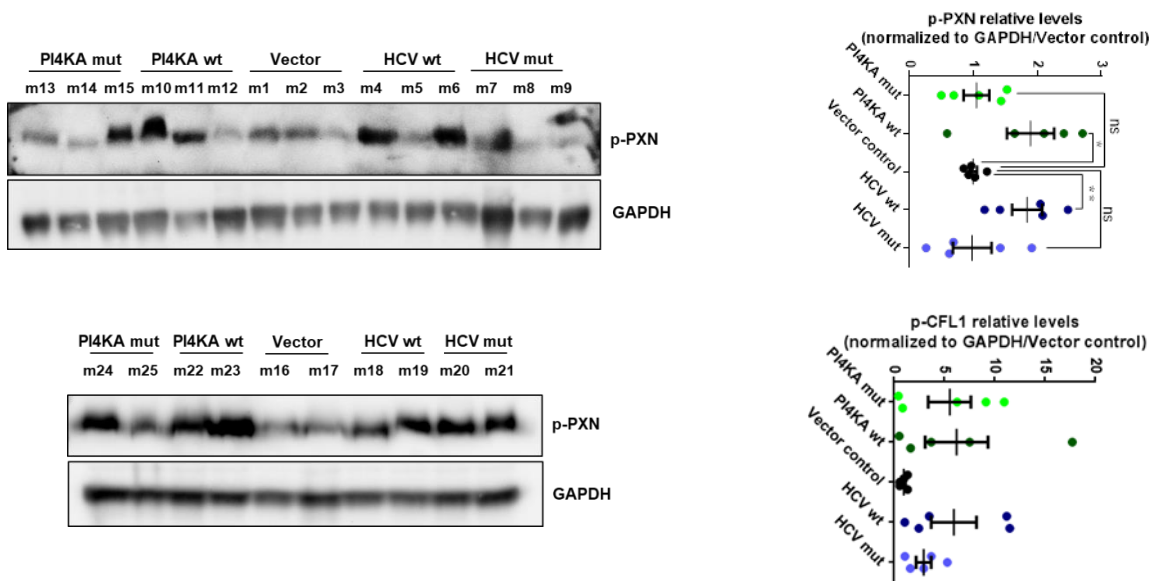


# RESULTS

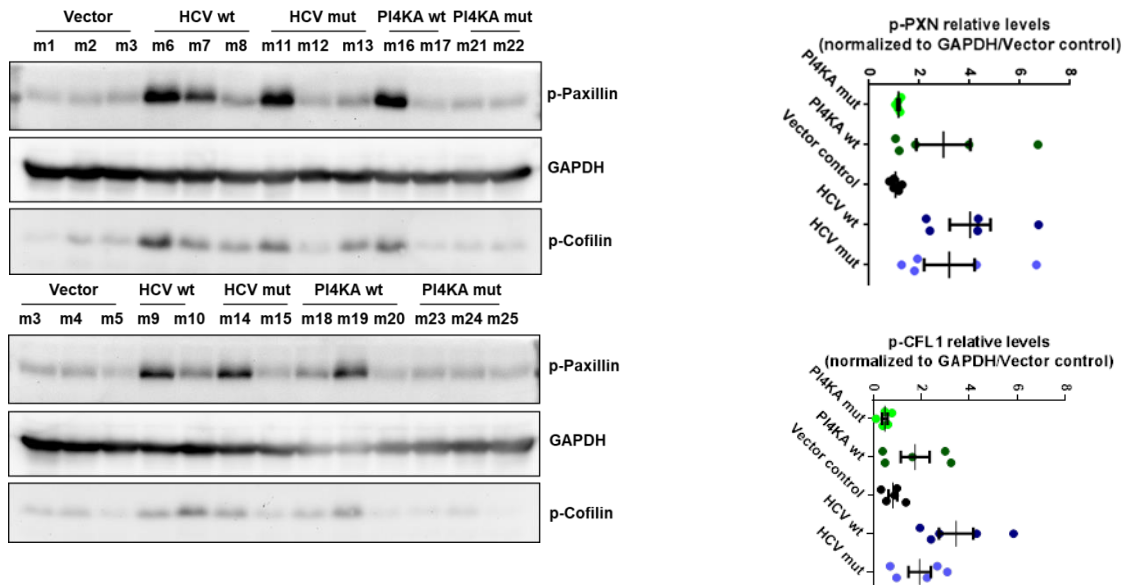
**A**



**B**



**C**



## RESULTS

D

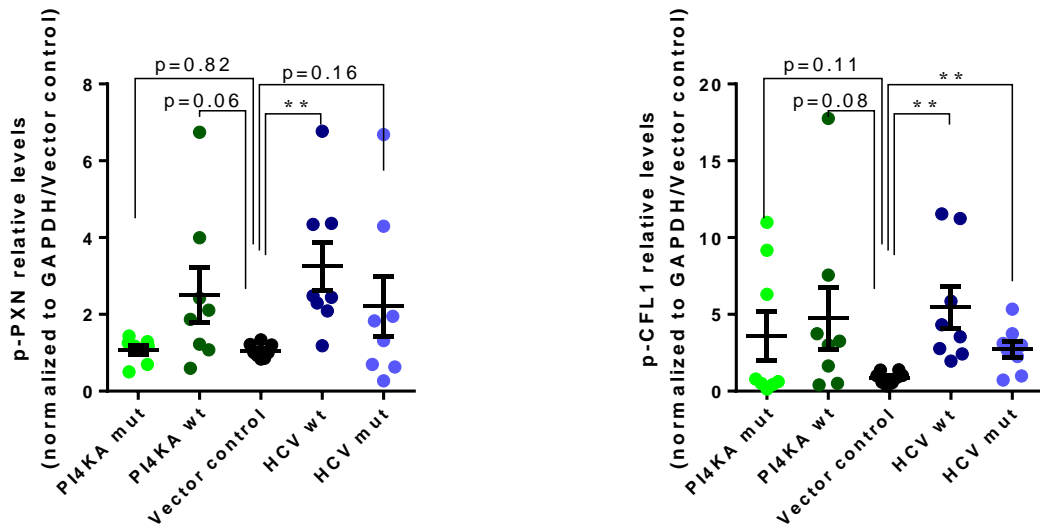


**Figure 33. Expressing PI4KA wt or HCV wt led to upregulation of p-paxillin and p-cofilin in livers of mice.** **A.** PI4KA (wt or the mutant D1957A) or HCV NS3-5B(wt or the mutant PPH) was cloned into Sleeping Beauty-transposon vector pCSMB or episomal DNA vector pSMART. Protein expressions of the genes were verified in Huh7-Lunet cells. **B.** The plasmids in **A.** were hydrodynamically injected into mice tail vein by the research group Darjus Tschaharganeh. Upper left panel: mice received pCSMB plasmids, 3 mice/ group. Lower left panel: mice received pSMART plasmids, 2 mice/ group. Mice livers were collected at 4 weeks post injection. Expression of p-paxillin and p-cofilin were verified by Western blot (left panel) and protein intensities were quantified and normalized to the GAPDH using Fiji (right panel). **C.** Similar to **B.** but all the mice received pCSMB plasmids, 5 mice/ group. **D.** Summary of the quantified relative levels of p-paxillin (left panel) and p-cofilin (right panel) in **B.** and **C.**

### 3.9.2. Injection of human liver cancer cells with modulated PI4KA expression into SCID mice

Another approach addressing PI4KA regulated cell migration and invasion *in vivo* was based on the transfer of tumor cells with different PI4KA expression levels into mice via injection and monitor tumor formation. To facilitate *in vivo* imaging, Huh7-Lunet cells stably expressing *Firefly*-luciferase were firstly established by lentiviral transduction. Lysates from these cells showed a high expression of luciferase (data not shown). These cells were further transduced with lentiviruses encoding shRNA to silence PI4KA or shNT. Morphological examination revealed the previous described differences between the two cell lines, confirming the functionality of shPI4KA (data not shown). These cells were then transferred to the research group of Professor Matti Sällberg at the Karolinska Institute for *in vivo* experiments. The cells were prepared in PBS at different densities and injected subcutaneously into the dorsal flank of SCID mice, devoid of adaptive immune responses to avoid destruction of the human cells by the murin immune system. *In vivo* imaging was performed at day 3, 5, 10, 14, 18 and 21 (**Figure 34**). In comparison to the mice adopting PI4KA knockdown cells, *in vivo* imaging showed in overall larger area of luciferase signal-positive cells in the case of control shNT, some of them developed over the time course (**Figure 34**). In contrast, signals of PI4KA silencing cells declined rapidly and many of them were already below the threshold (**Figure 34**). These data suggested that *in vivo* the liver

## RESULTS

cancer cells with high PI4KA expression could proliferate better and had more potential to grow into tumors than the cells with low PI4KA expression (PI4KA knockdown cells).

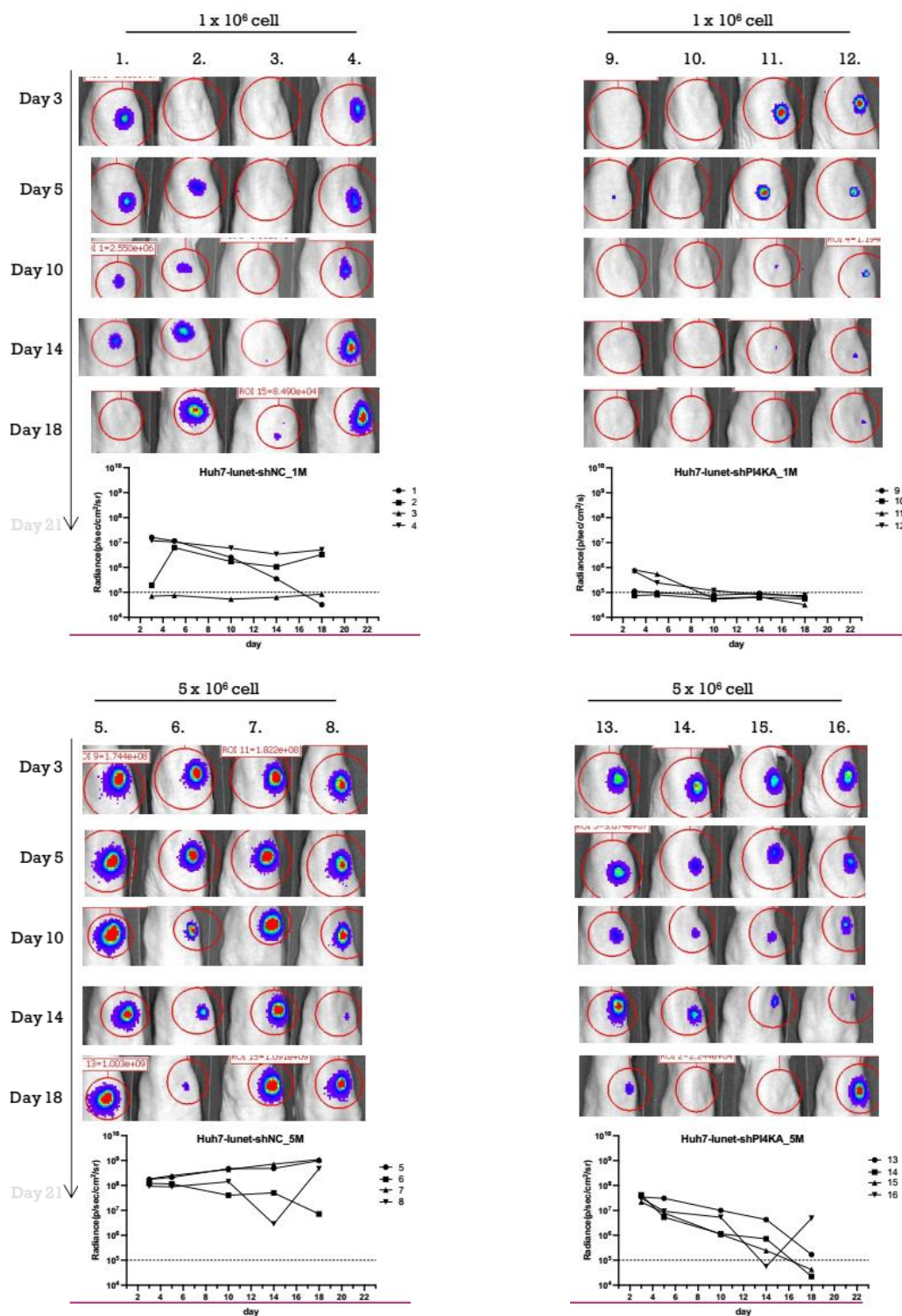


**Figure 34. IVIS signals were stronger in the mice incubated with control cells than with PI4KA-depleted cells.** (Data was provided by Jingyi Yan) Either  $1 \times 10^6$  cells or  $5 \times 10^6$  Huh7-Lunet-Luc-shNT and -shPI4KA cells were prepared in  $200 \mu\text{L}$  PBS and were injected subcutaneously into the dorsal flank of each mouse. *In vivo* imaging (IVIS) was performed at day 3, 5, 10, 14, 18 and 21.

## RESULTS

---

### 3.9.3. Autologous transfer of murine HCC derived cells with modulated PI4KA expression

In the previous section, I used human liver cells Huh7-Lunet and nude mice as recipients to monitor how these cells behave *in vivo* in regards to different levels of PI4KA. In addition, I employed injection of mouse liver hepatoma cells Hep55.1C, derived from C57BL/6 mice, into the autologous mouse strain. The research group of Professor Florian Kühnel (Medizinische Hochschule Hannover) kindly performed these experiments. I firstly created a stable Pi4ka knockdown cell line and the respective non targeting control (see **Figure 15D**). The PI4KA gene is conserved in many animals including mouse and the sequences of mouse Pi4ka and human PI4KA share high similarity. The shPI4KA sequence completely matched with coding sequence in mouse Pi4ka. Therefore, I could use the established shPI4KA to knockdown the gene in mouse cells. I indeed observed an approximately 80% reduction in the Pi4ka expression (**Figure 15D**). These Pi4ka knockdown cells also showed a strong decline in the invasiveness, similarly to the effects of PI4KA silencing on the human hepatoma cell lines as described previously (**Figure 15D**). The cells were intravenously infiltrated into immuno-competent mice C57BL/6 and growth of lung colonies was monitored as a surrogate characterize cell invasiveness *in vivo*, as an indicator for metastasis formation. At the day 26th post injection, the mice were sacrificed and tumor burden in their lungs were examined. By estimation without any solid measurement, in contrast to our expectation, the group observed a little more tumor burden in the shPI4KA samples than in the shNT samples. However, the parental Hep55.1C cells were also included in the experiment and they showed significantly higher tumor burden than the other treatments. No solid data however was provided by the group. In my hands, by contrast, shNT expressing cells did not show any differences compared to their respective parental cells. Due to the time limit of this project I decided to not follow this model further.

### 3.9.4. HCV infection of human-liver chimeric mice

My last attempt to verify some phenotypes observed in cell culture *in vivo* was to use human-liver chimeric mice (provided and performed by the research group of Professor Philip Meuleman at Ghent University). These mice were shown to be susceptible to infection by HCV and HBV, providing an important tool for studying these viruses *in vivo* (139). In this study, primary human hepatocytes were transplanted into homozygous uPA+/+-SCID mice and liver humanization was assessed by quantification of human albumin in mouse plasma. Viral inoculum from the serum obtained from a patient after liver transplantation, containing a novel gt1b isolate designated as GLT1 were intrasplenic injected into these mice. HCV load in blood plasma was quantified at a two-weekly base until the mice were sacrificed at 8 weeks post infection. Livers were collected and expressions of human albumin, HCV NS5A and p-paxillin were revealed by immunohistochemistry on consecutive slices which was performed by the research group of Professor Mathias Heikenwälder (University of Heidelberg). As shown in **Figure 35**, there was successful infection of HCV in the human hepatocytes engrafted in the mice. Moreover, p-paxillin was much more abundant in the case

## RESULTS

of the HCV-infected sample. This observation, even though as a single replicate, confirmed the phenotype that I observed in cell culture that HCV upregulated p-paxillin levels.

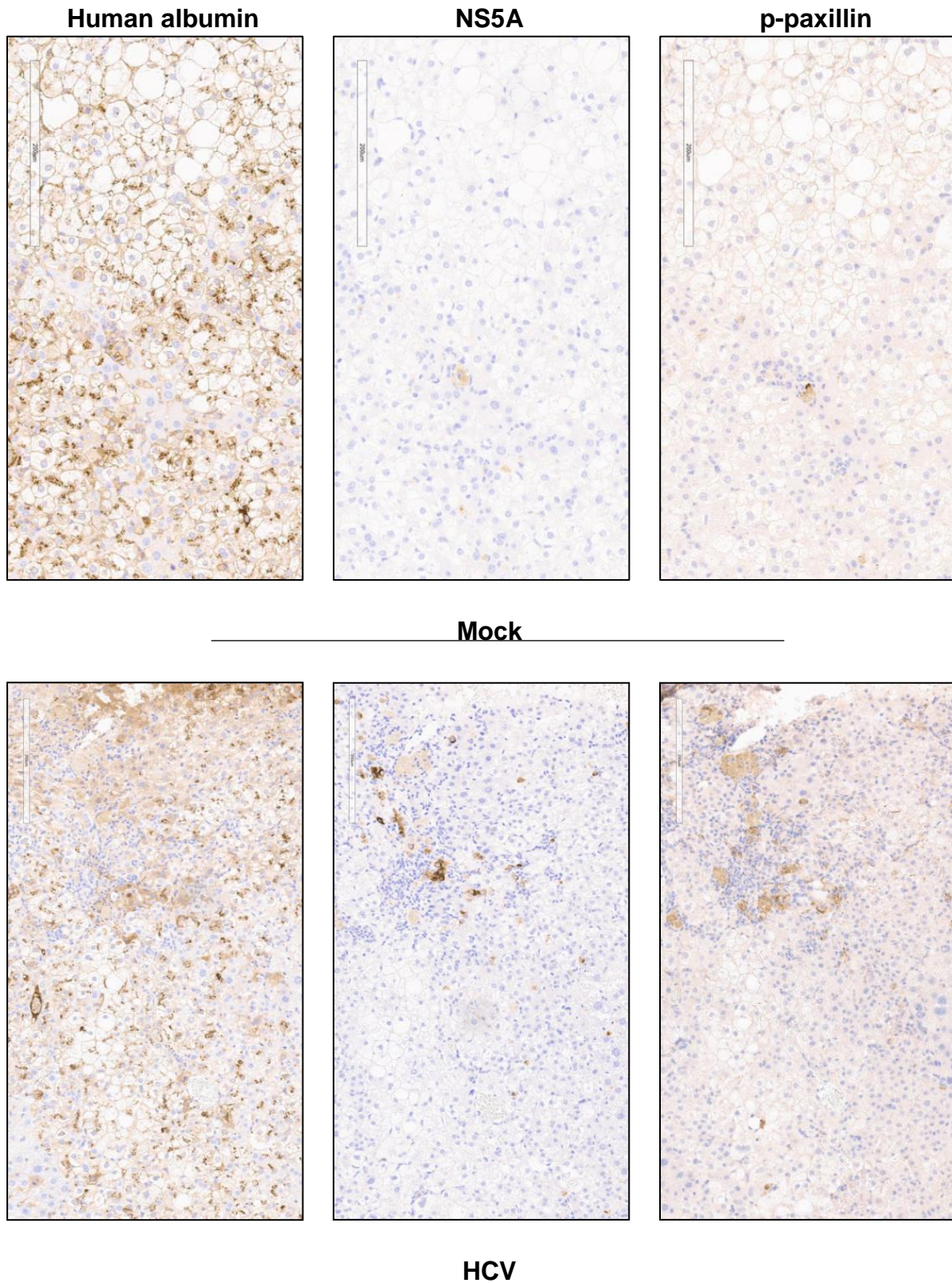


**Figure 35. HCV infection in mice led to an upregulation of p-paxillin.** Human hepatocytes were engrafted into homozygous uPA<sup>+/+</sup>-SCID mice. These mice were then infected with GLT1 wt high-titer post-transplant patient serum for 8 weeks. Mice livers were formalin fixed, paraffin embedded, cut and stained for human albumin, HCV NS5A and p-paxillin on consecutive slices.

# DISCUSSION

## 4. DISCUSSION

PI4KA is a well-known host factor for HCV replication. A recent work has shown an upregulation of this phospholipid kinase in HCC tissue and this overexpression of PI4KA was correlated with poor prognostic in liver cancer patient (74). It was however unknown how PI4KA contributed to the process of malignancy and whether the activation of the kinase by HCV could impact on liver pathogenesis. In this study I covered different aspects of PI4KA's functions on cell and cancer biology where the effects of HCV were also examined. My focus was firstly on characterization of PI4KA's roles in hepatocytes. Phenotypically, I found that PI4KA regulated cell morphology and favored cell motility which closely linked to its contribution to cytoskeleton rearrangement. Changes in many cytoskeletal components including stress actin fibers, microtubules, intermediate filaments and FAs were resulted from blocking expression or activity of the lipid kinase, highlighting PI4KA as a key signaling molecule in many important cell functions and thus the dysregulation such as elevated expression in HCC or enhanced activity by HCV could potentially contribute to liver pathogenesis. The investigation on mechanistic link between PI4KA and its controlled phenotypes uncovered a signaling cascade PI4KA/PIK3C2G/AKT2/p-paxillin and p-cofilin which contributed substantially to the PI4KA-mediated pathogenesis. Roles of HCV in this succession of events were also revealed which directly linked to its capability of PI4KA activation. The flow of these signaling events were illustrated in my proposed model (**Figure 36**) but further details will be discussed in the following sections.

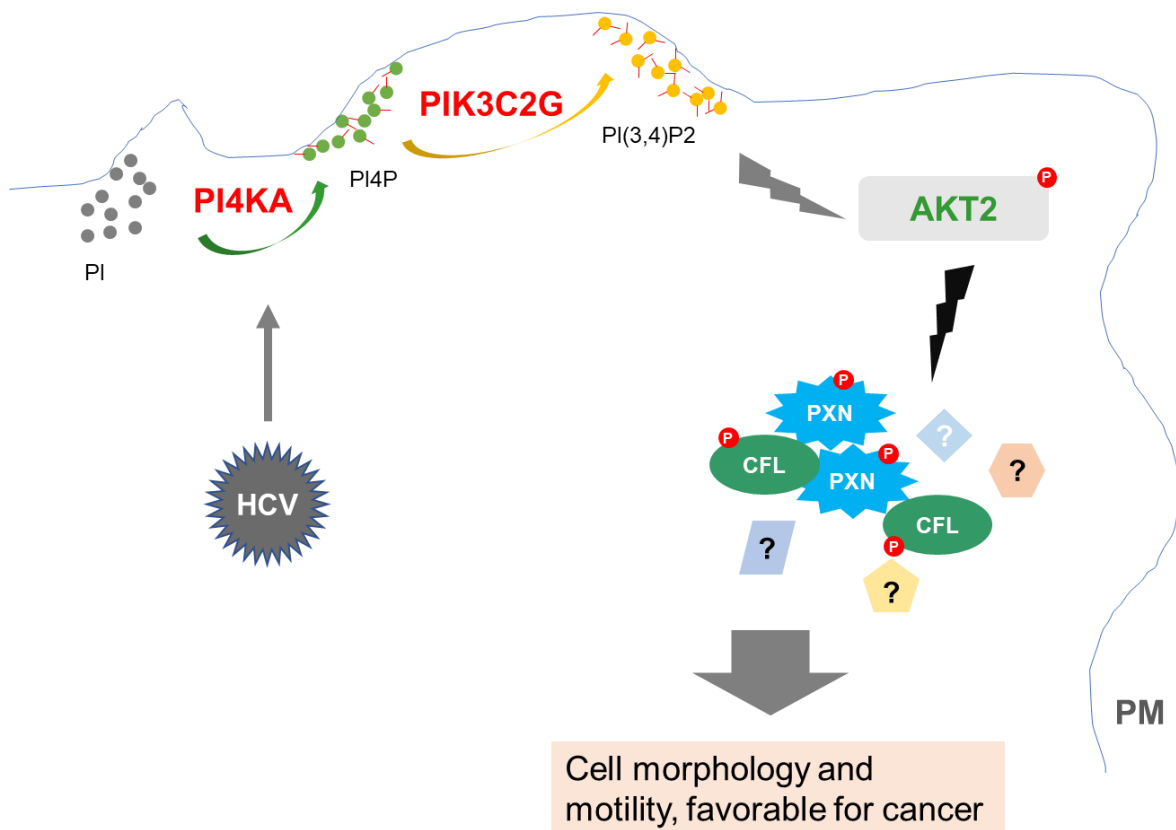


**Figure 36. Schematic model of the PI4KA's contribution to pathogenesis in the liver and the possible roles of HCV.** PI4P pools provided by PI4KA trigger PIK3C2G to synthesize PI(3,4)P2. These phosphoinositide molecules in turn activate AKT2 (and possibly other kinases) to promote

## DISCUSSION

---

phosphorylation of paxillin (and cofilin) and potentially additional factors regulating cytoskeleton rearrangements determining cell shape and favoring cell motility towards cancer progression. The contribution of HCV in this process is highlighted by its capability to activate PI4KA.

### 4.1. Important roles of PI4KA on cell morphology revealed by loss-of-function experiments

If PI4KA would play critical role in cell transduction pathways, in the context of highly expression of the protein in the human hepatoma cells, knocking down its expression or inhibiting its activity should exert an obvious effect on cell function. I firstly employed an shRNA previously shown specifically targeting PI4KA to check if depletion of the kinase could lead to any dramatic changes on signaling pathways, ideally revealed via a proteome or phosphoprotein array. I did not, however, expect that the silencing resulted in an obvious alteration in cell morphology which was reproducible and observed in several human liver hepatoma cell lines. Expressing PI4KA wt could fully revert the phenotype, indicating the specific effect of PI4KA on cell morphology.

Morphology is often neglected in cell culture, in parts since even clonal cell lines give rise to a substantial range of sizes and shapes. Although roles of PI4KA has been intensively studied in HCV replication in which silencing technology and inhibitor treatment were employed countlessly (77,78,79,80,81,82,84,85), there was no report so far, to my knowledge, of the effects of PI4KA reduction or inhibition on cell shape. However, my studies using shRNAs, rescue experiments and PI4KA inhibitors all agreed on the conclusion that PI4KA was important for cell morphology, at least in the liver cells and this function was specific to the kinase and was not found in any other members of the PI4K family.

My finding is, in fact, in line with previous studies on PI4KA's homologs and orthologs which have shown their importance in normal morphogenesis. These include the works on zebrafish showing the necessity of PI4KA for pectoral fin development (140) and its requirement for erythroid differentiation (108). Furthermore Yavari et al. (141) showed that in *Drosophila* Stt4 (an ortholog of PI4KA) was crucial for smoothed activation during wing imaginal disc development. A study by Tan J et al. (142) in *Drosophila melanogaster* further indicated that PI4KA deletion led to morphological defects. The protein was claimed to be essential for structural integrity of the plasma membrane during oogenesis and act as a key regulator of cortical integrity and trafficking events at the plasma membrane. In this study, PI4KA deletion also led to recessive lethality (and hemizygous males died shortly after embryogenesis as first instar larvae). They also showed that deletion of PI4KA caused irregular egg chamber morphology. Several morphological alterations were found including altered location of nurse cell nuclei in the ooplasm, rather than being restricted to the anterior of the egg chamber, irregular organization of the overlying layer of follicle cells, lacking dorsal appendages in egg chambers. In mice, PI4KA is required for the myelin formation and myeloid formation and differentiation and is crucial for gastrointestinal stability (108). Moreover, sciatic nerves of mutant mice with PI4KA inactivation in Schwann cells (cross-bred between conditional knockout mice of the *Pi4ka* gene (105) and B6N.FVB-Tg(Mpz-cre)<sup>26Mes/J</sup> transgenic mice (143)) were completely transparent and soft which were distinctly different from the control mice with white and firm nerves. These mice also showed



## DISCUSSION

---

a striking reduction in myelin thickness with severe impacts on nerve conductivity and motor functions. My finding on a previously not-yet-deciphered contribution of the PI4KA on cell shape is, therefore, adding up to the list of its pleiotropic roles on morphogenesis. This observation was as well a very important cornerstone of my study, encouraging me to further study functional contribution of this phospholipid kinase on liver cell signaling pathways and its potential consequences on pathogenesis.

### **4.2. Role of PI4KA on cell migration and invasion**

Cell shape is an important aspect of cell biology. Alterations in cell shape often reflect significant changes in cytoskeleton rearrangement which could eventually affect various other aspects of cell functions (37,38). Despite the significant impact on cell morphology, I found no remarkable effect of PI4KA silencing or inhibition on cell proliferation. However, migration and invasion of the hepatoma cells were significantly reduced by the lack of PI4KA. It was in accordance with the observation of reduced EMT features in the PI4KA knockdown cells in comparison with the control. My finding is, indeed, in line with previous studies showing the importance of this kinase on migratory and invasive properties of cancer cells, although via different signaling pathways.

These include the work by Alvarez-Prats A et al. (144) on Schwann cells, the cells in the peripheral nervous system that produce the myelin sheath around neuronal axons, which showed that inhibition of PI4KA by PI4KA-A1 inhibitor led to a significant reduction in cell migration even though the PI3K activation was still intact. This was the result of a completely broken-down actin organization with reduced numbers of stress fibers but enhanced cortical actin. Furthermore, according to the work of Sbrissa D et al. (145), ablation of PI4KA reduced cell invasion induced by CXCR4. This G protein coupled receptor recruited PI4KA to the plasma membrane for PI4P production by interacting with EFR3B and TTC7B. PI4P was also found on the invasive projections in the CXCR4 expressing cells. Moreover, there was an increase in PI4KA expression in metastatic tumors compared to the primary tumor counterparts and normal adjacent tissue, revealed by data set from extracted NCBI and IHC, highlighting the PI4KA's role in tumor metastasis. Silencing of PI4KA reduced cell invasion without affecting the cell proliferation, in agreement with my observation in the human hepatoma cells. In addition, Kim JH et al. (146) showed that in clear-cell renal-cell carcinoma, PI4KA expression was elevated in the tumor tissues compared with the adjacent normal tissues, both at mRNA and protein levels which promoted renal tumor progression via the WNK1-TRPC6-NFAT pathway. Wound-healing assay and Boyden chamber assay also revealed that PI4KA knockdown in Caki1 and ACHN cells reduced cell migration and invasion. My findings and the works of others therefore highlighted the necessity of PI4KA in cell motility which potentially contributes significantly in cancer progression and could mechanistically contribute to the previously observed (74) poor prognosis and increase in metastasis in HCCs with enhanced PI4KA expression.

### **4.3. Role of PI4KA on cytoskeleton and FAs**

The significant impact of PI4KA on cell morphology and cell motility led me to decipher the roles of PI4KA on cytoskeleton rearrangement in liver cells. I found that all the major

## DISCUSSION

---

cytoskeleton components, including actin filaments, microtubules and intermediate filaments as well as FAs were significantly altered in response to the differences in PI4KA expression and enzyme activity. These phenotypes were strongly associated with the effects of PI4KA on cell morphology and cell motility, indicating that PI4KA is an important regulator of the cytoskeleton contributing significantly to cancer cell malignancy.

Indeed a work on *Saccharomyces cerevisiae* (147) has highlighted crucial roles of Stt4p, a PI4KA's ortholog, in actin cytoskeleton organization and its contribution to maintain vacuole morphology and cell wall integrity. Stt4p via remodeling actin cytoskeleton and cell wall also regulated cell size or polarized growth. In *Drosophila melanogaster*, lacking PI4KA strongly affected F-actin (142). There was a huge loss in cortical F-actin in early female germ line clones (GLCs), followed by aggregations of F-actin into or across the oocyte in late stage. Buckled and disorganized F-actin along the oocyte cortex was found in the mutant lacking PI4KA, in contrast to the smooth and rigid appearance in the wt control. Furthermore, lectin staining and transmission electron micrographs revealed the loss of plasma membrane in these mutant GLCs. In human nerve cells, depletion of PI4KA affected the balance of actin polymerization and depolymerization as well as a prominent loss of stress fibers (144). These phenotypes are, indeed, to a certain extent reminiscent of the phenotypes which I observed in human hepatoma cells lacking PI4KA.

There had not been a clear connection between PI4KA and FAs. However PI4KB has been implied in regulation of FAs, cell shape and cell morphology (37). In this study, PI4P-containing vesicles were shown to translocate to the migratory leading edge during migration and some of them were found to tether to and fuse with FAs. Reduction of FA numbers and reduction of cell motility caused by silencing of PI4KA in my study seems to be counter-intuitive, however this relationship is more complex than usually thought. FA is not only required for cell attachment but also play crucial roles in cell migration. Cellular stress fibers connect with ECM via FAs which translate the force on actin fibers into cell movement. How PI4KA regulates cell migration and invasion via regulating cytoskeleton components and FA should be further studied in detail using advanced technologies, including electron microscopy and live-cell imaging. However, my studies clearly unraveled the signaling pathway starting with increased PI4P concentrations and ending in phosphorylation of PXN and CFL1, which are critical regulators of FAs.

### **4.4. Identification of p-paxillin and p-cofilin as cytoskeletal proteins regulated by PI4KA**

I found that PI4KA regulated cytoskeleton organization via upregulating phosphorylation of paxillin and to a lesser extent cofilin. Contribution of paxillin to liver carcinogenesis has been highlighted in previous studies. In HCC patient samples, there was an association between high paxillin expression with low differentiation, with the presence of portal vein thrombosis, and with extra-hepatic metastasis (148), indicating the link with high malignancy potential. Furthermore, higher expression of paxillin was found in liver metastases than in paired primary lesions in patients with stage IV colorectal cancer (149). In addition, several studies have suggested the importance of tyrosine phosphorylations Y31/118 of paxillin on cancer development. These include the requirement of paxillin phosphorylation for the collagen-

## DISCUSSION

---

induced migration of the rat bladder carcinoma NBT-II cells (150). Furthermore, migration of human melanoma cells on vitronectin (151) and invasive property of cervical and prostate cancers (152,153) also required tyrosine phosphorylation of paxillin.

It is, however, not excluded that PI4KA could regulate other cytoskeletal components as well. In fact, using a cytoskeleton array applied on PI4KA inhibitor treated cells I identified many other cytoskeleton proteins which could be potential targets of PI4KA (**Appendix 3**). Silencing of PI4KA led to alterations in all the main constituents of cytoskeleton including actin filaments, tubulin and intermediate filaments as well as FAs, indicating that PI4KA exerted its function in many aspects of the cytoskeleton and thus many other cytoskeletal proteins could be targeted by PI4KA. However, based on changes in p-paxillin and p-cofilin, I could study the mechanism how these events occurred in liver cells. In addition, only ectopically expressing PI4KA wt but not any single downstream components could fully rescue the loss-of-function phenotypes induced by PI4KA silencing, indicating that this pathway is much more complex than it is presented here and it is required further investigation to fully understand the whole process.

### **4.5. Discovering PIK3C2G as a downstream kinase of the pathway**

In this study, by performing a screen on 12 phospholipid kinases which are connected to PI4P metabolism, I identified PIK3C2G as the only kinase showing similar regulation on cell morphology and the two cytoskeletal proteins p-paxillin and p-cofilin in comparison with PI4KA. Furthermore, silencing of this kinase also led to reductions in cell motility (migration and invasion) and the number of FAs and to disruption of actin filament meshwork as similarly as observed in the case of knocking down PI4KA. These findings argue for the role of PIK3C2G as a direct downstream kinase of PI4KA in the signaling pathway which regulates cytoskeleton and exerts effects on cell morphology and cell movement.

In addition to PIK3C2G, I also found that silencing of PIK3CD also led to reductions of p-paxillin and p-cofilin, however the magnitude of reduction was not comparable to PI4KA knockdown. Furthermore, the gene depletion did not alter cell shape as observed in the case of PI4KA silencing. PIK3CD belongs to the PIK3 class I family which can convert PI(4,5)P<sub>2</sub> to PI(3,4,5)P<sub>3</sub> from which PI(3,4)P<sub>2</sub> can also be synthesized by some phosphatases. I therefore reasoned that the effects observed with PIK3CD silencing could be due to partial loss of PI(3,4)P<sub>2</sub> products which could exert its effects on the cytoskeletal pathway. This hypothesis was further supported by the observation that loss of PI4KA or PIK3C2G did not alter plasma membrane PI(3,4,5)P<sub>3</sub> levels, suggesting only minor impacts of this phosphoinositide on the pathway. However signaling pathways are often complex and many molecules often cooperate to regulate a pathway, therefore I cannot exclude the possibility that PI(3,4,5)P<sub>3</sub> or other phosphoinositides could also work downstream of PI4P in regulating cell shape and motility in the liver. My data, nevertheless, highlighted PI(3,4)P<sub>2</sub> as a main downstream effector of the signal transduction pathway in HCC derived cells studied in this thesis.

Another possibility could be that in some cases phospholipid kinases of the same family could provide enough of their respective phosphoinositide product if one of its member is

## DISCUSSION

---

missing due to the redundancy of the systems, and therefore individual silencing of a kinase as performed in my screen could not reveal the possible importance of other phosphoinositides than PI4P and PI(3,4)P<sub>2</sub>. This question could possibly be addressed by targeting multiple kinases in the same family using siRNAs, however this approach could also pose other problems such as effects on cell death or cell growth if depleting all crucial phosphoinositides. On the other hand, phosphoinositide kinases in a same family usually have distinct subcellular localization and therefore contribute to different pools of a specific phosphoinositide in cells (6,154,155). For instance, while PI4K2A and PI4K2B are mainly localized at endosomes and the trans golgi network, PI4KA is mainly found in the ER but also transiently at the plasma membrane and PI4KB is known to distribute to the Golgi and trans Golgi network (6,155), being responsible for the production of different subcellular fractions of PI4P. This also explains why lacking one lipid kinase is detrimental for cells, such as lethality found in mice with PI4KA knocked out (23,105). Above all, my data indicated that PI4KA and PIK3C2G are the two phospholipid kinases playing major roles in regulating cell shape and motility via interacting with components of cytoskeleton in our cell culture models.

PIK3C2G was found to be expressed mainly in the liver and some traces were detected in pancreas (130,156). In the liver, it was localized to hepatic parenchyma. Lack of PIK3C2G in mice led to insulin resistance and reductions in glycogen deposits in liver and increased fat storages. However, the mutant mice looked indistinguishable with the wt mice and did not show any signs of growth defects. Interestingly, *Pik3c2g*<sup>-/-</sup> mice showed impairment of AKT2 activation (reduced phosphorylation at both sites) but did not affect AKT1 phosphorylation upon insulin stimulation at later time. Furthermore these mice showed reduced PI(3,4)P<sub>2</sub> spatially localized on early endosomes but not PI(3,4,5)P<sub>3</sub> accumulation at the plasma membrane in response to insulin treatment. These findings were to some extent in agreement with my data on the roles of PIK3C2G in regulation of cytoskeleton and further supported the idea of targeting PIK3C2G instead of PI4KA for local and specific effects.

Few studies have suggested important function of PIK3C2G on biology and diseases development of the liver. During liver regeneration after partial hepatectomy expression of PIK3C2G is increased in a time-dependent manner, implying a possible involvement of the kinase in some yet-undefined liver-specific functions (154,156). PIK3C2G was also found to link to cancer. There was a significant association between mutations in the PIK3C2G gene and poor prognosis in patients with intrahepatic cholangiocellular carcinoma (ICC) (154,157). Low copy number of PIK3C2G in stage III colorectal cancer patients treated with oxaliplatin was correlated with increased probability of recurrence and increased risk of death (154,158). Furthermore, some PIK3C2G single nucleotide polymorphism (SNPs) were found to link with increased risk of developing type 2 diabetes in a Japanese population, diabetic nephropathy, hyperlipidemia and myocardial infarction, and high body mass index, highlighting an important function of PIK3C2G in regulating cell metabolism (154,159,160,161,162). However, the role of this protein on cancer development seems to be controversial. The work by Li A. et al. (163) indicated that low copy number of PIK3C2G was associated with increased risk of both recurrence and death in colorectal cancer patients

## DISCUSSION

---

(with stage III disease) treated with oxaliplatin, it was still a question how PIK3C2G functioned in that case since the protein is mainly found in liver and only traces were detected in few other tissues.

To study further the role of PIK3C2G on liver cell biology and cancer biology, I have tried to monitor localization of PIK3C2G in cell using antibodies which were claimed to be specific against the kinase by the manufacturers. There were only 2 antibodies available and we had tried using both but none of them revealed specific signal of the protein in Western blot and immunofluorescence analysis (data not shown and 122). The investigation on how PIK3C2G contributes to the signaling pathways was therefore still open for many questions. Work in the future could focus on establishing a stable cell line expressing PIK3C2G with a small tag or fused to an autofluorescent protein, with an aim to detect localization of the kinase in cells and understand more about the mechanism. Furthermore, the gene encoded for this protein has 3 isoforms and it would be interesting to study which isoform contributed mainly to the signaling pathways in liver pathogenesis. More importantly, little is known about PIK3C2G's roles in cell migration and invasion, especially in liver cancer. My data for the first time showed that this lipid kinase played important role in cell motility in liver cancer cells. Silencing of this kinase led to reductions in both cell migration and invasion. This is consistent with the role of PI(3,4)P<sub>2</sub> in cell motility. Further detail how PIK3C2G contributes to these cellular functions will be facilitated by live-cell imaging studies or inhibitor studies and will pave the way for a potential target in liver cancer therapy.

### 4.6. Detection of PI(3,4)P<sub>2</sub>

PI(3,4)P<sub>2</sub> is present at very low concentration in cells and research on this phospholipid was limited. Only recently this molecule has attracted more focus due to its uncovered roles in many cell functions, including cancer development. One reason that limits the studies on PI(3,4)P<sub>2</sub> is the availability of sensitive methods for detection. There are ELISA, biosensors and antibodies available to detect PI(3,4)P<sub>2</sub> as well as other phosphoinositides in cells. Biosensors using the PH domains from Tapp1 and p47phox fused to fluorescent proteins have been widely used to detect PI(3,4)P<sub>2</sub> (164). This approach allows monitoring intracellular distribution and changes in relative levels of this molecule, is in particular useful for live-cell imaging. However, overexpression of biosensors may interfere with interactions between the phosphoinositide and endogenous proteins, leading to misinterpretation of the phenotypes observed. More importantly, besides the main target PI(3,4)P<sub>2</sub> these biosensors can also bind to other phosphoinositides, in most cases PI(3,4,5)P<sub>3</sub>, posing a major concern about their specificity. Another limitation of using biosensors is that these molecules do not equally show affinity to all PI(3,4)P<sub>2</sub> pools in cells (164). Although antibodies can only be used for fixed cells, their specificity is a major advantage for quantification of phosphoinositides in cells. This is, to my knowledge, the first study showing PI(3,4)P<sub>2</sub> in cells using a specific antibody and linking PI4KA expression and activity with plasma membrane PI(3,4)P<sub>2</sub> levels. Furthermore, plasma membrane pools of the other two phosphoinositides with connection to PI4P; PI(4,5)P<sub>2</sub> and PI(3,4,5)P<sub>3</sub>; remained unchanged upon alterations of PI4KA expression. This was in line with several previous studies showing that PI(4,5)P<sub>2</sub> levels were not changed in cultured cells when PI4KA was inhibited (105) or inactivated (23).

## DISCUSSION

---

Furthermore, a study by Alvarez-Prats A et al. (144) has shown that prolonged inhibition of PI4KA resulted in a large reduction of plasma membrane PI4P levels, but did not lead to changes in plasma membrane PI(4,5)P2 levels. Instead, the reductions were found prominently in phosphatidylserine, phosphatidylethanolamine, and sphingomyelin content. In prostate cancer cells, knockdown of PI4KA led to reduced-levels of PI4P and PI(3,4)P2 but increased levels of PI(4,5)P2 and PI(3,4,5)P3 (145).

Although for a long time there had been little attention on PI(3,4)P2, several recent studies have suggested important roles of this low abundant phosphoinositide in cell and cancer biology. Many important cellular processes were found under control of PI(3,4)P2, including formation of podosome (165), membrane ruffle (166), formation (167) and maturation (168) of lamellipodia which are all crucial for cell movement. PI(3,4)P2 was actively involved in rearrangements of cytoskeleton at the cell plasma membrane (169). Reduced cell motility was found in PI(3,4)P2 depleted B cells during chemotaxis (170). In breast cancer cells, PI(3,4)P2 but not PI(3,4,5)P3 was the key for lamellipodia formation which favored cell motility and invasion (171). In particular, generation of PI(3,4)P2 supports cell membrane ruffling and lamellipodia formation, leading to cell invasion, whereas inhibition of its production led to formation of stress fibers and FA, resulting in cell spreading and increased cell area (171). Via a screen on phospholipid kinases which work in connection with PI4P, my unexpected identification of PI(3,4)P2 as an important messenger in regulating cytoskeletal pathways and cell motility is, therefore, further supporting the role of this molecule in important cell functions and signaling pathways.

### 4.7. Identification of AKT2 as the downstream kinase

In order to regulate the cytoskeletal proteins p-paxillin and p-cofilin which in turn contribute to important cell functions such as cell adhesion, migration, invasion and morphogenesis, signals from the phosphoinositides required the activation of a protein kinase. In order to identify the potential kinases which worked as mediator in the signaling pathways, I firstly aim to identify which kinase could be regulated by PI4KA/PIK3C2G. Using a protein kinase array in combination with validation in Western blot analysis, I found out that silencing of either PI4KA or PIK3C2G consistently led to significant reductions in phosphorylation of AKT2. In cells there are 3 AKT isoforms: AKT1, AKT2 and AKT3. Accumulation of PI(3,4)P2 or PI(3,4,5)P2 recruits and activates AKT via engagement of its PH domain. Phosphorylation of the two key residues on AKT, T308/309/305 and S473/474/472 (AKT1/2/3, respectively) is necessary to achieve maximal activation of the kinase. Activated AKTs in turn phosphorylate many downstream targets. Many proteins with a consensus recognition motif of R-X-R-X-X-S/T-f (where X is any amino acid and f denotes a preference for large hydrophobic residues) are direct targets of AKT. Phosphorylations by AKT are performed on Ser and Thr residues. More than 100 AKT substrates have been reported. They belong to many protein classes, including kinases, transcription factors, regulators of small G proteins and vesicle trafficking and cell cycle, metabolic enzymes, E3 ubiquitin ligases, etc. mTOR, GSK3, FOXO are the 3 main signaling pathways regulated by AKT, in turn cell survival, proliferation, metabolism and many important cell functions are under controlled of this kinase (172). Since the kinase array which I used in my study only covered a small part of human kinases, there was a high

## DISCUSSION

---

possibility that other kinases could also be targeted by the two phosphoinositides. Indeed ectopically expressing the constitutive active AKT2 or applying pan AKT activator could only revert partially the morphological changes as well as loss of p-paxillin and p-cofilin caused by silencing or inhibition of PI4KA, despite the full recovery of AKT2 activity. It could also be argued that localization of AKT2 played important role in this signaling cascade and that the exogenous expression or stimulation could not mimic fully the endogenous AKT2. However, all these observations implied that the transduction pathways were likely much more complex than presented here with involvements of many other proteins or molecules and future works will hopefully uncover these complex processes. My data, nevertheless still highlighted the importance of AKT2 as a kinase relaying signals from PI4P/PI(3,4)P2 to p-paxillin, p-cofilin and further downstream to regulate cell morphology and other important cell functions. My findings were also in agreement with previous works which indicated that PI(3,4)P2 selectively activated AKT2 at both the plasma membrane and early endosomes via preferential binding to its PH domain (173). In addition, my observations that AKT2 was enwrapping around the PI(3,4)P2-containing structures localized at the plasma membrane further strengthen my knowledge on how these two molecules interact each other in cells. To my knowledge, it was the first time that a close connection between the two signaling molecules was revealed using immunofluorescence. Spatial and temporal activation of AKT2 by PI(3,4)P2 under regulation of PI4KA could also be an interesting topic for future studies. How AKT2 colocalizes and interacts with paxillin and if AKT2 regulates cofilin and actin stress fibers still remain elusive but are interesting topics for future studies as well.

A previous study has shown that activation of AKT1 was hampered by silencing of PI4KA (144). It was indeed in agreement with my study that the level of AKT1 phosphorylation was reduced upon PI4KA depletion. However, the effect was much stronger in my study on the activation of AKT2. Roles of the two AKT isoforms on cell and cancer biology are still contradictory. However the common finding was that AKT1 is important for motility in fibroblasts and endothelial cells whereas AKT2 is important for epithelial cells motility (129). In lung cancer, AKT2 exerted important role in cellular proliferation and colony formation as well as cellular motility and invasion (174). However Zhou GL et al. (175) showed that in mouse embryo fibroblast cell, knockout of AKT2 reduced cell size, but resulted in more lamellipodia. Loss of AKT2 led to aberrant cell ruffling. Expression of AKT2 but not AKT1 could rescue the dorsal ruffle phenotype. Loss of AKT2 increased cell migration. My study highlighted the role of AKT2 as the mediator in regulating cytoskeletal proteins, in particular promoting p-paxillin which could potentially contribute to motility of cancer cells.

### **4.8. Roles of HCV**

In this study, I found that HCV could enhance phosphorylation of the two cytoskeletal proteins p-paxillin and p-cofilin as well as phosphorylation of AKT2. Furthermore, FA numbers in the HCV-infected cells were more abundant than in the mock control. HCV also promotes invasiveness of the Huh7-Lunet cells. These phenotypes induced by HCV were correlated with the capability of PI4KA activation, indicating that the lipid kinase activity was the main driver of the phenotypes. However, as mentioned earlier, besides activating PI4KA HCV also manipulated other proteins and their signaling pathways. Therefore, I did not

## DISCUSSION

---

exclude the possibility that other factors could contribute to the phenotypes observed in HCV-infected cells or HCV-expressing cells. Moreover the phenotypes observed were much more pronounced in the case of infection than in expression models. One factor could likely contribute to this difference was that with expression model, I could achieve only a maximum of 40-50% cells being HCV positive. In contrast almost every cell showed positive signals of HCV NS5A at the time of harvesting in the infection model. Moreover, the lack of HCV structural proteins in expressing system could also contribute to the discrepancy.

Some previous studies have suggested the connection of HCV with paxillin and AKT, however to some extent showed several differences to my study. According to the work by Alisi et al. (176), HCV upregulated total paxillin levels revealed by western blot but the p-paxillin levels were not examined. They also showed that HCV promoted cellular proliferation, migration and invasion but reduced adhesiveness without showing the FA numbers. In my study, however, the levels of p-paxillin and numbers of FA were highly upregulated by HCV which was in agreement with the activation of PI4KA. This discrepancy could not be explained by differences in cell lines or virus used since I have tested several cell lines and HCV genotypes which were included in their study. Furthermore, although using different arrays Ziyad et al. (108) and I (**Appendix 2**) both identified p-paxillin, but not total paxillin as a target of PI4KA. With regards to AKT, a previous work by Liu Z et al. (131) showed that HCV transiently activated AKT1 for its viral entry. However how AKT2 was regulated by HCV had remained unknown. In my study, the levels of AKT2 were examined when most of the cells were positive with HCV at day 4-6 post infection. I found a significant upregulation of AKT2 phosphorylation in the case of HCV Jc1-infected cells. I did not examine the activation of AKT2 at earlier time points because my interest was on signaling pathways regulated by HCV via activation of PI4KA when the virus was already established, as a model for persistent infection and potential impact on pathogenesis. I also investigated the activation of AKT2 as well as phosphorylation of paxillin and cofilin with the other two HCV genotypes for which I could achieve moderate infection levels. The gt 3a isolate DBN3a but not the gt 1a isolate TN also showed an upregulation of p-AKT2, p-paxillin and p-cofilin, albeit with lower fold induction in comparison with the Jc1. This was correlated with the levels of PI4P induced by different HCV viruses. However, I could not exclude the possibility that replication capacity also contribute to this observation. Among the three HCV viruses, Jc1 was the most efficient in terms of replication, followed by DBN3a and TN, respectively. Nevertheless, using adenovirus-mediated gene expression I found that levels of p-paxillin was associated with expression of HCV wt in regardless of replication but dependent on PI4P induction capacity, also in PHH, which are considered the most physiological liver-derived cell culture model.

HCV contributes significantly to HCC and is known to induce metastasis (177,178,179). The mechanism is not yet well understood but it has been suggested that, on the one hand, HCV can act directly as an oncogenic factor but on the other hand, inflammatory responses caused by the infection is another important factor for HCC (177,178,179). Core and NS5A are the two HCV proteins which have been frequently linked to the development of HCC and metastasis. HCV NS5A has been shown to enhance AKT activity via suppression of PTEN,



## DISCUSSION

---

in turn supporting cancer cells survival (180). Furthermore, proliferation and metastasis of HCC cells were promoted by HCV NS5A via activation of the AKT/ GSK3 $\beta$ / $\beta$ -catenin pathway (181). Interestingly, the replication of HCV in the tumor was reduced in comparison to the surrounding nontumorous areas (182). HCV seems to induce multi protumorous factors, leading to HCC development of HCC. My study therefore contributes to better understanding of HCV-induced HCC.

Several other aspects could also be interesting for future studies. These include how HCV enhanced levels of plasma membrane PI(3,4)P2. Whether this upregulation of PI(3,4)P2 observed in HCV-infected cells were solely due to an upsurge in PI4P production still remained to be answered. Furthermore how HCV regulated PIK3C2G is still an open question. It could be interesting to investigate if HCV activates the kinase or promotes its translocation to plasma membrane. However it is clear that HCV does not only activate PI4KA but also manipulate other host proteins and signaling pathways. Therefore the phenotypes observed in my models could also result from additional contributions of other signaling pathways. It is therefore important to note that in this study, HCV was used as a supporting tool but not exclusive for studying functional roles of PI4KA. I found indeed HCV-activated PI4KA positively regulated levels of PI(3,4)P2/p-AKT2/p-paxillin (and to a lesser extent p-cofilin) as well as cell motility and FA numbers which could potentially contribute to HCV-induced pathogenesis. Since HCV is known as one of the main etiology of HCC, it would be interesting to investigate further *in vivo* if blocking the PI4KA/PIK3C2G/pAKT2/p-paxillin could improve the outcomes of HCC and metastasis burdence.

### 4.9. Efforts to validate key phenotypes in more physiological models

In this study, I have used Huh7-derived cell lines as central models for my studies. However several key phenotypes were also validated in other cell liver cell lines, including Hep3B, HepG2, HHT4 and PHH. Furthermore, expressing human PI4KA or HCV proteins NS3-5B in mice also confirmed my cell culture data that PI4KA wt but not mutant increased levels of p-paxillin and to a lesser extent p-cofilin and HCV performed the similar contribution due to its activation of PI4KA. Furthermore, chimeric mice infected with HCV also showed higher expression of p-paxillin in immunohistochemistry. We further found that hepatocytes of those mice which received plasmid expressing HCV or PI4KA wt were larger than the control mice (**Appendix 1**). Furthermore Huh7 shNT revealed more IVIS signals than the shPI4KA in mice. Potential metastasis of the transplanted cells with different PI4KA expression could be examined by applying a model demonstrated by Ninio L et al. (183), quantifying numbers of human DNAs in different mice organs. These data supported my hypothesis in cell culture that PI4KA is important for liver cancer development, acting on cytoskeleton rearrangements via at least two phosphoproteins paxillin and cofilin and in turn exerting effects on cell morphology, and that HCV contributed to these phenotypes via activation of PI4KA. However these data were still limited and I hope in the future to establish more robust models to study function of PI4KA *in vivo*. There are two general approaches for studying invasion in mice: genetically engineered mouse models (GEMMs) and transplantation of tumor cells or tumor tissue into host mice. These two strategies are both suitable for investigation of early

## DISCUSSION

---

invasiveness but distant metastases are not frequently observed in the former approach (184) although some recently established GEMMs allowed studying metastasis of several cancers, including HCC with closer metastasis rates and tropisms to human cancers (184,185). Therefore, studying far distant metastasis and therapeutic options still rely mainly on syngeneic and xenograft models using cancer cell transplantation. In deed, by transplanting a highly tumorigenic HCV replicon cell line S3-GFP into  $\gamma$ -irradiated SCID mice, Hazari S et al. (186) observed a formation of subcutaneous tumors and diffuse metastasis of HCC throughout the liver lobes after 2 and 4 weeks, respectively. The model of chimeric mice infected with HCV used in this study could be therefore a valuable tool for future investigations, aiming at better understanding how HCV infection in the long run leads to development of HCC and metastasis and how important the pathway PI4KA/PIK3C2G/AKT2 contributes to the clinical outcome. Therapeutic interventions could then be applied in this model to obtain an optimal treatment. Still other animal models should be developed and applied with an aim to mimic HCV infection in human hepatocytes with fully functional immune responses.

### **4.10. Implications of PI4KA, PIK3C2G and AKT2 in cancer progression and as cancer therapeutic targets**

In recent years, several studies have suggested important roles of PI4KA in development of different types of cancer via different signaling pathways. In prostate cancer, it was shown that CXCL12 and its receptor CXCR4 play key roles in mediating prostate cancer bone metastasis and PI4KA was identified as a CXCR4 regulator. In CXCR4-expressing cells, PI4KA protein expression was elevated by approximately 2 fold without significant change in mRNA levels. This linked to the role of CXCR4 in regulating translational machinery involved in mTORC1 signaling. Furthermore, PI4KA activity was found to be upregulated in these cells. CXCR4 directly interacted with PI4KA adaptor proteins associated with PI4KA in lipid rafts and recruited PI4KA to the plasma membrane to induce PI4P production. Suppression of PI4KA reduced cellular invasion mediated by CXCR4. Interestingly, PI4P was found to localize on the invasive projections in CXCR4-expressing cells. More importantly, human tumor studies demonstrated increased expression of PI4KA in metastatic tumor versus the primary tumor counterpart (145).

PI4KA was further shown to be involved in WNK1-mediated  $Ca^{2+}$  signaling in the development of clear-cell renal-cell carcinoma (ccRCC), the most common type of renal cancer. In this context expression of TRPC6 which had previously linked to renal pathologies, such as focal and segmental glomerulosclerosis, fibrosis, and RCC together with that of WNK1, PI4KA and the nuclear factor of activated T cells cytoplasmic 1 (NFATc1) were elevated in the tumor tissues compared with the adjacent normal tissues. TRPC6 acted as a predominant molecular component of receptor-operated  $Ca^{2+}$  entry mechanism in ccRCC cells and its activation was blunted by depleting PI4KA. Knockdown of PI4KA or other components in the WNK1-PI4KIII $\alpha$ -mediated TRPC6-NFATc1 pathway also attenuated proliferation and migration of ccRCC (146).

In pancreatic cancer cells, PI4KA was associated with oncogenic KRAS signaling. PI4KA converts PI to PI4P at the PM. ORP5 and ORP8 then mediate the exchange of PM PI4P with

## DISCUSSION

---

PtdSer from the ER. PI4KA inhibition by inhibitor C7 led to mislocalization of KRAS from the plasma membrane and inhibited growth of cancer cells by reducing PI4P, and in turn plasma membrane phosphatidyl serine (187). ERF3, an adapter protein which recruits PI4KA to plasma membrane also contributed to oncogenic KRAS signaling and transformation of cancer cells. In this context, binding of activated KRAS with ERF3 led to recruitment of PI4KA to the plasma membrane, in turn induced higher levels of PI4P and PS and stimulated oncogenic signaling and transformation via maintaining and promoting localization and nanoclustering of KRAS at the plasma membrane (188).

It is also worth to notice that inhibition of PI4KA radiosensitizes in a human tumor xenograft and an immune-competent syngeneic murine tumor model. Mechanistically, inhibition of PI4K effectively down regulated the PI3K pathway *in vitro*. Radiation in combination with simeprevir, an HCV antiviral with activity of PI4KA inhibition significantly attenuated tumor growth in a breast cancer xenograft model which is related in part in down-regulation of PI3K $\delta$  expression (189).

Indeed, my study is in line with these findings, showing that PI4KA is important for cell morphology and cell motility of liver cancer cells, favoring cancer progression via modulating cytoskeleton components. PI4KA could therefore be a potential therapeutic target for HCC, especially HCV-related HCC. Several chemical compounds have been developed to target specifically PI4KA (105). Although genetic ablation of PI4KA led to lethality in adult mice, challenging it as a putative therapeutic target, PI4KA inhibitors used at proper concentrations showed no cytotoxicity (105). Moreover, effects of these drugs on cancer progression, especially on metastasis of HCC have never been studied.

PIK3C2G, in contrast to other PIK3C2 proteins, is expressed restrictedly in the liver and to a minor extent in the pancreas. Furthermore, PIK3C2G is only involved in the production of only single phosphoinositide product PI(3,4)P<sub>2</sub> (6). The specificity of PIK3C2G could be advantageous for being a therapeutic target. Due to its restricted expression it is expected that such compounds should have less severe side effects than PI4KA inhibitors if they are applied *in vivo*. Research studies on PIK3C2G are, however, still limited. A specific PIK3C2G inhibitor is not available, yet a recent work by Freitag et al. (190) had shown some compounds which could be promising for specifically targeting the kinase. These compounds were screened in a nonradiometric ADP Glo Assay against eight PI3K isoforms *in vitro* and act at nanomolar concentrations. However, so far effects in the context of cell culture or *in vivo* have not been studied. Applying these compounds in Huh7-Lunet cells using a wide range of concentration, Julia Kersten nevertheless did not notice any alteration in cell morphology nor levels of p-paxillin and p-cofilin (122). This had raised a concern over uptake and/or the metabolism of these compounds. Could these macromolecules pass the cell plasma membrane and other barriers in cells to target the kinase? How were these compounds processed in cells? What were their half-lives? These questions should be addressed before any further studies about their effects on cell biology would be carried out. In fact, Bojjireddy N et al. (105) has shown that there were significant variations in the potency of the compounds to inhibit purified PI4KA *in vitro* and to inhibit PI4P synthesis at the PM, implying the differences in their ability to reach the relevant cellular compartments

## DISCUSSION

---

despite similar chemistries. Work in the future focusing on screening PIK3C2G inhibitors in cell culture and *in vivo* thus will be important and will serve as the basis to understand further the clinical impact on inhibiting this kinase on cell signaling pathways.

In addition to PI4KA and PIK3C2G, my work also identified AKT2 as an important signaling component downstream of the pathway that regulates HCV-activated PI4KA-induced liver pathogenesis. The AKT pathway plays essential roles in tumorigenesis and tumor metastasis by controlling crucial cell functions, including cell survival, proliferation, migration and differentiation. This pathway is frequently found dysregulated in many human cancers (172,191,192). Overexpression and activation of AKT, especially AKT2 is found to correlate with the aggressiveness of cancer and poor survival rates in lung, breast, ovarian, gastric, colorectal and pancreatic cancers (172,191,192,193,194,195). Moreover, AKT2 but not other AKT isoforms expression correlates with prognosis of human HCC (196). More importantly, among the 3 isoforms liver was shown to express predominantly AKT2, and deletion of this isoform significantly impaired hepatic AKT activity and the occurrence of HCC in c-Met-transfected mice (197). AKT, specifically AKT2 is therefore a potential therapeutic target for treatment of liver cancer. However, due to high sequence homology, the development of Akt-specific and isoform-selective inhibitors has been predicted to be challenging (191). Still several compounds showing specificity against AKT2 over other isoforms have been developed (198). Future studies should further investigate on using these specific inhibitors on treatment and prevention of HCC and metastasis both *in vitro* and *in vivo*, with or without the presence of HCV.

### 4.11. Outlook

In summary, my data shed a light on the importance of the phosphoinositides PI4P and PI(3,4)P<sub>2</sub> in regulating signaling pathways connected to cytoskeleton and in turn promoting cell migration and invasion as well as shaping cell morphology. Due to its low concentration in cells, PI(3,4)P<sub>2</sub> was not considered as an important phosphoinositide. However, recent studies have highlighted important contribution of this signaling molecule in different cell functions. With the advancement of new technologies it is believed that more important functions of this molecule in cell biology and diseases will be discovered. The kinases and phosphatases responsible for its metabolism will also be central in many future studies. Expression of PIK3C2G, one of the kinases responsible for synthesizing PI(3,4)P<sub>2</sub> is more restricted, especially more liver specific, and thus could provide an alternative clinical target in treatment of cancer treatment over PI4KA which silencing or inhibition of it was shown to be lethal *in vivo* and therefore has not been considered as a therapeutic target. How PIK3C2G regulate cytoskeletal signaling pathway and if targeting the kinase could prevent cancer progression will be further addressed in the coming years with the development of suitable antibodies and specific inhibitors which could work in cell culture and *in vivo*. Furthermore, impact of the interference of PIK3C2G in HCV-infected cells will also be an interesting topic for future studies. The importance of phosphoinositides PI4P and PI(3,4)P<sub>2</sub>

## DISCUSSION

---

in the presented signaling pathways could also be further examined by exogenously introducing these phosphoinositides in the respective kinase-silenced cells. It could be facilitated by using immunofluorescence or other imaging techniques to investigate if these exogenous phosphoinositides can be delivered to the target sites. Furthermore, there are several inhibitors of PI4KA which were shown to selectively inhibit PI4KA activity and therefore other PI4KA inhibitors could also be included to support for the current data. Future studies should investigate if these PI4KA inhibitors could be applied for liver cancer treatment and if metastasis could be prevented by these treatments. Furthermore, more compounds which can specifically inhibit PI4KA activity with fewer side effects should be developed. More importantly, suitable animal models which can facilitate studies on the role of PI4KA and HCV on HCC progression and metastasis should be established.

## 5. REFERENCES

1. Thapa N, Tan X, Choi S, Lambert PF, Rapraeger AC, Anderson RA. The Hidden Conundrum of Phosphoinositide Signaling in Cancer. *Trends Cancer*. 2016 Jul;2(7):378-390. doi: 10.1016/j.trecan.2016.05.009. Epub 2016 Jun 20. PMID: 27819060; PMCID: PMC5094282.
2. Luo J, Cantley L. Phosphoinositide biology - messages from lipids. *Nat Cell Biol*. 2000 Oct;2(10):E190. doi: 10.1038/35036447. PMID: 11025682.
3. Jensen JB, Dickson EJ, Falkenburger BH. Phospholipids | Lipid Signaling and Ion Channels. *Encyclopedia of Biological Chemistry III (Third Edition)*. Elsevier. 2021:537-544. Doi: 10.1016/B978-0-12-819460-7.00110-9. ISBN 9780128220405.
4. Dickson EJ, Hille B. Understanding phosphoinositides: rare, dynamic, and essential membrane phospholipids. *Biochem J*. 2019 Jan 7;476(1):1-23. doi: 10.1042/BCJ20180022. PMID: 30617162; PMCID: PMC6342281.
5. Bunney TD, Katan M. Phosphoinositide signalling in cancer: beyond PI3K and PTEN. *Nat Rev Cancer*. 2010 May;10(5):342-52. doi: 10.1038/nrc2842. PMID: 20414202.
6. Burke JE. Structural Basis for Regulation of Phosphoinositide Kinases and Their Involvement in Human Disease. *Mol Cell*. 2018 Sep 6;71(5):653-673. doi: 10.1016/j.molcel.2018.08.005. PMID: 30193094.
7. Hammond GRV, Burke JE. Novel roles of phosphoinositides in signaling, lipid transport, and disease. *Curr Opin Cell Biol*. 2020 Apr;63:57-67. doi: 10.1016/j.ceb.2019.12.007. Epub 2020 Jan 20. PMID: 31972475; PMCID: PMC7247936.
8. Volpatti JR, Al-Maawali A, Smith L, Al-Hashim A, Brill JA, Dowling JJ. The expanding spectrum of neurological disorders of phosphoinositide metabolism. *Dis Model Mech*. 2019 Aug 13;12(8):dmm038174. doi: 10.1242/dmm.038174. PMID: 31413155; PMCID: PMC6737944.
9. D'Angelo G, Vicinanza M, Di Campli A, De Matteis MA. The multiple roles of PtdIns(4)P -- not just the precursor of PtdIns(4,5)P2. *J Cell Sci*. 2008 Jun 15;121(Pt 12):1955-63. doi: 10.1242/jcs.023630. PMID: 18525025.
10. De Matteis MA, Wilson C, D'Angelo G. Phosphatidylinositol-4-phosphate: the Golgi and beyond. *Bioessays*. 2013 Jul;35(7):612-22. doi: 10.1002/bies.201200180. Epub 2013 May 27. Erratum in: *Bioessays*. 2013 Aug;35(8):756. PMID: 23712958.
11. Balla A, Balla T. Phosphatidylinositol 4-kinases: old enzymes with emerging functions. *Trends Cell Biol*. 2006 Jul;16(7):351-61. doi: 10.1016/j.tcb.2006.05.003. Epub 2006 Jun 21. PMID: 16793271.
12. Batrouni AG, Baskin JM. The chemistry and biology of phosphatidylinositol 4-phosphate at the plasma membrane. *Bioorg Med Chem*. 2021 Jun 15;40:116190. doi: 10.1016/j.bmc.2021.116190. Epub 2021 May 1. PMID: 33965837; PMCID: PMC8169619.
13. Balla T. Phosphoinositides: tiny lipids with giant impact on cell regulation. *Physiol Rev*. 2013 Jul;93(3):1019-137. doi: 10.1152/physrev.00028.2012. PMID: 23899561; PMCID: PMC3962547.
14. Dorobantu CM, Albulescu L, Harak C, Feng Q, van Kampen M, Strating JR, Gorbalenya AE, Lohmann V, van der Schaar HM, van Kuppeveld FJ. Modulation of the Host Lipid Landscape to Promote RNA Virus Replication: The Picornavirus Encephalomyocarditis Virus Converges on the Pathway Used by Hepatitis C Virus. *PLoS Pathog*. 2015 Sep 25;11(9):e1005185. doi: 10.1371/journal.ppat.1005185. PMID: 26406250; PMCID: PMC4583462.

## REFERENCES

---

15. Arita M, Kojima H, Nagano T, Okabe T, Wakita T, Shimizu H. Phosphatidylinositol 4-kinase III beta is a target of enviroxime-like compounds for antipoliiovirus activity. *J Virol.* 2011 Mar;85(5):2364-72. doi: 10.1128/JVI.02249-10. Epub 2010 Dec 22. PMID: 21177810; PMCID: PMC3067798.
16. Hsu NY, Ilnytska O, Belov G, Santiana M, Chen YH, Takvorian PM, Pau C, van der Schaar H, Kaushik-Basu N, Balla T, Cameron CE, Ehrenfeld E, van Kuppeveld FJ, Altan-Bonnet N. Viral reorganization of the secretory pathway generates distinct organelles for RNA replication. *Cell.* 2010 May 28;141(5):799-811. doi: 10.1016/j.cell.2010.03.050. PMID: 20510927; PMCID: PMC2982146.
17. Greninger AL, Knudsen GM, Betegon M, Burlingame AL, Derisi JL. The 3A protein from multiple picornaviruses utilizes the golgi adaptor protein ACBD3 to recruit PI4KIII $\beta$ . *J Virol.* 2012 Apr;86(7):3605-16. doi: 10.1128/JVI.06778-11. Epub 2012 Jan 18. PMID: 22258260; PMCID: PMC3302542.
18. Sasaki J, Ishikawa K, Arita M, Taniguchi K. ACBD3-mediated recruitment of PI4KB to picornavirus RNA replication sites. *EMBO J.* 2012 Feb 1;31(3):754-66. doi: 10.1038/emboj.2011.429. Epub 2011 Nov 29. PMID: 22124328; PMCID: PMC3273392.
19. Altan-Bonnet N, Balla T. Phosphatidylinositol 4-kinases: hostages harnessed to build panviral replication platforms. *Trends Biochem Sci.* 2012 Jul;37(7):293-302. doi: 10.1016/j.tibs.2012.03.004. Epub 2012 May 25. PMID: 22633842; PMCID: PMC3389303.
20. Harak C, Radujkovic D, Taveneau C, Reiss S, Klein R, Bressanelli S, Lohmann V. Mapping of functional domains of the lipid kinase phosphatidylinositol 4-kinase type III alpha involved in enzymatic activity and hepatitis C virus replication. *J Virol.* 2014 Sep 1;88(17):9909-26. doi: 10.1128/JVI.01063-14. Epub 2014 Jun 11. PMID: 24920820; PMCID: PMC4136347.
21. Lees JA, Zhang Y, Oh MS, Schauder CM, Yu X, Baskin JM, Dobbs K, Notarangelo LD, De Camilli P, Walz T, Reinisch KM. Architecture of the human PI4KIII $\alpha$  lipid kinase complex. *Proc Natl Acad Sci U S A.* 2017 Dec 26;114(52):13720-13725. doi: 10.1073/pnas.1718471115. Epub 2017 Dec 11. PMID: 29229838; PMCID: PMC5748228.
22. Vaillancourt FH, Brault M, Pilote L, Uyttersprot N, Gaillard ET, Stoltz JH, Knight BL, Pantages L, McFarland M, Breitfelder S, Chiu TT, Mahrouche L, Faucher AM, Cartier M, Cordingley MG, Bethell RC, Jiang H, White PW, Kukulj G. Evaluation of phosphatidylinositol-4-kinase III $\alpha$  as a hepatitis C virus drug target. *J Virol.* 2012 Nov;86(21):11595-607. doi: 10.1128/JVI.01320-12. Epub 2012 Aug 15. PMID: 22896614; PMCID: PMC3486294.
23. Nakatsu F, Baskin JM, Chung J, Tanner LB, Shui G, Lee SY, Pirruccello M, Hao M, Ingolia NT, Wenk MR, De Camilli P. PtdIns4P synthesis by PI4KIII $\alpha$  at the plasma membrane and its impact on plasma membrane identity. *J Cell Biol.* 2012 Dec 10;199(6):1003-16. doi: 10.1083/jcb.201206095. PMID: 23229899; PMCID: PMC3518224.
24. Gehrman T, Gülkan H, Suer S, Herberg FW, Balla A, Vereb G, Mayr GW, Heilmeyer LM Jr. Functional expression and characterisation of a new human phosphatidylinositol 4-kinase PI4K230. *Biochim Biophys Acta.* 1999 Mar 25;1437(3):341-56. doi: 10.1016/s1388-1981(99)00029-3. PMID: 10101268.
25. Gehrman T, Heilmeyer LM Jr. Phosphatidylinositol 4-kinases. *Eur J Biochem.* 1998 Apr 15;253(2):357-70. doi: 10.1046/j.1432-1327.1998.2530357.x. PMID: 9654085.

## REFERENCES

---

26. Kakuk A, Friedländer E, Vereb G Jr, Kása A, Balla A, Balla T, Heilmeyer LM Jr, Gergely P, Vereb G. Nucleolar localization of phosphatidylinositol 4-kinase PI4K230 in various mammalian cells. *Cytometry A*. 2006 Dec 1;69(12):1174-83. doi: 10.1002/cyto.a.20347. PMID: 17131383.
27. Kakuk A, Friedländer E, Vereb G Jr, Lisboa D, Bagossi P, Tóth G, Gergely P, Vereb G. Nuclear and nucleolar localization signals and their targeting function in phosphatidylinositol 4-kinase PI4K230. *Exp Cell Res*. 2008 Aug 1;314(13):2376-88. doi: 10.1016/j.yexcr.2008.05.006. Epub 2008 May 27. PMID: 18585705.
28. Lees JA, Zhang Y, Oh MS, Schauder CM, Yu X, Baskin JM, Dobbs K, Notarangelo LD, De Camilli P, Walz T, Reinisch KM. Architecture of the human PI4KIII $\alpha$  lipid kinase complex. *Proc Natl Acad Sci U S A*. 2017 Dec 26;114(52):13720-13725. doi: 10.1073/pnas.1718471115. Epub 2017 Dec 11. PMID: 29229838; PMCID: PMC5748228.
29. Dornan GL, Dalwadi U, Hamelin DJ, Hoffmann RM, Yip CK, Burke JE. Probing the Architecture, Dynamics, and Inhibition of the PI4KIII $\alpha$ /TTC7/FAM126 Complex. *J Mol Biol*. 2018 Sep 14;430(18 Pt B):3129-3142. doi: 10.1016/j.jmb.2018.07.020. Epub 2018 Jul 18. PMID: 30031006.
30. Di Paolo G, De Camilli P. Phosphoinositides in cell regulation and membrane dynamics. *Nature*. 2006 Oct 12;443(7112):651-7. doi: 10.1038/nature05185. PMID: 17035995.
31. Saarikangas J, Zhao H, Lappalainen P. Regulation of the actin cytoskeleton-plasma membrane interplay by phosphoinositides. *Physiol Rev*. 2010 Jan;90(1):259-89. doi: 10.1152/physrev.00036.2009. PMID: 20086078.
32. Hohmann T, Dehghani F. The Cytoskeleton-A Complex Interacting Meshwork. *Cells*. 2019 Apr 18;8(4):362. doi: 10.3390/cells8040362. PMID: 31003495; PMCID: PMC6523135.
33. Fletcher DA, Mullins RD. Cell mechanics and the cytoskeleton. *Nature*. 2010 Jan 28;463(7280):485-92. doi: 10.1038/nature08908. PMID: 20110992; PMCID: PMC2851742.
34. Fife CM, McCarroll JA, Kavallaris M. Movers and shakers: cell cytoskeleton in cancer metastasis. *Br J Pharmacol*. 2014 Dec;171(24):5507-23. doi: 10.1111/bph.12704. Epub 2014 Jul 2. Erratum in: *Br J Pharmacol*. 2017 Jan;174(1):116. PMID: 24665826; PMCID: PMC4290699.
35. Friedl P, Wolf K. Tumour-cell invasion and migration: diversity and escape mechanisms. *Nat Rev Cancer*. 2003 May;3(5):362-74. doi: 10.1038/nrc1075. PMID: 12724734.
36. Yamaguchi H, Condeelis J. Regulation of the actin cytoskeleton in cancer cell migration and invasion. *Biochim Biophys Acta*. 2007 May;1773(5):642-52. doi: 10.1016/j.bbamcr.2006.07.001. Epub 2006 Jul 14. PMID: 16926057; PMCID: PMC4266238.
37. Bilodeau P, Jacobsen D, Law-Vinh D, Lee JM. Phosphatidylinositol 4-kinase III beta regulates cell shape, migration, and focal adhesion number. *Mol Biol Cell*. 2020 Aug 1;31(17):1904-1916. doi: 10.1091/mbc.E19-11-0600. Epub 2020 Jun 17. PMID: 32583740; PMCID: PMC7525810.
38. Luxenburg C, Zaidel-Bar R. From cell shape to cell fate via the cytoskeleton - Insights from the epidermis. *Exp Cell Res*. 2019 May 15;378(2):232-237. doi: 10.1016/j.yexcr.2019.03.016. Epub 2019 Mar 12. PMID: 30872138.



## REFERENCES

---

39. Olson MF, Sahai E. The actin cytoskeleton in cancer cell motility. *Clin Exp Metastasis*. 2009;26(4):273-87. doi: 10.1007/s10585-008-9174-2. Epub 2008 May 23. PMID: 18498004.
40. Nelson CM, Khauv D, Bissell MJ, Radisky DC. Change in cell shape is required for matrix metalloproteinase-induced epithelial-mesenchymal transition of mammary epithelial cells. *J Cell Biochem*. 2008 Sep 1;105(1):25-33. doi: 10.1002/jcb.21821. PMID: 18506791; PMCID: PMC2838485.
41. D'Anselmi F, Valerio M, Cucina A, Galli L, Proietti S, Dinicola S, Pasqualato A, Manetti C, Ricci G, Giuliani A, Bizzarri M. Metabolism and cell shape in cancer: a fractal analysis. *Int J Biochem Cell Biol*. 2011 Jul;43(7):1052-8. doi: 10.1016/j.biocel.2010.05.002. Epub 2010 May 10. PMID: 20460170.
42. Lyons SM, Alizadeh E, Mannheimer J, Schuamberg K, Castle J, Schroder B, Turk P, Thamm D, Prasad A. Changes in cell shape are correlated with metastatic potential in murine and human osteosarcomas. *Biol Open*. 2016 Feb 12;5(3):289-99. doi: 10.1242/bio.013409. PMID: 26873952; PMCID: PMC4810736.
43. Legerstee K, Houtsmuller AB. A Layered View on Focal Adhesions. *Biology (Basel)*. 2021 Nov 16;10(11):1189. doi: 10.3390/biology10111189. PMID: 34827182; PMCID: PMC8614905.
44. Kim DH, Wirtz D. Focal adhesion size uniquely predicts cell migration. *FASEB J*. 2013 Apr;27(4):1351-61. doi: 10.1096/fj.12-220160. Epub 2012 Dec 19. PMID: 23254340; PMCID: PMC3606534.
45. What are stress fibers? <https://www.mechanobio.info/cytoskeleton-dynamics/what-are-stress-fibers/>
46. Adhesion molecules and complexes. <https://www.reading.ac.uk/nitricoxide/intro/migration/adhesion.htm>
47. Trefts E, Gannon M, Wasserman DH. The liver. *Curr Biol*. 2017 Nov 6;27(21):R1147-R1151. doi: 10.1016/j.cub.2017.09.019. PMID: 29112863; PMCID: PMC5897118.
48. Llovet JM, Kelley RK, Villanueva A, Singal AG, Pikarsky E, Roayaie S, Lencioni R, Koike K, Zucman-Rossi J, Finn RS. Hepatocellular carcinoma. *Nat Rev Dis Primers*. 2021 Jan 21;7(1):6. doi: 10.1038/s41572-020-00240-3. PMID: 33479224.
49. Llovet JM, Kelley RK, Villanueva A, Singal AG, Pikarsky E, Roayaie S, Lencioni R, Koike K, Zucman-Rossi J, Finn RS. Hepatocellular carcinoma. *Nat Rev Dis Primers*. 2021 Jan 21;7(1):6. doi: 10.1038/s41572-020-00240-3. PMID: 33479224.
50. Editorial: Non-A, non-B? *Lancet*. 1975 Jul 12;2(7924):64-5. PMID: 49656.
51. Ansaldi F, Orsi A, Sticchi L, Bruzzone B, Icardi G. Hepatitis C virus in the new era: perspectives in epidemiology, prevention, diagnostics and predictors of response to therapy. *World J Gastroenterol*. 2014 Aug 7;20(29):9633-52. doi: 10.3748/wjg.v20.i29.9633. PMID: 25110404; PMCID: PMC4123355.
52. Houghton M. Hepatitis C Virus: 30 Years after Its Discovery. *Cold Spring Harb Perspect Med*. 2019 Dec 2;9(12):a037069. doi: 10.1101/cshperspect.a037069. PMID: 31501269; PMCID: PMC6886456.
53. Choo QL, Kuo G, Weiner AJ, Overby LR, Bradley DW, Houghton M. Isolation of a cDNA clone derived from a blood-borne non-A, non-B viral hepatitis genome. *Science*. 1989 Apr 21;244(4902):359-62. doi: 10.1126/science.2523562. PMID: 2523562.
54. Pol S, Lagaye S. The remarkable history of the hepatitis C virus. *Genes Immun*. 2019 May;20(5):436-446. doi: 10.1038/s41435-019-0066-z. Epub 2019 Apr 25. PMID: 31019253.

## REFERENCES

---

55. Sebastiani G, Gkouvatsos K, Pantopoulos K. Chronic hepatitis C and liver fibrosis. *World J Gastroenterol.* 2014 Aug 28;20(32):11033-53. doi: 10.3748/wjg.v20.i32.11033. PMID: 25170193; PMCID: PMC4145747.
56. Smith DB, Bukh J, Kuiken C, Muerhoff AS, Rice CM, Stapleton JT, Simmonds P. Expanded classification of hepatitis C virus into 7 genotypes and 67 subtypes: updated criteria and genotype assignment web resource. *Hepatology.* 2014 Jan;59(1):318-27. doi: 10.1002/hep.26744. PMID: 24115039; PMCID: PMC4063340.
57. Dubuisson J, Cosset FL. Virology and cell biology of the hepatitis C virus life cycle: an update. *J Hepatol.* 2014 Nov;61(1 Suppl):S3-S13. doi: 10.1016/j.jhep.2014.06.031. Epub 2014 Nov 3. PMID: 25443344.
58. Chevaliez S, Pawlotsky JM. Virology of hepatitis C virus infection. *Best Pract Res Clin Gastroenterol.* 2012 Aug;26(4):381-9. doi: 10.1016/j.bpg.2012.09.006. PMID: 23199498.
59. Roger S, Ducancelle A, Le Guillou-Guillemette H, Gaudy C, Lunel F. HCV virology and diagnosis. *Clin Res Hepatol Gastroenterol.* 2021 May;45(3):101626. doi: 10.1016/j.clinre.2021.101626. Epub 2021 Feb 23. PMID: 33636428.
60. Lohmann V. Hepatitis C virus cell culture models: an encomium on basic research paving the road to therapy development. *Med Microbiol Immunol.* 2019 Feb;208(1):3-24. doi: 10.1007/s00430-018-0566-x. Epub 2018 Oct 8. PMID: 30298360.
61. Lohmann V, Bartenschlager R. On the history of hepatitis C virus cell culture systems. *J Med Chem.* 2014 Mar 13;57(5):1627-42. doi: 10.1021/jm401401n. Epub 2013 Nov 21. PMID: 24164647.
62. Gerold G, Pietschmann T. The HCV life cycle: *in vitro* tissue culture systems and therapeutic targets. *Dig Dis.* 2014;32(5):525-37. doi: 10.1159/000360830. Epub 2014 Jul 14. PMID: 25034285.
63. Pietschmann T, Kaul A, Koutsoudakis G, Shavinskaya A, Kallis S, Steinmann E, Abid K, Negro F, Dreux M, Cosset FL, Bartenschlager R. Construction and characterization of infectious intragenotypic and intergenotypic hepatitis C virus chimeras. *Proc Natl Acad Sci U S A.* 2006 May 9;103(19):7408-13. doi: 10.1073/pnas.0504877103. Epub 2006 May 1. PMID: 16651538; PMCID: PMC1455439.
64. Li YP, Ramirez S, Mikkelsen L, Bukh J. Efficient infectious cell culture systems of the hepatitis C virus (HCV) prototype strains HCV-1 and H77. *J Virol.* 2015 Jan;89(1):811-23. doi: 10.1128/JVI.02877-14. Epub 2014 Oct 29. PMID: 25355880; PMCID: PMC4301150.
65. Li YP, Ramirez S, Jensen SB, Purcell RH, Gottwein JM, Bukh J. Highly efficient full-length hepatitis C virus genotype 1 (strain TN) infectious culture system. *Proc Natl Acad Sci U S A.* 2012 Nov 27;109(48):19757-62. doi: 10.1073/pnas.1218260109. Epub 2012 Nov 14. PMID: 23151512; PMCID: PMC3511766.
66. Ramirez S, Mikkelsen LS, Gottwein JM, Bukh J. Robust HCV Genotype 3a Infectious Cell Culture System Permits Identification of Escape Variants With Resistance to Sofosbuvir. *Gastroenterology.* 2016 Nov;151(5):973-985.e2. doi: 10.1053/j.gastro.2016.07.013. Epub 2016 Jul 22. PMID: 27453546.
67. Gottwein JM, Scheel TK, Hoegh AM, Lademann JB, Eugen-Olsen J, Lisby G, Bukh J. Robust hepatitis C genotype 3a cell culture releasing adapted intergenotypic 3a/2a (S52/JFH1) viruses. *Gastroenterology.* 2007 Nov;133(5):1614-26. doi: 10.1053/j.gastro.2007.08.005. Epub 2007 Aug 3. PMID: 17983807.

## REFERENCES

---

68. Scheel TK, Gottwein JM, Jensen TB, Prentoe JC, Hoegh AM, Alter HJ, Eugen-Olsen J, Bukh J. Development of JFH1-based cell culture systems for hepatitis C virus genotype 4a and evidence for cross-genotype neutralization. *Proc Natl Acad Sci U S A*. 2008 Jan 22;105(3):997-1002. doi: 10.1073/pnas.0711044105. Epub 2008 Jan 14. PMID: 18195353; PMCID: PMC2242719.
69. Jensen TB, Gottwein JM, Scheel TK, Hoegh AM, Eugen-Olsen J, Bukh J. Highly efficient JFH1-based cell-culture system for hepatitis C virus genotype 5a: failure of homologous neutralizing-antibody treatment to control infection. *J Infect Dis*. 2008 Dec 15;198(12):1756-65. doi: 10.1086/593021. PMID: 19032070.
70. Gottwein JM, Scheel TK, Jensen TB, Lademann JB, Prentoe JC, Knudsen ML, Hoegh AM, Bukh J. Development and characterization of hepatitis C virus genotype 1-7 cell culture systems: role of CD81 and scavenger receptor class B type I and effect of antiviral drugs. *Hepatology*. 2009 Feb;49(2):364-77. doi: 10.1002/hep.22673. PMID: 19148942.
71. Sainz B Jr, Barretto N, Yu X, Corcoran P, Uprichard SL. Permissiveness of human hepatoma cell lines for HCV infection. *Virology*. 2012 Jan 24;9:30. doi: 10.1186/1743-422X-9-30. PMID: 22273112; PMCID: PMC3317838.
72. Bartenschlager R, Lohmann V. Novel cell culture systems for the hepatitis C virus. *Antiviral Res*. 2001 Oct;52(1):1-17. doi: 10.1016/s0166-3542(01)00164-4. PMID: 11530183.
73. Wilson GK, Stamataki Z. *In vitro* systems for the study of hepatitis C virus infection. *Int J Hepatol*. 2012;2012:292591. doi: 10.1155/2012/292591. Epub 2012 Sep 27. PMID: 23056952; PMCID: PMC3465938.
74. Ilboudo A, Nault JC, Dubois-Pot-Schneider H, Corlu A, Zucman-Rossi J, Samson M, Le Seyec J. Overexpression of phosphatidylinositol 4-kinase type III $\alpha$  is associated with undifferentiated status and poor prognosis of human hepatocellular carcinoma. *BMC Cancer*. 2014 Jan 6;14:7. doi: 10.1186/1471-2407-14-7. PMID: 24393405; PMCID: PMC3898250.
75. Harak C, Meyrath M, Romero-Brey I, Schenk C, Gondeau C, Schult P, Esser-Nobis K, Saeed M, Neddermann P, Schnitzler P, Gotthardt D, Perez-Del-Pulgar S, Neumann-Haefelin C, Thimme R, Meuleman P, Vondran FW, De Francesco R, Rice CM, Bartenschlager R, Lohmann V. Tuning a cellular lipid kinase activity adapts hepatitis C virus to replication in cell culture. *Nat Microbiol*. 2016 Dec 19;2:16247. doi: 10.1038/nmicrobiol.2016.247. Erratum in: *Nat Microbiol*. 2017 Jan 23;2:17012. PMID: 27991882.
76. Vercauteren K, de Jong YP, Meuleman P. Animal models for the study of HCV. *Curr Opin Virol*. 2015 Aug;13:67-74. doi: 10.1016/j.coviro.2015.04.009. Epub 2015 May 23. PMID: 26304554; PMCID: PMC4549803.
77. Tai AW, Benita Y, Peng LF, Kim SS, Sakamoto N, Xavier RJ, Chung RT. A functional genomic screen identifies cellular cofactors of hepatitis C virus replication. *Cell Host Microbe*. 2009 Mar 19;5(3):298-307. doi: 10.1016/j.chom.2009.02.001. PMID: 19286138; PMCID: PMC2756022.
78. Berger KL, Cooper JD, Heaton NS, Yoon R, Oakland TE, Jordan TX, Mateu G, Grakoui A, Randall G. Roles for endocytic trafficking and phosphatidylinositol 4-kinase III  $\alpha$  in hepatitis C virus replication. *Proc Natl Acad Sci U S A*. 2009 May 5;106(18):7577-82. doi: 10.1073/pnas.0902693106. Epub 2009 Apr 17. PMID: 19376974; PMCID: PMC2678598.

## REFERENCES

---

79. Borawski J, Troke P, Puyang X, Gibaja V, Zhao S, Mickanin C, Leighton-Davies J, Wilson CJ, Myer V, Cornellataracido I, Baryza J, Tallarico J, Joberty G, Bantscheff M, Schirle M, Bouwmeester T, Mathy JE, Lin K, Compton T, Labow M, Wiedmann B, Gaither LA. Class III phosphatidylinositol 4-kinase alpha and beta are novel host factor regulators of hepatitis C virus replication. *J Virol.* 2009 Oct;83(19):10058-74. doi: 10.1128/JVI.02418-08. Epub 2009 Jul 15. PMID: 19605471; PMCID: PMC2748049.
80. Trotard M, Lepère-Douard C, Régeard M, Piquet-Pellorce C, Lavillette D, Cosset FL, Gripon P, Le Seyec J. Kinases required in hepatitis C virus entry and replication highlighted by small interference RNA screening. *FASEB J.* 2009 Nov;23(11):3780-9. doi: 10.1096/fj.09-131920. Epub 2009 Jul 16. PMID: 19608626.
81. Reiss S, Rebhan I, Backes P, Romero-Brey I, Erfle H, Matula P, Kaderali L, Poenisch M, Blankenburg H, Hiet MS, Longerich T, Diehl S, Ramirez F, Balla T, Rohr K, Kaul A, Bühler S, Pepperkok R, Lengauer T, Albrecht M, Eils R, Schirmacher P, Lohmann V, Bartenschlager R. Recruitment and activation of a lipid kinase by hepatitis C virus NS5A is essential for integrity of the membranous replication compartment. *Cell Host Microbe.* 2011 Jan 20;9(1):32-45. doi: 10.1016/j.chom.2010.12.002. PMID: 21238945; PMCID: PMC3433060.
82. Lim YS, Hwang SB. Hepatitis C virus NS5A protein interacts with phosphatidylinositol 4-kinase type IIIalpha and regulates viral propagation. *J Biol Chem.* 2011 Apr 1;286(13):11290-8. doi: 10.1074/jbc.M110.194472. Epub 2011 Feb 5. PMID: 21297162; PMCID: PMC3064185.
83. Lohmann V, Hoffmann S, Herian U, Penin F, Bartenschlager R. Viral and cellular determinants of hepatitis C virus RNA replication in cell culture. *J Virol.* 2003 Mar;77(5):3007-19. doi: 10.1128/jvi.77.5.3007-3019.2003. PMID: 12584326; PMCID: PMC149776.
84. Berger KL, Kelly SM, Jordan TX, Tartell MA, Randall G. Hepatitis C virus stimulates the phosphatidylinositol 4-kinase III alpha-dependent phosphatidylinositol 4-phosphate production that is essential for its replication. *J Virol.* 2011 Sep;85(17):8870-83. doi: 10.1128/JVI.00059-11. Epub 2011 Jun 22. PMID: 21697487; PMCID: PMC3165839.
85. Tai AW, Salloum S. The role of the phosphatidylinositol 4-kinase PI4KA in hepatitis C virus-induced host membrane rearrangement. *PLoS One.* 2011;6(10):e26300. doi: 10.1371/journal.pone.0026300. Epub 2011 Oct 12. PMID: 22022594; PMCID: PMC3192179.
86. Paul D, Madan V, Bartenschlager R. Hepatitis C virus RNA replication and assembly: living on the fat of the land. *Cell Host Microbe.* 2014 Nov 12;16(5):569-79. doi: 10.1016/j.chom.2014.10.008. Epub 2014 Nov 12. PMID: 25525790; PMCID: PMC7172941.
87. Reiss S, Harak C, Romero-Brey I, Radujkovic D, Klein R, Ruggieri A, Rebhan I, Bartenschlager R, Lohmann V. The lipid kinase phosphatidylinositol-4 kinase III alpha regulates the phosphorylation status of hepatitis C virus NS5A. *PLoS Pathog.* 2013 May;9(5):e1003359. doi: 10.1371/journal.ppat.1003359. Epub 2013 May 9. PMID: 23675303; PMCID: PMC3649985.
88. Bost AG, Venable D, Liu L, Heinz BA. Cytoskeletal requirements for hepatitis C virus (HCV) RNA synthesis in the HCV replicon cell culture system. *J Virol.* 2003 Apr;77(7):4401-8. doi: 10.1128/jvi.77.7.4401-4408.2003. PMID: 12634397; PMCID: PMC150619.

## REFERENCES

---

89. Lai CK, Jeng KS, Machida K, Lai MM. Association of hepatitis C virus replication complexes with microtubules and actin filaments is dependent on the interaction of NS3 and NS5A. *J Virol.* 2008 Sep;82(17):8838-48. doi: 10.1128/JVI.00398-08. Epub 2008 Jun 18. PMID: 18562541; PMCID: PMC2519648.
90. Roohvand F, Maillard P, Lavergne JP, Boulant S, Walic M, Andréo U, Goueslain L, Helle F, Mallet A, McLauchlan J, Budkowska A. Initiation of hepatitis C virus infection requires the dynamic microtubule network: role of the viral nucleocapsid protein. *J Biol Chem.* 2009 May 15;284(20):13778-13791. doi: 10.1074/jbc.M807873200. Epub 2009 Mar 6. PMID: 19269968; PMCID: PMC2679479.
91. Boulant S, Douglas MW, Moody L, Budkowska A, Targett-Adams P, McLauchlan J. Hepatitis C virus core protein induces lipid droplet redistribution in a microtubule- and dynein-dependent manner. *Traffic.* 2008 Aug;9(8):1268-82. doi: 10.1111/j.1600-0854.2008.00767.x. Epub 2008 May 17. PMID: 18489704.
92. Khera L, Paul C, Kaul R. Hepatitis C Virus Mediated Metastasis in Hepatocellular Carcinoma as a Therapeutic Target for Cancer Management. *Curr Drug Metab.* 2018;19(3):224-235. doi: 10.2174/1389200219666180129110942. PMID: 29380693.
93. Ninio L, Nissani A, Meirson T, Domovitz T, Genna A, Twafra S, Srikanth KD, Dabour R, Avraham E, Davidovich A, Gil-Henn H, Gal-Tanamy M. Hepatitis C Virus Enhances the Invasiveness of Hepatocellular Carcinoma via EGFR-Mediated Invadopodia Formation and Activation. *Cells.* 2019 Nov 5;8(11):1395. doi: 10.3390/cells8111395. PMID: 31694343; PMCID: PMC6912298.
94. Vescovo T, Refolo G, Vitagliano G, Fimia GM, Piacentini M. Molecular mechanisms of hepatitis C virus-induced hepatocellular carcinoma. *Clin Microbiol Infect.* 2016 Oct;22(10):853-861. doi: 10.1016/j.cmi.2016.07.019. Epub 2016 Jul 28. PMID: 27476823.
95. Grant SG, Jessee J, Bloom FR, Hanahan D. Differential plasmid rescue from transgenic mouse DNAs into *Escherichia coli* methylation-restriction mutants. *Proc Natl Acad Sci U S A.* 1990 Jun;87(12):4645-9. doi: 10.1073/pnas.87.12.4645. PMID: 2162051; PMCID: PMC54173.
96. Hanahan D. Studies on transformation of *Escherichia coli* with plasmids. *J Mol Biol.* 1983 Jun 5;166(4):557-80. doi: 10.1016/s0022-2836(83)80284-8. PMID: 6345791.
97. Matthew Ferenc. Plasmids 101: Common Lab *E. coli* Strains. <https://blog.addgene.org/plasmids-101-common-lab-e-coli-strains>.
98. Graham FL, Smiley J, Russell WC, Nairn R. Characteristics of a human cell line transformed by DNA from human adenovirus type 5. *J Gen Virol.* 1977 Jul;36(1):59-74. doi: 10.1099/0022-1317-36-1-59. PMID: 886304.
99. AdEasy Adenoviral Vector System. Instruction Manual. Agilent Technologies. <https://www.agilent.com/cs/library/usermanuals/public/240009.pdf>.
100. Kato T, Date T, Murayama A, Morikawa K, Akazawa D, Wakita T. Cell culture and infection system for hepatitis C virus. *Nat Protoc.* 2006;1(5):2334-9. doi: 10.1038/nprot.2006.395. PMID: 17406476.
101. Lindenbach BD. Measuring HCV infectivity produced in cell culture and in vivo. *Methods Mol Biol.* 2009;510:329-36. doi: 10.1007/978-1-59745-394-3\_24. PMID: 19009272.
102. Binder M, Quinkert D, Bochkarova O, Klein R, Kezmic N, Bartenschlager R, Lohmann V. Identification of determinants involved in initiation of hepatitis C virus RNA synthesis by using intergenotypic replicase chimeras. *J Virol.* 2007 May;81(10):5270-83. doi: 10.1128/JVI.00032-07. Epub 2007 Mar 7. PMID: 17344294; PMCID: PMC1900214.

## REFERENCES

---

103. Hammond GR, Schiavo G, Irvine RF. Immunocytochemical techniques reveal multiple, distinct cellular pools of PtdIns4P and PtdIns(4,5)P(2). *Biochem J.* 2009 Jul 29;422(1):23-35. doi: 10.1042/BJ20090428. PMID: 19508231; PMCID: PMC2722159.
104. PI(3,4)P2 Mass ELISA. Description: 96-well ELISA Assay for Detection and Quantification of PI(3,4)P2 from cells. Echelon Biosciences Inc. [https://echelon-inc.com/wp-content/uploads/2019/09/TDS\\_K-3800\\_Rev8.pdf](https://echelon-inc.com/wp-content/uploads/2019/09/TDS_K-3800_Rev8.pdf)
105. Bojjireddy N, Botyanszki J, Hammond G, Creech D, Peterson R, Kemp DC, Snead M, Brown R, Morrison A, Wilson S, Harrison S, Moore C, Balla T. Pharmacological and genetic targeting of the PI4KA enzyme reveals its important role in maintaining plasma membrane phosphatidylinositol 4-phosphate and phosphatidylinositol 4,5-bisphosphate levels. *J Biol Chem.* 2014 Feb 28;289(9):6120-32. doi: 10.1074/jbc.M113.531426. Epub 2014 Jan 10. PMID: 24415756; PMCID: PMC3937678.
106. Hall A. The cytoskeleton and cancer. *Cancer Metastasis Rev.* 2009 Jun;28(1-2):5-14. doi: 10.1007/s10555-008-9166-3. PMID: 19153674.
107. Cooper GM. *The Cell: A Molecular Approach.* 2nd edition. Sunderland (MA): Sinauer Associates; 2000. Chapter 11, The Cytoskeleton and Cell Movement. Available from: <https://www.ncbi.nlm.nih.gov/books/NBK9893/>
108. Ziyad S, Riordan JD, Cavanaugh AM, Su T, Hernandez GE, Hilfenhaus G, Morselli M, Huynh K, Wang K, Chen JN, Dupuy AJ, Iruela-Arispe ML. A Forward Genetic Screen Targeting the Endothelium Reveals a Regulatory Role for the Lipid Kinase Pi4ka in Myelo- and Erythropoiesis. *Cell Rep.* 2018 Jan 30;22(5):1211-1224. doi: 10.1016/j.celrep.2018.01.017. PMID: 29386109; PMCID: PMC5828030.
109. Schaller MD. Paxillin: a focal adhesion-associated adaptor protein. *Oncogene.* 2001 Oct 1;20(44):6459-72. doi: 10.1038/sj.onc.1204786. PMID: 11607845.
110. Bamburg JR, Bernstein BW. Roles of ADF/cofilin in actin polymerization and beyond. *F1000 Biol Reports* 2010 Aug 19, 2:62. <https://doi.org/10.3410/B2-62>.
111. Blackstone BN, Li R, Ackerman WE 4th, Ghadiali SN, Powell HM, Kniss DA. Myoferlin depletion elevates focal adhesion kinase and paxillin phosphorylation and enhances cell-matrix adhesion in breast cancer cells. *Am J Physiol Cell Physiol.* 2015 Apr 15;308(8):C642-9. doi: 10.1152/ajpcell.00276.2014. Epub 2015 Jan 28. PMID: 25631868.
112. Fusté NP, Fernández-Hernández R, Cemeli T, Mirantes C, Pedraza N, Rafel M, Torres-Rosell J, Colomina N, Ferrezuelo F, Dolcet X, Garí E. Cytoplasmic cyclin D1 regulates cell invasion and metastasis through the phosphorylation of paxillin. *Nat Commun.* 2016 May 16;7:11581. doi: 10.1038/ncomms11581. PMID: 27181366; PMCID: PMC4873647.
113. Liu Z, Chu S, Yao S, Li Y, Fan S, Sun X, Su L, Liu X. CD74 interacts with CD44 and enhances tumorigenesis and metastasis via RHOA-mediated cofilin phosphorylation in human breast cancer cells. *Oncotarget.* 2016 Oct 18;7(42):68303-68313. doi: 10.18632/oncotarget.11945. PMID: 27626171; PMCID: PMC5356556.
114. Lv D, Li L, Lu Q, Li Y, Xie F, Li H, Cao J, Liu M, Wu D, He L, Chen L. PAK1-cofilin phosphorylation mediates human lung adenocarcinoma cells migration induced by apelin-13. *Clin Exp Pharmacol Physiol.* 2016 May;43(5):569-79. doi: 10.1111/1440-1681.12563. PMID: 26918678.
115. Quizi JL, Baron K, Al-Zahrani KN, O'Reilly P, Sriram RK, Conway J, Laurin AA, Sabourin LA. SLK-mediated phosphorylation of paxillin is required for focal adhesion turnover and cell migration. *Oncogene.* 2013 Sep 26;32(39):4656-63. doi: 10.1038/onc.2012.488. Epub 2012 Nov 5. PMID: 23128389.

## REFERENCES

---

116. Wu DW, Wu TC, Wu JY, Cheng YW, Chen YC, Lee MC, Chen CY, Lee H. Phosphorylation of paxillin confers cisplatin resistance in non-small cell lung cancer via activating ERK-mediated Bcl-2 expression. *Oncogene*. 2014 Aug 28;33(35):4385-95. doi: 10.1038/onc.2013.389. Epub 2013 Oct 7. PMID: 24096476.
117. Bravo-Cordero JJ, Magalhaes MA, Eddy RJ, Hodgson L, Condeelis J. Functions of cofilin in cell locomotion and invasion. *Nat Rev Mol Cell Biol*. 2013 Jul;14(7):405-15. doi: 10.1038/nrm3609. Epub 2013 Jun 19. PMID: 23778968; PMCID: PMC3878614.
118. Alfahad D, Alharethi S, Alharbi B, Mawlood K, Dash P. PtdIns(4,5)P<sub>2</sub> and PtdIns(3,4,5)P<sub>3</sub> dynamics during focal adhesions assembly and disassembly in a cancer cell line. *Turk J Biol*. 2020 Dec 14;44(6):381-392. doi: 10.3906/biy-2004-108. PMID: 33402865; PMCID: PMC7759192.
119. Zhou J, Bronowska A, Le Coq J, Lietha D, Gräter F. Allosteric regulation of focal adhesion kinase by PIP<sub>2</sub> and ATP. *Biophys J*. 2015 Feb 3;108(3):698-705. doi: 10.1016/j.bpj.2014.11.3454. PMID: 25650936; PMCID: PMC4317530.
120. Hilpelä P, Vartiainen MK, Lappalainen P. Regulation of the actin cytoskeleton by PI(4,5)P<sub>2</sub> and PI(3,4,5)P<sub>3</sub>. *Curr Top Microbiol Immunol*. 2004;282:117-63. doi: 10.1007/978-3-642-18805-3\_5. PMID: 14594216.
121. Katan M, Cockcroft S. Phosphatidylinositol(4,5)bisphosphate: diverse functions at the plasma membrane. *Essays Biochem*. 2020 Sep 23;64(3):513-531. doi: 10.1042/EBC20200041. PMID: 32844214; PMCID: PMC7517351.
122. Kersten J. 2021. Characterisation of PI4KA/ PIK3C2γ roles in cytoskeleton-regulation of liver cell lines. Master thesis. University of Heidelberg. Heidelberg, Germany.
123. Bianco A, Reghellin V, Donnici L, Fenu S, Alvarez R, Baruffa C, Peri F, Pagani M, Abrignani S, Neddermann P, De Francesco R. Metabolism of phosphatidylinositol 4-kinase IIIα-dependent PI4P is subverted by HCV and is targeted by a 4-anilino quinazoline with antiviral activity. *PLoS Pathog*. 2012;8(3):e1002576. doi: 10.1371/journal.ppat.1002576. Epub 2012 Mar 8. PMID: 22412376; PMCID: PMC3297592.
124. Feng Z, Yu CH. PI(3,4)P<sub>2</sub>-mediated membrane tubulation promotes integrin trafficking and invasive cell migration. *Proc Natl Acad Sci U S A*. 2021 May 11;118(19):e2017645118. doi: 10.1073/pnas.2017645118. PMID: 33947811; PMCID: PMC8126793.
125. Brown MC, Cary LA, Jamieson JS, Cooper JA, Turner CE. Src and FAK kinases cooperate to phosphorylate paxillin kinase linker, stimulate its focal adhesion localization, and regulate cell spreading and protrusiveness. *Mol Biol Cell*. 2005 Sep;16(9):4316-28. doi: 10.1091/mbc.e05-02-0131. Epub 2005 Jul 6. PMID: 16000375; PMCID: PMC1196340.
126. López-Colomé AM, Lee-Rivera I, Benavides-Hidalgo R, López E. Paxillin: a crossroad in pathological cell migration. *J Hematol Oncol*. 2017 Feb 18;10(1):50. doi: 10.1186/s13045-017-0418-y. PMID: 28214467; PMCID: PMC5316197.
127. Bolós V, Gasent JM, López-Tarruella S, Grande E. The dual kinase complex FAK-Src as a promising therapeutic target in cancer. *Onco Targets Ther*. 2010 Jun 24;3:83-97. doi: 10.2147/ott.s6909. PMID: 20616959; PMCID: PMC2895777.
128. Koseoglu S, Lu Z, Kumar C, Kirschmeier P, Zou J. AKT1, AKT2 and AKT3-dependent cell survival is cell line-specific and knockdown of all three isoforms

## REFERENCES

---

- selectively induces apoptosis in 20 human tumor cell lines. *Cancer Biol Ther.* 2007 May;6(5):755-62. doi: 10.4161/cbt.6.5.3995. Epub 2007 Feb 9. PMID: 17426444.
129. Fortier AM, Asselin E, Cadrin M. Functional specificity of Akt isoforms in cancer progression. *Biomol Concepts.* 2011 Apr 1;2(1-2):1-11. doi: 10.1515/bmc.2011.003. PMID: 25962016.
130. Braccini L, Ciraolo E, Campa CC, Perino A, Longo DL, Tibolla G, Pregnolato M, Cao Y, Tassone B, Damilano F, Laffargue M, Calautti E, Falasca M, Norata GD, Backer JM, Hirsch E. PI3K-C2 $\gamma$  is a Rab5 effector selectively controlling endosomal Akt2 activation downstream of insulin signalling. *Nat Commun.* 2015 Jun 23;6:7400. doi: 10.1038/ncomms8400. PMID: 26100075; PMCID: PMC4479417.
131. Liu Z, Tian Y, Machida K, Lai MM, Luo G, Fong SK, Ou JH. Transient activation of the PI3K-AKT pathway by hepatitis C virus to enhance viral entry. *J Biol Chem.* 2012 Dec 7;287(50):41922-30. doi: 10.1074/jbc.M112.414789. Epub 2012 Oct 24. PMID: 23095753; PMCID: PMC3516739.
132. Mannová P, Beretta L. Activation of the N-Ras-PI3K-Akt-mTOR pathway by hepatitis C virus: control of cell survival and viral replication. *J Virol.* 2005 Jul;79(14):8742-9. doi: 10.1128/JVI.79.14.8742-8749.2005. PMID: 15994768; PMCID: PMC1168775.
133. Shi Q, Hoffman B, Liu Q. PI3K-Akt signaling pathway upregulates hepatitis C virus RNA translation through the activation of SREBPs. *Virology.* 2016 Mar;490:99-108. doi: 10.1016/j.virol.2016.01.012. Epub 2016 Feb 6. PMID: 26855332.
134. Jo H, Mondal S, Tan D, Nagata E, Takizawa S, Sharma AK, Hou Q, Shanmugasundaram K, Prasad A, Tung JK, Tejada AO, Man H, Rigby AC, Luo HR. Small molecule-induced cytosolic activation of protein kinase Akt rescues ischemia-elicited neuronal death. *Proc Natl Acad Sci U S A.* 2012 Jun 26;109(26):10581-6. doi: 10.1073/pnas.1202810109. Epub 2012 Jun 11. PMID: 22689977; PMCID: PMC3387065.
135. Tschaharganeh DF, Xue W, Calvisi DF, Evert M, Michurina TV, Dow LE, Banito A, Katz SF, Kasthuber ER, Weissmueller S, Huang CH, Lechel A, Andersen JB, Capper D, Zender L, Longerich T, Enikolopov G, Lowe SW. p53-dependent Nestin regulation links tumor suppression to cellular plasticity in liver cancer. *Cell.* 2014 Jul 31;158(3):579-92. doi: 10.1016/j.cell.2014.05.051. Erratum in: *Cell.* 2016 Jun 2;165(6):1546-1547. PMID: 25083869; PMCID: PMC4221237.
136. Bell JB, Podetz-Pedersen KM, Aronovich EL, Belur LR, Mclvor RS, Hackett PB. Preferential delivery of the Sleeping Beauty transposon system to livers of mice by hydrodynamic injection. *Nat Protoc.* 2007;2(12):3153-65. doi: 10.1038/nprot.2007.471. PMID: 18079715; PMCID: PMC2548418.
137. Argyros O, Wong SP, Niceta M, Waddington SN, Howe SJ, Coutelle C, Miller AD, Harbottle RP. Persistent episomal transgene expression in liver following delivery of a scaffold/matrix attachment region containing non-viral vector. *Gene Ther.* 2008 Dec;15(24):1593-605. doi: 10.1038/gt.2008.113. Epub 2008 Jul 17. PMID: 18633447.
138. Bozza M, Green EW, Espinet E, De Roia A, Klein C, Vogel V, Offringa R, Williams JA, Sprick M, Harbottle RP. Novel Non-integrating DNA Nano-S/MAR Vectors Restore Gene Function in Isogenic Patient-Derived Pancreatic Tumor Models. *Mol Ther Methods Clin Dev.* 2020 Apr 25;17:957-968. doi: 10.1016/j.omtm.2020.04.017. PMID: 32420409; PMCID: PMC7218229.
139. Meuleman P, Libbrecht L, De Vos R, de Hemptinne B, Gevaert K, Vandekerckhove J, Roskams T, Leroux-Roels G. Morphological and biochemical



## REFERENCES

---

- characterization of a human liver in a uPA-SCID mouse chimera. *Hepatology*. 2005 Apr;41(4):847-56. doi: 10.1002/hep.20657. PMID: 15791625.
140. Ma H, Blake T, Chitnis A, Liu P, Balla T. Crucial role of phosphatidylinositol 4-kinase IIIalpha in development of zebrafish pectoral fin is linked to phosphoinositide 3-kinase and FGF signaling. *J Cell Sci*. 2009 Dec 1;122(Pt 23):4303-10. doi: 10.1242/jcs.057646. Epub 2009 Nov 3. PMID: 19887586; PMCID: PMC2779132.
141. Yavari A, Nagaraj R, Owusu-Ansah E, Folick A, Ngo K, Hillman T, Call G, Rohatgi R, Scott MP, Banerjee U. Role of lipid metabolism in smoothed derepression in hedgehog signaling. *Dev Cell*. 2010 Jul 20;19(1):54-65. doi: 10.1016/j.devcel.2010.06.007. PMID: 20643350; PMCID: PMC2945252.
142. Tan J, Oh K, Burgess J, Hipfner DR, Brill JA. PI4KIII $\alpha$  is required for cortical integrity and cell polarity during *Drosophila* oogenesis. *J Cell Sci*. 2014 Mar 1;127(Pt 5):954-66. doi: 10.1242/jcs.129031. Epub 2014 Jan 10. Erratum in: *J Cell Sci*. 2014 Jun 1;127(Pt 11):2601. PMID: 24413170.
143. Feltri ML, D'Antonio M, Previtali S, Fasolini M, Messing A, Wrabetz L. P0-Cre transgenic mice for inactivation of adhesion molecules in Schwann cells. *Ann N Y Acad Sci*. 1999 Sep 14;883:116-23. PMID: 10586237.
144. Alvarez-Prats A, Bjelobaba I, Aldworth Z, Baba T, Abebe D, Kim YJ, Stojilkovic SS, Stopfer M, Balla T. Schwann-Cell-Specific Deletion of Phosphatidylinositol 4-Kinase Alpha Causes Aberrant Myelination. *Cell Rep*. 2018 Jun 5;23(10):2881-2890. doi: 10.1016/j.celrep.2018.05.019. PMID: 29874576; PMCID: PMC7268203.
145. Sbrissa D, Semaan L, Govindarajan B, Li Y, Caruthers NJ, Stemmer PM, Cher ML, Sethi S, Vaishampayan U, Shisheva A, Chinni SR. A novel cross-talk between CXCR4 and PI4KIII $\alpha$  in prostate cancer cells. *Oncogene*. 2019 Jan;38(3):332-344. doi: 10.1038/s41388-018-0448-0. Epub 2018 Aug 15. PMID: 30111818; PMCID: PMC6336684.
146. Kim JH, Hwang KH, Eom M, Kim M, Park EY, Jeong Y, Park KS, Cha SK. WNK1 promotes renal tumor progression by activating TRPC6-NFAT pathway. *FASEB J*. 2019 Jul;33(7):8588-8599. doi: 10.1096/fj.201802019RR. Epub 2019 Apr 25. PMID: 31022353.
147. Audhya A, Foti M, Emr SD. Distinct roles for the yeast phosphatidylinositol 4-kinases, Stt4p and Pik1p, in secretion, cell growth, and organelle membrane dynamics. *Mol Biol Cell*. 2000 Aug;11(8):2673-89. doi: 10.1091/mbc.11.8.2673. PMID: 10930462; PMCID: PMC14948.
148. Li, H. G., Xie, D. R., Shen, X. M., Li, H. H., Zeng, H., & Zeng, Y. J. (2005). Clinicopathological significance of expression of paxillin, syndecan-1 and EMMPRIN in hepatocellular carcinoma. *World journal of gastroenterology*, 11(10), 1445–1451. <https://doi.org/10.3748/wjg.v11.i10.1445>
149. Wen, L., Zhang, X., Zhang, J., Chen, S., Ma, Y., Hu, J., Yue, T., Wang, J., Zhu, J., Wu, T., & Wang, X. (2020). Paxillin knockdown suppresses metastasis and epithelial-mesenchymal transition in colorectal cancer via the ERK signalling pathway. *Oncology reports*, 44(3), 1105–1115. <https://doi.org/10.3892/or.2020.7687>
150. Petit V, Boyer B, Lentz D, Turner CE, Thiery JP, Vallés AM. Phosphorylation of tyrosine residues 31 and 118 on paxillin regulates cell migration through an association with CRK in NBT-II cells. *J Cell Biol*. 2000 Mar 6;148(5):957-70. doi: 10.1083/jcb.148.5.957. PMID: 10704446; PMCID: PMC2174549.
151. Aznavoorian S, Stracke ML, Parsons J, McClanahan J, Liotta LA. Integrin alphavbeta3 mediates chemotactic and haptotactic motility in human melanoma cells

## REFERENCES

---

- through different signaling pathways. *J Biol Chem.* 1996 Feb 9;271(6):3247-54. doi: 10.1074/jbc.271.6.3247. PMID: 8621727.
152. Aprikian AG, Tremblay L, Han K, Chevalier S. Bombesin stimulates the motility of human prostate-carcinoma cells through tyrosine phosphorylation of focal adhesion kinase and of integrin-associated proteins. *Int J Cancer.* 1997 Jul 29;72(3):498-504. doi: 10.1002/(sici)1097-0215(19970729)72:3<498::aid-ijc19>3.0.co;2-8. PMID: 9247295.
153. McCormack SJ, Brazinski SE, Moore JL Jr, Werness BA, Goldstein DJ. Activation of the focal adhesion kinase signal transduction pathway in cervical carcinoma cell lines and human genital epithelial cells immortalized with human papillomavirus type 18. *Oncogene.* 1997 Jul 17;15(3):265-74. doi: 10.1038/sj.onc.1201186. PMID: 9233761.
154. Margaria JP, Ratto E, Gozzelino L, Li H, Hirsch E. Class II PI3Ks at the Intersection between Signal Transduction and Membrane Trafficking. *Biomolecules.* 2019;9(3):104. Published 2019 Mar 15. doi:10.3390/biom9030104.
155. Clayton EL, Minogue S, Waugh MG. Mammalian phosphatidylinositol 4-kinases as modulators of membrane trafficking and lipid signaling networks. *Prog Lipid Res.* 2013 Jul;52(3):294-304. doi: 10.1016/j.plipres.2013.04.002. Epub 2013 Apr 19. PMID: 23608234; PMCID: PMC3989048.
156. Ono F, Nakagawa T, Saito S, Owada Y, Sakagami H, Goto K, Suzuki M, Matsuno S, Kondo H. A novel class II phosphoinositide 3-kinase predominantly expressed in the liver and its enhanced expression during liver regeneration. *J Biol Chem.* 1998 Mar 27;273(13):7731-6. doi: 10.1074/jbc.273.13.7731. PMID: 9516481.
157. Ruzzenente A, Fassan M, Conci S, Simbolo M, Lawlor RT, Pedrazzani C, Capelli P, D'Onofrio M, Iacono C, Scarpa A, Guglielmi A. Cholangiocarcinoma Heterogeneity Revealed by Multigene Mutational Profiling: Clinical and Prognostic Relevance in Surgically Resected Patients. *Ann Surg Oncol.* 2016 May;23(5):1699-707. doi: 10.1245/s10434-015-5046-6. Epub 2015 Dec 30. PMID: 26717940.
158. Li A, Chen H, Lin M, Zhang C, Tang E, Peng J, Wei Q, Li H, Yin L. PIK3C2G copy number is associated with clinical outcomes of colorectal cancer patients treated with oxaliplatin. *Int J Clin Exp Med.* 2015 Jan 15;8(1):1137-43. PMID: 25785104; PMCID: PMC4358559.
159. Daimon M, Sato H, Oizumi T, Toriyama S, Saito T, Karasawa S, Jimbu Y, Wada K, Kameda W, Susa S, Yamaguchi H, Emi M, Muramatsu M, Kubota I, Kawata S, Kato T. Association of the PIK3C2G gene polymorphisms with type 2 DM in a Japanese population. *Biochem Biophys Res Commun.* 2008 Jan 18;365(3):466-71. doi: 10.1016/j.bbrc.2007.10.180. Epub 2007 Nov 6. PMID: 17991425.
160. Saeed M. Locus and gene-based GWAS meta-analysis identifies new diabetic nephropathy genes. *Immunogenetics.* 2018 Jun;70(6):347-353. doi: 10.1007/s00251-017-1044-0. Epub 2017 Nov 16. PMID: 29147756.
161. Shia WC, Ku TH, Tsao YM, Hsia CH, Chang YM, Huang CH, Chung YC, Hsu SL, Liang KW, Hsu FR. Genetic copy number variants in myocardial infarction patients with hyperlipidemia. *BMC Genomics.* 2011 Nov 30;12 Suppl 3(Suppl 3):S23. doi: 10.1186/1471-2164-12-S3-S23. Epub 2011 Nov 30. PMID: 22369086; PMCID: PMC3333183.
162. Anderson D, Cordell HJ, Fakiola M, Francis RW, Syn G, Scaman ES, Davis E, Miles SJ, McLeay T, Jamieson SE, Blackwell JM. First genome-wide association study in an Australian aboriginal population provides insights into genetic risk factors

## REFERENCES

---

- for body mass index and type 2 diabetes. *PLoS One*. 2015 Mar 11;10(3):e0119333. doi: 10.1371/journal.pone.0119333. PMID: 25760438; PMCID: PMC4356593.
163. Li A, Chen H, Lin M, Zhang C, Tang E, Peng J, Wei Q, Li H, Yin L. PIK3C2G copy number is associated with clinical outcomes of colorectal cancer patients treated with oxaliplatin. *Int J Clin Exp Med*. 2015 Jan 15;8(1):1137-43. PMID: 25785104; PMCID: PMC4358559.
164. Idevall-Hagren O, De Camilli P. Detection and manipulation of phosphoinositides. *Biochim Biophys Acta*. 2015 Jun;1851(6):736-45. doi: 10.1016/j.bbali.2014.12.008. Epub 2014 Dec 13. PMID: 25514766; PMCID: PMC4863076.
165. Prasad N, Topping RS, Decker SJ. Src family tyrosine kinases regulate adhesion-dependent tyrosine phosphorylation of 5'-inositol phosphatase SHIP2 during cell attachment and spreading on collagen I. *J Cell Sci*. 2002 Oct 1;115(Pt 19):3807-15. doi: 10.1242/jcs.00070. PMID: 12235291.
166. Hasegawa J, Tokuda E, Tenno T, Tsujita K, Sawai H, Hiroaki H, Takenawa T, Itoh T. SH3YL1 regulates dorsal ruffle formation by a novel phosphoinositide-binding domain. *J Cell Biol*. 2011 May 30;193(5):901-16. doi: 10.1083/jcb.201012161. PMID: 21624956; PMCID: PMC3105542.
167. Krause M, Gautreau A. Steering cell migration: lamellipodium dynamics and the regulation of directional persistence. *Nat Rev Mol Cell Biol*. 2014 Sep;15(9):577-90. doi: 10.1038/nrm3861. PMID: 25145849.
168. Sharma VP, Eddy R, Entenberg D, Kai M, Gertler FB, Condeelis J. Tks5 and SHIP2 regulate invadopodium maturation, but not initiation, in breast carcinoma cells. *Curr Biol*. 2013 Nov 4;23(21):2079-89. doi: 10.1016/j.cub.2013.08.044. Epub 2013 Oct 24. PMID: 24206842; PMCID: PMC3882144.
169. Hawkins PT, Stephens LR. Emerging evidence of signalling roles for PI(3,4)P2 in Class I and II PI3K-regulated pathways. *Biochem Soc Trans*. 2016 Feb;44(1):307-14. doi: 10.1042/BST20150248. PMID: 26862220.
170. Li H, Wu X, Hou S, Malek M, Kielkowska A, Noh E, Makondo KJ, Du Q, Wilkins JA, Johnston JB, Gibson SB, Lin F, Marshall AJ. Phosphatidylinositol-3,4-Bisphosphate and Its Binding Protein Lamellipodin Regulate Chemotaxis of Malignant B Lymphocytes. *J Immunol*. 2016 Jan 15;196(2):586-95. doi: 10.4049/jimmunol.1500630. Epub 2015 Dec 22. PMID: 26695371.
171. Fukumoto M, Ijuin T, Takenawa T. PI(3,4)P2 plays critical roles in the regulation of focal adhesion dynamics of MDA-MB-231 breast cancer cells. *Cancer Sci*. 2017 May;108(5):941-951. doi: 10.1111/cas.13215. Epub 2017 May 11. PMID: 28247964; PMCID: PMC5448597.
172. Manning BD, Toker A. AKT/PKB Signaling: Navigating the Network. *Cell*. 2017 Apr 20;169(3):381-405. doi: 10.1016/j.cell.2017.04.001. PMID: 28431241; PMCID: PMC5546324.
173. Liu SL, Wang ZG, Hu Y, Xin Y, Singaram I, Gorai S, Zhou X, Shim Y, Min JH, Gong LW, Hay N, Zhang J, Cho W. Quantitative Lipid Imaging Reveals a New Signaling Function of Phosphatidylinositol-3,4-Bisphosphate: Isoform- and Site-Specific Activation of Akt. *Mol Cell*. 2018 Sep 20;71(6):1092-1104.e5. doi: 10.1016/j.molcel.2018.07.035. Epub 2018 Aug 30. PMID: 30174291; PMCID: PMC6214670.
174. Attoub, S., Arafat, K., Kamel Hammadi, N. et al. Akt2 knock-down reveals its contribution to human lung cancer cell proliferation, growth, motility, invasion and

## REFERENCES

---

- endothelial cell tube formation. *Sci Rep* 5, 12759 (2015). <https://doi.org/10.1038/srep12759>
175. Zhou GL, Tucker DF, Bae SS, Bhatheja K, Birnbaum MJ, Field J. Opposing roles for Akt1 and Akt2 in Rac/Pak signaling and cell migration. *J Biol Chem*. 2006 Nov 24;281(47):36443-53. doi: 10.1074/jbc.M600788200. Epub 2006 Oct 1. PMID: 17012749.
176. Alisi A, Arciello M, Petrini S, Conti B, Missale G, Balsano C. Focal adhesion kinase (FAK) mediates the induction of pro-oncogenic and fibrogenic phenotypes in hepatitis C virus (HCV)-infected cells. *PLoS One*. 2012;7(8):e44147. doi: 10.1371/journal.pone.0044147. Epub 2012 Aug 28. PMID: 22937161; PMCID: PMC3429423.
177. Goossens N, Hoshida Y. Hepatitis C virus-induced hepatocellular carcinoma. *Clin Mol Hepatol*. 2015 Jun;21(2):105-14. doi: 10.3350/cmh.2015.21.2.105. Epub 2015 Jun 26. PMID: 26157746; PMCID: PMC4493352.
178. de Oliveria Andrade LJ, D'Oliveira A, Melo RC, De Souza EC, Costa Silva CA, Paraná R. Association between hepatitis C and hepatocellular carcinoma. *J Glob Infect Dis*. 2009 Jan;1(1):33-7. doi: 10.4103/0974-777X.52979. PMID: 20300384; PMCID: PMC2840947
179. Khera L, Paul C, Kaul R. Hepatitis C Virus Mediated Metastasis in Hepatocellular Carcinoma as a Therapeutic Target for Cancer Management. *Curr Drug Metab*. 2018;19(3):224-235. doi: 10.2174/1389200219666180129110942. PMID: 29380693.
180. Cheng D, Zhang L, Yang G, Zhao L, Peng F, Tian Y, Xiao X, Chung RT, Gong G. Hepatitis C virus NS5A drives a PTEN-PI3K/AKT feedback loop to support cell survival. *Liver Int*. 2015 Jun;35(6):1682-91. doi: 10.1111/liv.12733. Epub 2014 Dec 4. PMID: 25388655.
181. Han Y, Niu J, Wang D, Li Y. Hepatitis C Virus Protein Interaction Network Analysis Based on Hepatocellular Carcinoma. *PLoS One*. 2016 Apr 26;11(4):e0153882. doi: 10.1371/journal.pone.0153882. PMID: 27115606; PMCID: PMC4846009.
182. Harouaka D, Engle RE, Wollenberg K, Diaz G, Tice AB, Zamboni F, Govindarajan S, Alter H, Kleiner DE, Farci P. Diminished viral replication and compartmentalization of hepatitis C virus in hepatocellular carcinoma tissue. *Proc Natl Acad Sci U S A*. 2016 Feb 2;113(5):1375-80. doi: 10.1073/pnas.1516879113. Epub 2016 Jan 19. PMID: 26787866; PMCID: PMC4747736.
183. Ninio L, Nissani A, Meirson T, Domovitz T, Genna A, Twafrá S, Srikanth KD, Dabour R, Avraham E, Davidovich A, Gil-Henn H, Gal-Tanamy M. Hepatitis C Virus Enhances the Invasiveness of Hepatocellular Carcinoma via EGFR-Mediated Invadopodia Formation and Activation. *Cells*. 2019 Nov 5;8(11):1395. doi: 10.3390/cells8111395. PMID: 31694343; PMCID: PMC6912298.
184. Rampetsreiter P, Casanova E, Eferl R. Genetically modified mouse models of cancer invasion and metastasis. *Drug Discov Today Dis Models*. 2011 Fall;8(2-3):67-74. doi: 10.1016/j.ddmod.2011.05.003. Epub 2011 Jul 1. PMID: 22577462; PMCID: PMC3334252.
185. Cho K, Ro SW, Seo SH, Jeon Y, Moon H, Kim DY, Kim SU. Genetically Engineered Mouse Models for Liver Cancer. *Cancers (Basel)*. 2019 Dec 19;12(1):14. doi: 10.3390/cancers12010014. PMID: 31861541; PMCID: PMC7016809.
186. Hazari S, Hefler HJ, Chandra PK, Poat B, Gunduz F, Ooms T, Wu T, Balart LA, Dash S. Hepatocellular carcinoma xenograft supports HCV replication: a mouse

## REFERENCES

---

- model for evaluating antivirals. *World J Gastroenterol*. 2011 Jan 21;17(3):300-12. doi: 10.3748/wjg.v17.i3.300. PMID: 21253388; PMCID: PMC3022289.
187. Kattan WE, Chen W, Ma X, Lan TH, van der Hoeven D, van der Hoeven R, Hancock JF. Targeting plasma membrane phosphatidylserine content to inhibit oncogenic KRAS function. *Life Sci Alliance*. 2019 Aug 26;2(5):e201900431. doi: 10.26508/lsa.201900431. PMID: 31451509; PMCID: PMC6709719.
188. Adhikari H, Kattan WE, Kumar S, Zhou P, Hancock JF, Counter CM. Oncogenic KRAS is dependent upon an EFR3A-PI4KA signaling axis for potent tumorigenic activity. *Nat Commun*. 2021 Sep 9;12(1):5248. doi: 10.1038/s41467-021-25523-5. PMID: 34504076; PMCID: PMC8429657.
189. Park Y, Park JM, Kim DH, Kwon J, Kim IA. Inhibition of PI4K III $\alpha$  radiosensitizes in human tumor xenograft and immune-competent syngeneic murine tumor model. *Oncotarget*. 2017 Nov 30;8(66):110392-110405. doi: 10.18632/oncotarget.22778. PMID: 29299156; PMCID: PMC5746391.
190. Freitag A, Prajwal P, Shymanets A, Harteneck C, Nürnberg B, Schächtele C, Kubbutat M, Totzke F, Laufer SA. Development of first lead structures for phosphoinositide 3-kinase-C2 $\gamma$  inhibitors. *J Med Chem*. 2015 Jan 8;58(1):212-21. doi: 10.1021/jm5006034. Epub 2014 Jul 14. PMID: 24983663.
191. Nitulescu GM, Margina D, Juzenas P, Peng Q, Olaru OT, Saloustros E, Fenga C, Spandidos DA, Libra M, Tsatsakis AM. Akt inhibitors in cancer treatment: The long journey from drug discovery to clinical use (Review). *Int J Oncol*. 2016 Mar;48(3):869-85. doi: 10.3892/ijo.2015.3306. Epub 2015 Dec 24. PMID: 26698230; PMCID: PMC4750533.
192. Cicenas J. The potential role of Akt phosphorylation in human cancers. *Int J Biol Markers*. 2008 Jan-Mar;23(1):1-9. doi: 10.5301/jbm.2008.618. PMID: 18409144.
193. Yuan ZQ, Sun M, Feldman RI, Wang G, Ma X, Jiang C, Coppola D, Nicosia SV, Cheng JQ. Frequent activation of AKT2 and induction of apoptosis by inhibition of phosphoinositide-3-OH kinase/Akt pathway in human ovarian cancer. *Oncogene*. 2000 May 4;19(19):2324-30. doi: 10.1038/sj.onc.1203598. PMID: 10822383.
194. Liu T, Zhu J, Du W, Ning W, Zhang Y, Zeng Y, Liu Z, Huang JA. AKT2 drives cancer progression and is negatively modulated by miR-124 in human lung adenocarcinoma. *Respir Res*. 2020 Sep 1;21(1):227. doi: 10.1186/s12931-020-01491-0. PMID: 32873299; PMCID: PMC7466426.
195. Hinz N, Jücker M. Distinct functions of AKT isoforms in breast cancer: a comprehensive review. *Cell Commun Signal*. 2019 Nov 21;17(1):154. doi: 10.1186/s12964-019-0450-3. PMID: 31752925; PMCID: PMC6873690.
196. Xu X, Sakon M, Nagano H, Hiraoka N, Yamamoto H, Hayashi N, Dono K, Nakamori S, Umeshita K, Ito Y, Matsuura N, Monden M. Akt2 expression correlates with prognosis of human hepatocellular carcinoma. *Oncol Rep*. 2004 Jan;11(1):25-32. PMID: 14654898.
197. Wang C, Che L, Hu J, Zhang S, Jiang L, Latte G, Demartis MI, Tao J, Gui B, Pilo MG, Ribback S, Dombrowski F, Evert M, Calvisi DF, Chen X. Activated mutant forms of PIK3CA cooperate with RasV12 or c-Met to induce liver tumour formation in mice via AKT2/mTORC1 cascade. *Liver Int*. 2016 Aug;36(8):1176-86. doi: 10.1111/liv.13055. Epub 2016 Jan 30. PMID: 26716908; PMCID: PMC4929046.
198. Hayashi Y, Morimoto J, Suga H. In vitro selection of anti-Akt2 thioether-macrocyclic peptides leading to isoform-selective inhibitors. *ACS Chem Biol*. 2012 Mar 16;7(3):607-13. doi: 10.1021/cb200388k. Epub 2012 Jan 24. PMID: 22273180.

## PUBLICATIONS AND PRESENTATIONS

### Publications

#### **Convergent use of phosphatidic acid for hepatitis C virus and SARS-CoV-2 replication organelle formation**

Tabata K, Prasad V, Paul D, Lee JY, Pham MT, Twu WI, Neufeldt CJ, Cortese M, Cerikan B, Stahl Y, Joecks S, **Tran CS**, Lüchtenborg C, V'kovski P, Hörmann K, Müller AC, Zitzmann C, Haselmann U, Beneke J, Kaderali L, Erfle H, Thiel V, Lohmann V, Superti-Furga G, Brügger B, Bartenschlager R.

Nat Commun. 2021 Dec 14;12(1):7276. doi: 10.1038/s41467-021-27511-1

#### **PACSIN2 interacts with nonstructural protein 5A and regulates hepatitis C virus assembly**

Lap P Nguyen, **Si C Tran**, Shiro Suetsugu, Yun-Sook Lim, Soon B Hwang

J Virol. 2020 Feb 14;94(5):e01531-19. doi: 10.1128/JVI.01531-19

#### **Hepatitis C Virus Modulates Solute carrier family 3 member 2 for Viral Propagation**

Ngan N T Nguyen , Yun-Sook Lim , Lap P Nguyen , **Si C Tran** , Trang T D Luong, Tram T T Nguyen , Hang T Pham, Han N Mai, Jae-Woong Choi, Sang-Seop Han, Soon B Hwang

Sci Rep. 2018 Oct 19;8(1):15486. doi: 10.1038/s41598-018-33861-6

#### **Hepatitis C virus-induced Rab32 aggregation and its implications for virion assembly.**

Tu M. Pham, **Si C. Tran**, Yun-Sook Lim, Soon B. Hwang. 2017.

J Virol. 2017 Jan 18;91(3):e01662-16. doi: 10.1128/JVI.01662-16

#### **Hepatitis C virus nonstructural 5A protein interacts with Abelson interactor 1 and modulates Epidermal Growth Factor-mediated MEK/ERK signaling pathway.**

Van T.T. Huynh\*, Yun-Sook Lim\*, **Si C. Tran\***, Tu M. Pham, Lam N. Nguyen, Soon B. Hwang

J Biol Chem. 2016 Oct 21;291(43):22607-22617. doi: 10.1074/jbc.M116.727081

#### **Nonstructural 3 protein of hepatitis C virus modulates the tribbles homolog 3/Akt signaling pathway for persistent viral infection.**

**Si C. Tran**, Tu M. Pham, Lam N. Nguyen, Eun-Mee Park, Yun-Sook Lim, Soon B. Hwang.

J Virol. 2016 Jul 27;90(16):7231-7247. doi: 10.1128/JVI.00326-16.

### Presentations

#### **27<sup>th</sup> International Symposium on Hepatitis C Virus and Related Viruses**

Montreal, Canada, 2021 (Virtually)

Talk: Contribution of the cellular lipid kinase PI4KA to Hepatitis C virus induced liver pathogenesis

#### **26<sup>th</sup> International Symposium on Hepatitis C Virus and Related Viruses**

Seoul, South Korea, 2019

Poster: Contribution of the cellular lipid kinase PI4KA to Hepatitis C virus induced liver pathogenesis

## PUBLICATIONS AND PRESENTATIONS

---

### **29th Annual Meeting of the Society for Virology (GfV)**

Düsseldorf, Germany, 2019

Poster: Contribution of the cellular lipid kinase PI4KA to Hepatitis C virus induced liver pathogenesis

### **International Conference of the Korean Society for Molecular and Cellular Biology**

Seoul, South Korea, 2015

Poster: Hepatitis C virus suppresses Tribbles homolog 3-mediated apoptosis via NS3 for its own propagation

### **7th Indochina Conference on Pharmaceutical Sciences.**

Bangkok, Thailand, 2011

Poster: Screening raw materials in Vietnam for chondroitin extraction.

## APPENDIX

**Appendix 1. Histological evaluation of mice livers expressing PI4KA or HCV NS3-5B plasmids.** Evaluation was carried out twice, the first time was blind, the second time control group was known. Control: 01-05, HCV wt 06-10, HCV mut 11-15, PI4KA wt 16-20, PI4KA mut 21-25.

CMCP – Center for Model System and Comparative Pathology  
Pathologisches Institut | Im Neuenheimer Feld 224 | D-69120 Heidelberg  
Kooperationspartner: Dr. med. vet. Tanja Poth



### Histopathologische Beurteilung

CMCP-Projektnummer: v0699

Projekttitel: "Hepatitis C virus induced dysregulation of lipid metabolism and implications for HCC development"

Projektleiter / Einrichtung: Prof. Dr. Volker Lohmann, Molekulare Virologie, Zentrum für Infektiologie, UKHD

#### **Legend:**

Steatosis: evaluation at 40 x magnification, considering only the hepatocytes

Zone 1 = periportal, Zone 2 = midzonal, Zone 3 = centrolobular

<sup>1</sup>Displacement of the nucleus to the side; <sup>2</sup>no displacement of the nucleus, contiguous patches

<sup>3</sup>Cellular enlargement more than 1.5 times the normal hepatocyte diameter

<sup>4</sup>Average of 5 different areas at 40 x magnification; <sup>5</sup>more than background lesions

<sup>6</sup>Small aggregates of macrophages; <sup>7</sup>contiguous patches

<sup>8</sup>in hepatocytes and macrophages

Stains: H&E, Sirius Red

#### **Comment:**

Multifocal pigment deposition (presumably lipofuscin) in samples #-03, #-05, #-09, #-10, #-12, #-13, #-20; Mild multifocal dystrophic calcification in #-20



# APPENDIX

CMCP – Center for Model System and Comparative Pathology  
 Pathologisches Institut | Im Neuenheimer Feld 224 | D-69120 Heidelberg  
 Kooperationspartner: Dr. med. vet. Tanja Poth



Histological feature	Definition	Score	Animal-ID v0699-											
			01	02	03	04	05	06	07	08	09	10	11	12
<b>Steatosis</b>														
A) Macrovesicular <sup>1</sup>	< 5 %	0	0	0	0	0	0	0	0	0	0	0	0	0
	5 - 33 %	1												
	34 - 66 %	2												
	> 66 %	3												
	Location	Zone 3	0											
	Zone 2	1												
	Zone 1	1												
	azonal	2												
	panazncinar	3												
B) Microvesicular <sup>2</sup>	< 5 %	0	0	0	0	0	0	0	0	0	0	0	0	0
	5 - 33 %	1			1			1	1		1			1
	34 - 66 %	2					2							
	> 66 %	3												
	Location	Zone 3	0											
	Zone 2	1			1			1	1		1			1
	Zone 1	1												
	azonal	2												
	panazncinar	3					3							
Hepatocellular Hypertrophy <sup>3</sup>	< 5 %	0	0	0	0	0	0	0	0	0	0	0	0	0
	5 - 33 %	1						1	1			1		
	34 - 66 %	2												
	> 66 %	3												
<b>Fibrosis</b>														
A: pericellular/perisinusoidal	mild/ moderate	1/2												
B: portal/periportal	mild/ moderate	1/2								1	1	1		
Both zones		2											2	2
Bridging fibrosis		3												
Cirrhosis		4												
<b>Inflammation</b>														
A) Lobular inflammation <sup>4</sup>	none (< 0,5 foci)	0	0	0	0	0	0	0	0	0	0	0	0	0
	0,5-1 foci/400x field	1												
	1-2 foci/400x field	2												
	> 2 foci/400x field	3												
B) Portal inflammation <sup>5</sup>	none	0	0	0	0	0	0	0	0	0	0	0	0	0
	mild/ moderate/severe	1/2/3			1									
Microgranulomas <sup>6</sup>	no/yes	0/1	1	1	1	1	1	1	1	1	1	1	1	1
Large lipogranulomas	no/yes	0/1	0	0	0	0	0	0	0	0	0	0	0	0
<b>Liver cell injury</b>														
Necrosis of cell groups	none/few/multiple/many foci	0/1/2/3	1	0	1	2	1	1	0	0	0	0	1	1
Apoptotic hepatocytes	none/few	0	0	0	0	0	0	0	0	0	0	0	0	0
	many	1												
Bile pigment deposition <sup>8</sup>	no/yes	0/1	0	0	0	0	0	0	0	0	0	0	0	0
<b>Other findings</b>														
Bile duct proliferation	none/mild/ moderate/severe	0/1/2/3	0	0	1	1	0	1	1	1	1	1	1	1
<b>Sum of Score</b>		0 - 35	<b>2</b>	<b>1</b>	<b>4</b>	<b>6</b>	<b>2</b>	<b>9</b>	<b>5</b>	<b>5</b>	<b>3</b>	<b>6</b>	<b>5</b>	<b>7</b>
Score according to KLEINER DE et al., Hepatology (2005), modified by Liang et al., PLOS (2014) and adopted for the present study														
Proliferative Lesions		/	none	none	none	none	none	none	none	none	none	none	none	none

Die Diagnose ist eine Urkunde, deren Verwendung zu wissenschaftlichen oder gutachterlichen Zwecken nur mit ausdrücklicher Genehmigung des CMCP zulässig ist.

## APPENDIX

CMCP – Center for Model System and Comparative Pathology  
 Pathologisches Institut | Im Neuenheimer Feld 224 | D-69120 Heidelberg  
 Kooperationspartner: Dr. med. vet. Tanja Poth



Histological feature	Definition	Score	Animal-ID v0699-																				
			13	14	15	16	17	18	19	20	21	22	23	24	25								
<b>Steatosis</b>																							
A) Macrovesicular <sup>1</sup>	< 5 %	0	0	0	0	0	0	0	0	0	0	0	0	0	0	0	0	0	0	0	0	0	0
	5 - 33 %	1																					
	34 - 66 %	2																					
	> 66 %	3																					
	Location																						
	Zone 3	0																					
	Zone 2	1																					
	Zone 1	1																					
	azonal	2																					
	panazncinar	3																					
B) Microvesicular <sup>2</sup>	< 5 %	0	0	0				0														0	0
	5 - 33 %	1			1	1			1	1	1	1	1	1	1	1	1	1	1	1	1		
	34 - 66 %	2																					
	> 66 %	3																					
	Location																						
	Zone 3	0																					
	Zone 2	1			1	1			1	1	1	1	1	1	1	1	1	1	1	1	1		
	Zone 1	1																					
	azonal	2																					
	panazncinar	3																					
Hepatocellular Hypertrophy <sup>3</sup>	< 5 %	0	0	0				0	0					0	0							0	0
	5 - 33 %	1			1	1				1	1										1		
	34 - 66 %	2																					
	> 66 %	3																					
<b>Fibrosis</b>	none	0	0	0	0	0	0	0	0	0	0	0	0	0	0	0	0	0	0	0	0	0	0
A: pericellular/perisinusoidal	mild/ moderate	1/2																					
B: portal/periportal	mild/ moderate	1/2																					
Both zones		2																					
Bridging fibrosis		3																					
Cirrhosis		4																					
<b>Inflammation</b>																							
A) Lobular inflammation <sup>4</sup>	none (< 0,5 foci)	0	0	0	0	0	0	0	0	0	0	0	0	0	0	0	0	0	0	0	0	0	0
	0,5-1 foci/400x field	1																					
	1-2 foci/400x field	2																					
	> 2 foci/400x field	3																					
B) Portal inflammation <sup>5</sup>	none	0	0	0	0	0	0	0	0	0	0	0	0	0	0	0	0	0	0	0	0	0	0
	mild/ moderate/severe	1/2/3																					
Microgranulomas <sup>6</sup>	no/yes	0/1	0	1	0	0	0	0	1	0	0	0	0	1	0	0	1	0	0	0	0	1	1
Large lipogranulomas	no/yes	0/1	0	0	0	0	0	0	0	0	0	0	0	0	0	0	0	0	0	0	0	0	0
<b>Liver cell injury</b>																							
Necrosis of cell groups	none/few/multiple/many foci	0/1/2/3	0	1	0	1	0	0	0	0	1	1	0	1	0	1	0	0	0	0	0	0	0
Apoptotic hepatocytes	none/few	0	0	0	0	0	0	0	0	0	0	0	0	0	0	0	0	0	0	0	0	0	0
	many	1																					
Bile pigment deposition <sup>8</sup>	no/yes	0/1	0	0	0	0	0	0	0	0	0	0	0	0	0	0	0	0	0	0	0	0	0
<b>Other findings</b>																							
Bile duct proliferation	none/mild/ moderate/severe	0/1/2/3	1	1	0	0	0	1	0	0	0	0	0	0	0	0	0	0	0	0	0	0	0
<b>Sum of Score</b>		0 - 35	1	3	3	4	0	4	3	4	3	4	3	3	4	0	1						
Score according to KLEINER DE et al., Hepatology (2005), modified by Liang et al., PLOS (2014) and adopted for the present study																							
Proliferative Lesions	/	none	none	none	none	none	none	none	none	none	none	none	none	none	none	none	none	none	none	none	none	none	none

Erstellt/freigegeben am 11.01.2022

Dr. med. vet. Tanja Poth,  
 Fachtierärztin für Pathologie

Die Diagnose ist eine Urkunde, deren Verwendung zu wissenschaftlichen oder gutachterlichen Zwecken nur mit ausdrücklicher Genehmigung des CMCP zulässig ist.

## APPENDIX

**Appendix 2. Fold change of cytoskeleton proteins (phosphorylated and total forms) revealed by a Cytoskeleton Phospho Antibody Array (BioCat).** Note the color codes for fold change: □: 0.6-0.79; □: 0.4-0.59; □: 1.21-1.40; □: 1.41-1.60 □: >2.0

Antibody List (phosphorylated protein)	Fold Change PI4KA F1/DMSO	Antibody List (phosphorylated protein)	Fold Change PI4KA F1/DMSO
Actin Pan (a/b/g) (Phospho-Tyr55/53)	1.41	MEK1 (Phospho-Thr286)	1.17
Calmodulin (Phospho-Thr79/Ser81)	0.74	MEK1 (Phospho-Thr291)	1.08
CaMK1-alpha (Phospho-Thr177)	0.96	MEK1 (Phospho-Ser298)	0.47
CaMK2 (Phospho-Thr286)	1.18	MEK2 (Phospho-Thr394)	0.82
CaMK2-beta/gamma/delta (Phospho-Thr287)	0.59	Merlin (Phospho-Ser10)	1.31
CaMK4 (Phospho-Thr196/200)	1.01	Merlin (Phospho-Ser518)	1.14
Cofilin (Phospho-Ser3)	2.13	MKK3/MAP2K3 (Phospho-Ser189)	1.08
Cortactin (Phospho-Tyr421)	0.98	MKK3/MAP2K3 (Phospho-Thr222)	0.7
Cortactin (Phospho-Tyr466)	0.96	MKK6 (Phospho-Ser207)	0.96
c-Raf (Phospho-Ser296)	1.06	MKK7/MAP2K7 (Phospho-Ser271)	0.73
c-Raf (Phospho-Ser43)	1.11	Myosin regulatory light chain 2 (Phospho-Ser18)	0.92
CrkII (Phospho-Tyr221)	0.97	p130Cas (Phospho-Tyr165)	1.01
ERK1-p44/42 MAP Kinase (Phospho-Thr202)	0.98	p130Cas (Phospho-Tyr410)	0.99
ERK1-p44/42 MAP Kinase (Phospho-Tyr204)	1.03	Paxillin (Phospho-Tyr118)	1.02
ERK3 (Phospho-Ser189)	0.94	Paxillin (Phospho-Tyr31)	0.7
Ezrin (Phospho-Tyr353)	1.05	PI3-kinase p85-subunit alpha/gamma (Phospho-Tyr467/Tyr199)	0.66
Ezrin (Phospho-Tyr478)	0.99	PKA CAT (Phospho-Thr197)	1.31
Ezrin (Phospho-Thr566)	1.01	PKC alpha (Phospho-Tyr657)	1.12
FAK (Phospho-Tyr397)	0.92	PKC alpha/beta II (Phospho-Thr638)	1.17
FAK (Phospho-Tyr407)	1.36	PKC pan activation site (Phospho)	1.15
FAK (Phospho-Tyr576)	1.29	PLC beta-3 (Phospho-Ser1105)	1.25
FAK (Phospho-Tyr861)	1	PLC beta-3 (Phospho-Ser537)	0.96
FAK (Phospho-Ser910)	0.91	Rac1/cdc42 (Phospho-Ser71)	0.86
FAK (Phospho-Tyr925)	0.9	Rho/Rac guanine nucleotide exchange factor 2 (Phospho-Ser885)	0.77
Filamin A (Phospho-Ser2152)	1.24	Src (Phospho-Tyr418)	0.52
Gab2 (Phospho-Ser159)	0.97	Src (Phospho-Tyr529)	1.01
GTPase activating protein (Phospho-Ser387)	1.3	Src (Phospho-Ser75)	0.98
LIMK1 (Phospho-Thr508)	1.19	VASP (Phospho-Ser157)	1.02
MEK1 (Phospho-Ser217)	1.04	VASP (Phospho-Ser238)	1.02
MEK1 (Phospho-Ser221)	0.99		

## APPENDIX

Antibody List (total protein)	Fold Change PI4KA F1/DMSO	Antibody List (total protein)	Fold Change PI4KA F1/DMSO
Actin alpha-1 skeletal muscle (N-term)	1.02	MEK1 (Ab-221)	0.96
Actin alpha-2/3 (N-term)	0.92	MEK1 (Ab-286)	0.69
Actin Pan (a/b/g) (Ab-55/53)	0.65	MEK1 (Ab-291)	0.76
ACTN1 (F-Actin) (inter)	0.81	MEK1 (Ab-298)	0.65
Beta actin	0.93	MEK2 (Ab-394)	1.18
Calmodulin (Ab-79/81)	1.3	MEKKK 1 (inter)	0.86
CaMK1-alpha (Ab-177)	1	MEKKK 4 (inter)	0.92
CaMK1-beta (inter)	0.81	Merlin (Ab-10)	0.74
CaMK2 (Ab-286)	0.73	Merlin (Ab-518)	0.79
CaMK2-beta/gamma (inter)	0.88	MKK3/MAP2K3 (Ab-189)	0.89
CaMK2-beta/gamma/delta (Ab-287)	1.34	MKK3/MAP2K3 (Ab-222)	1.19
CaMK4 (Ab-196/200)	0.93	MKK6 (Ab-207)	1.04
CaMK5 (inter)	0.77	MKK7/MAP2K7 (Ab-271)	1.11
Cofilin (Ab-3)	0.5	Myosin regulatory light chain 2 (Ab-18)	1.1
Cortactin (Ab-421)	0.86	NCK2 (C-term)	0.99
Cortactin (Ab-466)	0.79	p130Cas (Ab-165)	1.01
c-Raf (Ab-296)	0.92	p130Cas (Ab-410)	1.14
c-Raf (Ab-43)	0.82	Paxillin (Ab-118)	0.92
Crkl (Ab-221)	0.88	Paxillin (Ab-31)	1.17
ERK1/2 (N-term)	0.83	PI3-kinase p85-subunit alpha/gamma (Ab-467/199)	1.26
ERK1-p44/42 MAP Kinase (Ab-202)	0.82	PIP5K (inter)	0.83
ERK1-p44/42 MAP Kinase (Ab-204)	0.82	PKA CAT (Ab-197)	0.8
ERK3 (Ab-189)	0.96	PKC alpha (Ab-657)	0.87
Ezrin (Ab-353)	0.96	PKC alpha/beta II (Ab-638)	0.8
Ezrin (Ab-478)	1.05	PKC pan activation site	0.8
Ezrin (Ab-566)	0.86	PLC beta-3 (Ab-1105)	0.98
FAK (Ab-397)	0.89	PLC beta-3 (Ab-537)	0.93
FAK (Ab-407)	0.83	Rac1/cdc42 (Ab-71)	0.82
FAK (Ab-576)	0.92	Rho/Rac guanine nucleotide exchange factor 2 (Ab-885)	1.18
FAK (Ab-861)	1.06	Src (Ab-418)	1.04
FAK (Ab-910)	0.77	Src (Ab-529)	0.9
FAK (Ab-925)	0.9	Src (Ab-75)	1.16
Filamin A (Ab-2152)	0.72	VASP (Ab-157)	0.76
Gab2 (Ab-159)	1.04	VASP (Ab-238)	0.88
GAPDH	0.75	WASP (Ab-290)	0.99
GTPase activating protein (Ab-387)	0.65	WAVE1 (Ab-125)	0.98
LIMK1 (Ab-508)	0.9		
LIMK1/2 (Ab-508/505)	0.85		
MEK1 (Ab-217)	0.82		

## APPENDIX

### Appendix 3. qPCR primers used in this study

Primer	Sequence (5'-3')	Target mRNAs
19FE01	CAGCTCTGACCAAGTGGAGAT	PI4KA
19FE02	GCGGATGGTTGCATTTGGAA	
19FE03	CCTGCTCAACCATAAGCTCCC	PI4KB
19FE04	AGTTTTCTACGGACCTCGTACT	
19FE05	CTCCAGCGGAAGCTACTTCG	PI4K2A
19FE06	TCCACTTAGGATTAAGATGCCCA	
19FE07	ACCCAAATCAGAAGAGCCTTATG	PI4K2B
19FE08	CAAGGGCAGCAGACCTTATG	
19FE09	GGTGCCATCCAGTTAGGCATT	
19FE10	CGTAGAAATCTTGCATGAGGACA	PIP5K1A
19FE11	CTGGGAATAGGATACACAGTGGG	
19FE12	GCTGGGTAGGAACACACTTTC	PIP5K1B
19FE13	AGACCGTCATGCACAAGGAG	
19FE14	CAGTACAGCCCATAGAACTTGG	PIP5K1C
19FE15	CCACGACCATCATCAGGTGAA	
19FE16	CCTCACGGAGGCATTCTAAAGT	PIK3CA
19FE17	TATTTGGACTTTGCGACAAGACT	
19FE18	TCGAACGTACTGGTCTGGATAG	PIK3CB
19FE19	AAGGAGGAGAATCAGAGCGTT	
19FE20	GAAGAGCGGCTCATACTGGG	PIK3CD
19FE21	GGCGAAACGCCCATCAAAAA	
19FE22	GACTCCCGTGCAGTCATCC	PIK3CG
19FE23	AAATGGGACCAGTAGTTTGCC	
19FE24	GGGTTTGTGCGGTGATTGGTA	PIK3C2A
19FE25	TCAGGGCAATGGGGAACAC	
19FE26	CGTAACAGCTTGAGGTCGGTC	PIK3C2B
19FE27	ATCAACCCCATTTCTTAGCCA	
19FE28	CCAGGAGAGTTCACGGCTTTT	PIK3C2G
19MAR01	GGCTACCATGAGCAGCTTACC	
19MAR02	CTGTGAGGTCGGTGTTCCG	PIK3CG
19FE29	CTGCTGGAAGTGAACGCTGTA	
19FE30	GGGGCTGTTAGTCTCTGGGA	PXN
19FE31	TTCAACGACATGAAGGTGCGT	
19FE32	TCCTCCAGGATGATGTTCTTCT	CFL1
18MAY01	CAATGTAGCGGTCACCCAAG	
18MAY02	ACATTCCTGAGGCTCGTTCA	NS3-5B JFH1
18MAR01	ACGCAGAAAGCGTCTAGCCAT	
18MAR02	TACTCACCGGTTCCGCAGA	HCV Con1
18MAR03	TCTGCGGAACCGGTGAGTA	
18MAR04	GGGCATAGAGTGGGTTTATCCA	HCV JFH1
18MAR05	GAAGGTGAAGGTCGGAGTC	
18MAR06	GAAGATGGTGATGGGATTTT	GAPDH
18MAR07	AACTGGAACGGTGAAGGTG	
18MAR08	AGAGAAGTGGGGTGGCTTTT	$\beta$ -actin
20AU01	ATGTGCCCAGTAGATTTTCATGG	
20AU02	CCAATACACTTTTGGAAAGACCCC	mouse PI4KA
20AU03	AGGTCGGTGTGAACGGATTTG	
20AU04	GGGGTCGTTGATGGCAACA	mouse GAPDH

## APPENDIX

### Appendix 4. Primers used for cloning shRNAs

Primer	Sequence (5'-3')	Purpose
19JA02	tcgagaaggtatatTGCTGTTGACAGTGAGCGAGCTGATAGTGGCATGATTGAATAGTGAAGCCACAGATGTATTCAATCATGCCACTATCAGCCGCCTACTGCCTCGG	D11 shPI4KB
19JA16	aatTCCGAGGCAGTAGGCCAGGCTGATAGTGGCATGATTGAATACATCTGTGGCTTCACTATTCAATCATGCCACTATCAGCTCGCTCACTGTCAACAGCAatataccttc	
19JA03	tcgagaaggtatatTGCTGTTGACAGTGAGCGAACAGACTGGGTGGTGGTGAAGTAGTGAAGCCACAGATGTACTTCACCACCACCCAGTCTGTGTGCCTACTGCCTCGG	D12 shPI4K2A
19JA17	aatTCCGAGGCAGTAGGCCACACAGACTGGGTGGTGGTGAAGTACATCTGTGGCTTCACTACTTCACCACCACCCAGTCTGTTGCTCACTGTCAACAGCAatataccttc	
19JA04	tcgagaaggtatatTGCTGTTGACAGTGAGCGAAGTCACAATTTGAAAGATTAGTAGTGAAGCCACAGATGTACTAATCTTTCAAATTGTGACTGTGCCTACTGCCTCGG	D13 shPI4K2B
19JA18	aatTCCGAGGCAGTAGGCCACAGTCACAATTTGAAAGATTAGTACATCTGTGGCTTCACTACTAATCTTTCAAATTGTGACTTCGCTCACTGTCAACAGCAatataccttc	
19JA05	tcgagaaggtatatTGCTGTTGACAGTGAGCGACCTCTTGATGTCAATCCATAATAGTGAAGCCACAGATGTATTATGGATTGACATCAAGAGGCTGCCTACTGCCTCGG	D14 shPIP5K1A
19JA19	aatTCCGAGGCAGTAGGCCAGCCTCTTGATGTCAATCCATAATACATCTGTGGCTTCACTATTATGGATTGACATCAAGAGGTGCTCACTGTCAACAGCAatataccttc	
19JA06	tcgagaaggtatatTGCTGTTGACAGTGAGCGCGGAGATTGTGTCCTCAATTAGTAGTGAAGCCACAGATGTACTAATTGAGGACACAATCTCCTGCCTACTGCCTCGG	D15 shPIP5K1B
19JA20	aatTCCGAGGCAGTAGGCCAAGGAGATTGTGTCCTCAATTAGTACATCTGTGGCTTCACTACTAATTGAGGACACAATCTCCGCGCTCACTGTCAACAGCAatataccttc	
19JA07	tcgagaaggtatatTGCTGTTGACAGTGAGCGACCAGAGCACCTCAGATGAGAATAGTGAAGCCACAGATGTATTCTCATCTGAGGTGCTCTGGTGCTACTGCCTCGG	D16 shPIP5K1C
19JA21	aatTCCGAGGCAGTAGGCCACCCAGAGCACCTCAGATGAGAATACATCTGTGGCTTCACTATTCTCATCTGAGGTGCTCTGGTGCCTCACTGTCAACAGCAatataccttc	
19JA08	tcgagaaggtatatTGCTGTTGACAGTGAGCGCGGCCAGTACCTCATGGATTAGTAGTGAAGCCACAGATGTACTAATCCATGAGGTACTGGCCATGCCTACTGCCTCGG	D17 shPIK3CA
19JA22	aatTCCGAGGCAGTAGGCCATGGCCAGTACCTCATGGATTAGTACATCTGTGGCTTCACTACTAATCCATGAGGTACTGGCCGCGCTCACTGTCAACAGCAatataccttc	
19JA09	tcgagaaggtatatTGCTGTTGACAGTGAGCGCGGTCTTCATTTCTGATGAACTAGTGAAGCCACAGATGTAGTTCATCAGGAAATGAAGACCATGCCTACTGCCTCGG	D18 shPIK3CB
19JA23	aatTCCGAGGCAGTAGGCCATGGTCTTCATTTCTGATGAACTACATCTGTGGCTTCACTAGTTCATCAGGAAATGAAGACCGCGCTCACTGTCAACAGCAatataccttc	
19JA10	tcgagaaggtatatTGCTGTTGACAGTGAGCGATTTGTCCATGTGATTCAAGCAGTAGTGAAGCCACAGATGTACTGCTGAATCACATGGACAAAGTGCTACTGCCTCGG	D19 shPIK3CD
19JA24	aatTCCGAGGCAGTAGGCCACTTTGTCCATGTGATTGAGCAGTACATCTGTGGCTTCACTACTGCTGAATCACATGGACAAATCGCTCACTGTCAACAGCAatataccttc	

**APPENDIX**

19JA11	tcgagaaggtatatTGCTGTTGACAGTGAGCGAACAGAGGAGGTGCTGTG GAATTAGTGAAGCCACAGATGTAATTCCACAGCACCTCCTCTGTGTG CCTACTGCCTCGG	D20 shPIK3CG
19JA25	aatTCCGAGGCAGTAGGCACACAGAGGAGGTGCTGTGGAATTACATC TGTGGCTTCACTAATTCCACAGCACCTCCTCTGTTCGCTCACTGTCA ACAGCAatataccttc	
19JA12	tcgagaaggtatatTGCTGTTGACAGTGAGCGAGCCTACAACCTTGATAAGA AAGTAGTGAAGCCACAGATGTACTTTCTTATCAAGTTGTAGGCCTGC CTACTGCCTCGG	D21 shPIK3C2A
19JA26	aatTCCGAGGCAGTAGGCAGGCCTACAACCTTGATAAGAAAGTACATC TGTGGCTTCACTACTTTCTTATCAAGTTGTAGGCTCGCTCACTGTCA ACAGCAatataccttc	
19JA13	tcgagaaggtatatTGCTGTTGACAGTGAGCGACCAGACAGTGTCATCCT GCAGTAGTGAAGCCACAGATGTACTGCAGGATGACACTGTCTGGCT GCCTACTGCCTCGG	D22 shPIK3C2B
19JA27	aatTCCGAGGCAGTAGGCAGCCAGACAGTGTCATCCTGCAGTACATC TGTGGCTTCACTACTGCAGGATGACACTGTCTGGTCGCTCACTGTC AACAGCAatataccttc	
19JA14	tcgagaaggtatatTGCTGTTGACAGTGAGCGACCACTTACAATGAAATTG TAGTAGTGAAGCCACAGATGTACTACAATTTTCATTGTAAGTGGGTGC CTACTGCCTCGG	D23 shPIK3C2G
19JA28	aatTCCGAGGCAGTAGGCACCCACTTACAATGAAATTGTAGTACATCT GTGGCTTCACTACTACAATTTTCATTGTAAGTGGTCGCTCACTGTCAA CAGCAatataccttc	
19MAR04	tcgagaaggtatatTGCTGTTGACAGTGAGCGACGTGACTGCCTTGTCCTT AACTAGTGAAGCCACAGATGTAGTTAAGGACAAGGCAGTCACGGTG CCTACTGCCTCGG	D25 shPI4K2A
19MAR11	aatTCCGAGGCAGTAGGCACCGTGACTGCCTTGTCCTTAACTACATC TGTGGCTTCACTAGTTAAGGACAAGGCAGTCACGTCGCTCACTGTC AACAGCAatataccttc	
19MAR05	tcgagaaggtatatTGCTGTTGACAGTGAGCGCAGTGACAACATCATGGTC AAATAGTGAAGCCACAGATGATTTGACCATGATGTTGTCACTATGC CTACTGCCTCGG	D26 shPIK3CB
19MAR12	aatTCCGAGGCAGTAGGCATAGTGACAACATCATGGTCAAATACATC TGTGGCTTCACTATTTGACCATGATGTTGTCACTGCGCTCACTGTCA ACAGCAatataccttc	
19MAR06	tcgagaaggtatatTGCTGTTGACAGTGAGCGCGCTCATCAACTCACAGAT CAGTAGTGAAGCCACAGATGTACTGATCTGTGAGTTGATGAGCTTG CCTACTGCCTCGG	D27 shPIK3CD
19MAR13	aatTCCGAGGCAGTAGGCAAGCTCATCAACTCACAGATCAGTACATC TGTGGCTTCACTACTGATCTGTGAGTTGATGAGCGCGCTCACTGTC AACAGCAatataccttc	
19MAR08	tcgagaaggtatatTGCTGTTGACAGTGAGCGCGCCTACAACCTCATTGCGC AAGTAGTGAAGCCACAGATGTACTTGCGAATGAGGTTGTAGGCTTG CCTACTGCCTCGG	D29 shPIK3C2B
19MAR15	aatTCCGAGGCAGTAGGCAAGCCTACAACCTCATTGCGCAAGTACATC TGTGGCTTCACTACTTGCGAATGAGGTTGTAGGCGCGCTCACTGTC AACAGCAatataccttc	
19MAR09	tcgagaaggtatatTGCTGTTGACAGTGAGCGATCCAATTCTGTGCAGGTA AAGTAGTGAAGCCACAGATGTACTTTACCTGCACAGAATTGGAGTG CCTACTGCCTCGG	D30 shPIK3C2G
19MAR16	aatTCCGAGGCAGTAGGCACTCCAATTCTGTGCAGGTAAGTACATC TGTGGCTTCACTACTTTACCTGCACAGAATTGGATCGCTCACTGTCA ACAGCAatataccttc	
19MAR17	tcgagaaggtatatTGCTGTTGACAGTGAGCGATCTGATGGTGTCATCAAG GTGTAGTGAAGCCACAGATGTACACCTTGATGACACCATCAGAGTG CCTACTGCCTCGG	D31 shCFL1
19MAR19	aatTCCGAGGCAGTAGGCACTCTGATGGTGTCATCAAGGTGTACATC TGTGGCTTCACTACACCTTGATGACACCATCAGATCGCTCACTGTCA ACAGCAatataccttc	

## APPENDIX

19MAR18	tcgagaaggtatatTGCTGTTGACAGTGAGCGATTCTCAAGCTCTTCTGC TAGTAGTGAAGCCACAGATGTACTAGCAGAAGAGCTTGAGGAAGTG CCTACTGCCTCGG	D32 shPXN
19MAR20	aatTCCGAGGCAGTAGGCACTTCCTCAAGCTCTTCTGCTAGTACATCT GTGGCTTCACTACTAGCAGAAGAGCTTGAGGAATCGCTCACTGTCA ACAGCAatataccttc	
19AP01	tcgagaaggtatatTGCTGTTGACAGTGAGCGCATGCTTATTGTGAAGAGT AAATAGTGAAGCCACAGATGTATTTACTCTTCACAATAAGCATTTGC CTACTGCCTCGG	D33 shPIK3C2G
19AP02	aatTCCGAGGCAGTAGGCAAATGCTTATTGTGAAGAGTAAATACATCT GTGGCTTCACTATTTACTCTTCACAATAAGCATGCGCTCACTGTCAA CAGCAatataccttc	
19AP03	tcgagaaggtatatTGCTGTTGACAGTGAGCGATGGGAGTATATGAAACCT GATTAGTGAAGCCACAGATGTAATCAGGTTTCATATACTCCCACTGC CTACTGCCTCGG	D34 shPIK3C2G
19AP04	aatTCCGAGGCAGTAGGCACTGGGAGTATATGAAACCTGATTACATC TGTGGCTTCACTAATCAGGTTTCATATACTCCCATCGCTCACTGTCA ACAGCAatataccttc	
19AP05	tcgagaaggtatatTGCTGTTGACAGTGAGCGCCCAGACAATGTCTCTTAA CACTAGTGAAGCCACAGATGTAGTGTAAAGAGACATTGTCTGGATG CCTACTGCCTCGG	D35 shPIK3C2G
19AP06	aatTCCGAGGCAGTAGGCATCCAGACAATGTCTCTTAACACTACATCT GTGGCTTCACTAGTGTAAAGAGACATTGTCTGGCGCTCACTGTCA ACAGCAatataccttc	

### Appendix 5. Primers used for cloning PIK3C2G, PXN and CFL1

Gene	Cloning primers	
	Sense	Antisense
PIK3C2G	TT GGCGCGCC ATGGCATATTCTTGGCAAACGGATC	CC GCGATCGC TCAAATTATACTGTTTCCTAATGGA
CFL1	TT GGCGCGCC ATGGCCTCCGGTGTGGCTGT	CC GCGATCGC TCACAAAGGCTTGCCCTCCA
PXN	TT GGCGCGCC ATGGACGACCTCGACGCCCT	CC GCGATCGC CTAGCAGAAGAGCTTGAGGA

### Appendix 6. List of plasmids used in this study

Plasmid	Description
pFK-JFH1/J6/C-846_δg (Jc1)	Full length virus chimera
pFK-DBN3a cc	Gift from Jens Bukh
pFK-TNcc	Gift from Jens Bukh
pAPM shNT	Non-targeting shRNA, puromycin resistance
pAPM shPI4KA	Constitutive knockdown of PI4KA
pAPM shPI4KB	Constitutive knockdown of PI4KB
pAPM shPI4K2A	Constitutive knockdown of PI4K2A
pAPM shPI4K2B	Constitutive knockdown of PI4K2B
pAPM shPIP5K1A	Constitutive knockdown of PIP5K1A
pAPM shPIP5K1B	Constitutive knockdown of PIP5K1B
pAPM shPIP5K1C	Constitutive knockdown of PIP5K1C
pAPM shPIK3CA	Constitutive knockdown of PIK3CA
pAPM shPIK3CB	Constitutive knockdown of PIK3CB
pAPM shPIK3CD	Constitutive knockdown of PIK3CD
pAPM shPIK3C2A	Constitutive knockdown of PIK3C2A
pAPM shPIK3C2B	Constitutive knockdown of PIK3C2B
pAPM shPIK3C2G	Constitutive knockdown of PIK3C2G
pWPI BLR	Basic lentiviral transduction vector, blasticidin resistance
pWPI BLR HA-PI4KA wt	Stable expression of HA-tagged PI4KA wt
pWPI BLR HA-PI4KA D1957A	Stable expression of HA-tagged PI4KA D1957A



## APPENDIX

pWPI BLR PIK3C2G	Stable expression of PIK3C2G
pWPI BLR AKT2 Y474D	Stable expression of AKT2 Y474D
pWPI BLR PXN wt	Stable expression of PXN wt
pWPI BLR PXN Y31D	Stable expression of PXN Y31D
pWPI BLR CFL1 wt	Stable expression of CFL1 wt
pWPI BLR CFL1 S3A	Stable expression of CFL1 S3A
pWPI BLR CFL1 S3D	Stable expression of CFL1 S3D
pMD2.G	VSV-G envelope expressing plasmid
psPAX2	2 <sup>nd</sup> generation lentiviral packaging plasmid
pShuttle CMV vector	Shuttle vector for use in AdEasy system, under a CMV promoter
pShuttle CMV JFH NS3-5B wt	Expression of transgene JFH NS3-5B wt
pShuttle CMV JFH NS3-5B S2208A	Expression of transgene JFH NS3-5B S2208A
pShuttle CMV JFH NS3-5B PPH	Expression of transgene JFH NS3-5B PPH
pAdEasy CMV vector	Adenoviral vector for AdEasy system, recombine plasmid from the pShuttle CMV vector
pAdEasy CMV JFH NS3-5B wt	Recombine plasmid from pShuttle CMV JFH NS3-5B wt
pAdEasy CMV JFH NS3-5B S2208A	Recombine plasmid from pShuttle CMV JFH NS3-5B S2208A
pAdEasy CMV JFH NS3-5B PPH	Recombine plasmid from pShuttle CMV JFH NS3-5B PPH
pCMV-SB	transposase vector, encoding the enzyme mediating excision and integration of the GOI for use in Sleeping Beauty transposon system
pCSMB1-PI4KA wt	Transposon vector, containing binding sites flanking PI4KA wt
pCSMB2-PI4KA mutPPH	Transposon vector, containing binding sites flanking PI4KA D1957A
pCSMB3-NS3-5B wt	Transposon vector, containing binding sites flanking JFH NS3-5B wt
pCSMB4-NS3-5B mut	Transposon vector, containing binding sites flanking JFH NS3-5B PPH
pSMART <sub>t</sub> _HCV NS3-5B JFH wt GFP	pSMART <sub>t</sub> vector for expression of HCV NS3-5B and PI4KA wt and mutant
pSMART <sub>t</sub> _HCV NS3-5B JFH wt - emGFP	
pSMART <sub>t</sub> _HA-PI4KA wt	
pSMART <sub>t</sub> _HA-PI4KA mut D1957A	